UNIVERSITI MALAYA

ORIGINAL LITERARY WORK DECLARATION

Name of Candidate: Noraini Binti Ajit

Registration/Matric No: KGA 070031

Name of Degree: Master's Degree

Title of Project Paper/Research Report/Dissertation/Thesis ("this Work"):

Steel Connection Behaviour In Frame And Floor System At Elevated Temperature

Field of Study: Structural Steel Engineering

I do solemnly and sincerely declare that:

(1) I am the sole author/writer of this Work;
(2) This Work is original;
(3) Any use of any work in which copyright exists was done by way of fair dealing and for permitted purposes and any excerpt or extract from, or reference to or reproduction of any copyright work has been disclosed expressly and sufficiently and the title of the work and its authorship have been acknowledged in this Work;
(4) I do not have any actual knowledge nor do I ought reasonably to know that the making of this work constitutes an infringement of any copyright work;
(5) I hereby assign all and every rights in the copyright to this Work to the University of Malaya ("UM"), who henceforth shall be owner of the copyright in this Work and that any reproduction or use in any form or by any means whatsoever is prohibited without the written consent of UM having been first had and obtained;
(6) I am fully aware that if in the course of making this Work I have infringed any copyright whether intentionally or otherwise, I may be subject to legal action or any other action as may be determined by UM.

Candidate's Signature Date

Subscribed and solemnly declared before,

Witness's Signature Date

Name: Designation:

ABSTRACT

This thesis presents an analytical investigation on the influence of connection on the performance of steel frame structure and floor system under fire conditions. The connections are modeled through the use of Component Based Method. The implementation is undertaken within the advanced finite element program ADAPTIC, which accounts for material and geometric nonlinearities. Data from a compartment fire test of a four-storey composite building conducted in Gurun, Malaysia was adopted for simulation studies. For steel sub-frame, experimental test based on Coimbra Fire Test was used, which cover endplate connections under fire load. Based on the developed and validated numerical model, parametric studies were performed in order to identify parameters affected the performance of connection under elevated temperatures. Several factors are put into consideration to investigate the influence of connections as well as structural response due to temperature effect, geometric consideration, influence of composite slab and load ratio. From the studies carried out, it can be illustrated that the component based methods is one of the economical and faster solutions to study the behaviour of connection at elevated temperature. Comparison between the experimental and Component Based Method results shows that the developed connection model has the capability to predict the resistance and deformation capacity of semi-rigid connections under elevated temperatures with a satisfactory degree of accuracy. It is important to consider the actual connections configurations in assessing the overall structural response, so that in the beginning of designing stage, designer can estimate the capability of overall structure to resist natural fire accident. From the parametric studies, it can be illustrated that parameters related to connections may influence the overall performance of structures. Further studies on the ductility of connections at elevated temperatures are reviewed in order to identify the limitation of rotation capacity of connections under fire.

ABSTRAK

Tesis ini menerangkan penyelidikan secara analitikal terhadap pengaruh sambungan terhadap kelakuan kerangka keluli dan sistem lantai pada keadaan kebakaran. Sambungan dimodel menggunakan kaedah asas komponen (Component Based Method). Ianya dilaksana menggunakan analisa tidak terhingga ADAPTIC, yang mengambilkira ketidaklelurusan bahan dan geometri. Data daripada ujikaji kebakaran ke atas ruang bilik di dalam bangunan komposit empat tingkat yang dilakukan di Gurun, Malaysia telah digunakan untuk kerja-kerja simulasi. Untuk kerangka keluli, ujian eksperimen adalah berdasarkan kepada Ujian Kebakaran Coimbra, yang meliputi sambungan plat hujung. Berdasarkan kepada model yang dibina dan disahkan, kajian parameter telah dilakukan untuk mengenalpasti parameter yang memberi kesan kepada tindakan sambungan pada suhu yang tinggi. Beberapa faktor telah diambilkira untuk mengkaji pengaruh sambungan dan tindakan struktur disebabkan kesan suhu, pertimbangan geometri, pengaruh lantai komposit dan nisbah beban. Daripada kajian yang dilakukan, telah didapati bahawa yang kaedah asas komponen adalah salah satu kaedah yang ekonomik dan penyelesaian yang cepat untuk mengkaji perlakuan sambungan pada suhu tinggi. Perbandingan keputusan diantara eksperimen dan kaedah asas komponen menunjukkan model sambungan yang dibina mempunyai kebolehan untuk menganggar kebolehtahanan dan keupayaan putaran sambungan separa tegar pada suhu tinggi dengan nisbah ketepatan yang memuaskan. Adalah penting untuk mengambilkira kelakuan sebenar sambungan dalam menilai tindakbalas keseluruhan struktur, supaya di tahap awal proses rekabentuk, perekabentuk boleh menganggar kebolehan keseluruhan struktur untuk bertahan dalam situasi kebakaran.sebenar. Daripada kajian parameter, dapat ditunjukkan parameter yang berkaitan dengan sambungan boleh mempengaruhi kelakuan struktur secara keseluruhannya. Kajian

berkaitan kemuluran sesuatu sambungan di bawah suhu tinggi juga dikaji bagi mengenalpasti tahap keupayaan putaran sesuatu sambungan di bawah kebakaran.

ACKNOWLEDGEMENT

In the name of Allah, the Compassionate, the merciful, praise be to Allah, Lord of Universe and Peace and Prayers be upon His Final prophet and Massenger'.

First and foremost, I would like to express my special appreciation to my supervisor, Dr. Nor Hafizah Ramli @ Sulong for her supervision, guidance, advice and support in my Master studies. A special thanks to University Malaya in providing a scholarship and grand that helps in support in my studies.

I would also like to thanks to Prof. Siti Hamisah Tafsir from UTM Skudai Johor, for her co-operation in giving information for this studies. Beside that a special thanks to others researchers in this area that directly or indirectly contribute in giving information and data in completing this thesis.

Not forgotten to my beloved family and friends in giving their moral support and encouragement. Last but not less a sincere appreciation also goes to those who directly or indirectly involve in successfully my thesis.

TABLE OF CONTENTS

TABLE OF CONTENTS

TABLE OF CONTENTS

TABLE OF CONTENTS

TABLE OF CONTENTS

LIST OF FIGURES

LIST OF FIGURES

LIST OF FIGURES

LIST OF FIGURES

LIST OF FIGURES

LIST OF FIGURES

LIST OF FIGURES

LIST OF FIGURES

LIST OF TABLES

LIST OF TABLES

LIST OF SYMBOLS AND ABBREVIATIONS

Symbols	Description	Unit
T_b	Temperature of the bolt	°C
E	Elastic modulus	N/m^2
T_s	Temperature of steel	°C
f_y	Yield strength of steel at ambient temperature	N/m^2
f_{yT}	Yield strength of steel at a given temperature	N/m^2
f_{ub}	Ultimate strength of the bolt at ambient temperature	N/m^2
f_{ubT}	Ultimate strength of the bolt at a given temperature	N/m^2
ϕ	Rotation	rad
M	Moments	kNm
d_b	Bolt diameter	m
$M_{j,Rd}$	Moment resistance of the joint	kNm
t_w	Web thickness	m
h_b	Depth of the beam	m
h_c	Depth of column	m
Δ^f	Component failure displacement	m
K^e	Initial elastic stiffness	N/m
K^p	Post-limit stiffness	N/m
F^y	Yield Strength	N/m^2
Δ^y	Component yield displacement	m
γ	Deformation	m
ε_{cu}	Ultimate compressive strain	-
A_b	Area of bolt shank	m^2
t_{bh}	Thickness of bolt head	m
t_n	Thickness of nut	m
t_w	Thickness of washer	m
n_1	Distance from endplate edge to bolt head/nut/washer edge	m
k	Distance of bolt head/nut /washer whichever is appropriate	m
m_1	Distance from edge of bolt head/nut/ washer to fillet of endplate to beam web	m
L_{ep}	Total depth of endplate	m

LIST OF SYMBOLS AND ABBREVIATIONS

Symbols	Description	Unit
t_{ep}	Thickness of endplate	m
b_p	Endplate width	m
p_b	Minimum bolt pitch	m
α	Coefficient for the computation of the effective width for the bolt-row below the beam tension flange	-
d_{M16}	Diameter of M16 bolts	m
L_a	Total depth of angle	m
t_a	Angle thickness	m
g_{bl}	Gauge length of beam leg	m
b_{clr}	Bolt clearance	m
p_b	Minimum bolt pitch	m
g_{cl}	Gauge length of column leg	m
e_{cl}	Distance from bolt line to free edge of column leg	m
e_{bl}	Distance from bolt line to free edge of beam leg	m
r_a	Angle radius	rad

LIST OF SYMBOLS AND ABBREVIATIONS

Abbreviations	**Compound**
DWA/dwa	Double web angle
TSA	Top and seat angle
TSWA	Top, seat and double web angle
EXTEP	Extended end plate
FEP	Flush end plate
FEA	Finite element analysis
SRF	Strength reduction factor

CHAPTER 1.0 INTRODUCTION

1.1 BACKGROUND

Recent experimental investigations dealing with the performance of steel and composite buildings under fire conditions have provided greater insight into the actual behaviour mechanisms that occur at elevated temperatures. This has led to a wide recognition of the inadequacy of current design procedures. Consequently, there is a growing need for the development of performance-based design procedures which can provide a more rational representation of the behaviour.

Recently, investigations and studies on behaviour of structure under real fire test have increased considerably, including six tests carried out on eight-storey office building in UK at the Building Research Establishment's Cardington Laboratory on 16 Jan 2003 (Bailey, 1999). Fire tests on William Street Office Building, Collins Street Office Enclosure and German fire test on four-storey steel framed building at Struttgard- Vaihingen University, German. Besides that, a study on Basingstoke and Churchill plaza fire accident also gives a better understanding and proves that structures behave differently in real fire compared to standard fire test. In Malaysia, the first attempt in investigating the behaviour of full scale building under fire loading was carried out by Tapsir (2004) on a four-storey school building located in Gurun, Kedah.

In understanding the behaviour of structure under fire, several finite elements analysis software was emerged to model and analyzed the structure without resorting to highly expensive fire testing. A brief review of some finite element analysis programs used in the field of steel structure under fire was carried out by Wang (2002), Ramli Sulong (2005), Silva (2004, 2005 and 2008). These programs include research software such as ADAPTIC, Finite Element Analysis of Structures at elevated temperature FEAST, SAFIR and VULCAN in addition to commercial finite element packages which are ABAQUS, ANSYS and DIANA.

The earliest research carried on the structure behaviour under elevated temperature was carried out by Pettersson et al. (1976) and Witteveen et al. (1977), on the compartment and on frame structure. Other researchers such as Lawson et al. (1990), Leston-Jones (1997), Al-Jabri (1999), Spyrou et al. (2002), Wang (2007), Yu et al. (2007, 2008), Ding (2007) and Hu et al. (2008) are the names of researchers that report on the experimental test conducted on a connection at elevated temperature.

In the prescriptive approach, fire resistance periods are specified depending on the building's function and height above ground and can vary throughout the world. It is based on required fire resistance periods which referred to standard fire test carried on isolated member, not as a whole structure of building as for performance based approach. Traditionally, to determine fire protection applied on steel section, it is based on the thermal performance of steel section call section factor, H_p / A, where, H_p is the perimeter of section exposed to fire in' m' unit and A is the Cross-Sectional area of the steel member in 'm^2' unit and also the relation with fire resistance periods.

According to traditional testing, it proves that steel reach its critical temperature value of 550 ^oC, where at this stage the steel lost 40% of its strength. This value can be referred to strength reduction factors recorded for steel complying with Grade 43 to 50 in BS5950 Part 8. The typical prescriptive approach specifies the thickness of fire protection to steel elements to ensure the steel does not exceed a specified temperature for a given fire resistance period. In UK, the maximum temperatures of 550°C for columns and 620°C for beams supporting concrete floors are assumed. These temperatures are based on the assumption that a fully-stressed member at ambient conditions (designed to BS5950-1 or BS449) will lose its design safety margin when it reaches 550°C. The maximum temperature for beams supporting concrete floors is increased to 620°C since the top flange is at a lower temperature compared to the web and bottom flange. This is because the top flange is in contact with the concrete floor which acts as a heat sink (Bailey, 2007).

The prescriptive approach in developing fire-resistance ratings does not take account of the various factors that influence fire growth. Such factors include the fire load, distribution of the fire load, ceiling heights, ventilation, geometry of the room or space, the inherent fire resistance of the structure, and whether or not the space is protected by an automatic sprinkler system.

Lamont (2007) reported that performance based design of structure for fire is about treating fire as a load like wind, seismic or gravity loading and not necessarily about keeping the structure at low temperature. According to Bailey (2007), the performance based approach involves the assessment of three basic components include the likely fire behaviour, heat transfer to the structure and the structural response. The overall complexity of the design depends on the assumptions and methods adopted to predict each of the three design components.

There is a growing belief that there is a need to move away from the Building Codes approach to structural fire design - single structural element responses to a standardized small scale fire test. Locke (2007), reports that some of the concerns with the fire test method include the following:

- The cost and time required to conduct tests;
- Reproducibility between testing laboratories;
- The testing of single structural elements does not take account of the beneficial effects of adjacent structural components;
- The size of structural elements is limited by the size of the test furnace;
- The time-temperature curve represents only a fully developed fire;
- The benefits of sprinkler protection are not taken into account in the fire test; and
- The test does not evaluate the durability of fire-protective treatments under anticipated service conditions.

Design methods have been refined from solely based on capacity checks to more detailed guidelines for the assessment of strength, stiffness and rotational capacity. However, current provision focuses on ambient temperature condition with limited guidelines on connection design at elevated temperature. There is a gap and discrepancy on the behaviour and performance of structure at elevated temperature using prescriptive approach. The behaviour of structure at elevated temperature in actual condition is depending on the applied force and overall structure response including the response of connected members and joint.

In this thesis, the influence and behaviour of the joint at elevated temperature on the floor system and frame system will be investigated and presented. More individual components should be tested at elevated temperature to obtain their actual structural and thermal characteristics. It was shown that the inelastic performance of some of these components can play a critical role on the behaviour of the joint under fire conditions. The knowledge of joint at elevated temperature is beneficial in assessing the structural response with respect to progressive collapse and earthquake-fire situations. The behaviour of connections can be defined by knowing three basics parameter which are strength, stiffness and ductility. The behaviour of connections at ambient temperature is different with the behaviour of structure exposed to fire.

1.2 OBJECTIVES OF RESEARCH

1. To investigate steel connection behaviour at elevated temperature based on the recent developed connection model using component based method using ADAPTIC software.
2. To conduct parametric and sensitivity studies on steel connection in composite floor systems under fire loading based on Gurun Fire Test.
3. To investigate steel connection behaviour at elevated temperature in frame structures by using frame tests conducted in Coimbra University, Portugal.
4. To investigate the ductility demand of connection components and rotation capacity of steel joints at elevated temperature.

1.3 SCOPE OF RESEARCH

The scope of this research was to use the developed component based method by (Ramli, Sulung, 2005) to study on semi-rigid connections under elevated temperature. A verification of connection model against ambient and recent elevated temperature test were conducted. The simulation of connections in compartment exposed to fire on school building at Gurun Kedah was carried out using ADAPTIC (Izzudin, 1991). Several factors influenced the connection behaviour under fire will be investigated, focusing on the actual structural and thermal characteristics, ductility and performance of angle cleat connections used in Gurun Fire Test. Furthermore, numerical studies on steel frames with various connection configurations were carried out based on the recent completed experimental work on steel frame under natural fire conducted in Coimbra University, Portugal. Investigations of the ductility demand were carried out based on Cardigton fire test on frame structure for various connection configurations.

1.4 LAYOUT OF THE THESIS

The outlines of this thesis are briefly explained as follow:

Chapter Two presents a literature survey on existing experimental studies on steel joints at elevated temperature. Available methods for the modeling of connections are also reviewed, a list of researches whom using different methods are listed down as well. The literature review listed in this chapter are based on recent studies that related to the influences of connection behaviour on the structural response at elevated temperature were presented.

Chapter Three explains the development of modeling using component based method. ADAPTIC software is used in the implementation of the connection model using component based method which assembling the response of all components, typically represented by nonlinear springs.

Chapter Four validates work on current research available on steel connections at ambient as well as at elevated temperatures. At ambient temperature, the model was created as isolated connection model. As for elevated temperature, the validations work based on isolated connection, isolated beam, sub-frame and overall compartment condition were conducted against the experimental results.

Chapter Five describes several parametric and sensitivity studies undertaken in order to examine the influence of the connection behaviour on the performance of isolated beams, sub-frame and on floor system. Several factors are examined such as loading and boundary conditions, connection type and geometry, temperature effects, load ratio, mechanical properties, as well as temperature gradient. Besides, studies on ductility of steel connections were reviewed and identification of the gap in the current guideline was investigated.

Chapter Six consists of conclusion of the studies discussed in this thesis. Further recommendations and suggestions for future work to improve understanding on the performance of connection under elevated temperature were listed.

CHAPTER 2.0 LITERATURE REVIEW

2.1 INTRODUCTION

It is important to study the behaviour of steel structures under fire, as all structural members exposed to fire heat up and cause the properties of each member to decrease in value with increasing temperature. Observation on tests performed on isolated elements subjected to standard fire regimes does not model a natural fire. The failure of the World Trade Centre on 11th September 2001 and, in particular, of building WTC7 alerted the engineering profession to the possibility of connection failure under fire conditions. Investigations involving full-scale tests under natural fire are limited. The development of the Cardington Laboratory of the Building Research Establishment (BRE) has provided the opportunity to carry out several research projects and highlight the importance of connection performance of the structure as a whole.

Due to temperature increase, the component materials in buildings are susceptible to progressive decrease, and in particular the yield strength and elastic modulus of steel deteriorate relatively quickly. When assessing the realistic performance of building frames subjected to a typical compartment fire, the effects of the restraints of the heated flexural members at their ends and of the cooler portions of the frame outside of the compartment must be included.

Structural fire design codes such as BS5950: Part 8 (steel), Eurocode 3: part 1.2, were developed from standard fire tests in isolated beams and columns and there is general agreement that such tests ignore the significant structural contribution available through the interaction between members. This design methodology stems from the assumption that individual structural elements behave independently in fire, ignoring interactions that may be presented between various parts of the structure. Researches, and observations of structural behaviour under fire conditions, over the past 20 years,

have shown that load redistribution and large deflections of parts of the structure at the Fire Limit State are essential to the survival of the entire structure.

It has been proven that a building tested without fire protection as demonstrated by the Cardington fire test (Bailey, 1999) can reduce the cost of fire safety design where the eight-storey building was built from unprotected composite steel-frames. The fire test conducted on a school building in Gurun, Kedah, also built from locally manufacture steel without fire protection, had the same objective to reduce the cost of insulation by confidently proving that the steel itself has fire protection properties, (Tapsir, 2004). Beside that the benefit of this entire test is to address the limitations of the prescriptive method, at the same time allowing for some economies in construction cost (Wald, 2006).

Full scale fire tests indicate that when structures are at large deflections and high temperatures, the slab panel capacity is dependent on the tensile capacity of the reinforcement, which provide sufficient vertical support at the slab panel boundary (Cedeno, 2009). From existing research on an 8-storey office building for floor system under fire, the results show that primary and secondary beams undergo large structural deformations and develop large axial forces at the beam ends during the heating and cooling phases of the fire. These axial forces are greater than the tension capacities of the beam end shear connections at ambient and elevated temperatures (Bailey, 1999).

In all these cases, composite floors had demonstrated robustness and resistance to fire far greater than indicated by tests on single beams. The Cardington tests demonstrated that, when a significant numbers of beams are not protected, the slab acts as a membrane supported by cold perimeter beams and protected columns. As the unprotected beams lose their loads carrying capacity, the composite slab utilises its full bending capacity in spanning between the adjacent cooler members. With increasing displacement, the slab acts as a tensile member carrying the loads in the reinforcement

which then becomes the critical element of the floor construction. Using the conservative assumption of simply supported edges, the supports will not anchor these tensile forces and a compressive ring will form around the edges of the slab. Failure will only occur at large displacements with the fracture of the reinforcement. Reviews indicate that horizontal tensile forces during cooling of the connected beam under large rotations are associated with flexible end-plate joints (Wald, 2006).

This chapter gathers literature reviews focusing on the connection behaviour under elevated temperatures. The reviews include research studies on the behaviour of beam-to-column connection, beam-to-beam connection, isolated beam under elevated temperatures (boundary condition). Besides that, there was an evaluation of the floor system and frame structure focusing on the performance of connection under elevated temperatures.

A general understanding of structures under elevated temperature especially for steel frame and floor system needed further understanding and further design guidance. A list of researches is classified according to methods of investigation with further discussion on the behaviour of connection for isolated beam, floor system and frame structure for experimental work. Lastly, ductility studies on steel connections at elevated temperature were reviewed in order to discuss the ductility of steel connection models at elevated temperature developed using the component based method in chapter 5.

2.2 GENERAL BEHAVIOUR AND DESIGN OF JOINT

A clear definition of connection and joint is needed in order to determine the difference between these two terms. From EC3 Part 8, “connection” is the whole of the physical components which mechanically fasten the beam to the column and it is concentrated at the location where the fastening action occurs. An example of a connection is end plate, angles and bolts, where the joint is a zone where two or more members are interconnected. For design purposes, it is the assembly of all the basic components required to represent the behaviour during the transfer of the relevant interval forces and moment between the connected members. A beam-to-column joint consists of a web panel and either one connection (single sided joint configuration) or two connections (double sided joint configuration).

For conventional analysis and design of a steel-framed structure, the actual behavior of beam-to-column connections is simplified to the two idealized extremes of either rigid-joint or pinned-joint behavior. For a rigid-joint, the connection has sufficient rigidity to hold virtually unchanged original angles between intersecting members. For a pinned-joint, it is assumed that it can only transfer shear force between members and free to rotate. However most connections used in steel frames are actually exhibit semi-rigid deformation behaviour which can contribute substantially to overall force distribution in the members.

The characteristic of a joint can be easily understood by considering its rotation under applied load. Figure 2.1 shows the change of angle rotation of members under applied moment. The behaviour and classification of a connection can be undertaken by considering the moment-rotation curve shown in Figure 2.2. From the curve, the connection can be classified by strength, rigidity or by ductility. The joint behavioural characteristics can be represented by means of a moment–rotation (M–θ) curve that defines three main properties: moment resistance ($M_{j,Rd}$), rotational stiffness ($S_{j,ini}$ or S_j) and rotation capacity (ϕ_{Cd}).

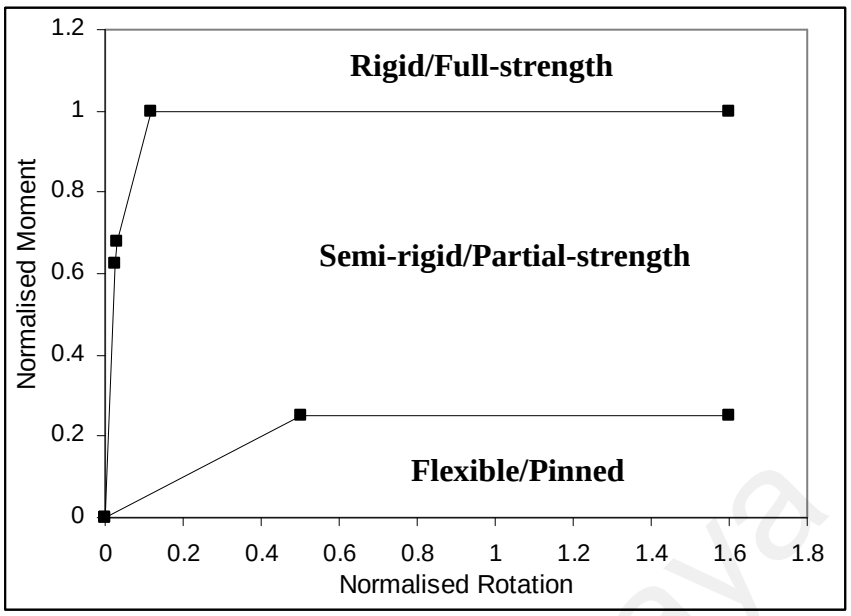

Figure 2.1 Classification of connection by using moment-rotation curve

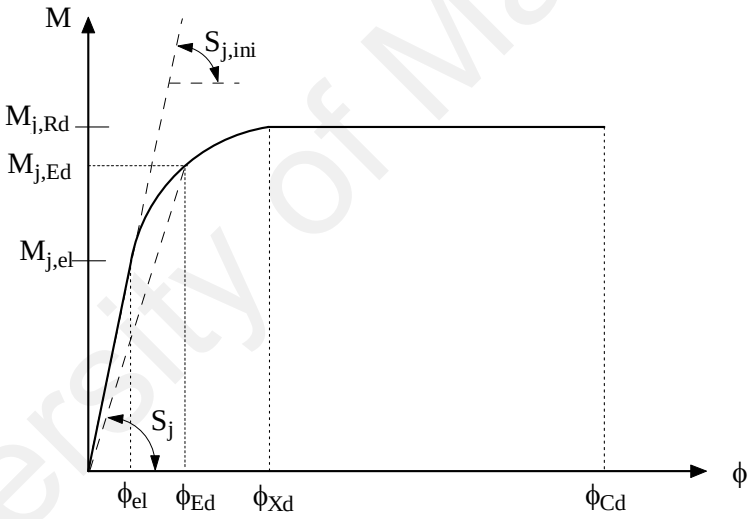

Figure 2.2 Design moment-rotation characteristic in EC3

Semi-rigid connections make the analysis somewhat difficult but lead to economy in member design. The analysis of semi-rigid connections is usually done by assuming linear rotational springs at the supports or by advanced analysis methods, which account for non-linear moment-rotation characteristics.

It should be noted, that in design practice for steel structures, it is important to consider the capability of the structure under elevated temperatures without considering any fire protection in the first place. The steel structure itself has the capability to resist fire for a certain period of time before collapse. The behaviour of connections at

ambient temperature is observed in order to further understand the behaviour of connection at elevated temperature.

2.3 STRUCTURAL RESPONSE AT ELEVATED TEMPERATURE

Beam-to-column connections represent one of the most important components of the structure for which reliable assessment and modelling are needed. However, only a few studies have been undertaken on the response of beam-to-column connections at elevated temperature. As a result, the current design procedures (EC3: Part 1.8) cannot deal with the actual scenarios occurring in the connection under fire loading.

Most of the available studies on the overall connection response focused primarily on moment-rotation characteristics. It should be noted in the fire case, the effect of beam thermal expansion and tensile membrane actions will induce axial forces in the connection. In addition, due to load redistributions that occur during a fire, strain reversals frequently occur.

On several occasions, the joint response governs the structural behaviour because of the failure of connection components in the tensile region due to high induced cooling strains. This has led to a wide recognition of the inadequacy of current design procedures (EC3: Part 1.8).

In assessing the fire response of steel joints, understanding of a global structural behaviour is needed rather than concentrating on the joint area. At elevated temperature, interaction between members will induce large value of axial forces combined with bending moment and shear force in the connection. In addition, the effect of actual fire loading conditions, particularly in the cooling phase requires extensive investigations to examine the effect of load reversal on the connections.

The characteristics of stress–strain at ambient temperature of steel are roughly bi-linear up to 2% strain, with a distinct yield plateau. At high temperature, BS5950:

Part 8 and EC3: Part 1.2 have adopted 0.5%, 1.5% and 2.0% strain limits for different situations at the fire limit state. The deterioration of steel strength for strain limits of 0.5% and 2.0% as considered in both BS5950: Part 8 and EC3: Part 1.2 is shown in Figure 2.3 (a) and Figure 2.3 (b) shows the stiffness reduction factor.

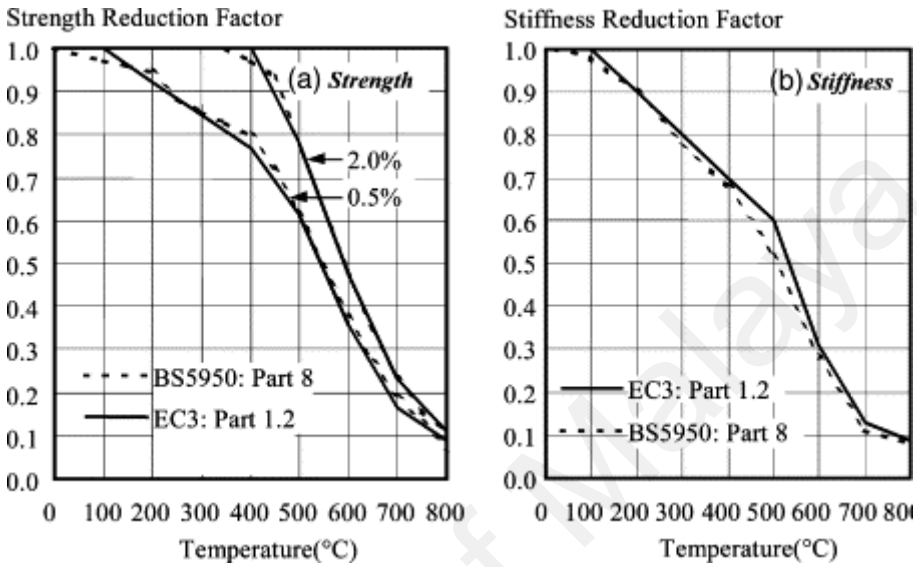

Figure 2.3 Degradation of strength and stiffness for Grade 43 steel with temperature.

In the analysis of structures at elevated temperature, parameters such as the elastic modulus, yield and ultimate stress, which represent the stiffness and strength of the connections needs to account for the degradation with increasing temperature. Table 2.1 presents typical strength and stiffness reduction factors used by Ramli Sulong (2005), as adopted in Al-Jabri et al. (2004), which gives a slightly different value to that in EC3.

Kirby (1991) reported the stress-strain behaviour of old structural mild steel BS 15 steel section by comparing mild steel grade 430A with 43A. Figure 2.4 and 2.5 illustrate that BS 15 steel is weaker than BS4360:Grade 43A. Although steel section under BS 15 is weaker compared to the more recent steel section BS4360, the performance of old steel structure under elevated temperature is reported to be as good as its modern counterpart.

Table 2.1 Strength and stiffness reduction factors for S275 steel at 1% strain level and proportional limit, respectively (Al-Jabri et al., 2004)

Steel Temperature T_s	Reduction factors at steel temperature T_s	
	Strength	Stiffness
	$k_{y,T}=f_{y,T}/f_y$	$k_{E,T}=E_{s,T}/E_s$
20^0 C	1.000	1.000
100^0 C	1.000	1.000
200^0 C	0.971	0.807
300^0 C	0.941	0.613
400^0 C	0.912	0.420
500^0 C	0.721	0.360
600^0 C	0.441	0.180
700^0 C	0.206	0.075
800^0 C	0.110	0.050
900^0 C	0.060	0.0375
1000^0 C	0.040	0.0250
1100^0 C	0.020	0.0125
1200^0 C	0.000	0.000

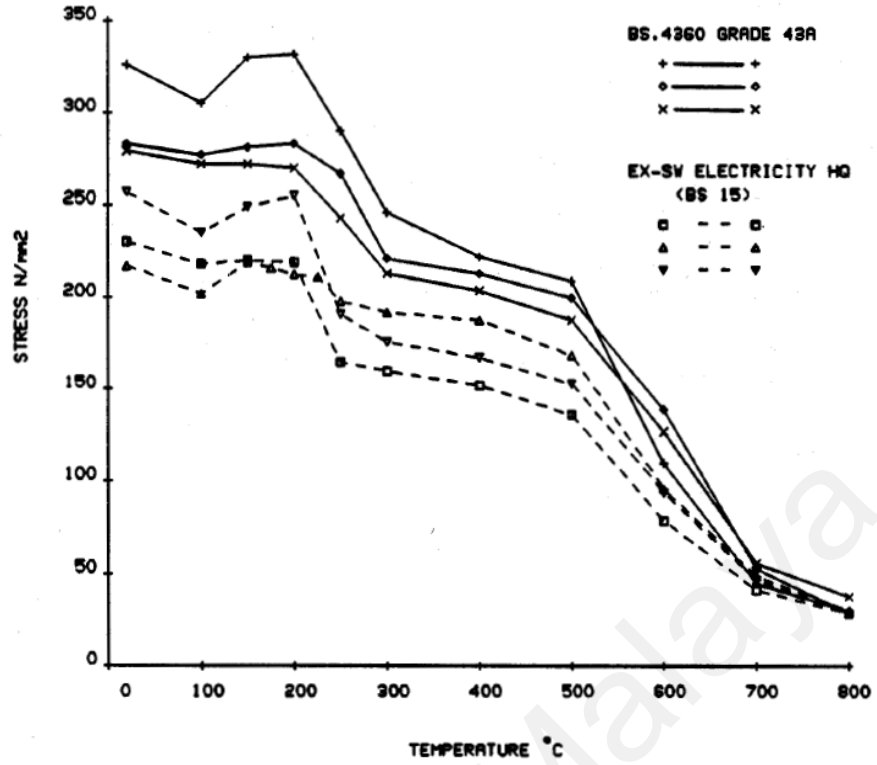

Figure 2.4 Relationship between 0.2% proof stress/LYS (Lower Yield Stress) and temperature, (Kirby, 1991)

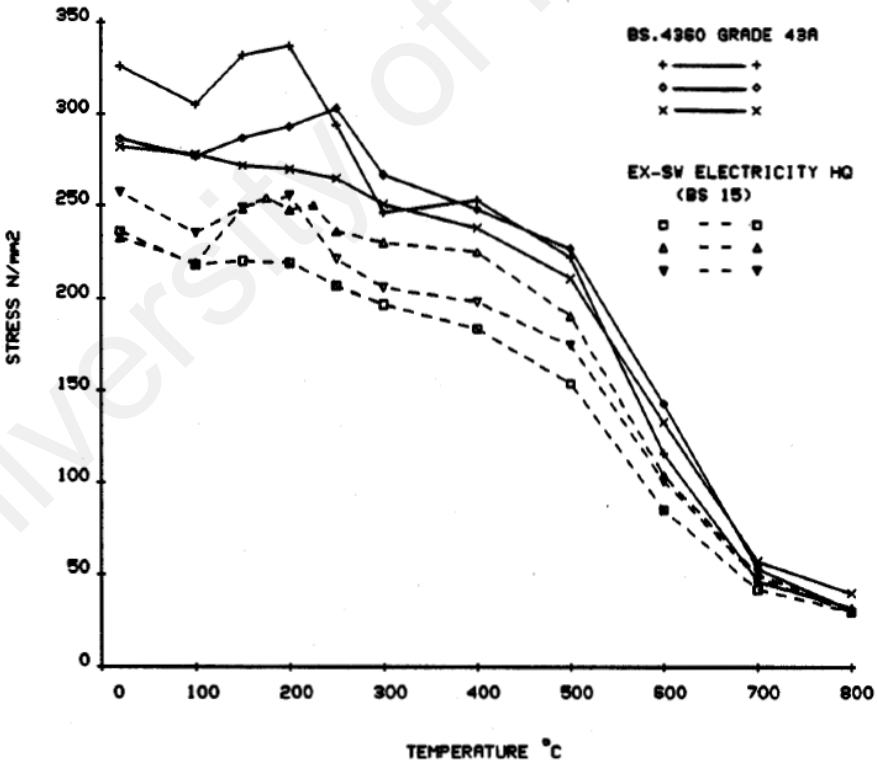

Figure 2.5 Relationship between the ratio $\sigma_{0.2}/p_y$ and Temperature (Kirby, 1991)

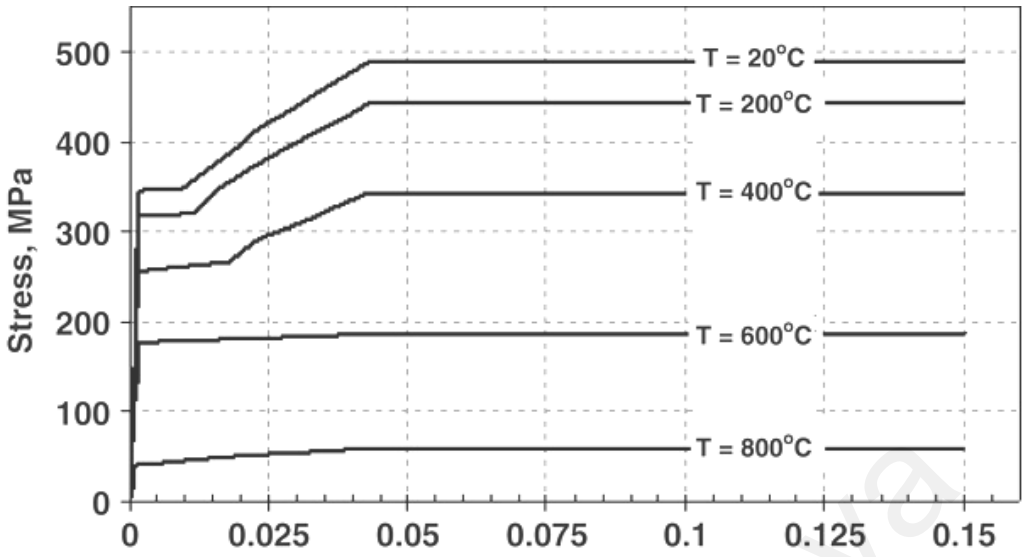

Figure 2.6 Stress-strain-temperature curves for structural steel including strain hardening, (Poh, 2001)

Temperature-stress strain relations for structural steel specified in the codes and standards (EC3: Part 1.2) do not specifically account for high-temperature creep that can be significant under fire exposure, especially prior to the failure of the member. Therefore, in an attempt to understand the effect of high-temperature creep to the response of steel restrained beams, temperature-stress strain relations were recommended by Poh (2001). Poh (2001) developed generalized temperature-stress-strain relations for structural steel based on large set of experimental data (Figure 2.6). These relations account for specific features, such as the yield plateau and the effect of strain hardening. These stress-strain relations have been validated against the specified relationships in codes and standards and they have been shown to give better predictions of fire resistance.

Degradation of bolt properties, mainly strength and stiffness at elevated temperature followed equation 2.1. A series of tests was conducted by Kirby (1995) on Grade 8.8 bolts at elevated temperature. From the finding a tri-linear relationship of bolt strength reduction factor (SRF) was proposed, as follows:

$$SRF = \begin{cases} 1.0 & T_b \le 300^oC \\ 1.0-(T_b-300) \times 0.2128 \times 10^{-2} & 300^oC \le T_b \le 680^oC \\ 0.17-(T_b-680) \times 0.513 \times 10^{-3} & 680^oC \le T_b \le 680^oC \end{cases} \quad (2.1)$$

where T_b is the temperature of the bolt.

Spyrou (2004), reports on how existing empirical models at ambient temperature, contained in design codes and standards need to be modified in order to be used at elevated temperatures.

As reported by Al-Jabri et al. (2004) Figure 2.7 shows are example of moment-rotation curve of flush and flexible end-plate connection at elevated temperatures. This is due to the behaviour of connections under elevated temperatures where the stiffness and strength of the connection become degraded with increasing temperature. The proposed moment rotation curve was only focused on isothermal tests. Further understanding on the behaviour of connections under anisothermal conditions are needed.

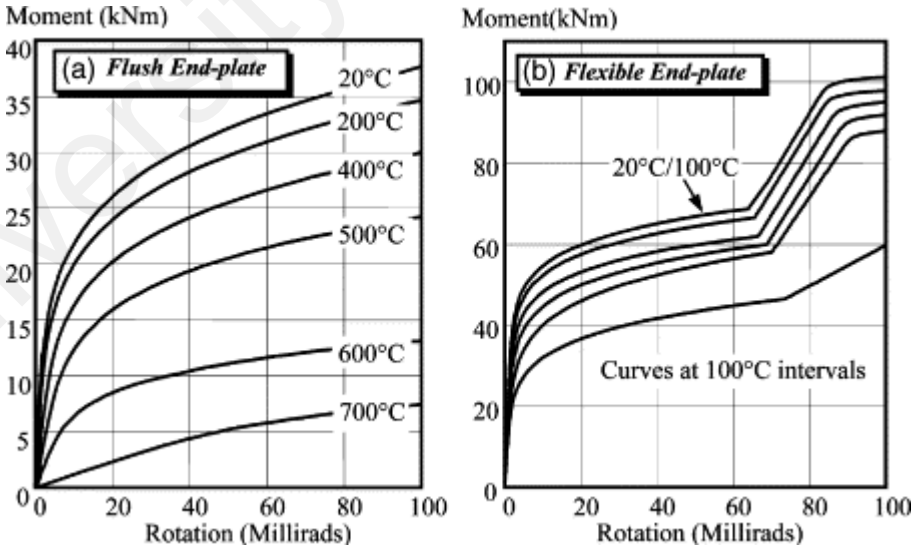

Figure 2.7 Moment–rotation–temperature curves for typical connections

Wang et al. (2007) recommended the following equation for determining the reduction of the elastic modulus and yielding strength of steel, according to Chinese technical code on fire safety of steel building structure, 2006. For steel plate and hot-rolled sections,

$$\begin{aligned} \frac{E_T}{E} &= \frac{7T_S - 4780}{6T_S - 4760} \qquad 20^O C \le T_S \le 600^O C \\ \frac{E_T}{E} &= \frac{1000 - T_S}{6T_S - 2800} \qquad 600^O C \le T_S \le 1000^O C \end{aligned} \tag{2.2}$$

$$\begin{aligned} &\frac{f_{yT}}{f_y} = 1.0 && 20^O C \le T_S \le 300^O C \\ &\frac{f_{yT}}{f_y} = 1.24\times10^{-8} T_S^3 - 2.096\times10^{-5} T_S^2 \\ &+ 9.228\times10^{-3} T_S - 0.2168 && 300^O C < T_S < 800^O C \\ &\frac{f_{yT}}{f_y} = 0.5 - \frac{T_S}{2000} && 800^O C \le T_S \le 1000^O C \end{aligned} \tag{2.3}$$

For steel bolts, the ultimate strength at elevated temperature is determined by

$$\frac{f_{ubT}}{f_{ub}} = -2\times10^{-6} \times T_b^2 + 7\times10^{-5} \times T_b + 1.0473 \qquad 20^O C \le T_b \le 700^O C \tag{2.4}$$

where E is the elastic modulus of steel at ambient temperature; E_T the elastic modulus of steel at a given temperature; T_s the temperature of steel in centigrade; f_y the yield strength of steel at ambient temperature; f_{yT} the yield strength of steel at a given temperature; f_{ub} the ultimate strength of the bolt at ambient temperature; f_{ubT} the ultimate strength of the bolt at a given temperature; and T_b is the temperature of the bolts. The decrease of the yield strength and elastic modulus of structural steel and the ultimate strength of high strength bolts with elevated temperatures are presented in Figure 2.8.

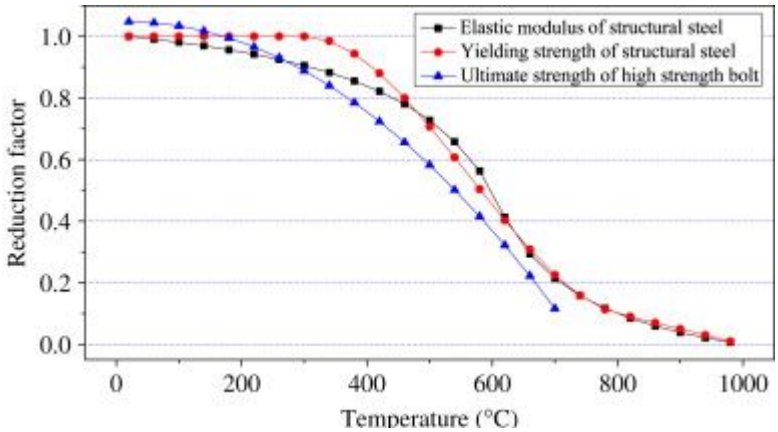

Figure 2.8 Yield strength and elastic modulus of structural steel and high strength bolts at elevated temperatures (Wang et al., 2007)

Some steel connections are cast with a composite slab, which under fire conditions retains most of its strength, which lower down the rate of degradation under fire due to reinforcement temperature is considerably lower than exposed steel.

A parametric study was carried on the Cardington Fire Tests on the structural response when subjected to different heating regimes applied in the concrete slab of composite floor slab system (Sanad, 2000). The mechanism that producing large deflections was caused by thermal bowing. Material's degradation and loading applied on the slab are additional factors that influence the behaviour of structures under fire. Reduction of slab mean temperature will cause the reduction of deflections; however another effect of this is an increasing of thermal gradient. The increasing of thermal gradients in the rib also initially produces increasing values of hogging moments that is caused by the end of rotational restrains.

The performances of composite floor systems subjected to compartment fire are discussed by Elghazouli (2001), which focuses on the influence of restraint to thermal expansion. This research is based on the fire experiments carried on full-scale multi-storey steel-framed building at Cardigton, UK. The studies discussed on the tests which is carried on internal steel beam (Test 1), plane frame test (Test 2) and corner

compartment test (Test 3). The most important observation found from the studies is the influence of the axial restraint that resists thermal expansion.

Eleven parametric studies on the overall corner floor and edge compartment with and without fire protection applied on the beam were reported by, Lamont (2003). Author concludes that the total moment resistance at the end of primary beam is the sum of the moment caused by the imposed load, composite thermal gradient, extra loading from the transverse secondary beams and effect of thermally induced compression. Comparison of beam behaviour when using fire protection or without fire protection was also studied. Results showed that fire protection influenced the temperature gradient in the structures and affected the behaviour of overall structure instability. Connection behaviour also plays an important role in transferring the applied force from connected members, which is not covered in the studies.

Studies carried by Yin (2004) reported that, if a steel beam is reliably provided with some axial restraints, catenary action will occur and will enable the beam to survive in a very high temperatures without collapse. Only minor effect occurs by the temperature distribution, rotational restraint or whether the beam will experience lateral torsional buckling or not. The level of axial restraint is the most important factor, since the beam's restraint comes from the adjacent structure including connections.

Real (2004) used SAFIR program to validate numerical results of a simple model presented in Eurocode 3, Part 1-2 (1995). A geometrical and materially non-linear code was developed to analysis structures by using three-dimensional (3D) beam element with a simply supported boundary at the end of beam. The simple models were based on the lateral-torsional buckling curve that are valid at room temperature lead to a safety level that depends on the slenderness of the beam. The results being unsafe for a certain range of slenderness. Based on previous studies Vila Real et al. (1999, 2001 and 2003) a new proposal for the lateral-torsional buckling resistance, based on numerical

calculations and a new beam design curve under elevated temperature has been proposed.

Abu (2006) investigates the phenomenon of thermal gradient in simply-supported thin slabs by using the Rayleigh-Ritz approach which modeling is referring to observations on Cardington tests. At elevated temperatures, thermal bowing of the slab induces double-curvature bending which generates full-depth cracking across the shorter span of the slab, which may leads to an eventually yield-line type of failure mechanism. The method has shown that different thermal expansion through the depth of a simply-supported slab can induce a considerable amount of tensile membrane action. Overall behaviour of compartment should also take into consideration of the behaviour of connection.

Additionally, Abu (2008) carried a finite element analysis using Bailey-BRE method in investigating the effects of reinforcements and vertical support on slab panel failure. The study also examines the effect of various degrees of protection on the development of the tensile membrane action mechanism. It has been observed that the tensile membrane action mechanism is lost when slab panel edge beams experience significant deflections.

Studies on the connection behaviour at elevated temperature are recently emerged. Apart from assessing the connection response through experimental work, another four methods can be used to investigate the behaviour of connection. These are empirical models, simplified analytical model, finite element analysis or component-based approach. Further review on the methods used to understand and investigate the behaviour of connections under elevated temperature by using experimental work is discussed. Available experimental work on beam-to-column connection under fire, sub-frame test and full-scale fire test are reported. In addition, further reviews on the understanding of connection behaviour using component based method were discussed.

2.4 METHODS IN EXAMINING CONNECTION RESPONSE UNDER FIRE

Currently there are five methods in understanding the behaviour of connection response under fire. The methods include experimental test, empirical models, simplified analytical approaches, finite element models and component-based approaches**.** This thesis will review on current studies of using these methods in examining the connection response.

2.4.1 Experimental Test at Elevated Temperature

2.4.1.1 Isolated Connection Test under Fire

Studies found that the strength and stiffness of structure reduce with an increasing temperature. Beside several parameters that may affect the behaviour of structure under elevated temperature, it should also take into consideration in design process, the slenderness of the members, geometrical properties of the connection, grade of bolt, tying force and mechanical properties of the connection. Observations from real fires show that, on several occasions, steel joints will fail, particularly their tensile components (such as bolts or end-plates). This is due to high cooling strains induced by the distortional deformation of the connected members (Bailey et al., 1999; Buchanan, 2002; Wald et al., 2006). Increasing numbers of studies focus on difference connections configurations under elevated temperature were carried out.

O'Connor and Martin (1998) generates a numerical model of steel framed buildings subjected to fire loading by using the results of four full-scale tests on a modern multi-storey composite steel building. The results indicate that unprotected steelwork behaves significantly better in frames than when acting as isolated members, thereby it indicates a need for robust computational techniques for evaluating the performance of entire structures than single isolated members.

Spyrou et al. (2002) used end plate connection which is equivalent to T-stub connection in the studies. The purpose of the experimental work is to investigate the

behaviour of the tension and compression zones (column web) within a steel beam-to-column joint at elevated temperatures. Parameters that have been investigated were the plate geometries, slenderness of the column web and the thickness of the flanges. From the experimental work, three failure modes of the T-stub in tension at elevated temperature had been identified.

Wang (2007) used EXTEP connection on four full-scale specimens made with H-shaped steel. A comparison of the capacity of joint that applied with rib stiffeners and without rib stiffeners were investigated, besides the differences of end-plate thickness between 12mm and 16mm were applied on the connection. The rib stiffener has significant influence on the critical temperature of the EXTEP joints. When the temperature of the specimen exceeded 400^0C, the vertical deflection at the end of the beam increased rapidly, and flexure deformation occurred in the column flange and the EXTEP for joint which are not stiffened at the column web. The thickness of the end-plate has some influences on the critical temperature of the joints. The thicker the rib stiffener and end-plate, the higher the critical temperature of the joints. From this research a Chinese technical code on fire safety of steel building structure, 2006, on the reduction of elastic modulus and strength of steel expressions are recommended.

Ding (2007) used fin plate, end plate, reverse channel and T-stub connections in his experimental tests. Experimental results of steel beam to concrete filled tubular (CFT) column in fire enable the development of better understanding and rational design methods for robust construction of different type of connection to resist extreme fire attack. From the experimental test conducted the main result shows that the reverse channel joint appeared to have higher stiffness and strength compared to T-stub joint in resisting the catenary action.

Hu (2008) conducted twelve tests that have been separated into three classes of initial loading angle, α of 55^0, 45^0 and 35^0 which represent as the tying forces by using

flexible end plate connections and test under different constant temperature 20^{o}C, 450 ^{o}C, 550 ^{o}C and 650 ^{o}C. Test results clearly shown that the resistance and ductility of steel connection are both decreased at high temperature. In addition, the reduction in rotation capacity of simple connection at high temperature is due to rupture of the end plates occurring before the beam flange contacts with the column flange which occurs at ambient temperature. This is due to the reduced rotation capacity of simple connections at high temperatures cause by rupture of the end plates occurring before the beam flange contacts with the column flange, which occurs at ambient temperatures as evidenced by the kink in the curve at about 6^{o} rotation. From observation, the tying capacities estimated by using the EC3 are likely to overestimate the real resistances of connections.

Yu (2008) investigated four types of connections including flush endplates, flexible endplates, fin plates and web cleats. These tests are carried out to see the behavior of connections under tying force by considering angle of loading, α of 55^{0}, 45^{0} and 35^{0} to generate a combination of shear and tying force. Results showed that the tying capacity decreased rapidly with the increased of temperature, and the connections have little residual resistance at 650^{0}C. Also, from result obtained, the web cleat connections have extremely high rotational capacity compared to other connection carried out. At ambient and elevated temperatures all fin plate connection the failure is govern by bolt shear.

Yu (2009) examined fin plate connections subjected to combinations of shear force and tying force, which loaded to large deformation and fracture. Test results indicate that bolts are vulnerable to shear fracture and that failure is usually controlled by bolt shear rather than by plate bearing. Fin plate connection resistance reduces rapidly with the increases of temperature.

Saedi Daryan and Yahyai (2009) carried out twelve experimental tests to study the effects of web angle, angle thickness, stiffeners and moment value on the bolted top-seat angle connections behaviour. Besides, author investigates the fire resistance capacity of the connection. Failure characteristics and fracture modes of specimens were studied, and results are presented in the form of temperature–rotation curves. From the experimental results obtained using temperature-resistant bolts, by increasing the thickness of angles and decreasing the applied moment on connections, the connection's strength at elevated temperature can be increased. Connections made of structural steel fully deteriorate at temperatures greater than 900 ^{0}C, and the connection stiffness at this temperature reaches zero. In this study the web angle does not significantly increase the capacity of the connection to withstand high temperatures. This may occur because the premature tension failure of bolts in these connections does not allow the capacity of the angles to be fully used, particularly for web angles.

Saedi Daryan and Bahrampoor (2009) carried out four experiment tests on Khorjini connection using ISO834 and ASTM E119 curve with different amount of moment applied. Results were presented as temperature–rotation and moment–rotation curves which then were compared with finite-element models. Besides that, Saedi Daryan and Yahyai (2009) carried 12 full-scale tests by using bolted top-seat angle, (TSA) connections with difference parameters such as thickness of angles, grades of bolts and other geometrical and mechanical properties. The failure modes and deformation patterns of these specimens were studied and the results are shown as rotation-temperature curves.

Yu et al. (2009) studied on tying capacity of web angle connections between beams and columns subjected to different combinations of shear and tying force. Results show that web cleat connections have excellent rotational ductility, and their resistance reduces rapidly with increasing temperature due to failure of the critical

component of joint. Finite element simulations were also carried out to compare with test results.

Yang et al. (2009) carried out four specimens test under steady state and transient fire test based on ISO 834 with and without fire proofing by using welded flange-bolted web type moment connections. Parametric studies were conducted to examine the strength degradation of steel moment connection at elevated temperature. The studies found that the beam-to-column connection is able to retain its design strength up to 650 ^{0}C. However, the stiffness dropped to 25% of the value at ambient temperature. Ductile behaviour was observed on the connections, with necking and tearing at the top flange and local buckling at the bottom flange. It was also proved that the stability and integrity of steel connections can be ensured if proper fire-proofing materials were provided.

2.4.1.2 Sub Frame Test under Elevated Temperature

Traditional approach disregards the behaviour of joint in frame structure by assuming the joint either rigid or pin joint. To achieve a more accurate analysis of a structure, it would be advantageous to include the true behavior of the joints. Summaries of the test conducted on sub-frame in understanding the behaviour of semi-rigid joint in frame structure are reviewed.

Wang (2002) explained on a frame tests conducted in Fire Research Station and Corus such as on a rugby post frame (Cooke and Latham 1987), UK and a series of tests on sub-frames carried by University of Manchester, to examine in detail the role of the connections and axial restraint in affecting the fire resistance of a steel beam when subjected to fire (Liu, 2002). All experimental tests conducted on the Cardington tests which include test from isolated beams, frames and on compartments were also reported.

Santiago (2008) carried out an experimental test and numerical analysis using LUSAS and SAFIR which study on four types of connections with difference parameters which in total six experimental tests was conducted. The connections cover FEP, EXTEP, header plate and welded joint. Results showed a clear influence of the joint used in the test such as header plate, FEP, EXTEP and welded on the overall response of the sub-frame. The results show that the appearance of large tensile forces and the reversal of bending moment during the cooling phase may result in failure of the bolted joints.

Wald (2009) explained a fire test on a steel frame in Ostrava which was carried on 16 May 2006. The test conducted on three storey administrative building which was attached to a single storey framed building of the Ammoniac Separator II in the Mittal Steel Plant in Ostrava, Czech Republic. The beam-to-beam and beam-to-column connections were designed as simple end plate connections using two or six M20 bolts.

Chung (2010) carried two full-scale beam-to-column moment connections specimens that were tested at elevated temperatures according to the standard ISO-834 by using welded connection and were validated with 3D Finite Element Implicit Solver ABAQUS. From the test results shown, the proposed method fire-resistant steel can improve the fire-resistance of beam-to-column moment connections in steel structures which can effectively extend the fire endurance time, reduce structural deformation, and raise the critical temperature to failure for the beam-to column moment connections.

From the experiment test conducted on sub-frame, the important finding is that the connections can enhance the fire resistance of a beam by reducing some of the mid-span moment during the time when temperature is rising, despite the possibility of local flange buckling in the beam. Although the moment transfered by end-plate connections can be much larger than that given by the web-cleat connections, the advantage of the former is also made more noticeable by the catenary action, which does not appear to

the same extent in the cases with web-cleat connections. The catenary action is more pronounced in cases with lower load levels and higher axial restraint. However, it becomes obvious only at large deflection. From the test conducted also shows the conservatism of the Eurocode fire design EC3: Part 1.8. The calculated values show good and conservative predictions of the temperature in the fire compartment, (Liu, 2002).

2.4.1.3 Full Scale Fire Test

Isolated tests subjected to standard fire conditions do not reflect the actual behaviour of a complete building. Even the current design codes for fire resistance of structures are also based on isolated member tests subjected to standard fire conditions. Many aspects of behaviour occur due to the interaction between members cannot be predicted or observed in isolated tests. Therefore, a number of performance based approaches had been carried out to understand the behaviour of connection at elevated temperature such as Cardigton test.

The reason to carry out full-scale test because of the traditional isolated test does not give accurate or actual behaviour. It is also doubtful whether these results will be useful when dealing with the behaviour of frame connection. High cost and limitations of furnace used for experiment test are also one of the factors. Most of the tests concentrated on obtaining the moment-rotation relationships of isolated connections. Many aspects of behaviour occur due to the interaction between members cannot be observed from isolated tests. These include global or local failure of the structure, stresses and deformations due to the restraint of thermal expansion by the adjacent structure and redistribution of internal forces. It is known that even nominally ‘simple’ connections can resist significant moment at large rotation. At the severe deformation of a structure in fire, moments are transferred to the connection and to the adjacent members, and hence they may have a beneficial effect on the survival time of structure.

Tafsir (2004) reported local fire tests to study the behaviour of structural steel and also composite concrete/steel structure in real fire. In addition, it was carried out to prove and show the agreement between theoretical and simulation work to give more understanding on the structural member behaviour under fire condition. Ultimately, this test aims to prove that the steel itself has fire resistance capability; hence it can reduce the cost of structural steel construction by minimizing the use of fire protection.

Wald (2006) explained on experimental programme to investigate the global structural behaviour of a compartment on the 8-storey steel–concrete composite frame building at the Cardington laboratory during a BRE large-scale fire test. From The result supported the concept of unprotected beams and connections with protected columns as a viable system for composite floors. There are seven large-scale fire tests include test on isolated beam, frame structure and compartment.

Abecassis-Empis (2007) carried out two tests called The Dalmarnock tests in July 2006. Test one allowed the fire to develop freely to post-flashover conditions while test two incorporated sensor informed ventilation management. Fire tests were carried on a real high-rise building with furnished with regular living room/office. The main aim of the experiments was to collect a comprehensive set of data from a realistic fire scenario that had a resolution compatible with the output of field models.

Chlouba (2008) carried out a fire test in June 2006 on a structure of Ammoniac Separator II in company Mittal Steel Ostrava. The test was conducted on three storey steel structure with composite slab. The main objective is to understand more about connection temperatures and internal forces in the structure beside to study on behaviour of restrained, the heating of external steelwork and the effect of natural fire on sandwich panel, light timber based panels and timber concrete element.

Zhao (2008) carried out experimental of floor system under ISO fire condition. The objective of the test is to provide the evidence that steel and concrete composite floor with some of its steel beams that are not protected may ensure, with an adequate reinforcing steel mesh in concrete slab, a good fire performance can be shown even it is exposed to long ISO fire. From the result obtained, it can be concluded that the whole floor remains structurally robust under long duration of fire even with important failure of reinforcing steel mesh in concrete slab. Besides, the maximum deflection reaches less than twentieth of their span. The main result from the test found out that unprotected steel structure heated up to maximum value of 1040^0C and protected steel beam heated up to around 300^0C, this show that the contribution of fire protection in reducing the temperature of structure directly expose to fire.

2.4.2 Component-Based Method

Component-based approach is one of the suitable and simple methods to model connection behaviour compared to other analytical method such as empirical models, simplified analytical approaches and finite element model. This method is referred to as mechanical model by concentrating sources of deformability into single flexural springs arranged to an infinite small point at the intersection point of the axes of the connected members. The joint responses are simulated by combined springs representing bending and shear together based on its geometrical and mechanical properties. A review of component based approach has shown that a number of nonlinear FE program such as FEAST, SAFIR, VULCAN, ABAQUS, DIANA and ADAPTIC have been used in determining the connection response based on component method.

Spyrou (2002, 2004) is one of the researchers that carry out experimental test to see the important parameters behaviour of equivalent T-stub in tension and column web in compression within a steel beam-to-column joint at elevated temperatures. These studies are important in developing and understanding the active component in the

connection. The studies aiming at predicting the ultimate resistance of column webs subjected to concentrated forces. The studies reported on how existing empirical models at ambient temperature, contained in design codes and standards, may be modified for application at elevated temperatures. The study highlighted the discrepancies that exist between capacities calculated using current design standards and test results for column web capacities at ambient temperature.

Yin (2004) used a different elastic axial and rotational restraint of support to represent a semi-rigid connection. Parameters investigated include beam span, uniform and non-uniform temperature distributions, different levels of applied loads, and different levels of axial and rotational spring stiffness at the beam ends and lastly the effect of lateral torsional buckling. From the research carried out it is concluded that the large deflection behaviour of steel beams can significantly affect their survival temperature in fire. Indeed, if a realistic amount of axial restraint stiffness is available at the beam ends and fire engineering design is not concerned with the amount of large deflection in a beam, it is possible that the beam can have virtually unlimited survival temperature.

Beg (2004) studied on end-plate welded connection to determine the rotation capacity of moment connection. The parametric studied of column web in compression were performed by a set of different web slenderness with a range of axial forces. The result showed the deformation capacity is decreased with increasing of web slenderness.

Al-Jabri (2005) developed spring-stiffness model and calibrated with experimental test by Lawson (1990) at ambient as well as at elevated temperature by using FEP) and EXTEP connections. From the observation, the rib stiffener has significant influence on the critical temperature of the EXTEP joints. The thickness of the end-plate has also some influence on the critical temperature of the joints where the thicker the rib stiffener and end-plate, the higher the critical temperature of the joints.

The main references of this thesis are referred to research conducted by Ramli Sulong (2005) which developed a new model of connection using component-based approach. Validation works are carried on five connections types under monotonic and cyclic loading at ambient and elevated temperatures condition. The nonlinear finite element program, developed by Izzudin (1991) is used in implementing the connection model. The computer code for new connection is written using FORTRAN, after testing for independent mode, it is then implemented using advanced nonlinear analysis program ADAPTIC.

Five connection types were used in the studied by Ramli Sulong (2005) including double web angle, (DWA), flush end plate, (FEP), extended end plate (EXTEP), top and seat angle, (TSA) and combination of double web, top and seat angle, (TSWA). Calibration of development model with existing experimental test by Leston-Jones (1997) and Al-Jabri (1999) were done. A component-based model is utilised to assess the behaviour of isolated members and structural assemblages under fire conditions. An appropriate representation of the joint is shown to be important for the purpose of assessing the load and deformation levels imposed on the connection itself.

Wang (2007) used EXTEP joints to investigate the influence of rib stiffeners and depth of end-plates on fire-resistant capacity of the joints, by comparing the capacity of the joints with and without rib stiffeners and different depths of end-plate. Beside experimental work, the author also carried a spring-component model for predicting the behaviour of EXTEP at elevated temperature. The response of the joints subjected to elevated temperature can be predicted by assembling components, the stiffness and strength of which are assumed to degrade with increasing temperatures based on the recommendations presented in the Chinese Technical Code on Fire Safety of Steel Building Structure.

Florian Block (2007) summaries the derivation of the stiffness matrix of new element, based on a spring model, and the incorporation of the element into the non-linear finite element program, Vulcan by focusing on endplate connections.

Yu et al. (2009) developed a model of web angle connection and validated at ambient and elevated temperature. Web angle connections were subjected to various combinations of shear, tying and moment actions at elevated temperatures. Failure criteria determined from the tests have been introduced into the models for components such as web cleats and bolts in double shear. These tests showed that web cleat connections have very good tying resistance and rotational capacity, mainly due to large deformation of the web cleat.

Besides that, Yu et al. (2009) also carried out a study on the development of a T-stub model to capture the behaviour of endplate connections at large deformations. Connection designs at ambient temperature generally consider only the initial stiffness and the plastic resistance, whereas ductility and failure modes are more important for connections in fire, as large deformations are generally experienced. The model is based on the virtual work principle, which allows it to be easily applied to endplate connections, and considers material hardening after yielding for both the T-stub flange and the bolts. Compatibility between these two components is also maintained. Validation against T-stub tests at both ambient and elevated temperatures shows that the proposed model can predict the behaviour of T- stubs of various characteristics.

2.4.3 Analytical Model

This method begins with observation of test behaviour to identify the deformation sources and the collapsed mechanism of the connections. Then, simplified connection models were developed for predicting the initial connection stiffness by mean of elastic analysis. The prediction of ultimate moment capacity from plastic mechanism model can be observed from balance of internal and external works. Results from assumed model are verified with controled experimental work. Mathematical equation represents M-φ curve can be developed by using the predicted initial stiffness and ultimate moment capacity from the model.

Lien (2009) investigated the non-linear behaviour of structure under heating and cooling phases of a fire by using Vector Form Intrinsic Finite Element (VFIFE) method. Several numerical examples were fully studied to investigate the cooling behaviour of steel structures, and the proposed numerical model can effectively predict the nonlinear behaviour of such structures during both heating and cooling phases.

Heidarpour and Bradford (2010) formulated a flexibility method for undertaking the analysis of large steel frames subjected to fire loading. Methods of analysis for these framed structures are either plastic-zone or plastic-hinge based. The proposed method was used to model three frames; one small frame with rigid joints, one small frame with flexible joints and one large rigid-jointed frame with 104 members, and the results were compared with those of ABAQUS.

2.4.4 Finite Element Analysis

The great advantage of computer based modeling is evident; modifications to material data, altering dimensions and adding new load scenario to the prototype is radically possible at any stage of the simulation. The flexibility of computer based modelling gives the ability to evaluate the designed response at any point of the design,

while a real prototype needs sensors to measure quantities such as strain, temperature, flow speed or other physical quantities, simulation models provide these quantities without the effort of sacrificing time and cost on the model.

The connection behaviour at elevated temperature is weaker compared to assumed design at ambient temperature. A group of researchers from University of Sheffield simulate behaviour of isolated steel elements in furnace tests and after that extended to study the full-scale composite frame at Cardington during the 1990s. Several software approaches have been used to study the behaviour of beams and columns in isolation towards the performance of building structures as a whole. One of the Finite element softwares, Vulcan was developed in year 1998 by that research group and has been used widely in simulation.

Beside it, FERGAN is a group of researchers led by a team of academics at Centre for Advance Construction Studies, School of Civil and Environmental Engineering, Nanyang Technological University (NTU), Singapore. The research work is on the development of an efficient analytical tool to study structural behaviour in fire, FEM program (FEMFAN) has been developed for the analysis of steel frames in fire.

Yin and Wang (2004) carried out parametric studies on restrained steel beams accounting for different level of axial and rotational spring stiffness at beam end using finite element program ABAQUS. The parameters investigated include beam span, uniform and non-uniform temperature distributions, different levels of applied load, different levels of axial and rotational spring stiffness at the beam ends and the effect of lateral torsional buckling. The level of axial restraint is the most important factor as it affects the beam deflection and the catenary force under catenary action. The higher the axial restraint, the smaller the beam deflection, which is favourable for integrity of the fire compartment in which the restrained beam is located.

Lamont (2007) used ABAQUS finite element software analyse and study the behaviour of structure by applying fire protection to only external beams and when no beam are fire protected. Temperature in concrete and protected beam was calculated using adaptive finite element heat transfer research code (HADAPT). It is found that when the edge beams are protected, the floor slab tends to span in 2 directions because the edge beams provide sufficient support around the perimeter of the floor for tensile membrane action to develop. In the other hand when the edge beams are unprotected the slab tends to span in only one direction in a manner similar to a beam in catenary action.. In this study its shows that by applying fire protection to the edge beams where fix support were applied to joint the beam and slab appears to be a robust solution and allows 2-D membrane action to be supported and for greater lateral support to columns in the later stages of fires.

Al-Jabri et al. (2006) used ABAQUS software to validate experimental test on flush end-plate bolted connections. The connection components were modelled using three-dimensional brick elements, while the contact between the components was modelled using contact elements based on the Coulomb friction law. The model developed showed good agreement with experimental test and capable of predicting connection response at elevated temperatures to an acceptable degree of accuracy. The finite element model was used to establish the moment–rotation characteristics of the connections under the combined loading of a concentrated force and elevated temperature.

Besides that, Sarraj et al. (2007) also used ABAQUS in carry out a studied on Fin plate shear connections. A comparison on available experimental data at ambient and elevated temperatures and other analytical results shows that the model has a high level of accuracy. When the connection model was extended to include an attached beam, it was found that it eventually experiences large tensile force when exposed to fire.

Kodur and Dwaikat (2009) simulated a partial resistance to horizontal elongation of beam due to thermal exposure; an axial spring was used to exert lateral resistance. By using finite element software ANSYS, parametric studies indicate that fire scenario, load level, degree of end-restraint and high-temperature creep have significant influences on the behavior of beams under fire conditions. Creep, at room temperature, influences the behavior of steel structures, however, at elevated temperatures; creep becomes a dominant factor and significantly affects the response of steel structures. Higher load ratios induce higher mechanical stresses in the steel; therefore, high-temperature creep produces higher strains, leading to increased deflection in the beam.

Mao (2009) used ANSYS software to verify the full-scale fire tests implemented in the building fire laboratory center of the Architecture and Building Research Institute (ABRI) in Taiwan, in studying the effects on the stiffness of steel moment connections in addition to material properties and connection geometry. The numerical results show that the applied moments have significant effects on the stiffness of steel moment connections. However, the axial load of column, and shear and axial force of beam have less effect. The stiffness of steel beam-column connection is not affected by the transverse load pattern of beam. For constant temperature case (including ambient temperature case) with increasing transverse load on beam, the connection stiffness is constant when the connection is elastic, and it decreases with respect to the increase of transverse load of beam when the plastic strain occurs. For the cases of constant load with increasing temperature, the stiffness of steel moment connections increases in the first stage before approximately 300 ^{O}C, then a downturn occurs from the peak.

Dai et al. (2010) studied on five different types of semi-rigid joints: fin plate, flexible endplate, FEP, DWA and EXTEP. Validation of the numerical models (ABAQUS) is assessed through comparison of the simulation results with ten fire tests on restrained steel structural assemblies carried out by the University of Manchester.

Finite Element Model is one of alternative methods which could verify the behavior of connections and also used to predict the response of connections which unable to be performed experimentally. Besides that, the validation model may be used to conduct numerical parametric studies investigate wider parameters affecting the connection behaviour. This alternative method can reduce the cost of sample preparation, which varies in geometry and mechanical properties.

2.5 A STUDY ON JOINT DUCTILITY

The influence of connection flexibility on the elastic frame stability can be explained from example in Figure 2.9. The end rotation, ϕ of a simply supported beam under a uniform vertical load plus external negative applied moments M is given by:

$$\phi = \frac{q_b^3}{24EI_b} - \frac{Ml_b}{2EI_b} \tag{2.5}$$

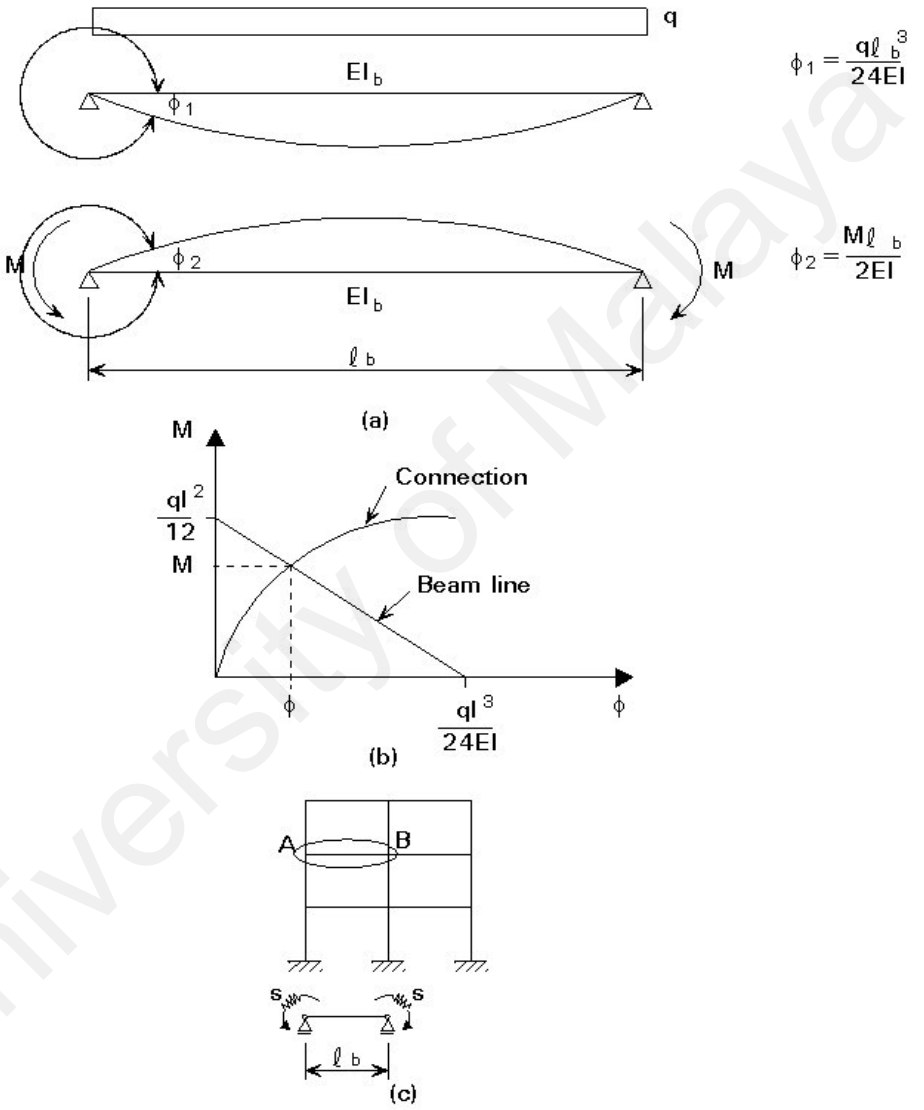

Figure 2.9 Beam-line and connection behaviour

The M-ϕ response represented by equation 2.5 is a straight line which is called as the beam line as show in Figure 2.9 (b). In real frames, the end moment restraint is provided by the rigidity of the connection S = M/ϕ as shown in Figure 2.9 (c) and therefore the actual end moment and the end rotation of the beam is given by the intersection of the beam line with the connection characteristic as shown in Figure 2.9

(b). The connection behaviour is characterized by its moment resistance M_{Rd}, its rotational capacity ϕ_{cd} and its rigidity $s = M/\phi$.

Evaluation of the behaviour of connections relies on the independent evaluation of strength, stiffness and ductility. Based on the current design BS EN 1993-1-8:2005, the way to determine the deformation capacity of joint are limited and no specific procedure to calculate rotational capacity. Most researchers' study on the behaviour of semi-rigid joints was focused on determining resistance and stiffness characteristic. This problem has been recognized by researchers in this area such as Silva et al. (2000) Girao Coelho et al. (2004) and Beg (2004).

Characterization of the joint ductility can be defined as the amount of plastic rotation that can be sustained while maintaining a certain percentage of its ultimate strength (Swanson, 1999). Ductility also is a measure of the ability of a material, section, structural element or structural system to sustain deformations prior to collapse without substantial loss of resistance. The evaluation of joint ductility is to ensure that sufficient rotation or deformation capacity is available to allow the chosen analysis type (elastic or plastic).

2.5.1 Design Requirement of Rotation Capacity at Ambient Temperature

The behaviour of moment-rotation characteristic of a joint can be represented as a non-linear curve as indicated in Figure 2.10 (EC3: Part 1.8). The joint rotation can be divided into three segments: elastic rotation ($\phi \le \phi_{el}$), transition rotation ($\phi_{el} < \phi \le \phi_{Xd}$) and plastic rotation ($\phi_{Xd} < \phi \le \phi_{Cd}$). The design rotation capacity ϕ_{Cd} of a joint is referring to maximum rotation of the design moment-rotation characteristic at the design moment resistance, $M_{j,Rd}$ of the connection.

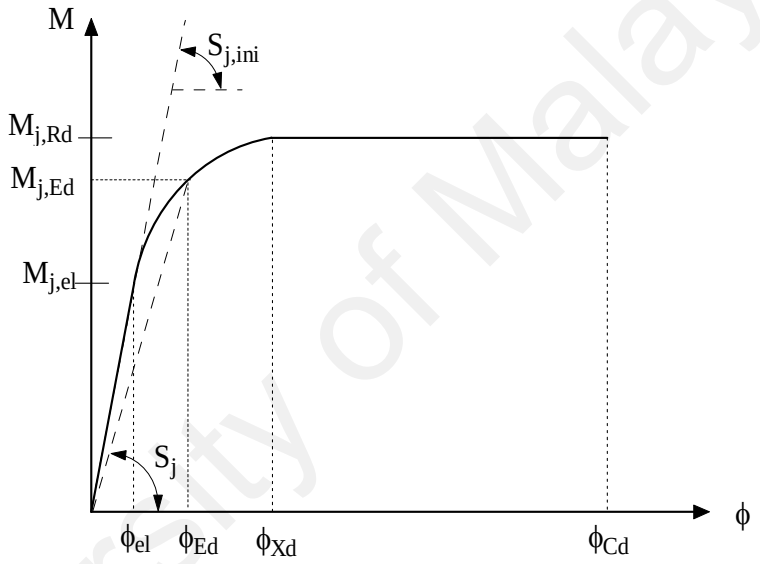

Figure 2.10 Design moment-rotation characteristic

The clause stated that for bolted joints in which the design moment resistance of the joint $M_{j,Rd}$ is governed by design resistance of the column web panel in shear, is assumed to have adequate rotation capacity of the connection for plastic global analysis provided that the column web slenderness satisfies:

$$d/t_w \le 69\varepsilon \tag{2.6}$$

where d is the web depth, t_w is the column web thickness. On the other hand, for joint either a bolted end-plate or angle flange cleat connection may be assumed to have sufficient rotation capacity for plastic analysis, which satisfied both of the following condition:

(i) The moment resistance of the joint is governed by the design resistance of either the column flange in bending or the end plate or tension flange cleat in bending and

(ii) The thickness *t* of either the column flange or the end plate or tension flange cleat should satisfy:

$$t \leq 0.36d\sqrt{\frac{f_{ub}}{f_y}} \tag{2.7}$$

where d is the bolt diameter, f_{ub} is the tensile strength of the bolt and f_y is the yield stress of the relevant basic component.

As for welded joints, the rotation capacity ϕ_{Cd} for a stiffened column web in compression but unstiffened in tension, is limited to:

$$\phi_{Cd} = 0.025h_c/h_b \tag{2.8}$$

where h_b and h_c are the depth of the beam and column. Its design moment resistance is not governed by the design shear resistance of the column web panel. For unstiffened welded joints the rotation capacity ϕ_{Cd} may be assumed to have minimum of 0.015 radians.

Alternatively from the above two cases, the rotation capacity of joints need not to be checked, provided that the design moment resistance of the joint, $M_{j.Rd}$ is at least 1.2 times the design plastic moment resistance $M_{pl.Rd}$ of the cross section of the connected member.

2.5.2 Ductility Studies at Ambient Temperature

There are a few studies of ductility of steel connection. Previous studies carried by Girao Coelho et al. (2004) identify the relationship of ductility by using characterization quantify by means of an index $\psi_{j,}$ that relates the rotation capacity of the joint, Φ_{Cd} to the rotation value corresponding to the joint plastic resistance, $\Phi_{Xd,}$

$$\psi_j = \Phi_{Cd}/\Phi_{Xd} \tag{2.9}$$

Kuhlmann et al. (1998) conducted an analytical method to calculate strength and stiffness to represent force-deformation curve. Further ductility evaluation determined as the deformation capacity of each component. Classes of ductility concluded by Kuhlmann et al. (1998) propose classification of ductility which is divided into three classes. By using bi-linear approximations of the force–deformation behaviour of each component, Silva et al. (2002) simplified the classification of components ductility as:

(i) Components with high ductility,

A simplified bi-linear force–deformation curves (Figure 2.11) that changes from an initial linear elastic mode into a second carrying mode which allows increasing deformation with increasing force. The deformation capacity of the component is nearly unlimited, not imposing any bounds on the overall rotation ability of the joint. K^e, K^{pl}, F^y and Δ^y are initial elastic stiffness, the post-limit stiffness, the strength and the yield displacement of the component respectively. It is noted that the component failure displacement, Δ^f, the limit displacement of the component is very high, so Δ^f / Δ^y may be taken as infinity. Some components falling into this classification are column web panel in shear, end-plate in bending, column flange in bending and beam web in tension

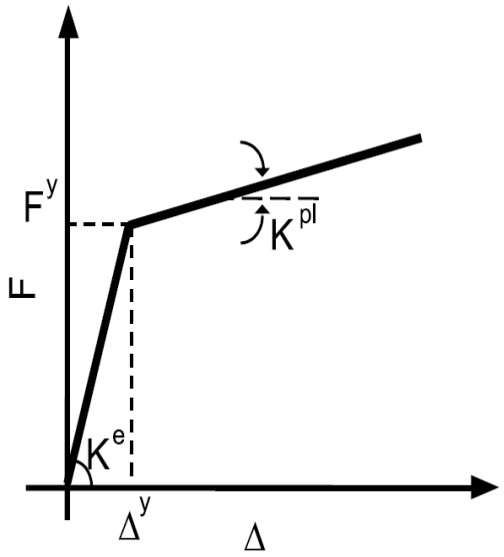

Figure 2.11 Bi-linear approximations for components with high ductility

(ii) Components with limited ductility

These components are characterised by a force–deformation curve exhibiting a limit point and a subsequent softening response (Figure 2.12). In this ductility class, it is required to define the collapsed displacement of the component, Δ^f. Components that fall into this category are column web in compression, column web in tension and beam flange and beam web in compression.

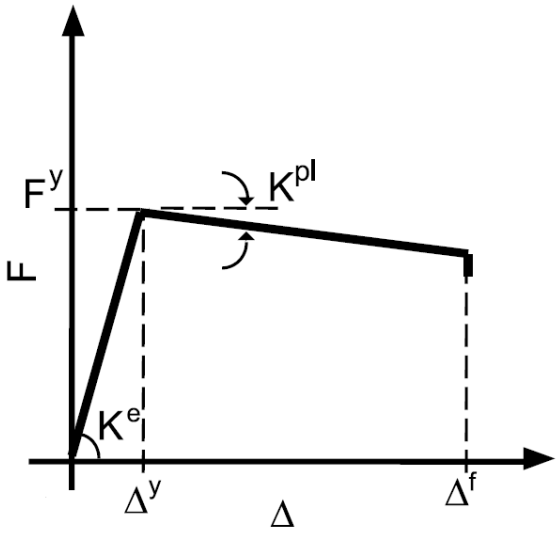

Figure 2.12 Bi-linear approximations for components with limited ductility

(iii) Components with brittle failure

Components classified in this category are components that behave linearly until it collapses, with very little deformation before failure (Figure 2.13). The force–deformation curve is represented as a linear approximation, from the curve shown that $\Delta^y = \Delta^f$. Components classified in this category are bolts in tension and welds.

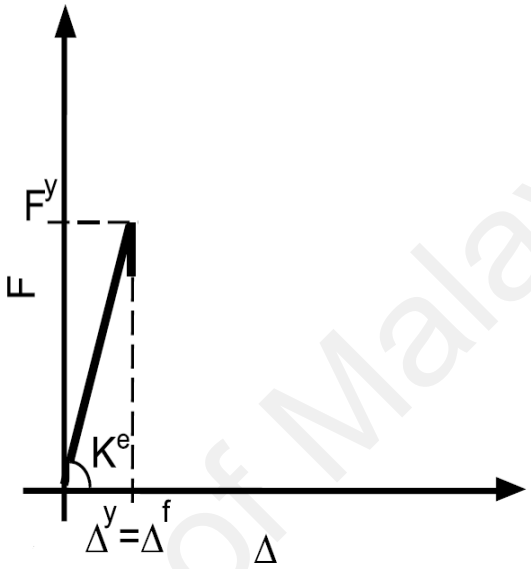

Figure 2.13 linear approximations for components with brittle failure

Ductility index φ_i for each component i, defined as,

$$\varphi_i = \Delta^f_i / \Delta^y_i \qquad (2.10)$$

Three ductility classes proposed by Kuhlmann et al. (1998)

Class 1—components with high ductility ($\varphi_i \geq \alpha$)

Class 2—components with limited ductility ($\beta \leq \varphi_i < \alpha$)

Class 3—components with brittle failure ($\varphi_i < \beta$)

Where α and β representing ductility limits for component classes. Kuhlmann et al. (1998), suggested that α = 20 and β = 3. Further study by Silva et al. (2002) considered in design, and in-line with the usual assumptions in plastic design, it seems reasonable to assume, for Class 1 components, a ductility index $\varphi_i = \infty$. On the other end, for Class 3 components, because of brittle behaviour, a safe estimate can be obtained with a ductility index of $\varphi_i = 1$ (elastic response) and for class 2 components, a

range of 4–5 seems reasonable to used. Silva et al. (2002) also proposes the ductility index can also be defined as:

$$\varphi_i = \theta_f / \theta_1 \quad (2.11)$$

Where θ_f is the rotation at failure and θ_1 is the rotation when the first component reaches its elastic limit.

The studies carried by Kuhlmann et al. (1998) and Silva et al. (2002) fill the gap and uncertainty in code which classified the ductility according to classes, compared to code that give general satisfaction of ductility requirement. Further studies on component for cleat angle also need further investigation.

A simple analytical expression for the deformation capacity of the components is derived by referring to end plate connection to upgrade the existing procedure of EN 1993-1-8 (Beg, 2004). The important components that may significantly contribute to the rotation capacity of the whole joint are: column web in compression, column web in tension, column web in shear, column flange in bending and end-plate in bending. Components related to the column web are relevant without stiffeners in the column that resist compression, tension or shear forces.

Simplified force–displacement relationships for each component following the idea of EN 1993-1-8 are defined, but there is no indication in the code how to calculate it. The procedure in determination of deformation capacity, δ_u, of individual components was proposed by Beg (2004) as follow:

1) FE analysis was calibrated for each component against the available test results.

2) A parametric study of the deformation behaviour of each component was performed by means of FE analysis. The main parameters were the level of the column axial force and the column web slenderness.

3) Based on these parametric studies, analytical expressions for δ_u were established.

For safe-sided results, displacements corresponding to the maximum resistance were taken as the deformation capacity. The deformation capacity was limited to the values reached at the relevant principal strain of 10% (column web) or 20% (T-stub) in the cases where force–displacement diagrams exhibited along plastic plateau.

Based on the test results of Kuhlmann and Kuhnemund (2000) the equivalent ultimate transverse strain for column web in compression can be determined as follows:

$$\varepsilon_u = \frac{\delta_u}{d} \tag{2.12}$$

where d is the depth of the web, ε_u can be regarded as a non-dimensional deformation capacity. The same equation 2.12 can be used for column web in tension, where deformation capacity, δ_u, with ε_u is a transverse strain corresponding to the ultimate resistance of the web and d is the depth of the web as in column web in compression.

For the web in shear, the tests of Dubina et al. (2000) were used to determine the ductility. The deformation capacity is not affected much where the relationship is linear. In determining the deformation capacity, three failure modes were proposed (Beg et al., 2004). For Mode 1 (complete yielding of the flange), ultimate displacements, δ_u, can be calculated from:

$$\delta_u = \phi\, m \tag{2.13}$$

where m distance between the two hinges in each column leg.

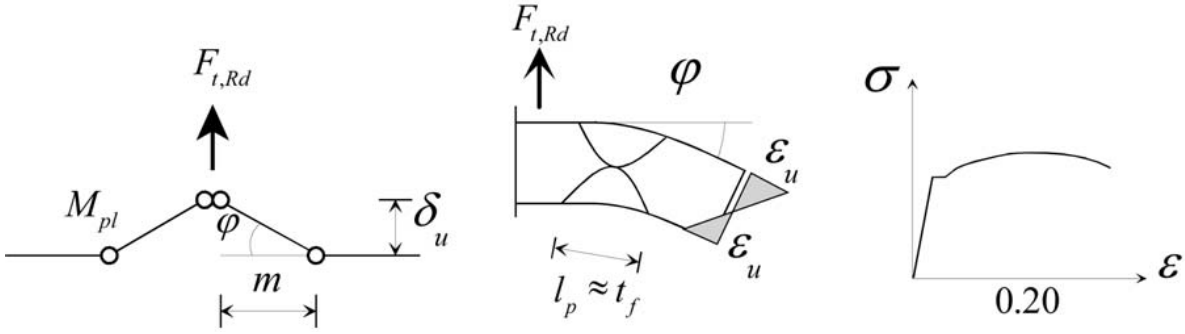

Figure 2.14 Deformation capacity δ_u- Mode 1, (Beg et al., 2004)

The rotation of the plastic hinge, φ, can be determined under the assumption that the maximum strain at the outer surface of the flange in bending, ε_u, cannot be larger than 0.20, in order to prevent tearing of the material, and that the length of the plastic hinge l_p can be approximately set equal to the thickness of the flange t_f. Accordingly, by referring to Figure 2.14, the rotation, φ is equal to:

$$\varphi = \frac{\varepsilon_u l_p}{t_f / 2} = \frac{\varepsilon_u t_f}{t_{f/2}} 2\varepsilon_u \tag{2.14}$$

Deformation capacity δ_u is then:

$$\delta_u = 2\ \varepsilon_u\ m = 0.4\ m \tag{2.15}$$

For mode 2 (bolt failure with yielding of the flange) plastic mechanism according to EN 1993-1-8 is shown in Figure 2.15 (a). Due to the local bending of flanges around bolts, the real deformation pattern is similar to the model in Figure 2.15 (b). The deformation capacity δ_u for model in figure 2.15 (b) is written as:

$$\delta_u = \phi_1 n + \phi_2 m \tag{2.16}$$

ϕ_1 is obtained from the plastic deformation of bolts

$$\phi_1 = \frac{\varepsilon_{ub} l_b}{n} \tag{2.17}$$

where ε_{ub} is the maximum strain allowed in bolts, to prevent rupture of bolts in tension, which is set equal to 0.1. l_b is the clamping length of bolts, including the thickness of washers. ϕ_2 can be expressed in terms of ϕ_1 as

$$\phi_2 = k\ \phi_1 \tag{2.18}$$

where k is an empirical factor with values between 1.0 and 5.0. Hence, 1.0 is a very conservative value and 3.0–4.0 is the value that is normally reached, the final expression for δ_u is then

$$\delta_u = 0.1 l_b \left(1 + k\frac{m}{n}\right) \tag{2.19}$$

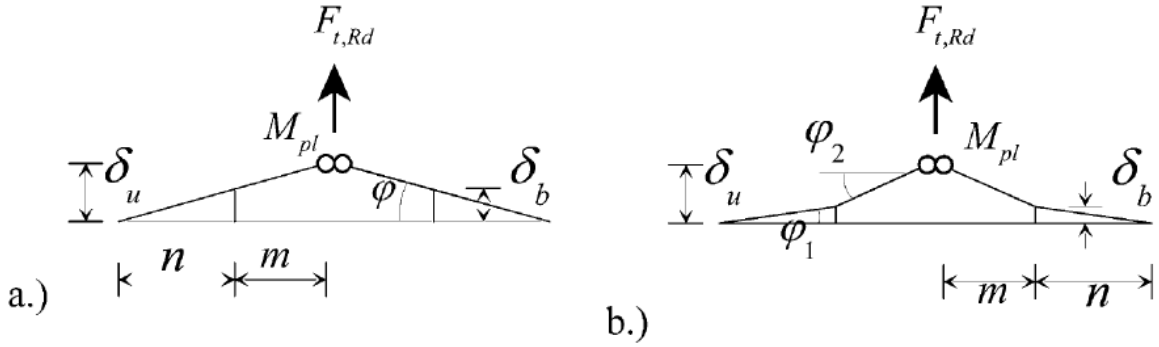

Figure 2.15 Deformation capacity δ_u- Mode 2, (Beg et al., 2004)

Mode 3 (bolt failure), the deformation capacity for this mode is simply the elongation of the bolts at failure:

$$\delta_u = \varepsilon_{ub}\, l_b = 0.1\, l_b \tag{2.20}$$

Determination of the rotation capacity of the entire joint can be shown in Figure 2.16 which δ_1 is deformation of component for column flange in bending column, δ_2 is deformation of component for web in tension, δ_3 is deformation of component for column web in compression, and γ_4 is deformation of component for column web in shear, so overall rotation for joint is illustrated in equation 2.21.

$$\phi_u = \frac{\delta_1 + \delta_2 + \delta_3}{h} + \gamma_4 \tag{2.21}$$

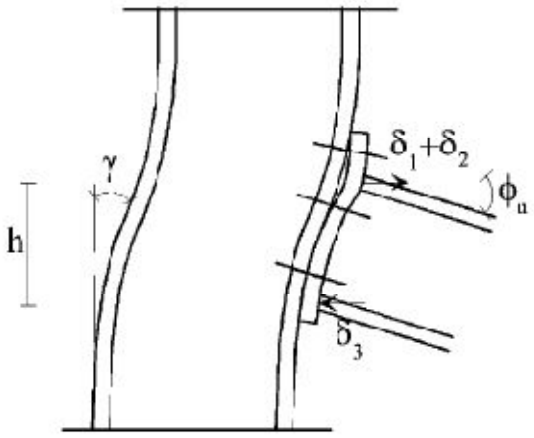

Figure 2.16 Rotation of joint, (Beg et al., 2004)

Beg et al. (2004) also carried out a statistical evaluation of the rotation capacity of typical moment connections with respect to the variation of the material properties f_y

and f_u of individual components influences the rotation capacity of a connection by using the Monte Carlo method. Criteria in reaching ultimate rotation θ_u were stated by maximum equivalent plastic strains reached in different parts of connection: 0.1 for column web in tension, compression on shear and 0.2 for column flange and end-plate in bending. The results show that considerable variation in rotation capacity is obtained in some cases.

Ramli Sulong (2005) studies on ductility of steel joint under combined axial-moment at ambient temperature. The connection is modelled as two coincident nodes, subjected to initial axial loading (tension and compression) followed by incremental of moment in ADAPTIC Finite Element Programme. Five types of connections are examined i.e. FEP, EXTEP, DWA, TSA and finally TSWA. By referring to studies by da Silva et al. (2002) and Kuhlmann et al. (1998), the deformation demand of the critical components located in the outermost bolt-row of the connection and the ductility index (defined as the ratio of failure-to-yield displacement) are determined. The same connection types will be used for further investigation on ductility at elevated temperature in this study.

2.5.3 Ductility Studies at Elevated Temperature

Limited studies can be found on joint ductility at elevated temperature. One of the studies was by Al-Jabri et al. (2005). In identifying the connection's rotation, φ, equation 2.22 were adopted at elevated temperature for flush end-plate and flexible end-plate connection based on displacement transducer readings (see Figure 2.17).

$$\varphi = \tan^{-1}(u/L) \tag{2.22}$$

From the studies, the connection behaviour for temperature–rotation curves of the connections are characterised by three regions. Linear response at early stage with an increasing temperature, followed by a curve-knee which indicates yielding of

connection, and finally a flat plateau at the end of analysis showing the failure of the connection.

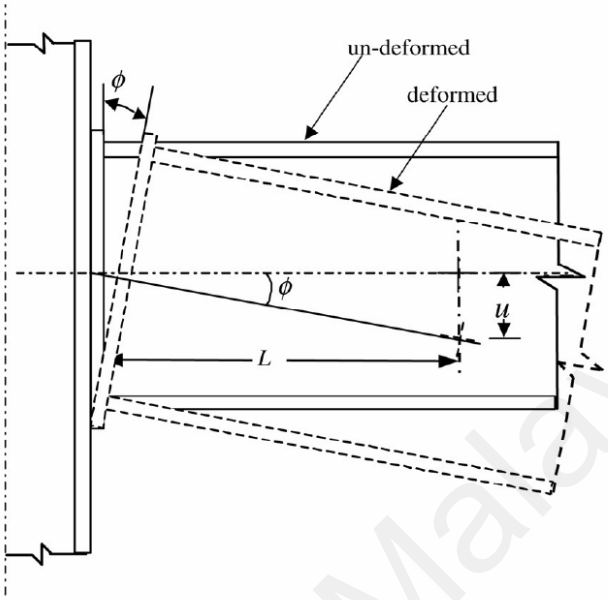

Figure 2.17 Rotation of the connection, (Al-Jabri, 2005)

Based on moment–rotation–temperature data obtained from the connection tests and fitted using a modified Ramberg–Osgood, expression to relate moment, temperature and rotation can be presented in a form of:

$$\varphi = (M/A) + 0.001(M/B)^n \tag{2.23}$$

where,

φ, M = connection rotation and the corresponding level of moment respectively;

A, B and n = temperature dependent parameters.

This equation is only valid for connections with single moment–rotation curves. For connections such as flexible end-plates connections possessing two stages of moment–rotation behaviour (before and after contact of the beam flange with column flange), two separate moment–rotation expressions are necessary in order to represent the response of the connection accurately. The second moment–rotation curve can be represented by Eq. (2.24).

$$\phi = \phi_1 + \frac{(M - M_1)}{A_1} + 0.01\left[\frac{(M - M_1)}{B_1}\right]^{n1} \quad (2.24)$$

Where, ϕ_1 = rotation at which the beam flange comes into with the column;

M_1 = moment corresponding with ϕ_1;

A_1, B_1 and n_1 = temperature dependent constants for stage two of response.

Dharma (2007) carried a studied on both bare steel beams and composite deck slab with re-entrant steel decking to investigate the ductility issue related to inelastic behaviour in the hogging moment regions under fire conditions and to propose the model of the moment-rotational relationships. The reason is that, in the event of fire, the temperatures of the joints are often lower than that of the member due to the shielding effect. This was observed during Cardington fire test (British Steel, 1998); hence the relative stiffness of the connections compared to the member is increased. Consequently, the rotation near the support is largely provided by the member. This analogous to a beam with a rigid joint and the member, instead of the connection, often fails by local flange and web buckling (Fig. 2.18). Thus, in the event of fire, the semi-rigid joints in effect behave like rigid joints since the steel section is relatively weaker due to higher temperatures.

(a) (b)

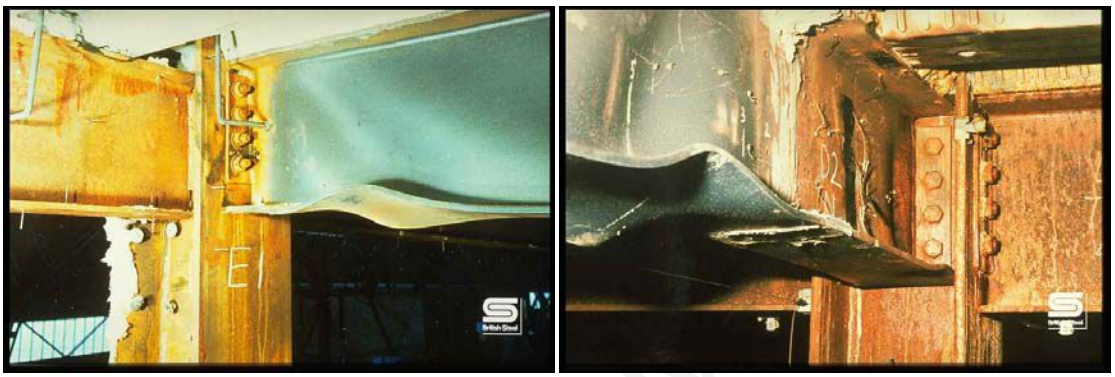

(c) (d)

Figure 2.18 Local Buckling Failures in Cardington Fire Test (Dharma, 2007)

2.6 CONCLUDING REMARKS

It is recognised that the current design code for the joint (EC3: Part 1.8) is limited only on the performance at ambient temperature. In understanding the true behaviour of steel connection at elevated temperature experimental works and other methods were developed such as empirical, analytical, component based method and finite element method.

In selecting methods to understand the characteristic of the connection, it depends on cost and time. For an accurate and realistic output of result, an experimental test can be used but it is too expensive to be practiced in everyday design and also takes time for setup. In order to undertake a practical method, alternative approaches can be used such as empirical, analytical, finite element models or even component based method which is already proven by some researches to be as accurate as experimental result.

Lean et al. (2009) in the studies reported that there are many experimental results that have been adopted as design codes, such as European recommendations for the fire safety of steel structures (ECCS), Eurocode 3, BS 5950: Part 8, and American Institute of Steel Construction (AISC). However, these studies focused on the structural behaviour during the heating phase, and ignoring the cooling process. This lead to further investigation of structure using performance based design compared to prescriptive based approached. There is need to focus on the understanding of structure behaviour under full scale test by taking into consideration the heating and cooling phases based on fire load applied beside the true behaviour of connection itself which plays an important role to connect between members.

Regarding the connection ductility, in order to avoid premature failure and to allow sufficient redistribution of moment, members should be designed to have sufficient rotational capacity (ductility) in fire. A review of ductility at ambient and elevated

temperature studies was carried out to understand further the true behaviour of ductility at elevated temperature.

CHAPTER 3.0 DEVELOPMENT OF NUMERICAL MODELS FOR JOINTS, FRAME AND FLOOR SYSTEM

3.1 INTRODUCTION

Numerical modeling is an alternative way in order to study the behaviour of structure at elevated temperature. Experimental test is a very practical way in evaluating the true behaviour of structure in real fire test but experiment test is costly compared to other methods. This study adopts component based method to determine the structural behaviour of joint at elevated temperature. This chapter explains on the method used in developing the connection model at ambient and elevated temperature. The capability and the development of the model is explained in detail. It starts with explanation of the connection itself by using component based method, followed by the development of connection model at ambient temperature for four connection types including DWA, TSWA, EXTEP and TSA connection. Detail explanation on modeling steel frame and composite floor systems at elevated temperature are presented. Results from the simulation are compared with the experimental tests to verify their accuracy in chapter 4.

3.2 CONNECTION MODEL

Connection models developed by Ramli Sulong (2005) implemented in ADAPTIC nonlinear finite element program, (Izzuddin, 1991) is employed in this study. Based on the component method, the approach requires identification of active components, evaluation of force–deformation relationships and assembling of component characteristics to obtain the overall joint response. In assessing the force–deformation relationship of each idealised component, the strength and stiffness properties are determined based on underlying mechanics principles.

The force-deformation characteristics of the active components are formulated in tri-linear monotonic, and then extended to account for cyclic loading, as illustrated in Figure 3.1. Massing's rule is adopted for the construction of the unloading and reloading paths, in developing the cyclic response of the force-deformation curve of a component. At elevated temperature, reduction factors for strength and stiffness are adopted to account for the degradation of elastic modulus, yield and ultimate stress with increasing temperature. The temperature-dependant properties for the various components are user-defined and can be modified if necessary. The model also allows quadratic temperature variation along the depth of a segment, which enables an accurate representation of the component temperature under consideration.

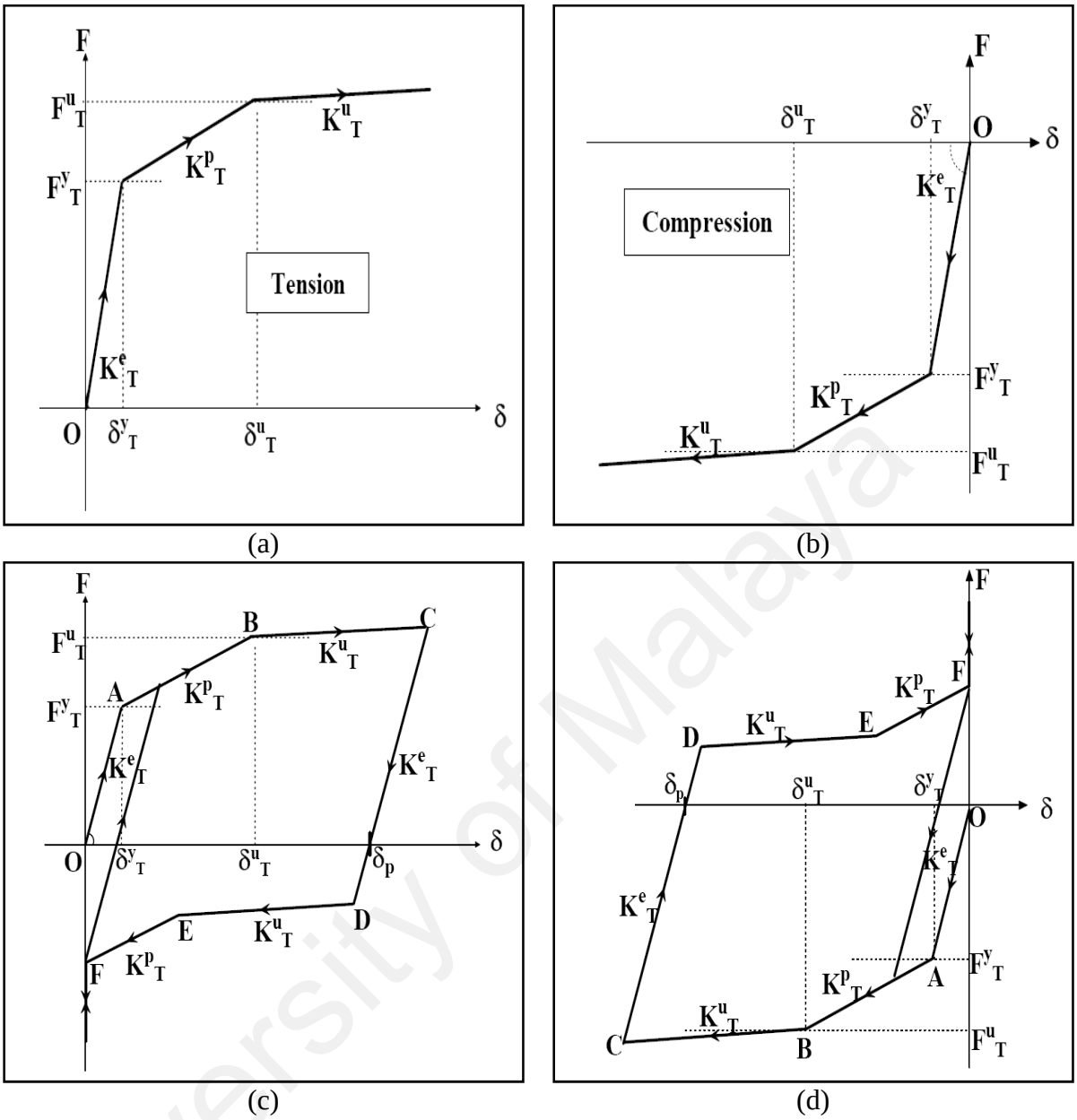

Figure 3.1 Tri-linear force–displacement relationships: (a) tension-type components: monotonic response; (b) compression-type components: monotonic response; (c) tension-type components: cyclic response; and (d) compression-type components cyclic response.

For every incremental step, the applied loading is distributed to the individual components in each connection layer depending on stiffness and resistance of the connection. The full range of moment-rotation is developed by assembling the active component by using appropriate element type of connection. The tri-linear response of an individual component is combined to give a multi-linear representation of the connection response until all components enter the plastic regions.

ADAPTIC software develop by Izzuddin (1991) is an adaptive static and dynamic structural analysis program used for the nonlinear analysis of steel and composite frames, slabs, shells and integrated structures. Version 1.1 of the manual covers mainly the frame analysis capabilities. Besides, this software also can study the behaviour of simple member to complex structure such as frame under different condition such as static, dynamic and under elevated temperature. The program can model 2D to 3D frame.

The connection model used in this work is based on the model developed by Ramli Sulong (2005). The connection model covers six types of connection which are FEP, EXTEP, DWA, TSA, TSWA and lastly fin plate. The computer code for the connection model is written in FORTRAN and involves full nonlinear and cyclic procedures covering generalised loading for all connection types under ambient and elevated temperature conditions. The procedure to develop connection model using component base method requires three steeps as follow:

1) Identification of the active components of the beam-to-column joint to be examined,
2) Evaluation of the stiffness and resistance characteristics for each individual basic component,
3) Assembly of the components for evaluating the response of the whole joint.

Descriptions on the development of component-based models of six types of connection DWA, TSA, TSWA, EXTEP, FEP connection and finally fin plate connection are explained as below:

Data entry in ADAPTIC will call three modules which are ‘type’, ‘material names’ and ‘parameters’,

1) Under module ‘type’, three entries are required:

   a. First entry is either ‘steel’ for bare steel connection or ‘composite’ for composite connection.

   b. In the second entry, the connection type has to be specified as follows:

   • ‘flush.endplate’ : FEP

   • ‘extended.endplate’ : EXTEP

   • ‘web.angles’ : DWA

   • ‘top.and.seat’ : TSA

   • ‘combination.web/top/seat’ : TSWA

   • ‘finplate’ : Finplate

   c. The third entries require the behaviour of panel zone, either ‘rigid’ where panel zone behaviour is omitted or ‘flexible’ where the flexibility of the panel zone is included.

2) Under ‘material names’, three material properties of the connection need to be entered, using a material model called ‘gen1’. The first material name provides the properties of the connecting elements depending on the connection configuration, either plates or angles. The second material name is the properties of bolts and the third material properties are related to the connected members, i.e. the beams and the column. For each material, mechanical properties are ultimate stress, elastic modulus, reduced strain hardening coefficient, yield stress and strain hardening coefficient, in sequence order.

3) The last module is ‘parameters’, the parameters here referring to geometrical properties of connection. The number of parameters varies according to connection types and parameters of the connecting element are as follows:

- FEP (13 parameters)
- EXTEP (26 parameters)
- DWA (12 parameters)
- TSA (23 parameters)
- TSWA (34 parameters)
- Finplate (8 parameters)

Details of these parameters are as follows:

a. FEP

- Bolt diameter, d_b
- Area of bolt shank, A_b
- Thickness of bolt head, t_{bh}
- Thickness of nut, t_n
- Thickness of washer, t_w
- Distance from endplate edge to bolt head/nut/washer edge, n_1
- Distance of bolt head/nut /washer whichever is appropriate, k
- Distance from edge of bolt head/nut/ washer to fillet of endplate to beam web, m_1
- Total depth of endplate, L_{ep}
- Thickness of endplate, t_{ep}
- Endplate width, b_p
- Minimum bolt pitch, p_b
- Coefficient for the computation of the effective width for the bolt-row below the beam tension flange, α

b. EXTEP

The geometrical properties of the EXTEP are double the properties of the flush endplate, accounting for different orientation of the T-stub components, but the details and order are the same. The only exception is for the last parameter, where the length of the extended part of the endplate is required.

c. DWA

- Bolt diameter, d_b
- Area of bolt shank, A_b
- Total depth of angle, L_a
- Angle thickness, t_a
- Gauge length of beam leg, g_{bl}
- Bolt clearance, b_{clr}
- Minimum bolt pitch, p_b
- Gauge length of column leg, g_{cl}
- Distance from bolt line to free edge of column leg, e_{cl}
- Distance from bolt line to free edge of beam leg, e_{bl}
- Angle radius, r_a
- Diameter of M16 bolts, d_{M16}

d. TSA

For top angle (12 parameters):

- Bolt diameter, d_b
- Area of bolt shank, A_b
- Total depth of angle, L_a
- Angle thickness, t_a
- Gauge length of beam leg, g_{bl}
- Bolt clearance, b_{clr}
- Minimum bolt pitch, p_b
- Gauge length of column leg, g_{cl}
- Distance from bolt line to free edge of column leg, e_{cl}
- Distance from bolt line to free edge of beam leg, e_{bl}
- Angle radius, r_a
- Diameter of M16 bolts, $dM16$

Similar dimensions are needed for seat angle (11 parameters) except for the diameter of M16 bolts.

e. TSWA

Connection parameters for this type are the combination of web angle and top and seat angles.

f. Finplate

- Bolt diameter, d_b
- Bolt hole diameter, d_0

- Total depth of plate, L_p
- Plate thickness, t_p
- Gauge length, a
- Width of plate, b_p
- Minimum bolt pitch, p_b
- Diameter of M16 bolts, d_{M16}

After the connection parameters are entered, another 14 parameters are needed: 11 parameters for the connected members, followed by Poisson ratio, number of layers and a flag to indicate preload or non-preload condition of the bolts. Connected member parameters are:

- Column depth, h_c
- Column flange width, b_c
- Thickness of column flange, t_{cf}
- Thickness of column web, t_{cw}
- Column radius, r_c
- Bolt pitch in column, p_b
- Distance from bolt line to free edge of column flange, n_c
- Distance from bolt line to fillet of column flange, m_c
- Beam depth, h_b
- Thickness of beam flange, t_{bf}
- Thickness of beam web, t_{bw}

3.3 MODELLING OF CONNECTION AT AMBIENT TEMPERATURE

The development of connection model at ambient temperature is to further validate the accuracy of the developed connection model (Ramli Sulong, 2005) and to prove that the model is capable of simulating the actual connection behaviour.

The development of models steps start with identifying mechanical and geometrical properties for connection and connected members. The currently proposed model by Ramli Sulong, 2005 is validated against the results of several experimental studies of connection types such as angle connection or end plate connection. It is acknowledged that there is extensive experimental data in the literature on steel connection response at ambient temperature.

In this thesis, a validation work of connection included for DWA connection (Yang and Lee, 2007), TSWA connection (Danesh et al., 2007), EXTEP connection (Girao Coelho, 2004) and TSA connection (Azizinamini et al., 1987 and Pirmoz et al., 2009).

EXTEP connections were selected in experimental result from Girao Coelho (2004). The tests ID used in validation work are FS1 and FS2; the difference between these connections is different of end plate thickness. Column had a section profile of HE340M (376.00 x 307.50 x 40.21), beam section profile of IPE300 (300 x 150 x 10.7) and M20 grade 8.8 bolts are used for the entire test. Refer figure 3.2 for geometrical properties and details of test and mechanical properties in Table 3.1 to 3.3.

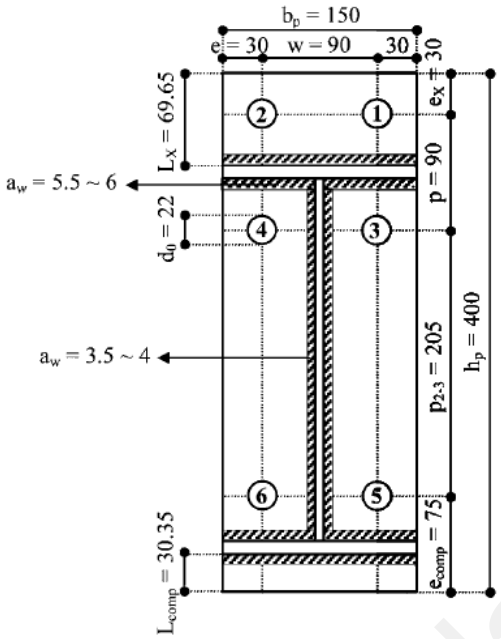

Figure 3.2 Geometrical properties of the connection, (Girao Coelho, 2004)

Table 3.1 Detail of test specimens, (Girao Coelho, 2004)

Test ID	Column		Beam		End Plate	
	Profile	Steel Grade	Profile	Steel Grade	t_p(mm)	Steel Grade
FS1	HE340M	S355	IPE300	S235	10	S355
FS2	HE340M	S355	IPE300	S235	15	S355

Table 3.2 Average characteristic values for the structural steels

Specimen		Steel grade	E (MPa)	E_{st}(MPa)	f_y (MPa)	f_u	p_y	ε_{st}	ε_{uni}	ε_u
End plate	t_p=10	S355	209856	2264	340.12	480.49	0.708	0.015	0.224	0.361
	t_p=15	S355	208538	2901	342.82	507.85	0.675	0.020	0.198	0.475
Beam	Web	S235	208332	1856	299.12	446.25	0.670	0.016	0.235	0.464
	Flange	S235	209496	1933	316.24	462.28	0.684	0.016	0.235	0.299

Table 3.3 Average characteristic values for the bolts

Batch	E(MPa)	*f*y(MPa)	*f*u(MPa)	ε_u
1	223166	857.33	913.78	0.272
2	222982	854.31	916.81	0.231

For the DWA connection (Yang and Lee, 2007) angle section of (L125 × 75 × 7) mm is used to connect (W 18 x 35) inch beam to (W14 x 90) inch column. The only difference among the specimens is the number of M20 bolts, which varies from three to five layers. All the bolt gauge length of each angle is 65 mm. Mechanical and geometrical properties of the connection are shown in Table 3.4 and Figure 3.3.

Table 3.4 Mechanical properties of angle specimen and bolt, (Yang and Lee, 2007)

Member	Young's modulus (N/mm^2)	Yield stress (N/mm^2)	Ultimate stress (N/mm^2)
Angle	202,762	318.50	469.42
Bolt	260,778	872.22	925.12

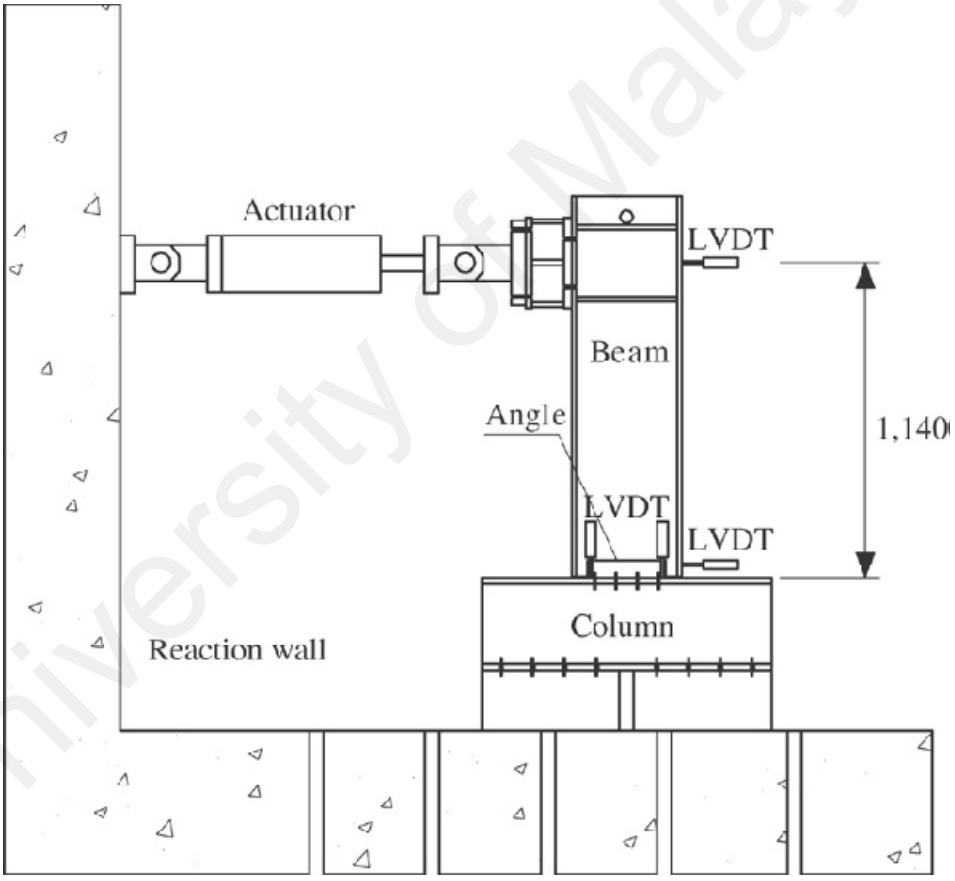

(a)

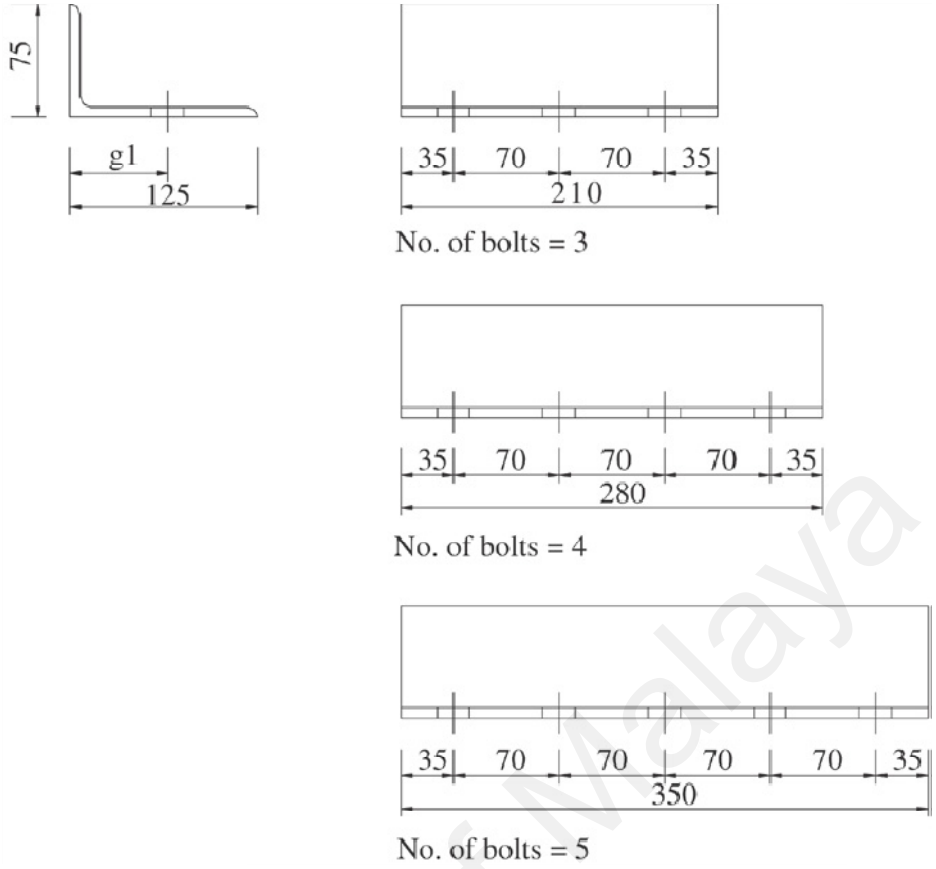

(b)

Figure 3.3 (a) Test set-up (b) Geometrical properties of angle connections, (Yang and Lee, 2007)

TSA connection tested by Pirmoz et al. (2009) is also adopted. The differences among the model are the bolt diameter, beam and column section and geometrical properties of angle connection. Details of geometrical properties for each specimen list in Table 3.5 and Figure 3.4 and 3.5 view test setup configuration and stress-strain relation for material.

Table 3.5 Geometrical properties of TSA connections (Pirmoz et al., 2009)

Specimen number	Bolt diameter (mm)	Column section	Beam Section	TSA's			
				Angle	Length (mm)	Gage (g) (mm)	Bolt spacing (p) (mm)
A1	22	W12x96 inch	W14x38 inch	(L6X4X3/8) inch	203.2	63.5	139.7
A2	22	W12x96 inch	W14x38 inch	L6X4X1/2 inch	203.2	63.5	139.7
W00	20	H400x300x12x8mm	H400x300x12x8mm	L150X100X 12 mm	200	55	120

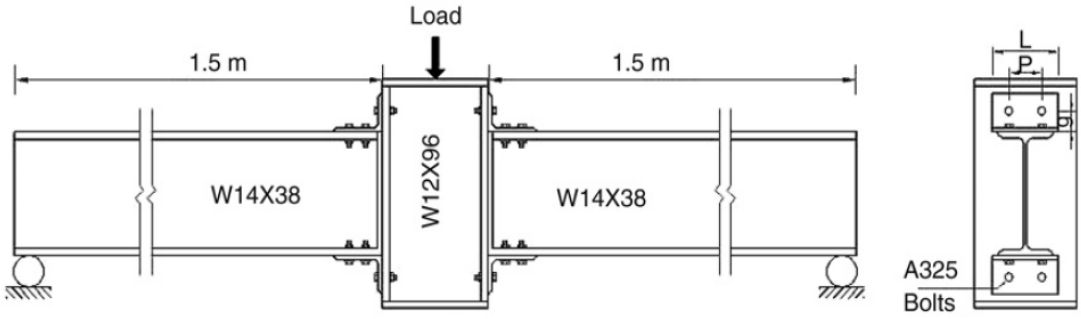

(a) Test setup configuration and connection parameter of A2 and A1 specimens

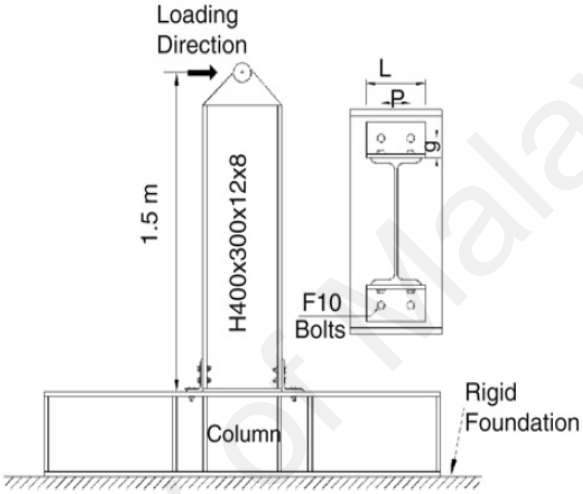

(b) Test setup configuration and connection parameters of W00 test

Figure 3.4 Test setup configurations.

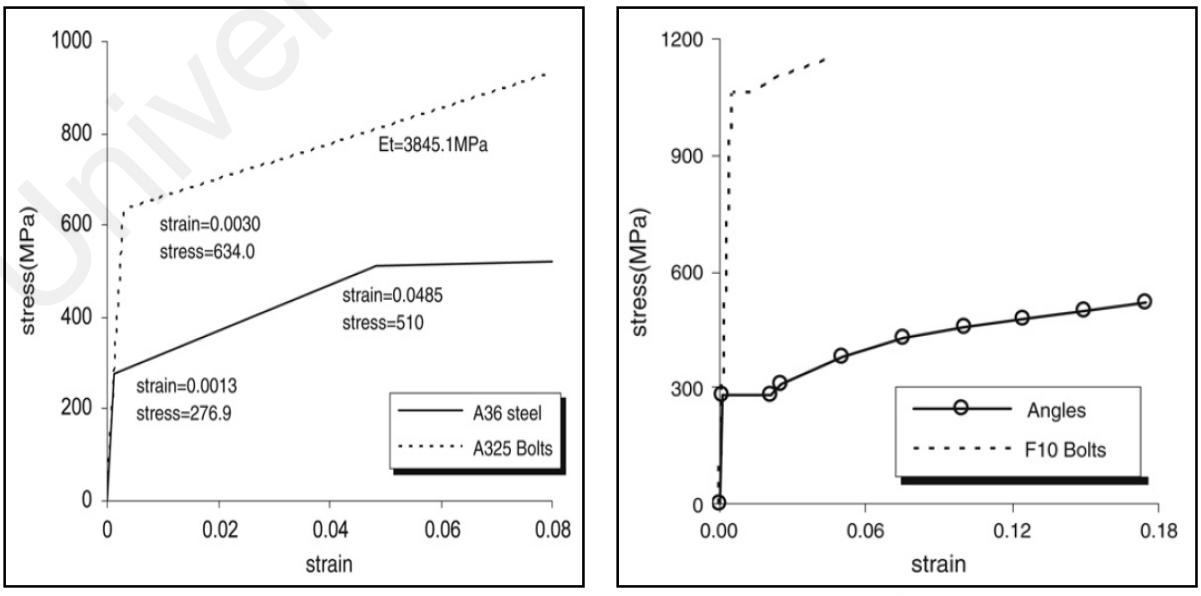

(a) (b)

Figure 3.5 Stress-strain relation of material (a) Material properties of beam, column, angle and bolt for A2 and (b) True uniaxial stress-strain relations of W00 angles (Pirmoz et al., 2009)

Two tests were selected to validate TSWA connection which is specimen number 8S1, 8S2 and 8S9 (Danesh et al., 2007). The differences between this two tests are the thickness of top and seat angle of the connection. Details of the specimen are given in Table 3.6, and illustration of geometrical properties of the connection is shown in Figure 3.6.

Table 3.6 Section and geometrical properties of the connections

Specimen number	Bolt diameter (mm)	Column section (inch)	Beam section (inch)	Top and seat angle				Web angle	
				Angle (inch)	Length (mm)	Gauge (g) (mm)	Bolt spacing (p) (mm)	Angle	Length (mm)
8S1	19.1	W12X58	W8X21	L 6X3-1/2X5/16	152.4	50.8	88.9	2L4X3-1/2X1/4	139.7
8S2	19.4	W12X58	W8X21	L6X3-1/2X3/8	152.4	50.8	88.9	2L4X3-1/2X1/4	139.7
8S9	22.3	W12X58	W8X21	L6X3-1/2X3/16	152.4	50.8	88.9	2L4X3-1/2X1/4	139.7

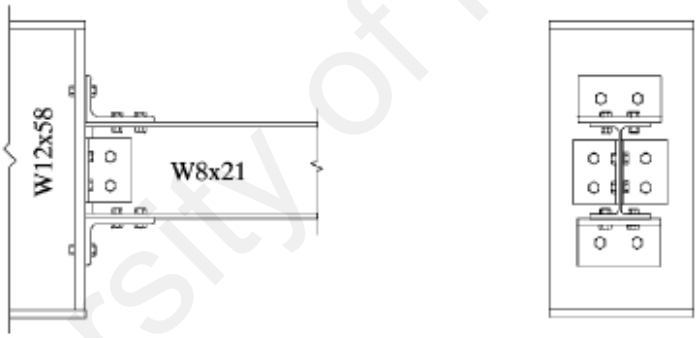

Figure 3.6 Column, beam and angle cross section (Danesh et al., 2007)

The model of isolated connection is analysed using 2D static with time-history loading control. Material model ‘gen1’ were applied for the material properties. Material properties need to be specified in the following order:

1. Ultimate strength, temperatures and reduction factors for quadlinear description,
2. Young’s modulus, temperatures and reduction factors,
3. Reduced strain hardening coefficient, temperatures and reduction factors,
4. Yield strength , temperatures and reduction factors,
5. Strain hardening coefficient, temperatures and reduction factors.

Further, an element ‘jbc2’ has been used to group the connection element which requires the specification of a number, connectivity and other modules. This element consists of two coincident nodes prior to loading plus a third node to determine the beam direction. Three modules need to be included namely module ‘type’, ‘material names’ and ‘parameters’. Under module ‘type’, three entries are required:

1. First entry is ‘steel’ for bare steel connection.
2. In the second entry, the connection type has to be specified as follows:
    - ‘extended.endplate’ : EXTEP for validation model by Girao Coelho (2004),
    - ‘web.angles’ : DWA for validation model by Yang and Lee (2007),
    - ‘top.and.seat’ : TSA for validation model by Pirmoz et al. (2009)
    - ‘combination.web/top/seat’: TSWA for validation model by Danesh et al. (2007).
3. The third entries in all case the behaviour of panel zone to be ‘rigid’ where panel zone behaviour is omitted.

Under second module of ‘material names’, three material properties of the connection need to be entered, using a material model called ‘gen1’. This model has already being explained earlier, connection configuration, properties of bolt and lastly properties of connected members need to be specified according to the order.

The last module is ‘parameters’, where geometrical properties of the connection are specified. The number of parameters varies according to connection types and parameters of the connecting element. This has already being explained under sub-chapter 3.2.

Further, an identification of nodes and connectivity, in 2D analysis 2 directions are required in x and y to define the direction of node responds. Next, this node is connected under element connectivity by grouping the node. Under boundary condition, 1 node is defined as rigid in all direction x, y and rz and another node is restrained in y direction and free to respond in axial and rotational direction. At ambient temperature, the loading condition is applied through incremental moments by controlling rotation using proportional load control.

Under Iterative strategy module specifies the iterative strategy applied during a load or a time step. Parameters that need to specify under this module are as follow:

1. ‘number.of.iterations’: The maximum number of iterations performed for each increment.
2. ‘initial.reformations’: The number of initial reformations of the tangent stiffness matrix within an increment.
3. ‘step.reduction’: The step reduction factor used when convergence is not achieved.
4. ‘divergence.iteration’: The iteration after which divergence checks are performed.
5. ‘maximum.convergence’: The maximum convergance value allowed for any iteration

The convergence criteria module, which defines convergence criteria for the iterative procedures, are based either on the out-of-balance norm or the maximum iterative displacement increment. Last but not least, output module, this module specifies the frequency of numerical output by including step reduction levels.

3.4 MODELLING OF FULL SCALE GURUN FIRE TEST

3.4.1 Description of Fire Test

A full scale fire test was carried out in Malaysia to study the performance of local steel product without fire protection under fire. The fire test was conducted on a 36m x 12m four storey steel-frame school building on the premise of Perwaja Sdn. Bhd. at Gurun, Kedah. Detail explanation on this fire test was presented by Tapsir (2004).

As shown in Figure 3.7 and 3.8, the school building consisted of four storey structural steel frame and the building foundation rests on steel H piles of size 350mm x 350mm x 105kg/m. The loading on the second and third floor consists of sandbags, appropriately placed and arranged at each floor as to represent the weight of walls and imposed loads, which equivalent to 35.7kg/m^2. Two types of floor system used were precast concrete slab and metal deck system. The fire test was carried out in the middle room located on the first floor, measuring 15m x 9.5m, which has precast concrete flooring. Precast concrete flooring was used on three-quarters of the first and second floor, and on entire third floor. The metal deck system was installed for the rest of first and second floor.

The precast concrete slab (65mm) had an 85 mm layer of concrete on the top, giving a total floor thickness of 150mm. The metal deck flooring was 110mm in thickness. Shear studs were installed on the main and secondary beams to provide fully restrained beam and composite behaviour between the beams and slab. A total of 952 shear studs were used on each floor. A layer of cement render was applied to the first floor slab. Concrete slab with strength of 25 N/mm^2 at 28 days strength was used.

For wall, two types of non-load bearing masonry units were used. The solid concrete brick was installed on the north and west sides of the middle room while the hollow blocks were installed at the east and south sides. Plaster cement was applied on

the brickworks. Total ventilation of 11.8m^2 from wire mesh above the windows remains opened during the test and all window and doors were closed.

The important part in the connection was made of 100 mm x 100mmx 10mm plate of angle cleats welded to the secondary beams. The flange faces of column were bolted to the main beams and the bolts were of grade A 325. The angle under the secondary beams was of the size 100 mm x 100mmx 12mm thick.

The fire test was carried out in the middle room located on the first floor, measuring 15m x 9.5m which had precast concrete flooring. In this test, two tons of wooden pallets were used and arranged to provide the service loading (Tapsir, 2004). 140 pieces of wooden pallets were used 14.75 kg/piece giving a total weight of 2, 065 kg. The stack contained of 10 wooden pallets with each dimension of 1.16 x 1.12 x 0.13 m.

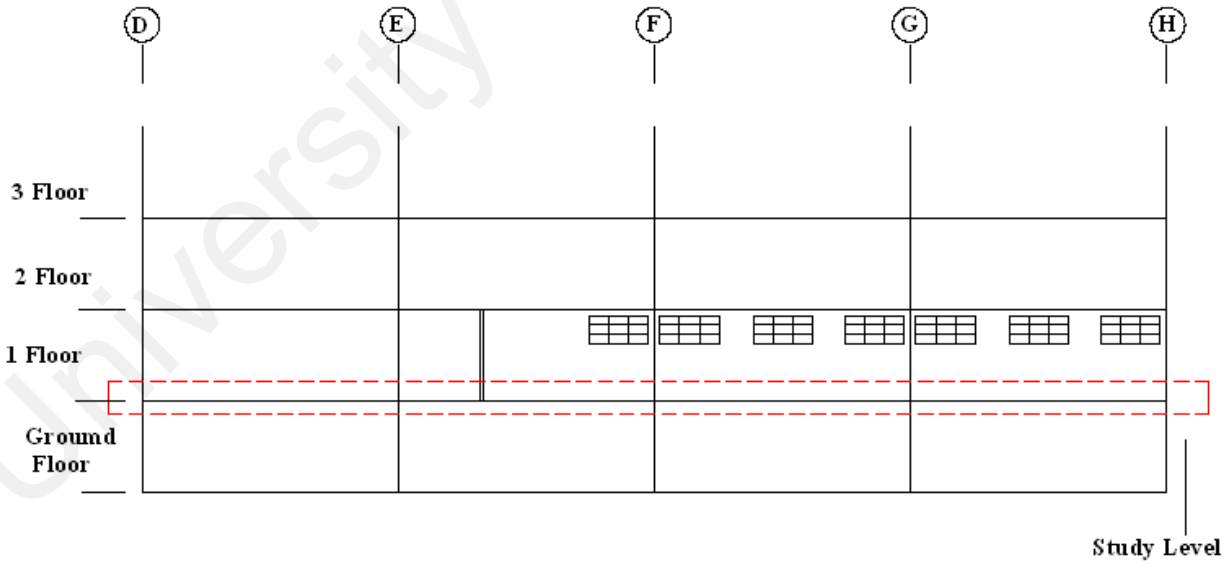

Figure 3.7 Side View of the School Building

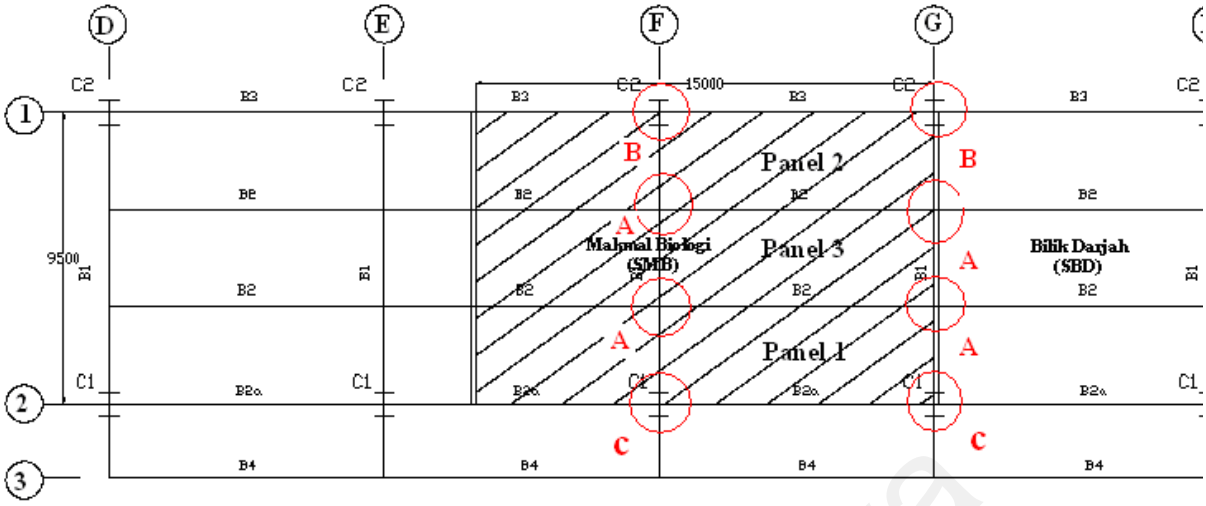

Figure 3.8 Compartment Area

Figure 3.9 shows panel 1, panel 2 and panel 3 in the compartment area which illustrate the beam size used in each panel. In addition, detail geometrical properties of connections used in each panel are demonstrated in Figure 3.10. The connections are seat and web angle connection, EXTEP and DWA connection.

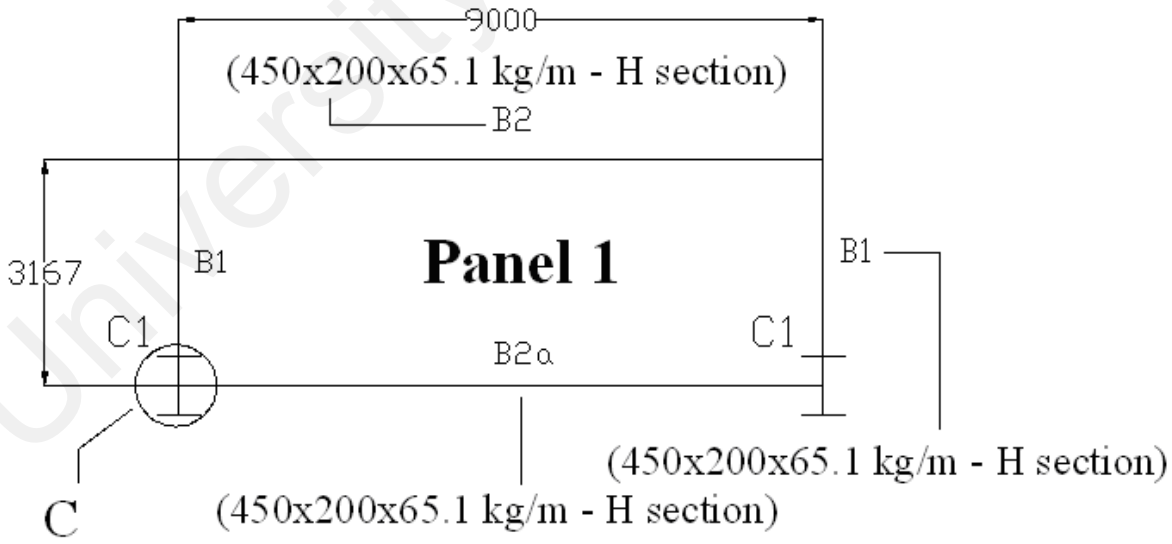

(a)

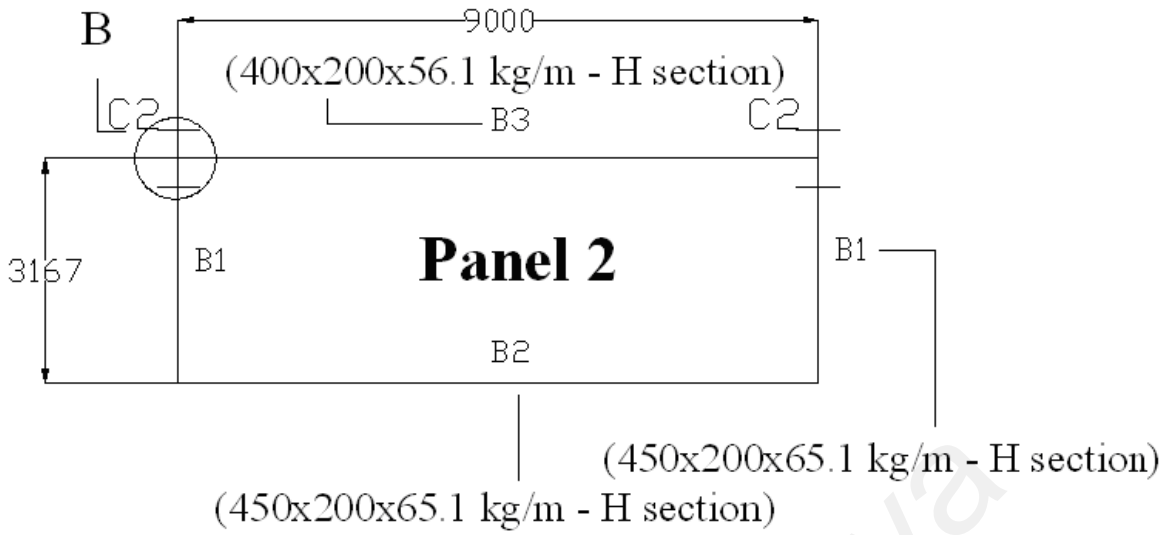

(b)

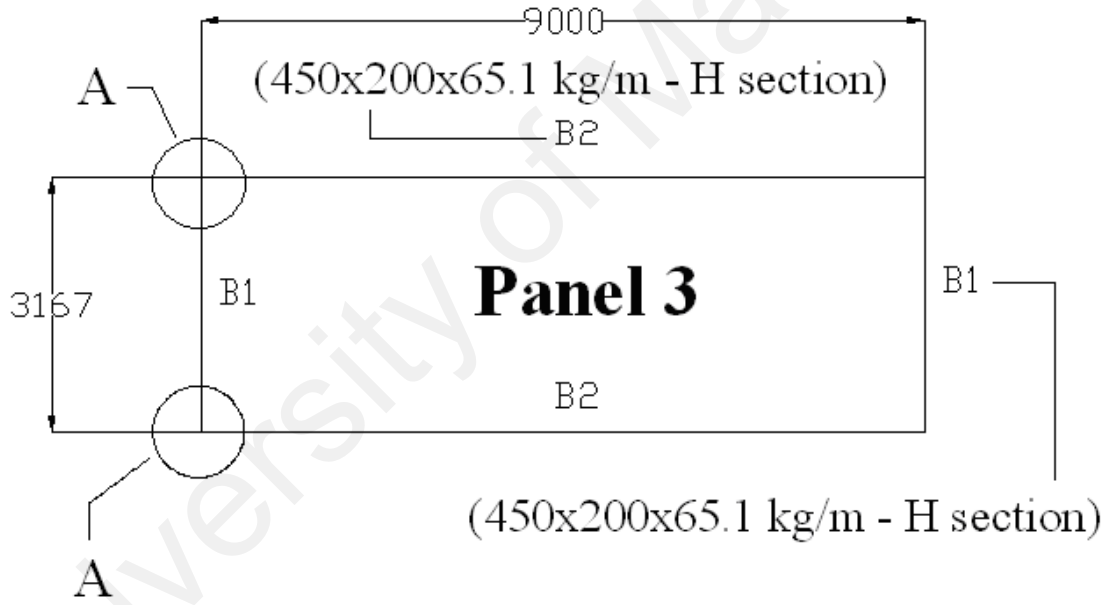

(c)

Figure 3.9 Panel 1, Panel 2 and Panel 3 in the compartment area

Figure 3.10 (a) and (b) show seat and web angle connection used to connect between secondary beams B3 with column C2 and between secondary beam B2a to main beam B1 (at grid F1, G1, F-2 and G-2). EXTEP connection was employed to connect main beam B1 to column C2 (Figure 3.10 (c)). Lastly, DWA connection was used to connect internal secondary beam B2 to main beam B1 (Figure 3.10(d)).

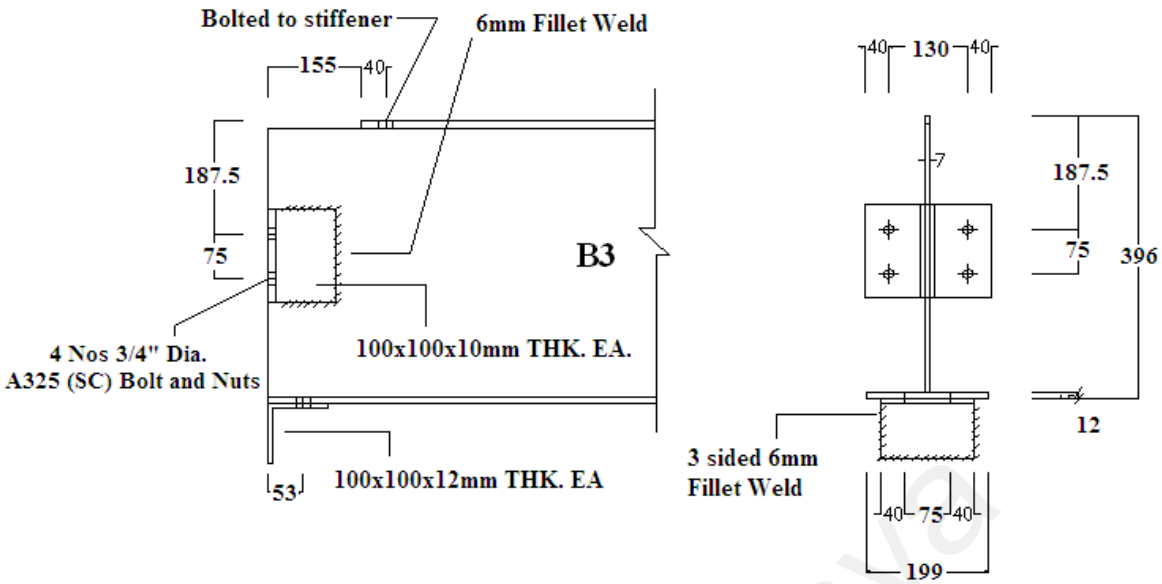

a) Side and cross section view of seat and web angle connection for detail connection between B3 and column C2

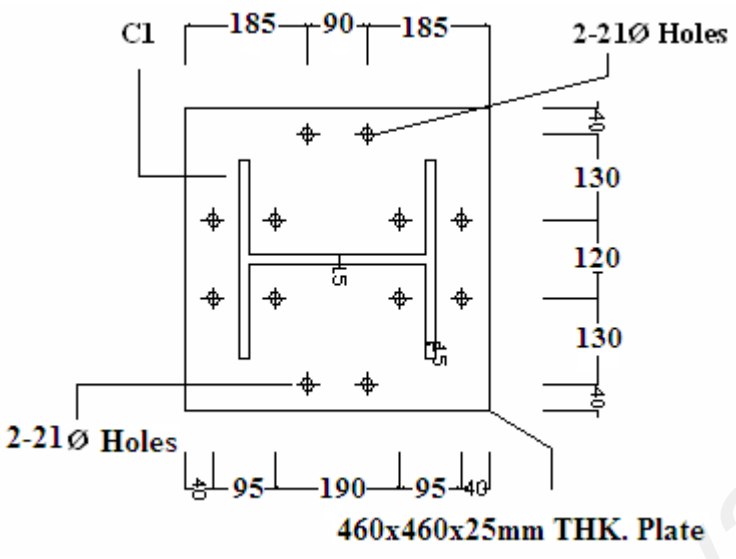

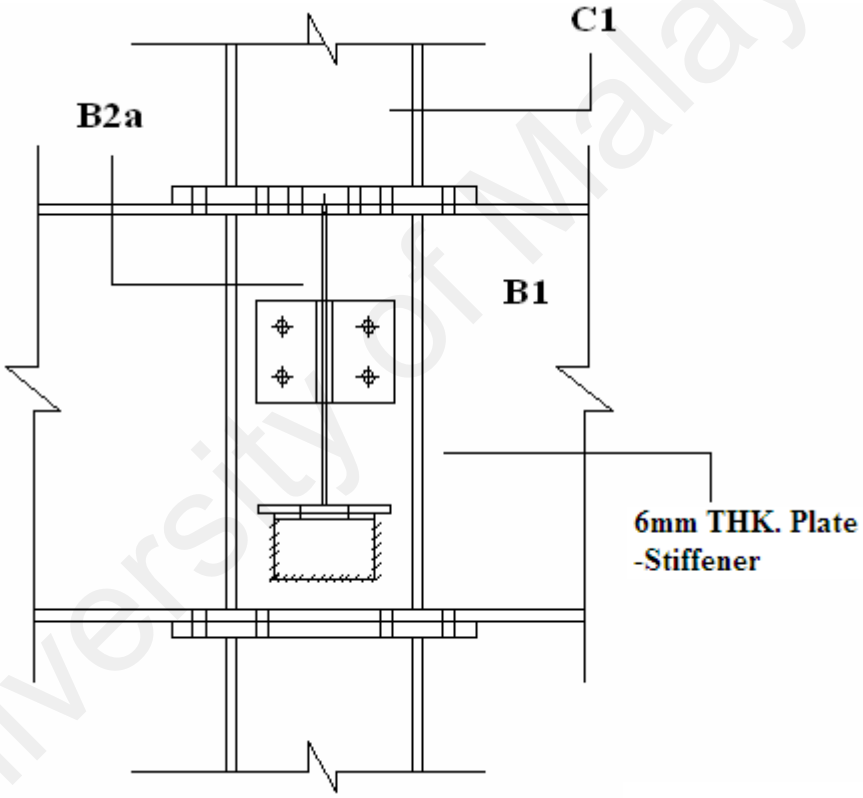

b) Plan and cross section view of seat and web angle connection between secondary beam B2a and main beam B1 in Figure 3.3

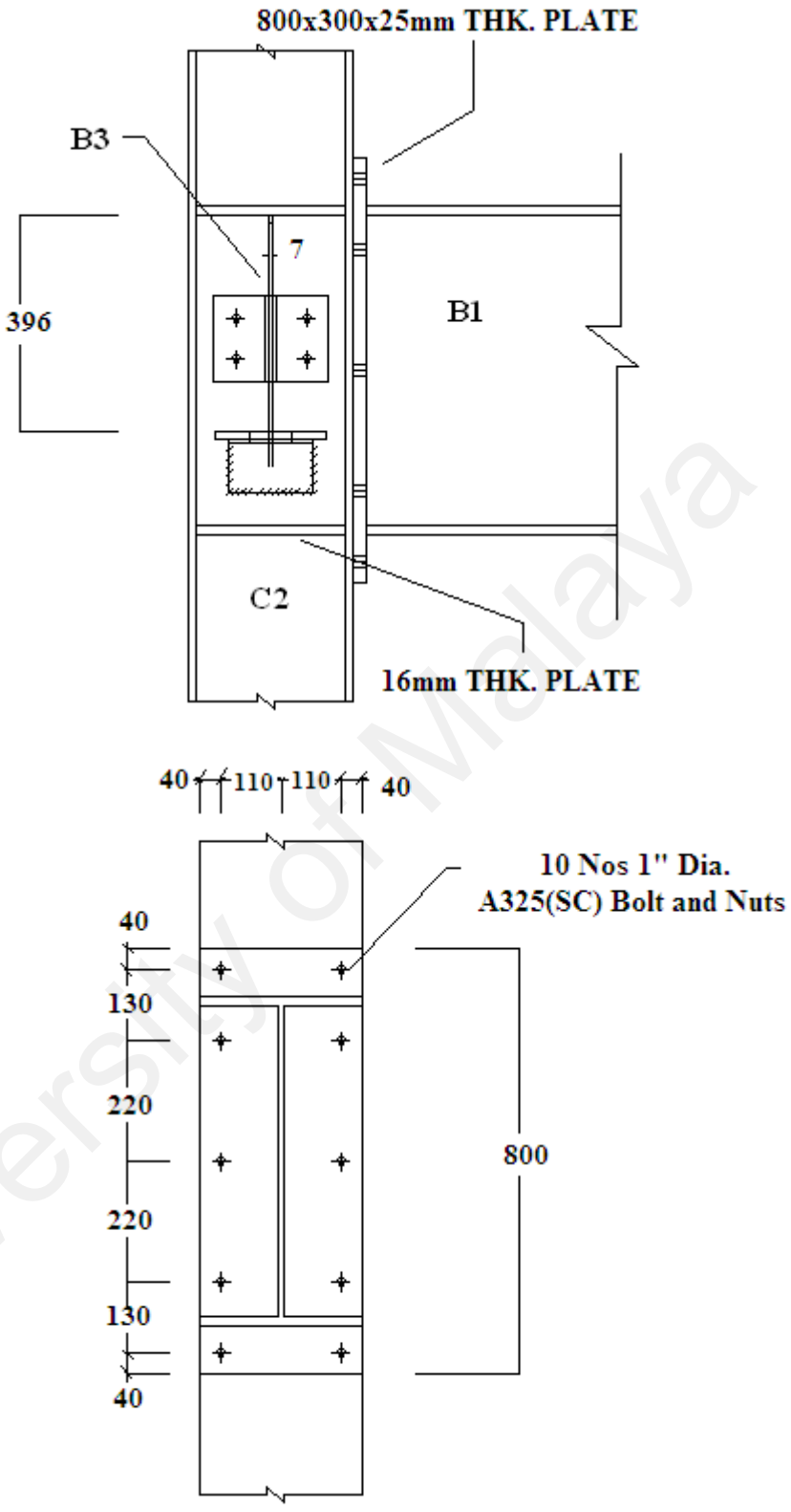

(c) EXTEP connections to connect between main beam, B1 and column C2

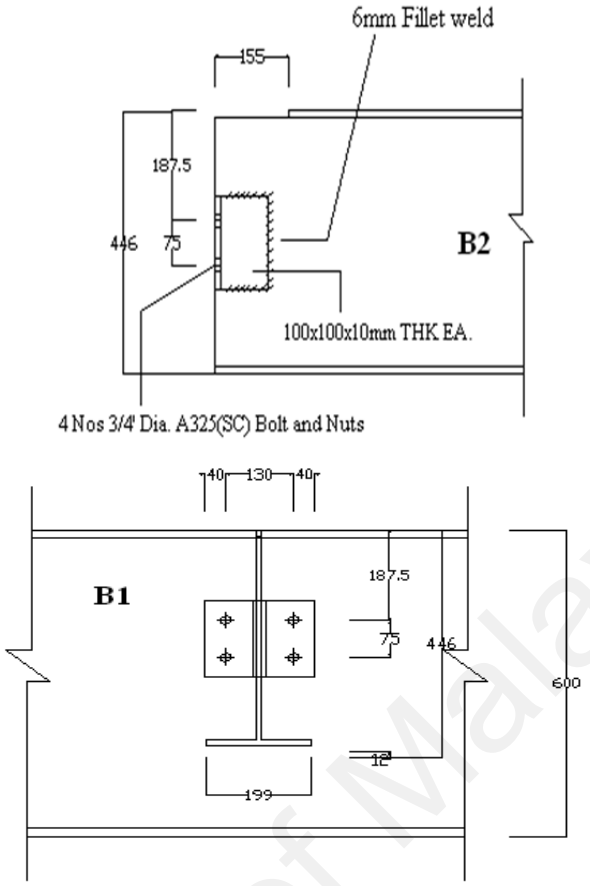

(d)DWA connections for detail A in Figure 3.3

Figure 3.10 Detail of geometrical properties of connections in the compartment area

Table 3.7 exemplifies the loading applied on the steel beam that has been calculated based on the use of the compartment. Details of beam and column sizes are illustrated in table 3.8.

Table 3.7 Applied Loading on the steel beam, (Tapsir, 2004)

Beams	Dimensions mmxkg/m	Load (kN)	Length (mm)	Moment of Inertia (cm^4)	Deflection (mm)
B1	600x300x133.0	168.19	9500	98950	20.82
B2	450x200x65.1	86.4	9000	28134	14.22
B2a	450x200x65.1	75.6	9000	28134	12.44
B3	400x200x56.1	41.31	9000	19771	9.67

Table 3.8 Geometric properties of steel section (Tapsir, 2004)

Section Designation	Depth of Section (mm)	Width of section (mm)	Web Thicknes (mm)	Flange Thickness (mm)
Beams				
250x125x29.0	250	125	6	9
400x200x56.1	396	199	7	11
450x200x65.1	446	199	8	12
600x300x133.0	582	300	12	17
Column				
300x300x83.5	294	302	12	12
300x300x105	300	305	15	15

In this work, the main focus of the study is to investigate the connection behaviour under fire loading on this school building. Two types of connection are examined, i.e. connection between main beam to secondary beam and connection between column to main beam. Figure 3.11 shows the time- temperature for DWA and EXTEP connection. Figure 3.12 shows result of time-temperature of secondary beam. The live load applied is assumed to be constant along the analysis and the temperature applied on the connection is assumed to be uniform along and across the section.

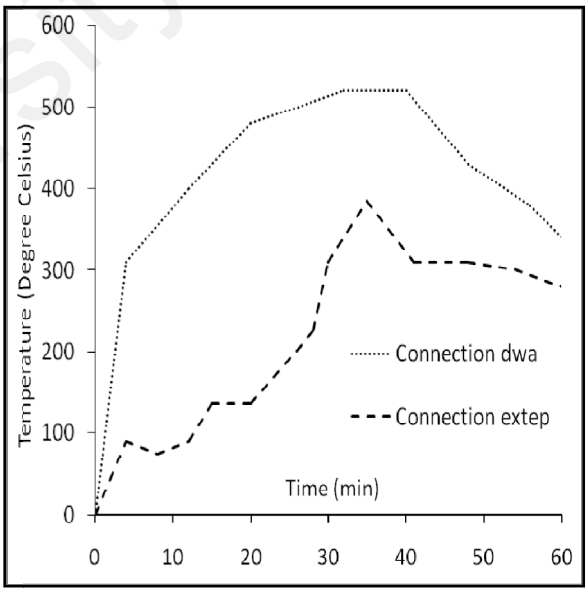

Figure 3.11 Time-temperature for connection that connects secondary beam B2 and main beam B1 at A using DWA and main beam, B1 to column C2 at B using EXTEP.

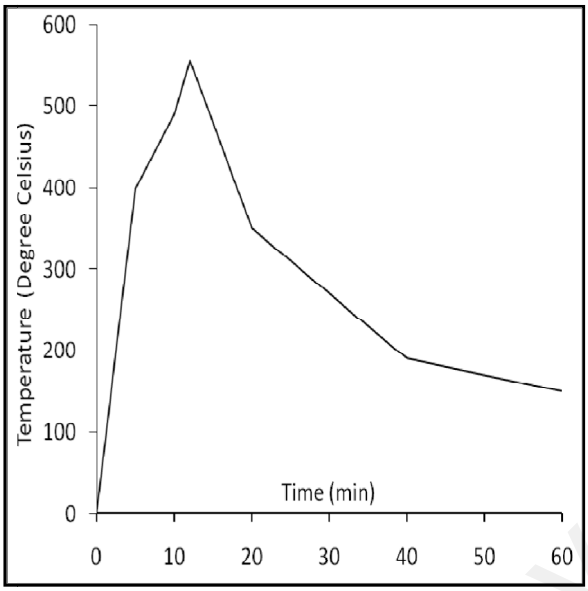

Figure 3.12 Time-temperature curve for secondary beam B2 (Tapsir, 2004)

3.4.2 Modelling With ADAPTIC Finite Element Program

3.4.2.1 Isolated Steel and Composite Beam

In this study, the modelling and simulation studies are divided into two parts, i.e. (i) Isolated steel and composite beam and (ii) Floor system. By referring to Figure 3.8, the compartment area is located in the first floor covering an area of 15 x 9.5 m. The compartment area can be divided into three panels i.e. Panel 1, Panel 2 and Panel 3. Panel 1 is supported by DWA and combination of web angle and seat angle connection, panel 2 is supported by DWA connection and panel 3 is supported by EXTEP and DWA. The details of beam sizes located in this compartment are shown in Figure 3.9 (a), (b) and (c).

The type of connections used to connect the structural element in this compartment area includes DWA, combined web and seat angle and EXTEP connections. Detailed geometrical properties of these connections at respective location are presented in Figure 3.10 (a) to (d). Structural modeling of isolated beam and floor system carried out in finite element analysis program, ADAPTIC is explained in detail in the next sections.

Modelling of the isolated beam case is divided into steel and composite beam. The purpose of modeling isolated steel beam is to investigate the influence of connection on the overall steel beam response. On the other hand, modeling of composite beam is very much closer to the actual beam in the fire compartment.

For both models, on the isolated secondary beam, B2 (450 x 200 x 65.1 kg/m) of 9.0 m is connected by DWA (Figure 3.10 (d)) at both ends to 9.5m length main beam (600 x 300 x 133 kg/m) are utilized. Taking advantage of symmetrical properties of this secondary beam, only half of the beam length is modeled.

In modeling the isolated steel beam, bilinear material steel model, 'stl4' which requires the specification of Young's modulus, the yield strength, the strain-hardening factor, the thermal strain and their variations with temperature is adopted in ADAPTIC. This material model allows reduction of steel material properties at elevated temperature. Yield strength value of 275 N/mm^2 and Young Modulus of 205 kN/mm^2 is adopted at ambient temperature. Reduction of these material properties with temperature is given in Figure 3.13. The increment of thermal strain with temperature is given in Figure 3.14, this follow EN 1993-1-2:2005.

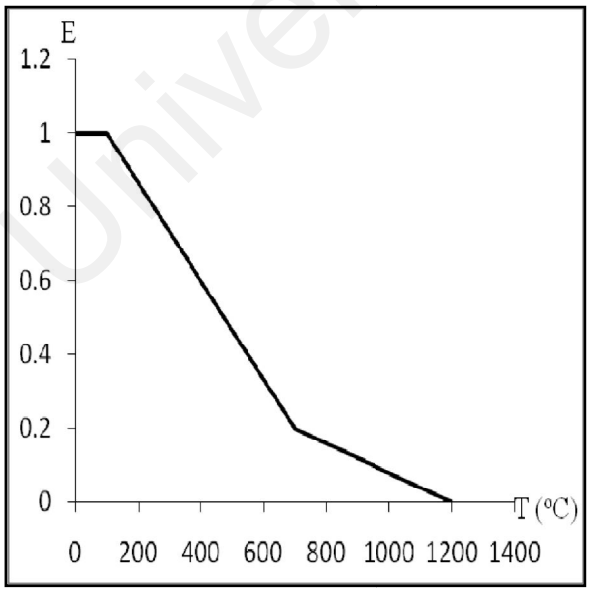

(a) Reduction of Elastic Modulus, E with temperature

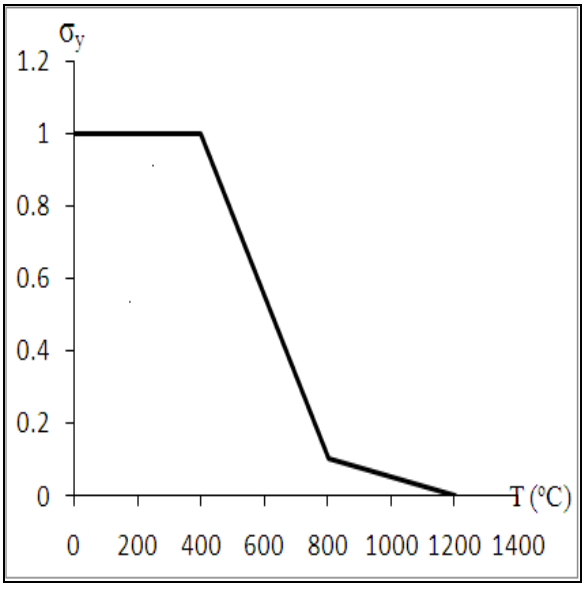

(b) Reduction of Yield Strength, σ_y with Temperature

Figure 3.13 Reduction of material properties with temperature

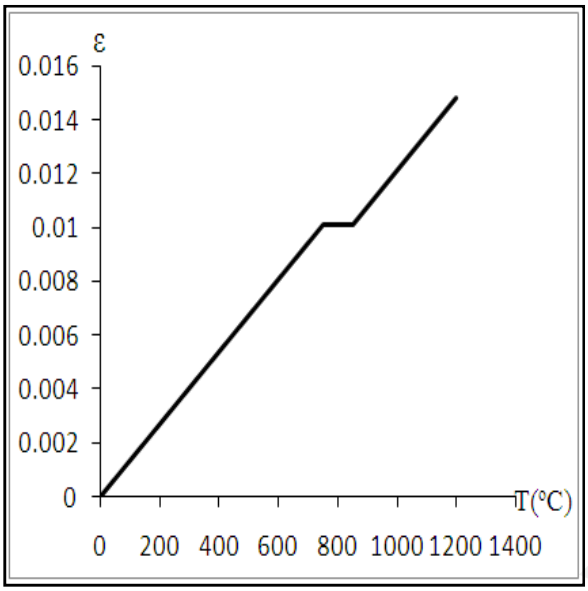

Figure 3.14 Thermal strain of steel as a function of temperature

The modelling of composite beam is carried out based on material models called 'con6', a tri-linear compressive concrete model for elevated temperature, with zero tensile response in ADAPTIC. In this material model, four material properties are required i.e. compressive strength (σ_c), compressive strain (ε_c), ultimate compressive strain (ε_{cu}), and thermal strain (ε_{th}).Variations of these materials with increasing temperature adopted in the model are given in Figure 3.15.

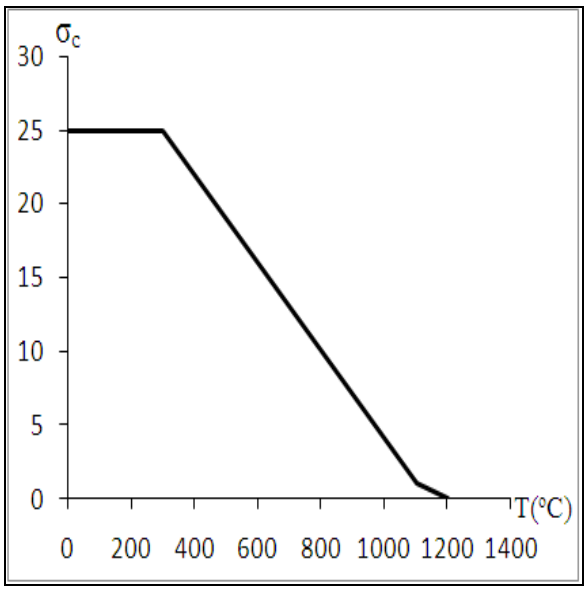

(a) Variation of compressive strength, σ_c with temperature

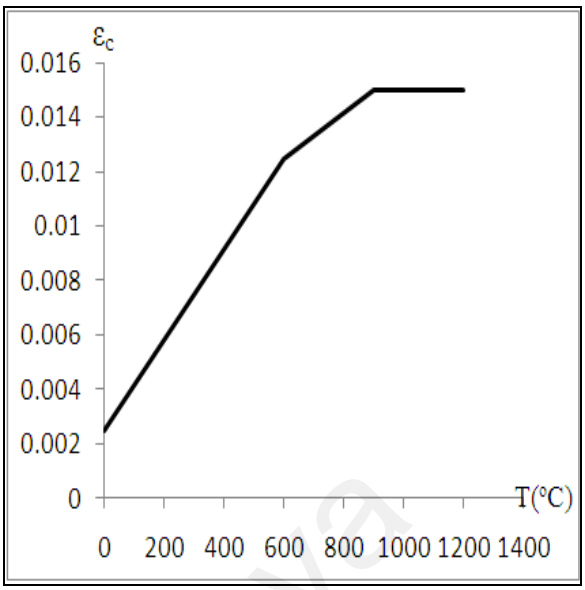

(b) Variation of compressive strain, ε_c with temperature

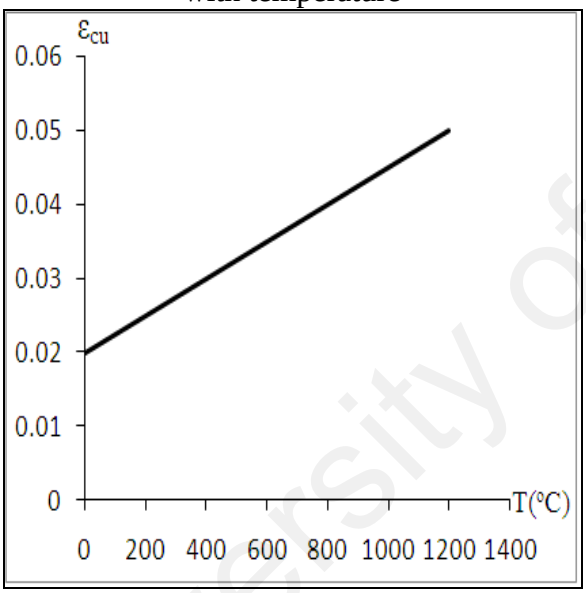

(c) Variation of ultimate compressive strain, ε_{cu} with temperature

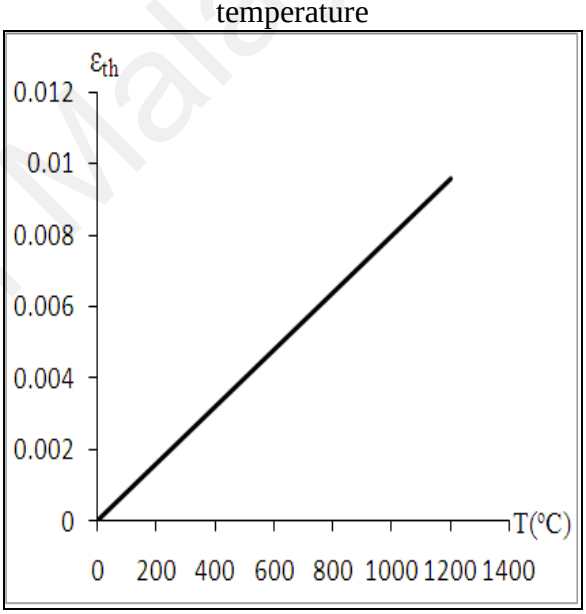

(d) Variation of thermal strain, ε_{th} with temperature

Figure 3.15 Variations of material properties with temperature

The overall depth of slab is 150mm, reinforced with two layers of wire mesh with an area of 193 mm^2/m in both directions using 'stl4' model element. The model considers 1 m effective width of the slab. The concrete slab is connected to the steel beam via shear stud connector, which is modeled as rigid link element 'lnk2' which is assume to be rigid in all direction.

For both steel and composite beam models, DWA connection is used. A detailed geometrical property of this connection is shown in Figure 3.10 (d). The joint is

modeled as ‘jbc2’ element in ADAPTIC with the type of ‘web.angle’ chosen. In showing the effect of welding between angle and column, the parameter of connected members is adjusted to give a very stiff response by increasing the thickness of column and by reducing the distance of bolt line. In this connection model, reduction of material properties of the angle, bolts and connected members with temperature need to be specified according to the order. These material properties are:

I. Ultimate strength
II. Elastic modulus
III. Reduced strain hardening coefficient
IV. Yield stress
V. Strain hardening coefficient

The material property at ambient temperature for this joint is given in Table 3.9. The reduction of this property with temperature taken place in quadrilinear fashion, with a reduction factor suggested by Al-Jabri et. al. (2004) in Figure 3.16 is adopted in this study.

Table 3.9 Material properties for each element at ambient temperature

Yield Strength	
Angle	275 N/mm^2
Bolt	634.32 N/mm^2
Connected member	275 N/mm^2
Ultimate Strength	
Angle	460 N/mm^2
Bolt	827 N/mm^2
Connected member	446.16 N/mm^2
Young Modulus	205 kN/mm^2

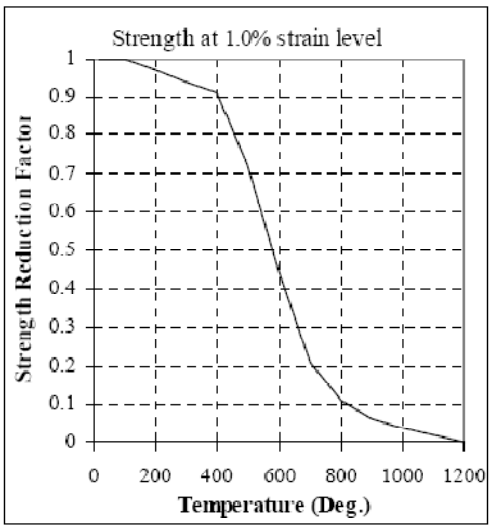

(a) Strength reduction factor

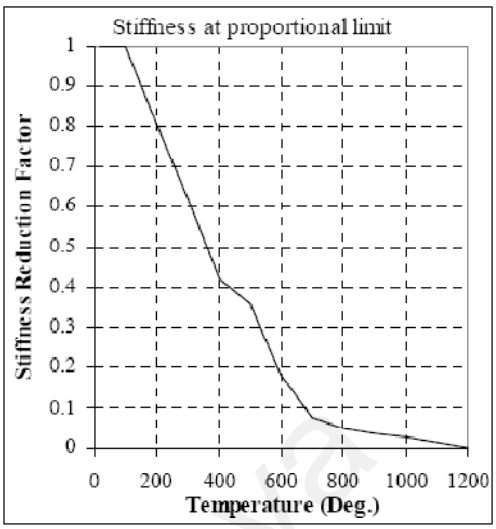

(b) Stiffness reduction factor

Figure 3.16 Degradation of bare-steel connection material properties with temperature (Al-Jabri et al., 2004)

For both steel and composite beam models, the load is applied in two forms, i.e. initial load and time history load. Initial load is taken as uniform load of 9.6 kN/m applied along the secondary beam of 9m span followed by time history loading in the form of time-temperature curve. Figure 3.11 (a) and 3.12 shows time-temperature applied to the connection element and neutral axis of the beam. Uniform temperature across and along the beam is assumed. A sample of data file for steel beam and composite beams are given in Appendix A1 and A2, respectively.

3.4.2.2 Floor System

Simulation of floor system is represented by modeling half of compartment area for panel 1, panel 2 and panel 3 (Figure 3.8). Only half of the compartment was model to simplify the model, taking into consideration of symmetrical support system. The purpose to model overall compartment is to examine the contribution of actual connection behaviour to overall compartment. Beside that this model can be used to study the factors influence the behaviour of compartment which were not recorded in experimental work such as detail response of connection at elevated temperature, even further studies on connection contribution to overall compartment can be studied using

develop model. In the case of floor system, the overall structural response may not be very sensitive to the connection idealization, however a realistic representation of the connections is important in order to assess the local load and deformation demands imposed on the joints.

To model the floor system, a grillage model was used (Figure 3.17), where all steel beams model were modeled as ‘stl4’ which already being explained in isolated modeling with same geometrical and mechanical properties. Sizes of beam and column in compartment can be referred to table 3.5. The steel beams are connected rigidly by 3D link element, ‘lnk3’ to composite floor ‘cbp3’ cubic elasto-plastic 3D beam-column element.

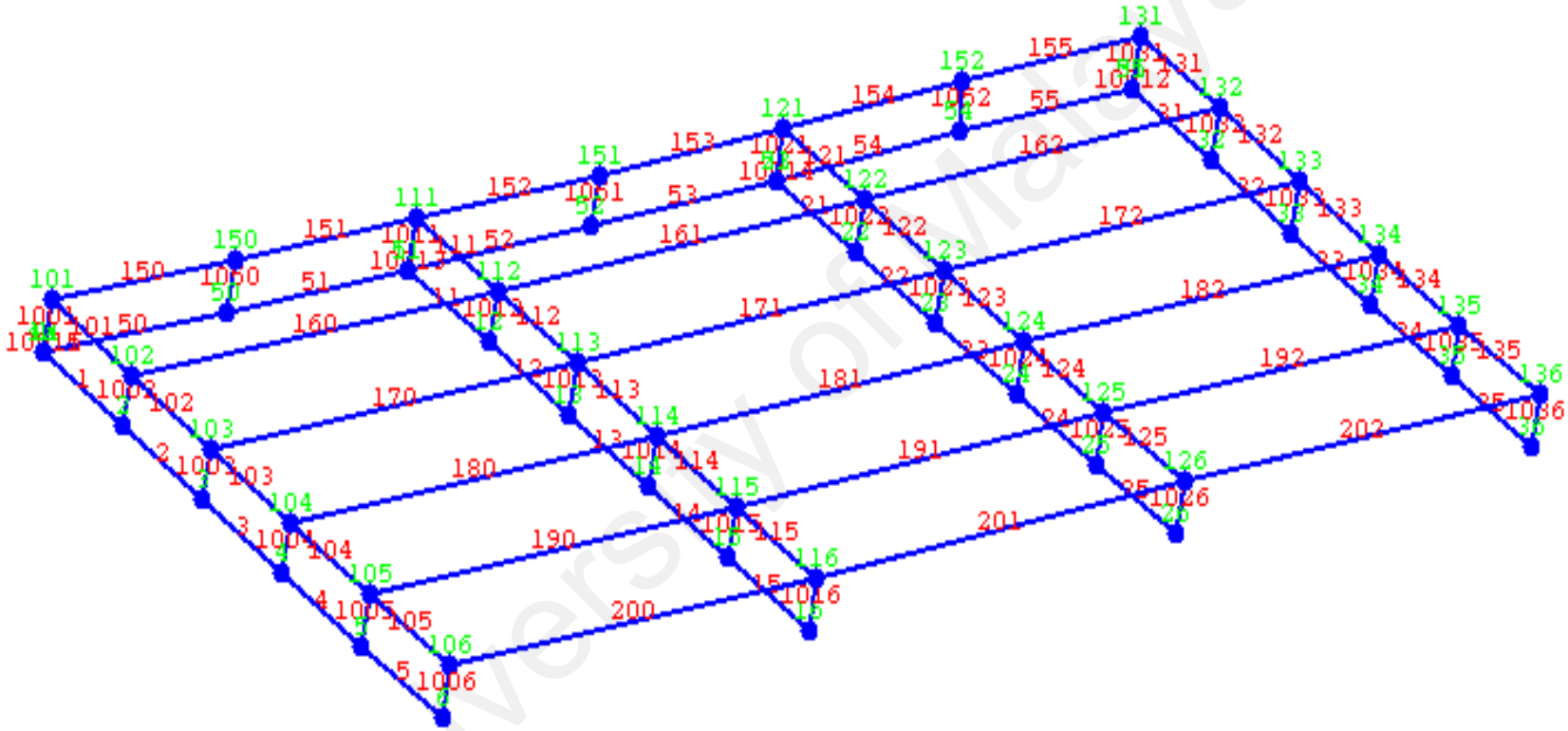

Figure 3.17 Grillage modelling of floor system, (Half of compartment for Panel 1, 2 and 3)

Actual geometrical and mechanical properties were used to model all connections in the compartment which cover DWA connection, seat and web angle and EXTEP connection. These connections used element 'jbc2' with connection type in model refer as 'web.angle', 'combination.web/top/seat' and 'extended.endplate'. The geometrical properties of connection as illustrated in Figure 3.10 and location for each connection is shown in Figure 3.9. The mechanical properties for all connections are the same as DWA explained in isolated beam modelling.

Load applied on the composite floor covers initial load and time history load. The initial load applied from Tapsir (2004) is total of uniform load applied on the floor consist of selfweight 3.6 kN/m^2, life load 3.0 kN/m^2, wall 2.6 kN/m^2 and finishing with 1.0 kN/m^2. Time history load is referred to time-temperature applied at the beam and connection. The time-temperature curve can be referred to Figure 3.11 and 3.12 considering a uniform temperature across and along the steel beam. Time-temperature curve applied on main beam is shown in Figure 3.18, sample of data file for grillage modelling of Gurun Fire Test is given in Appendix A3.

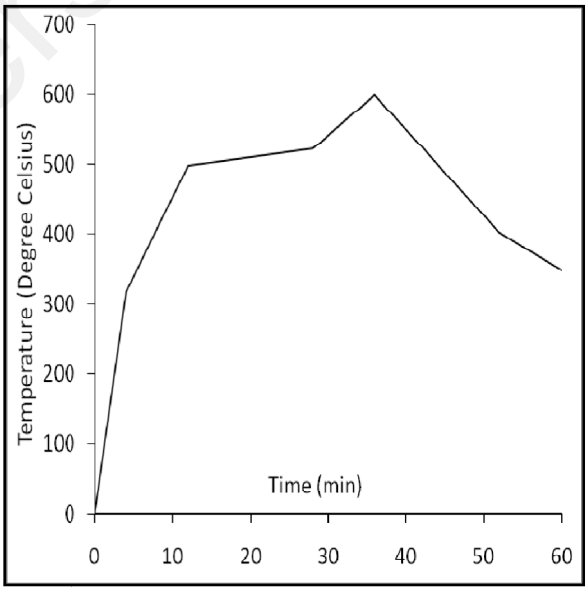

Figure 3.18 Time-temperature for main beam B1, (Tapsir, 2004)

3.5 MODELLING OF COIMBRA SUB-FRAME STEEL FIRE TEST

Six tests on steel sub-frame under natural fire were carried out at the Department of Civil Engineering of the University of Coimbra, Portugal (Santiago, 2008). The main objective of this test is to investigate the influence of different connection typologies on the behaviour of steel sub-structures under fire. The connection types involved in the investigation are header plate, FEP, EXTEP and welded. The dimensions of a steel sub-frame were chosen to reproduce the measured dimensions from the fire compartment of the 7th Cardington fire test (Wald et al., 2006).

3.5.1 Description of Test

A series of sub-frames testing conducted on two thermally insulated HEA300 (290 x 300 x 14mm) cross-section columns and an unprotected IPE300 (300 x 150 x 10.7mm) cross-section beam with 5.70 m free span, supporting a concrete slab (Figure 3.19).

The steel sub-frame was supported by two reaction frames (Figure 3.19) perpendicular to the plane of the frame. Pinned supports at the top of the columns, allowing free axial movement, the bottom of the columns was hinged and fixed to a reinforced concrete footing that was secured in position by Dywidag bars passing through the laboratory strong floor and fixed horizontally using a steel profile connecting both reinforced concrete footings. The geometrical properties for each connection study in the experimental work are shown in Figure 3.20 and the different parameters of beam-to-column configuration for each test can be seen from Table 3.10.

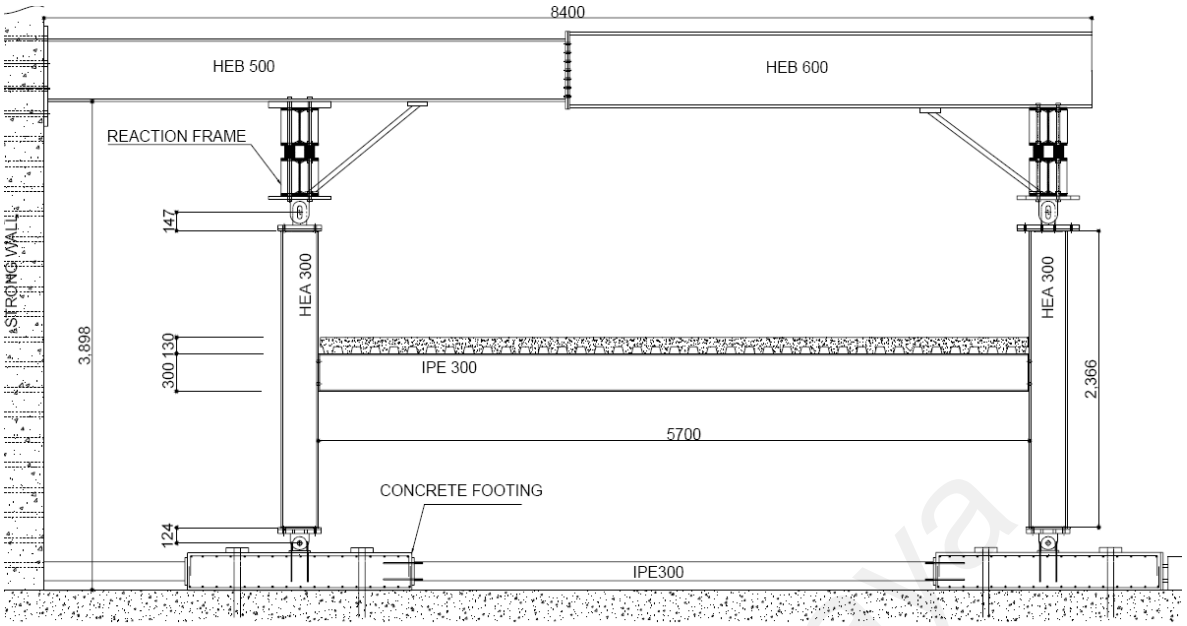

(a)

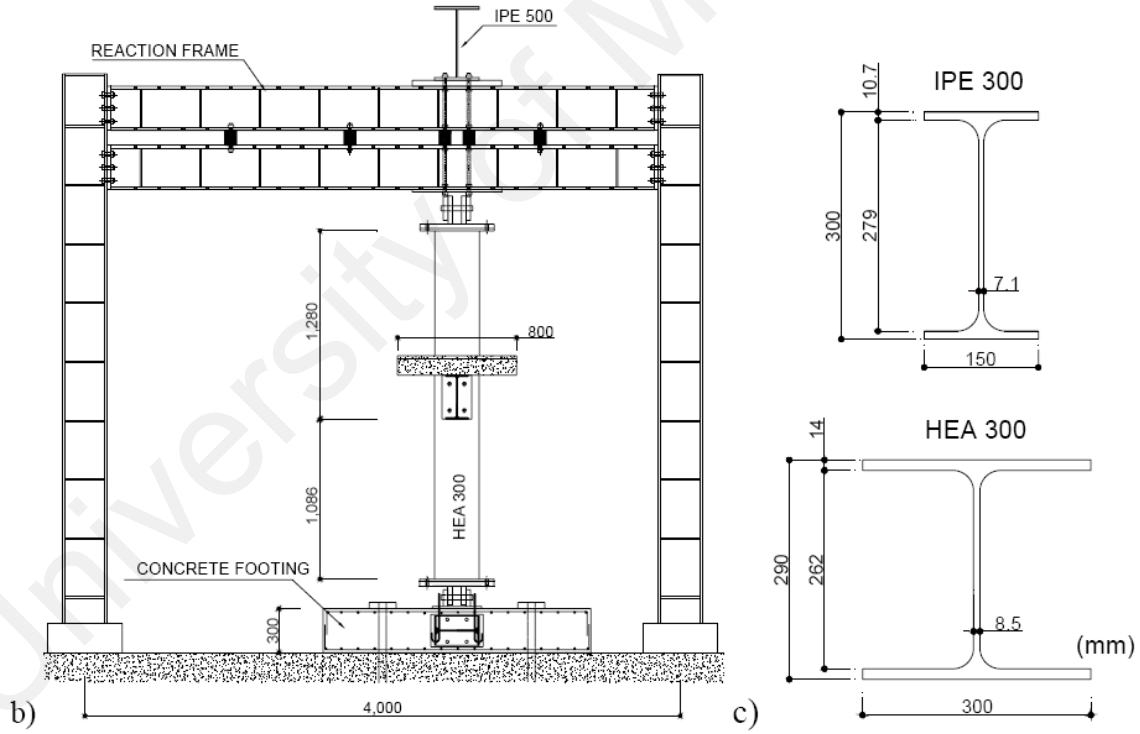

Figure 3.19 General layout: a) longitudinal view; b) lateral view; c) geometry of the profiles, (Santiago, 2008)

Table 3.10 Details of connection used for each test.

Test ID	Joint typology	End-plate dimensions (*mm)* and steel grade	Bolts / Weld (*a*f, *a*w, weld throat thickness, class, *mm*)
FJ01	FEP	(320×200×10); S275	2 bolt row M20, 8.8
FJ02		(320×200×16); S275	2 bolt row M20, 10.9
FJ03		(320×200×16); S275	2 bolt row M20, 8.8
EJ01	EXTEP	(385×200×16); S275	3 bolt row M20, 8.8

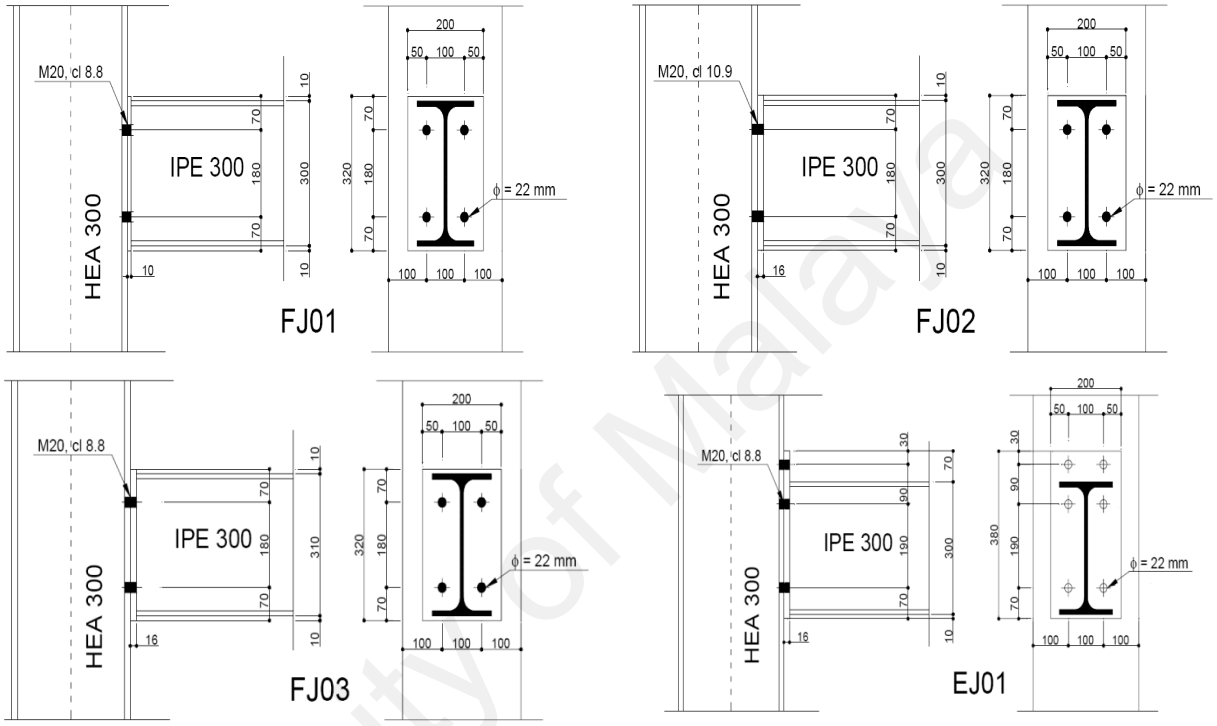

Figure 3.20 Geometrical properties of joints (Santiago, 2008)

Two different steel grades were used, S275 for the end plates and S355 for the steel sections and according to the European Standard EN 10025-1 (2004), the steel qualities are S275JR and S355J2G3. No coupon tests were carried out for the end-plate material. Reduction factor of mechanical properties for steel grade S355J2G3 are shown in Table 3.11. For bolt, two different classes of M20 bolts were used in the experiments, 8.8 and 10.9. Table 3.12 shown mechanical properties of bolt at ambient temperature.

Table 3.11 Mechanical properties of the structural steel S355J2G3.

n(test)	Temp.(^{o}C)	E(GPa)	$k_{E,\theta}$	*Fy*(Mpa)	$k_{y,\theta}$	*Fu*(Mpa)	$K_{u,\theta}$	ε_u(%)	Z(%)
3	20	209	1.00	385	1.00	491	1.00	30.8	63.2
2	100	190	0.91	436	1.13	492	1.00	12.0	66.9
2	200	195	0.93	347	0.90	553	1.13	13.5	52.5
2	300	177	0.84	277	0.72	557	1.14	21.8	48.8
2	400	173	0.83	266	0.69	493	1.00	18.4	52.1
2	500	120	0.58	231	0.60	370	0.75	19.2	39.3
2	600	108	0.51	182	0.47	221	0.45	16.0	27.5
1	700	41	0.19	95	0.25	173	0.35	27.4	73.4
3	800	18	0.09	41	0.11	51	0.10	37.1	37.2
2	900	2	0.01	23	0.06	37	0.07	23.7	18.8
2	1000	1	0.00	19	0.05	29	0.06	21.8	18.0

Table 3.12 Characteristic values for the bolts at room temperature.

n test	Bolts	E(GPa)		*Fy*(Mpa)		*Fu*(Mpa)		ε_u(%)	
		μ	*COV*(%)	*μ*	*COV*(%)	*μ*	*COV*(%)	*μ*	*COV*(%)
6	8.8	211.2	2.8	657.7	7.7	834.2	1.8	1.42	25.6
3	10.9	211.6	1.0	860	0.2	1078.7	0.2	1.30	32.2

For all experimental tests, the steel sub-frame were applied by a mechanical loading of two points on the beam top flange, 700 mm to either side of the beam mid-span and each concentrated load was equal to 20 kN. The beam after that was applied with thermal loading shown in Figure 3.21.

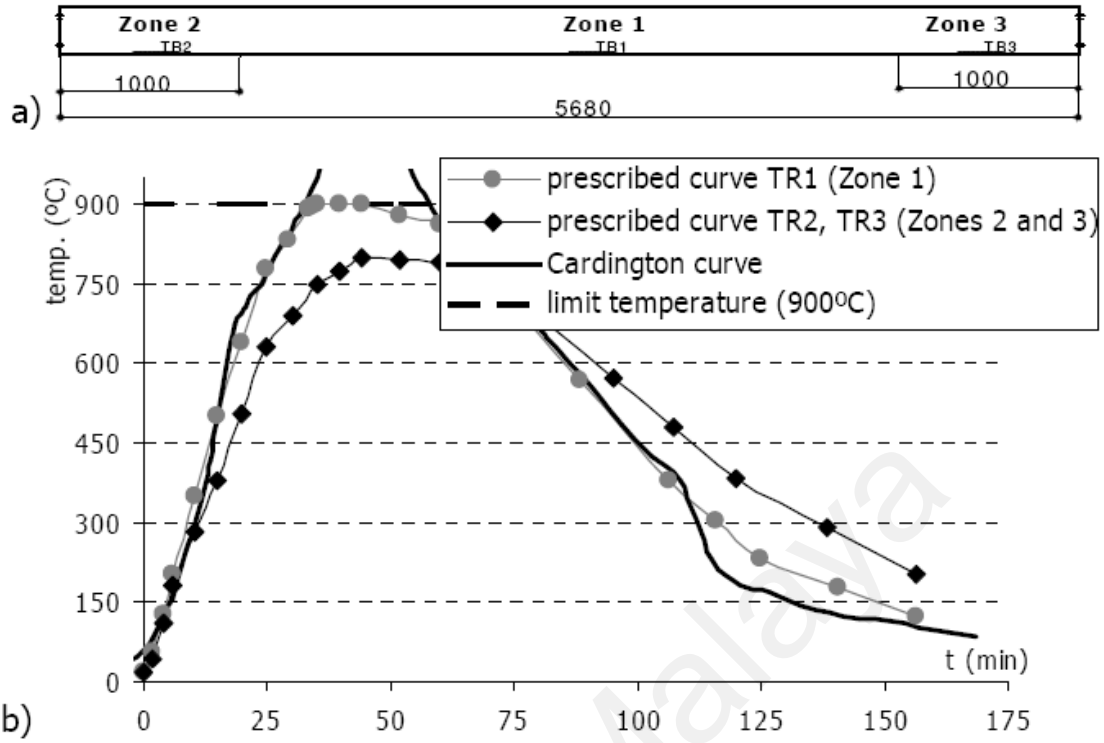

Figure 3.21 Thermal loading: a) definition of heating zones; b) time-temperature curves (Santiago, 2008)

3.5.2 Modelling of Sub-Frame with ADAPTIC Finite Element Program

In the simulation work on steel sub-frames, tests conducted by Santiago (2008) were used. All tests used beam and column sizes of IPE 300 and HEA300 (Figure 3.20). For both beam and column the same cubic elasto-plastic 2D beam-column element, 'cbp2' was used with 'stl4' bilinear material model. Yield strength value of 385 N/mm^2 and Young Modulus of 209 kN/mm^2 are adopted at ambient temperature. Reduction of these material properties with temperature is given in Table 3.13, and a simplified linear reduction of Elastic Modulus and yield strength is characterized in Figure 3.22. Figure 3.23 shows thermal strain of steel as a function of temperature.

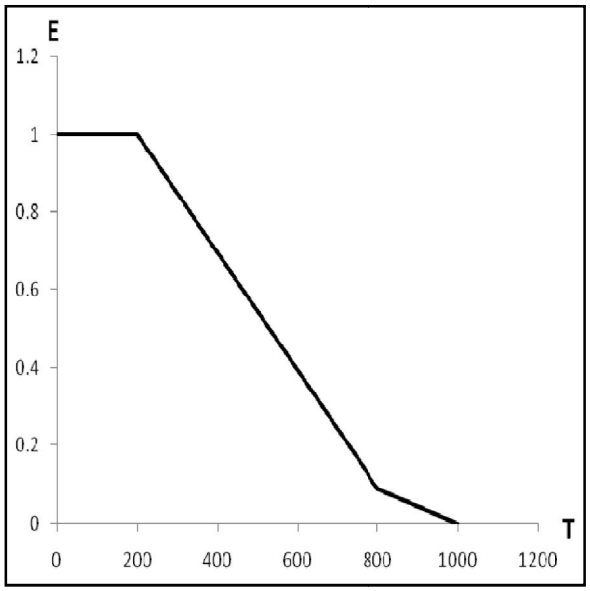

(a) Reduction of Elastic Modulus, E with temperature (^oC)

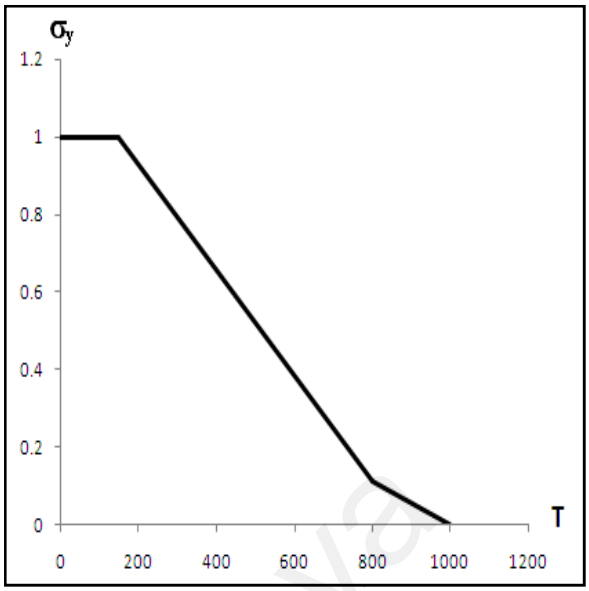

(b) Reduction of Yield Stress, σ_y with Temperature(^oC)

Figure 3.22 Reduction of material properties with temperature

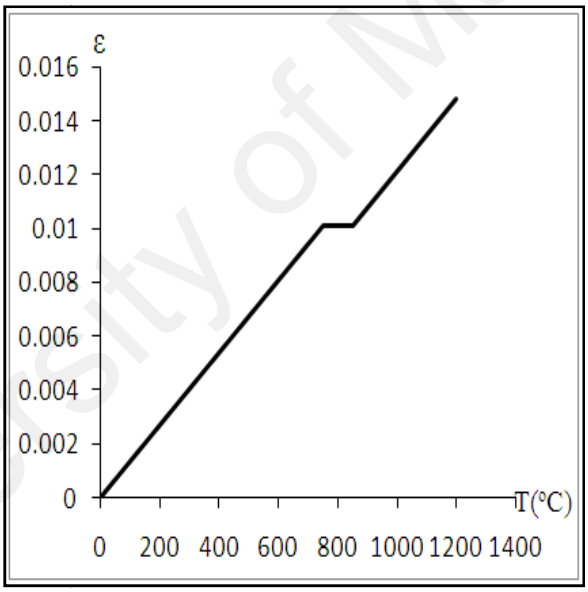

Figure 3.23 Thermal strain, ε of steel as a function of temperature

Four tests on end plate connection were used for validation. Table 3.10 shows the parameter variation used for FJ01, FJ02, FJ03 and EJ01. Geometrical properties of connection for each test can be referred to Figure 3.20. Element used for flush endplate connection is 'jbc2', with 'flush.endplate' type of model. Boundary condition at the top of column is restraint vertically and fully fix at the bottom of column. The mechanical properties used in the joint element are shown in Table 3.13. The reduction of this

property for end plate with temperature taken place in quadrilinear fashion, with a reduction factor suggested by Al-Jabri et al. (2004) is adopted in this study. Reduction factor of bolt properties followed equation 2.1 proposed by Kirby (1995) for bolt grade 8.8 and no record of strength reduction factor for bolt grade 10.9. Lastly, for connected member the reduction factor of mechanical properties followed Table 3.5 by simplified the curve to quadrilinear fashion.

Table 3.13 Material properties for each element at ambient temperature

Yield Strength	
End plate	275 N/mm^2
Bolt grade 8.8	657.7 N/mm^2
Bolt grade 10.9	860 N/mm^2
Connected member	385 N/mm^2
Ultimate Strength	
End plate	460 N/mm^2
Bolt grade 8.8	834.2 N/mm^2
Bolt grade 10.9	1078.7 N/mm^2
Connected member	491 N/mm^2
Young Modulus	
End plate	205 kN/mm^2
Bolt grade 8.8	211.2 kN/mm^2
Bolt grade 10.9	211.6 kN/mm^2
Connected member	209 kN/mm^2

Loading applied consists of initial loading of concentrated load of 20 kN located at 700 mm to either side of the beam mid-span and uniform load from floor equal to 2.1 kN/m. After that, a time-history load was applied at centre of the beam element according to zone (Figure 3.21). Time-temperature curve applied is represented in Figure 3.24 (a) at mid-span of the beam at zone 1 and Figure 3.24 (b) at zone 2 and zone 3. The model were assumed to have a linear temperature gradient across the beam section as shown in Table 3.14. The gradient is measured based on temperature difference between the top flange of beam and the bottom flange, divided by the depth of the beam.

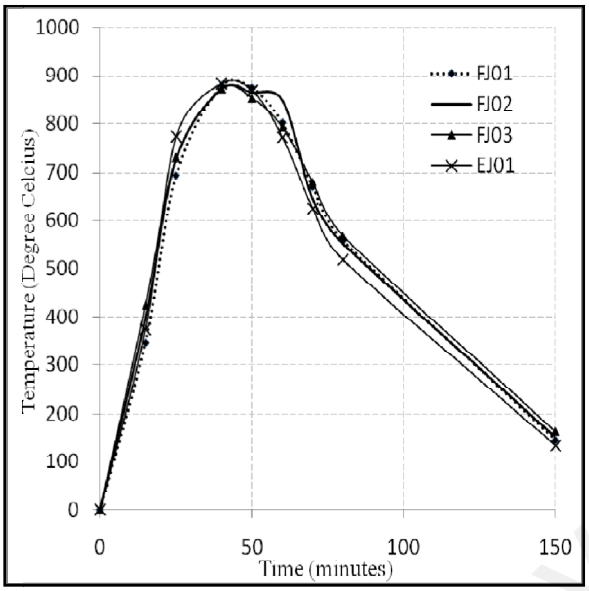

(a)

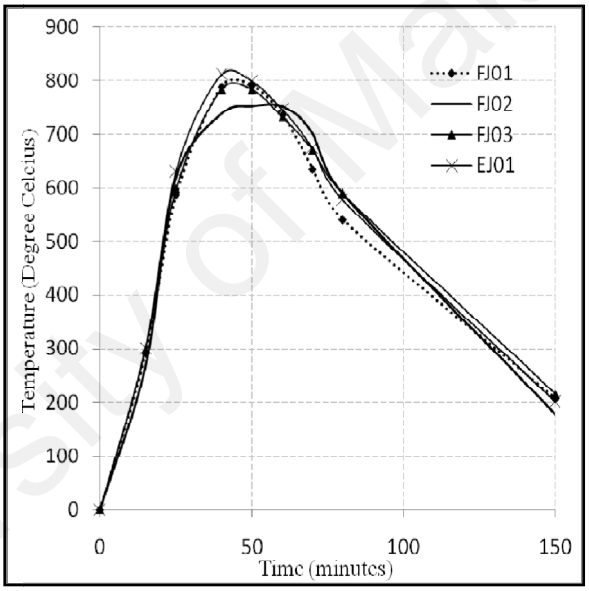

(b)

Figure 3.24 (a) Temperature at mid-span of beam (b) Temperature at beam element in zone 2 and 3

Table 3.14 (a) Temperature gradient across mid-span of beam (b) Temperature gradient across beam element in zone 2 and 3

(a)

Test	Temperature (^{o}C)							
	15min.	25min.	40min.	50min.	60min.	70min.	80min.	150min
FJ01	-670	-686.7	-356.7	-216.7	-116.7	-173.3	-176.7	183.3
FJ02	-310.0	-16.7	-80.0	-73.3	-66.7	-360.0	-316.7	-110.0
FJ03	-633.3	-506.7	-380.0	-273.3	-190.0	-130.0	-170.0	93.3
EJ01	-736.7	-573.3	-423.3	-376.7	-253.3	-110	-113.3	-86.67

(b)

Test	Temperature (^{o}C)							
	15min.	25min.	40min.	50min.	60min.	70min.	80min.	150min
FJ01	-423.3	-463.3	-250.0	-230.0	-170.0	-300.0	-336.7	16.7
FJ02	-546.7	-530.0	-283.3	-373.3	-320.0	-203.3	-233.3	73.3
FJ03	-460.0	-410.0	-320.0	-296.7	-303.3	-340.0	-350.0	30.0
EJ01	-590.0	-550.0	-260.0	-276.7	-310.0	-303.3	-310.0	16.7

3.6 CONCLUDING REMARKS

Connection model explained in this chapter used component-based method. The connection model was developed by Ramli Sulong (2005) and implemented in advanced nonlinear finite element analysis program, ADAPTIC (Izzuddin, 1991). Detail description of the procedure and capabilities of the connection model covering six connection types were explained in this chapter.

The simulation work in this thesis covers DWA connection, TSWA, EXTEP connection and TSA connection in order to further validate the connection model at ambient temperature using ADAPTIC software. At elevated temperature, DWA connection in composite floor system in Gurun Fire Test and end plate connection on sub-frame test by Santiago (2008) were used in validation works. In Chapter 4, the results of validations work against selected experimental data are presented and discussed.

CHAPTER 4.0 VALIDATION STUDIES

4.1 INTRODUCTION

This chapter presents validation studies of steel joints/structural system at ambient and elevated temperature. At ambient condition, simulation of isolated connection covering four types of connections i.e. DWA, TSA, TSWA and EXTEP connections were developed. Simulation work of connection at ambient temperature is carried out to further validate the accuracy of component based method, (Ramli Sulong, 2005) before further verification at elevated temperature.

At elevated temperature, validation of the joint response in composite floor system and steel subframe was carried out based on Gurun Fire Test, (Tapsir, 2004) and Coimbra Fire Test, (Santiago, 2008), respectively. The type of connection involve in Gurun Fire Test were DWA, EXTEP and, seat and web angle connections. Focus of validation result is given to double web angle due to existing of recorded data. For the Coimbra Fire Test, the focus is given to EXTEP and FEP connection.

4.2 AMBIENT TEMPERATURE CASE

Verification of connection model at ambient temperature was carried by comparing with recently existing fire tests including DWA connection (Yang and Lee, 2007), TSWA connection (Danesh et al., 2007), EXTEP connection (Girao Coelho, 2004 and Maggi et al., 2005) and TSA connection (Pirmoz et al., 2009).

4.2.1 Double web angle connections

Results shown in Figure 4.1 illustrate the comparison between experiment and finite element modeling. Table 4.1 compares result between numerical and experimental results for prediction of initial stiffness and capacity at ambient temperature. Data recorded that relative error for initial stiffness are 0.37, 0.18 and 0.01 for 3 layers, 4 layers and 5 layers. On the other hand relative errors for moment capacity are 0.28, 0.24 and 0.13. The discrepancy of the modeling is depending on the accuracy of mechanical and geometrical property applied for the modeling. Result shows that with an increasing row of bolt, initial stiffness and moment capacity of the connection will also increase.

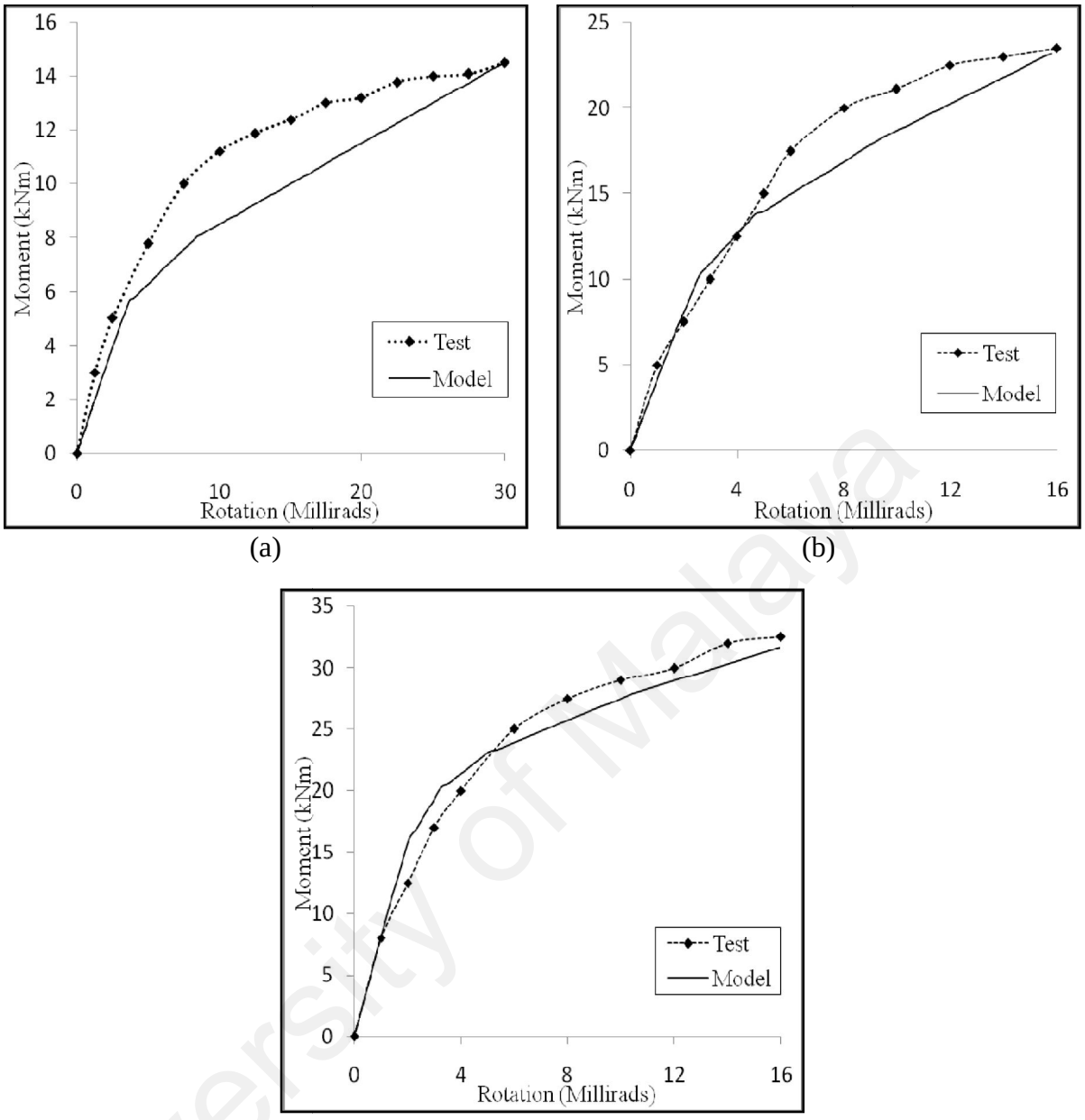

Figure 4.1 Comparison of moment-rotation curve of DWA connection for (a) three bolt row (3B-L-7-65), (b) four bolt row (4B-L-7-65), and (c) five bolt row (5B-L-7-65).

Table 4.1 Comparison between numerical and experimental results for the prediction of initial stiffness and capacity at ambient temperature

Layer	Initial Stiffness			Moment capacity		
	Numerical (kNm/rad)	Experimental (kNm/rad)	Relative error	Numerical (kNm)	Experimental (kNm)	Relative error
3	1549.18	2469.00	0.37	6.83	9.45	0.28
4	3968.99	4841.20	0.18	12.08	15.86	0.24
5	8111.05	8052.00	-0.01	20.89	24.00	0.13

4.2.2 Top-seat-web angles

Moment-rotation curve of the connection model were compared with experimental result. Result for comparison between experiment (Danesh et al., 2007), and modell in Figure 4.2 can be summarised in Table 4.2. The differences between the models is the thickness of top and seat angle of the connection and also bolt diameter as explained in chapter 3. The initial stiffness is overestimated for 8S1 and 8S2, these discrepancies particularly for angle connections are due to bolt slippage/bolt pretension, residual stresses and imperfections (which are not included in the model). In addition, other general inaccuracies in the overall shape of the curves are attributed to the tri-linear idealisation in the model of the nonlinear response of individual components, and possible discrepancies in material and geometric properties.

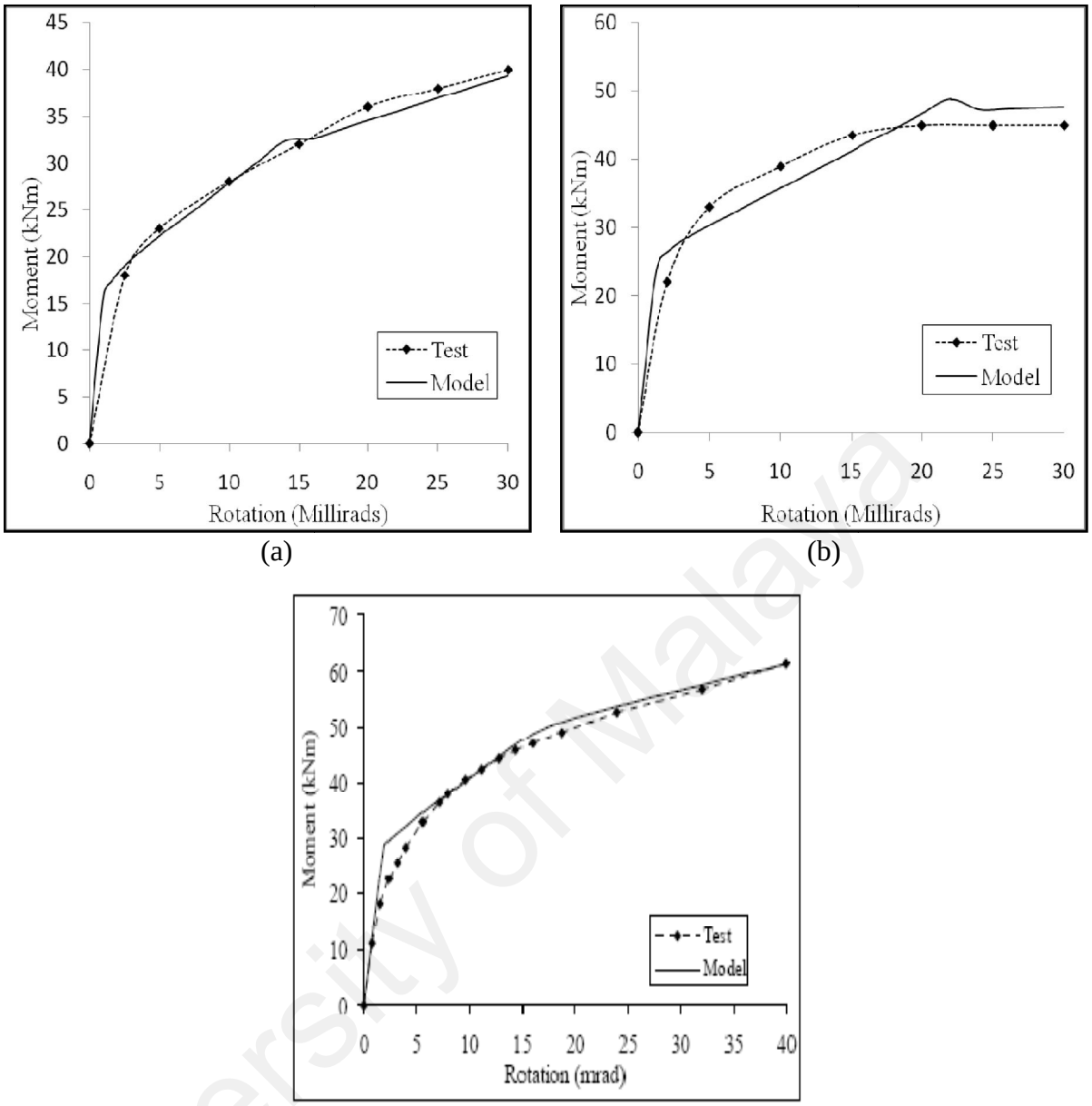

Figure 4.2 Moment-rotation response of TSWA connection for (a) 8S1 and (b) 8S2 (c) 8S9 (Danesh et al., 1987).

Table 4.2 Comparison between numerical and experimental results for the prediction of initial stiffness and capacity at ambient temperature

Author	Initial Stiffness			Moment capacity		
	Numerical (kNm/rad)	Experimental (kNm/rad)	Relative error	Numerical (kNm)	Experimental (kNm)	Relative error
8S1	9150.00	6400.00	-0.43	26.25	26.18	0.00
8S2	20000.00	16666.67	-0.20	44.60	42.25	-0.06
8S9	14450.00	14800.00	0.02	39.43	37.51	-0.05

4.2.3 Extended end plate connections

Validation of EXTEP test by Girao Coelho (2004) is illustrated in Figure 4.3. Same as validation work for TSWA by Danesh et al. (2007), the initial stiffness is overestimated due to bolt slippage/bolt pretension, residual stresses and imperfections (which are not included in the model). Relative error for both model are shown in table 4.3.

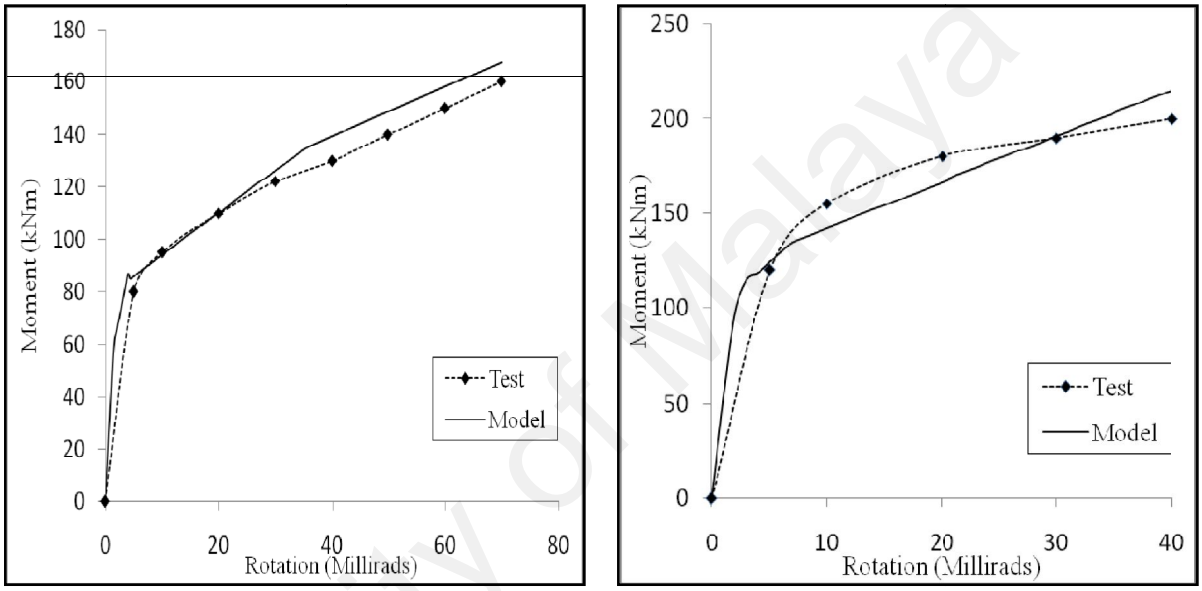

(a) (b)

Figure 4.3 Moment-rotation response of EXTEP connection for (a) FS1, (b) FS2, (Girao Coelho, 2004)

Table 4.3 Comparison between numerical and experimental results for the prediction of initial stiffness and capacity at ambient temperature

Model	Initial Stiffness			Moment capacity		
	Numerical (kNm/rad)	Experimental (kNm/rad)	Relative error	Numerical (kNm)	Experimental (kNm)	Relative error
FS1	38187.50	34660.00	-0.10	103.37	96.00	-0.08
FS2	38333.33	24000.00	-0.60	117.53	160.00	0.27

4.2.4 Top and seat angle connection

Three connection tests by Pirmoz et al. (2009) were selected to validate, this connection type i.e. A1, A2 and W00. The initial stiffness for TSA connection for model A2 and W00 (Pirmoz et al., 2009), are in good agreement with the test result. For model A1 a high stiffness builds in the modeling which represents about triple of the actual behaviour under testing. The model for A2 and W00 are closely predicted the behaviour with test result under elastic phase. Under plastic range all models closely represent the behaviour of experimental result. The geometrical properties of angle significantly influence the result of initial stiffness in the model.

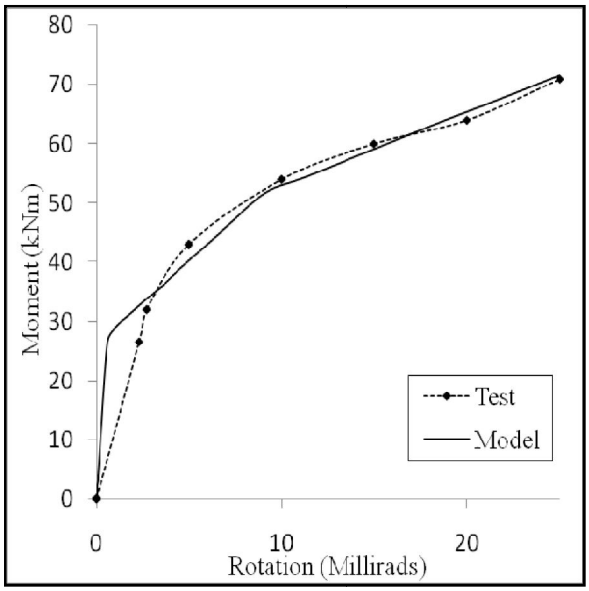

(a)

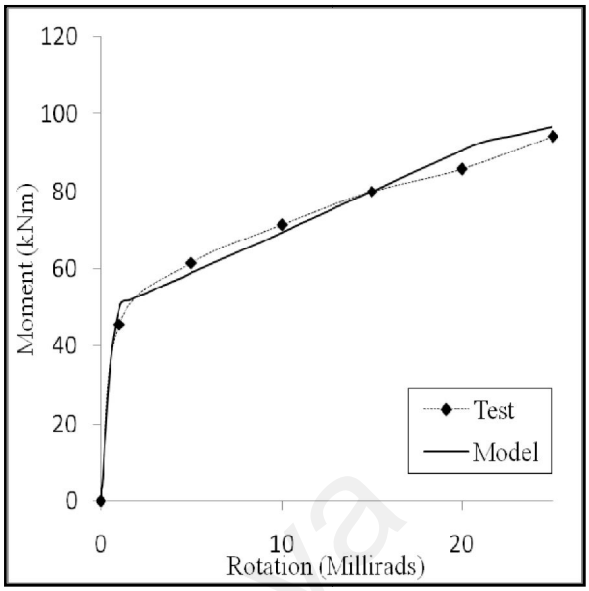

(b)

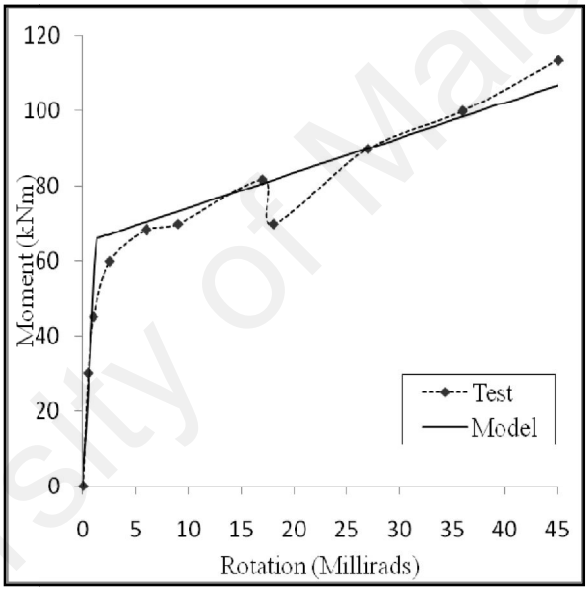

(c)

Figure 4.4 Moment-rotation response of TSA connection for (a) A1, (b) A2 and (c) W00 (Pirmoz et al., 2009)

Table 4.4 Comparison between numerical and experimental results for the prediction of initial stiffness and capacity at ambient temperature

Specimen	Initial Stiffness			Moment capacity		
	Numerical (kNm/rad)	Experimental (kNm/rad)	Relative error	Numerical (kNm)	Experimental (kNm)	Relative error
Test A1	45351.47	11521.74	-2.94	41.43	47.32	0.12
Test A2	47830.19	45720.00	-0.05	50.77	58.13	0.13
W00	54798.76	54799.51	0.00	66.00	62.70	-0.05

4.3 BEHAVIOUR OF CONNECTION AT ELEVATED TEMPERATURE

Validation of connection model on isolated connection under fire was reported in (Wang, 2007; Hu, 2008; Yu, 2008; Saedi Daryan and Yahyai, 2009; Burgess et al., 2009 and Chen et al., 2009). In this study, the focus is to investigate the connection response in composite floor system for locally produced steel product based on Gurun Fire Test. The focus is also given to examine the connection behaviour in steel sub-frame under natural fire based on Coimbra Fire Test.

4.3.1 Composite Floor System

4.3.1.1 Simulation of Gurun Fire Test-Isolated Beam

In this section the results of isolated steel and composite beam modeling as described in section 3.4.2.1 is validated against the test result. It is acknowledged that very limited validation studies can be conducted based on Gurun Fire Test since the recorded data is very scarce. The validation shown here is between the model for steel and composite beam against recorded mid-span deflection of secondary beam B2, (refer Figure 3.8).

Comparison of mid-span deflection of beam B2c (Figure 3.8) between the test result and isolated steel and composite beam model is shown in Figure 4.5. The test results given maximum deflection of 182 mm at 32 min, corresponding to maximum temperature of 556.2 ^{0}C. For the isolated steel beam model, very large deflection is observed i.e. 425 mm, whereas the isolated composite beam model given a maximum deflection of 138 mm. This is due to rigidity of the link on the secondary beam connected to composite floor. For both models, maximum deflections occur at 12 min, which correspond to maximum temperature recorded in the test as shown in Figure 3.7 (a). The deflection reduces thereafter due to cooling effect and distribution of internal forces to adjacent members.

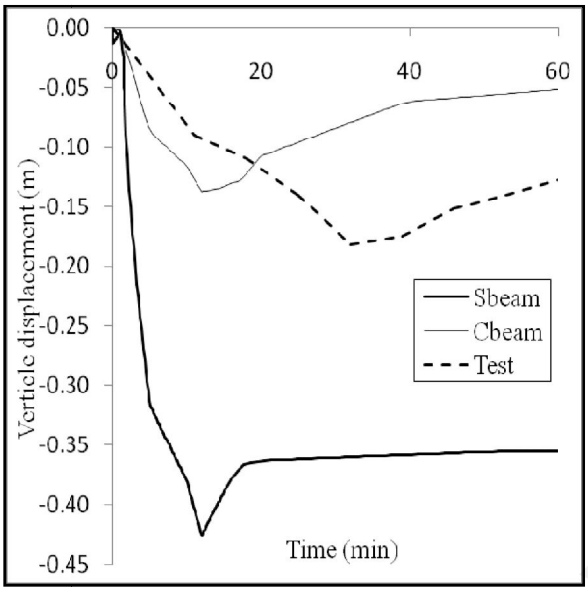

Figure 4.5 Comparison of vertical displacement for different modeling method

Very large discrepancies were observed between the two models and the test results because the actual structural elements under fire is the floor system, where restraint of structural elements in 3-Dimension may contribute to the overall response of the compartment area under fire. The different between the models also due to rigidity of the link on the secondary beam connected to composite floor. Validation of the floor system model against experimental result will be presented in next section.

4.3.1.2 Overall Simulation - Compartment of Gurun Fire Test

In this section, the results of floor system modelling as explained in section 3.4.2.2 is compared againt the test result. The 3-D model of the floor system with arrangement of the node and element numbering is shown in Figure 3.17. Verticle displacement obtained at the mid-span of the secondary beam (i.e. node 16 and 26) is compared against the test result as shown in Figure 4.6. Very close prediction of maximum displacement is obtained between the model and test results. However, there is quite large differences on the time when maximum displacement occurs between the model and test results. The model gives maximum displacement at the time when maximum temperature was applied on the compartment area, which is acceptable in

principle. The time-temperature curves applied on the member are shown in the temperature profile in Figure 3.11 and 3.12.

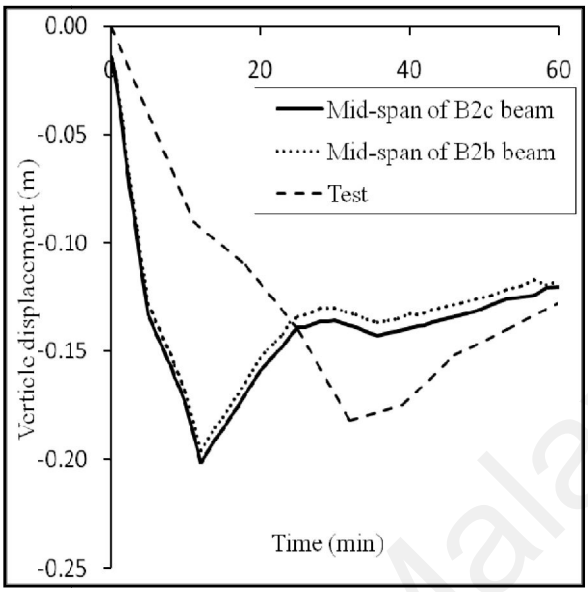

Figure 4.6 Vertical displacements against time at internal secondary beam in grillage modeling

In this compartment area, there are three connection types used i.e. TSWA connection to connect main beam to column C2 in minor axis, DWA connection to connect the secondary beam to the main beam and EXTEP connection to connect the main beam to column C2 in major axis. All geometrical properties involve in the modelling can be referred to Figure 3.5. Response of these connection at elevated temperature applied in the compartment area are given in Figure 4.7 to Figure 4.10.

Figure 4.7, shows time-axial force for different connection type in compartment. From the result, EXTEP resists the higher axial forces which is approximately 4000 kN followed by top-seat-web angle and lastly web angle connection. In compression region, the capacity of the connection is governed by column web component in compression. By calculation, the capacity of column web in compression is about 3,300 kN, the beam capacity in compression is near to 3,918 kN an additional of compression stiffener at column web is added to resist compression forces which govern an extra

support on the compression component of EXTEP connection. Axial force increases rapidly in heating phase and start to reduce until it reaches a constant value which is governed by connected members. In Figure 4.8, time-moment curve indicates that double web angle connection behaves almost like a pin connection with a small value of moment resistant due to small capacity of connection's component i.e. angle in bending.

Time-axial displacement curve in Figure 4.9 illustrates that double web angle connection gives higher displacement due to lower resistance compared to other connections in the compartment. Besides that, this connection was exposed to higher temperature compared to other connections. The response of time-rotation curve as given in Figure 4.10 shows that under heating phase, DWA connection and EXTEP connection rotate continuously with increasing temperature until they reach cooling phase the EXTEP gives a constant value of rotation. A reduction of rotation for DWA can be seen under cooling phase. The rotation of EXTEP connection drops after a certain time which is resulting to tensile forces resist by the connection. Different with TSWA start to rotate when it comes under tensile force due to the response of the critical component of the connection.

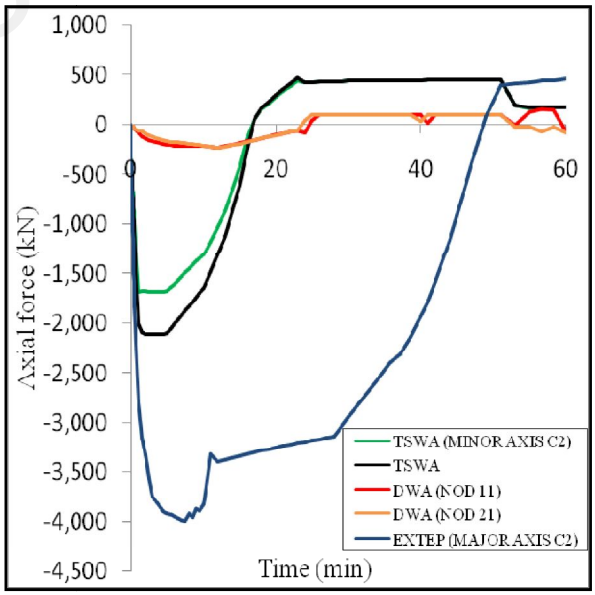

Figure 4.7 Time-axial forces for different support condition in the compartment area

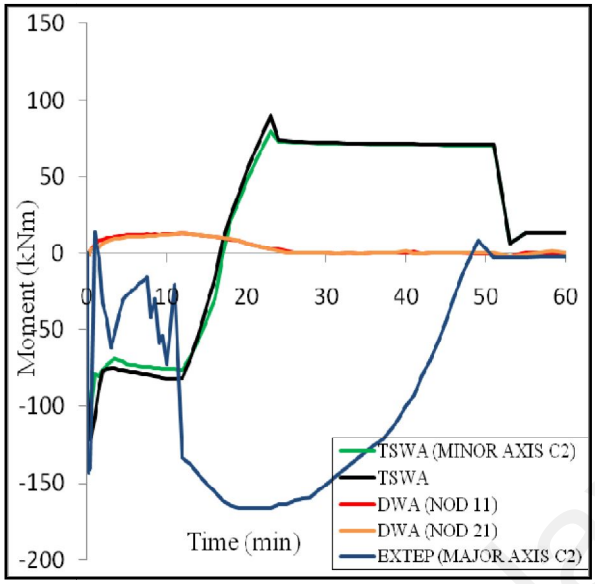

Figure 4.8 Time-moment for different support condition in the compartment area

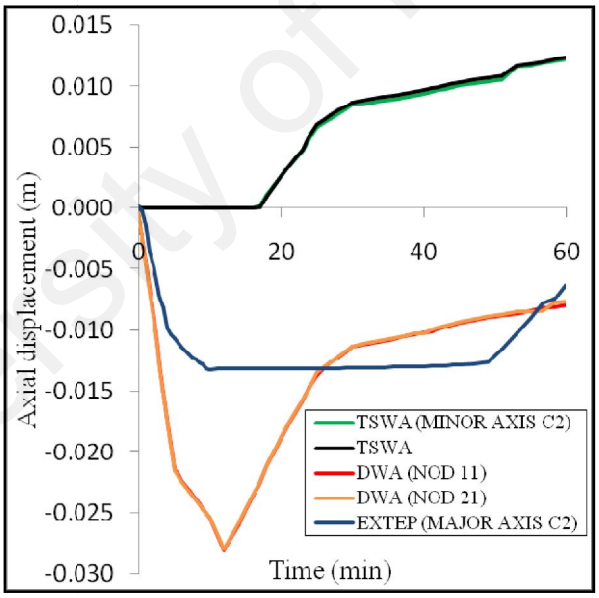

Figure 4.9 Time-axial displacements for different support condition

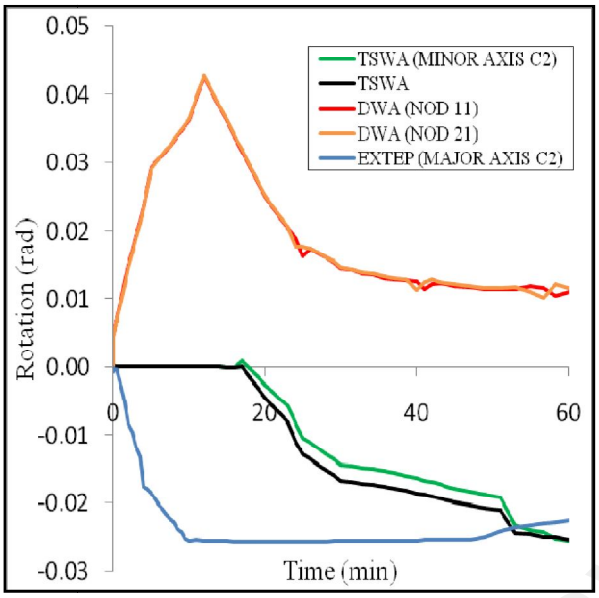

Figure 4.10 Time-rotation for different support condition

As recorded in the experiment, the temperature of the connections exposed to fire increased gradually with the room temperature. An increase in the room temperature caused the connection to expand and loses its strength. During the cooling phase of secondary beam (Time ≥ 12 minutes, Figure 3.12), the bolts and angle cleats connecting the two secondary beams to the main beams sheared off. Very high tensile forces caused the shearing of the end connections. This is because allowance for expansion and contraction have not been provided. All other connections have performed well during the fire (Tapsir, 2004).

4.3.2 Steel Sub-Frame

4.3.2.1 Simulation of model at ambient temperature

Before embarking into a complex frame analysis, it is important to ensure that the connection can be modeled accurately. Due to unavailable experiment result, the connection model is validated against the numerical model by Santiago (2008) for a series of connections applied in the sub-frame fire test. These connections include FEP connection (FJ01, FJ02 and FJ03) and EXTEP connection (EJ01). Figure 4.11 shows comparison result of the model with numerical analysis carried by Santiago (2008). Details of EXTEP connection model were explained in sub-chapter 3.5.2. Comparisons of the results show that the model can closely simulate the results of numerical model carried by Santiago (2008b).

From Figure 4.11 also, it can be seen that with an increasing number of bolt rows, moment resistance of the model also increases. For the EXTEP connection, Figure 4.11(d) shows that moment-rotation in the elastic range overestimated the stiffness obtained by Santiago's model due to resistance from extended parameter of the connection. EXTEP model demonstrates high moment resistance with lower rotation response at the beginning of analysis in elastic phases; the discrepancy is due to parameter of extended bolt. Santiago (2008) reported that for almost all bolted end-plate joints, bolt failure was reached before steel deformed; although it should be mentioned that before the bolt failure, yielding of several zones of the joint was observed.

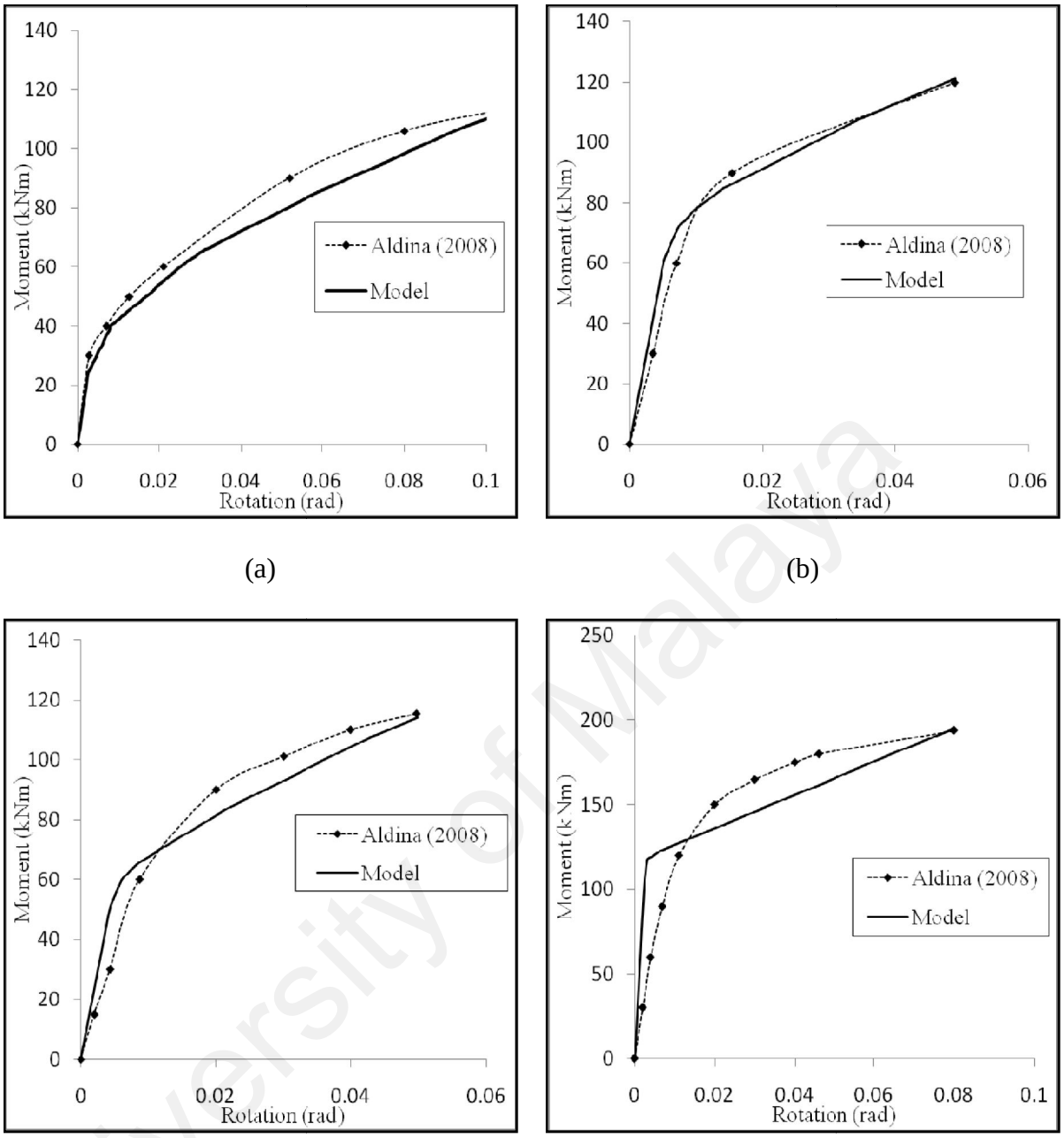

Figure 4.11 Moment-rotation curve for 2 bolt rows (a) FJ01 (b) FJ02 (c) FJ03 and 3 bolt rows (d) EJ01

4.3.2.2 Connection response at Elevated Temperature

The development of Finite Element model for the sub-frame structure (Santiago, 2008a) is explained in section 3.5.2. Figure 4.12 to 4.13 show comparison of Finite Element Model with experimented results of steel sub frame using end plate connection i.e FEP and EXTEP connection. In Figure 4.12, the model can closely predict the experiment results. The deflection for FJ02 and FJ03 is lower than FJ01 due to end plate thickness, where FJ01 use 10 mm thickness which influences the respond for end plate

in bending. Deflection of mid-beam increases gradually at the beginning of analysis for all models until it reaches at T = 24 min, the deformation keeps increasing rapidly after that due to reduction of strength and stiffness with increasing temperature. The recovery of the deformation can be seen in cooling phase (Time > 50 min).

Experimental test by Santiago (2008a,c) shows that most of the beams were able to sustain the load with reduced deflection up to 10 min ($\theta_0 < 150$ ºC); during this stage, the deflection was mainly due to the mechanical loading. Beyond that, due to the loss of stiffness, the mid-span deflection increased gradually. Beyond 20 min, a further rise in temperature ($\theta_0 > 550$ ºC) led to a progressive run-away of the beam deflection as the loss of stiffness and strength accelerated. In the case of the FJ02, EJ01 a maximum recorded deflection of 375 mm was approximately reached (these values were measured already during the cooling phase). Once the cooling phase started, the heated beams began to recover strength and stiffness from an inelastic state, together with a reduction of thermal strains. This induced tensile axial forces and the reversal of the deflection. Because of the limited range of the displacement transducers (400 mm), FJ01 curve was incomplete where a maximum deflection of 428 mm was measured at the end of the fire.

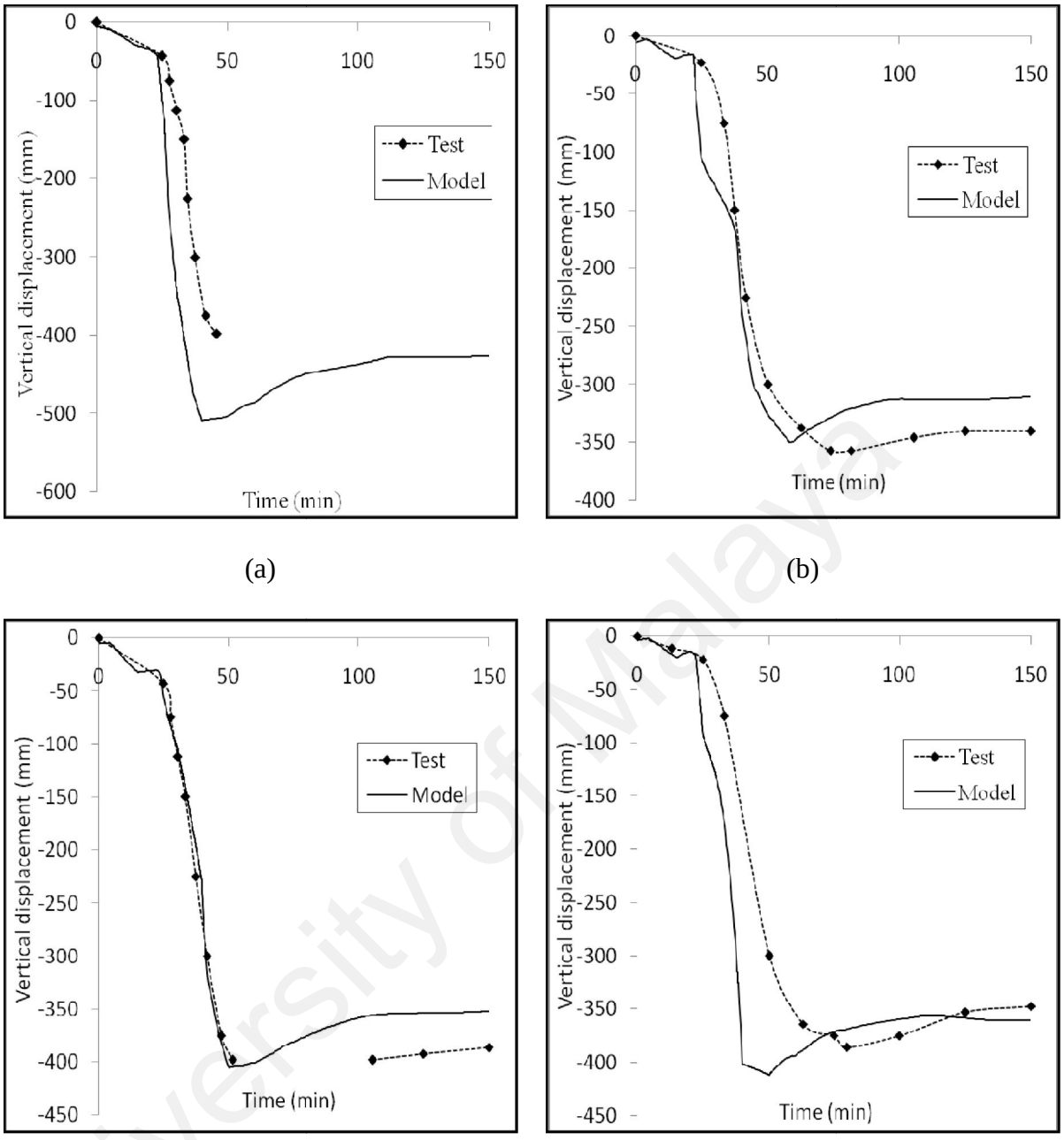

Figure 4.12 Time againts mid-span of beam displacement for (a) FJ01 (b) FJ02 (c) FJ03 and (d) EJ01

Figure 4.13 illustrates rotation of connections vs time. The rotation increases with an increasing bending force until it reaches cooling phase. Beyond this stage, the rotation reduces until the end of analysis because the beam behaviour is governed by the connection tension resistance.

Figure 4.14 then shows a comparison of axial force response vs time between test and developed model. The tests results demonstrated the appearance of large tensile forces during the cooling phase (see Figure 3.21 for Time-Temperature curve); they

also demonstrated that these forces may result in failure of the joint. It can be seen that in the compression region the connection model illustrated a good agreement with the test result until it goes into the tension region. In the tension region, the capacity of the model underestimated the experimental value due to the onset of yielding of the critical component under tensile forces. For the experimental results, there are reserve strength due to strain hardening of the material and redistribution of the applied forces to other active components, which resulted in higher capacity. For all developed models, the maximum value of compressive force is near to 500 kN compared to test result where each specimen showed that the maximum value of compressive force between 600 kN to 800 kN. For all models, the change from compression force to tension force begins when it comes to cooling phase.

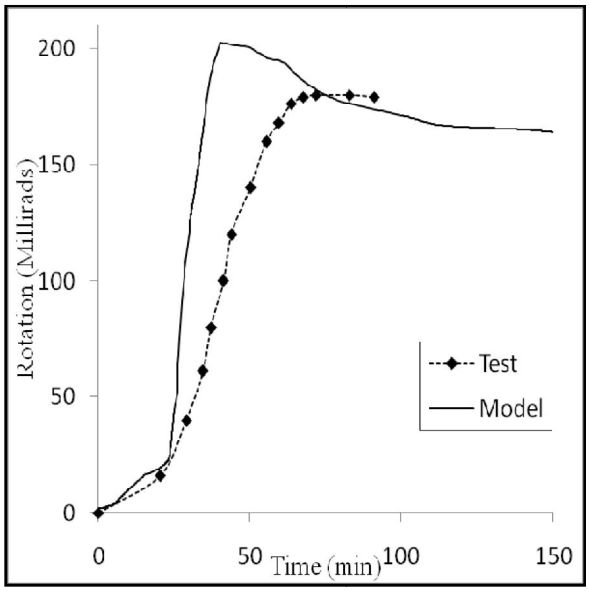

(a)

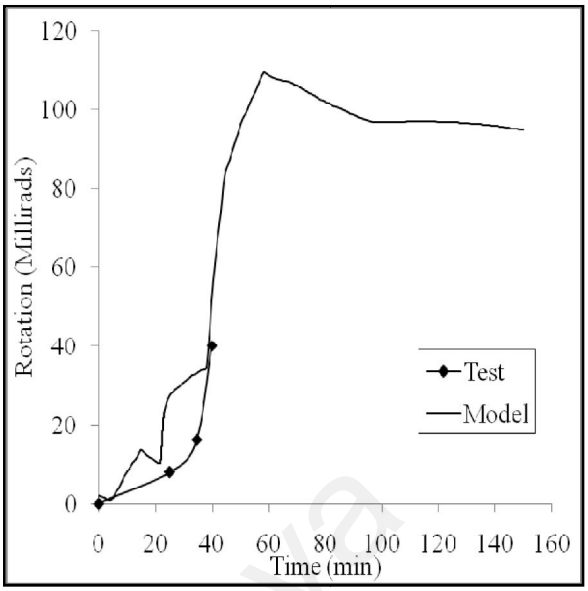

(b)

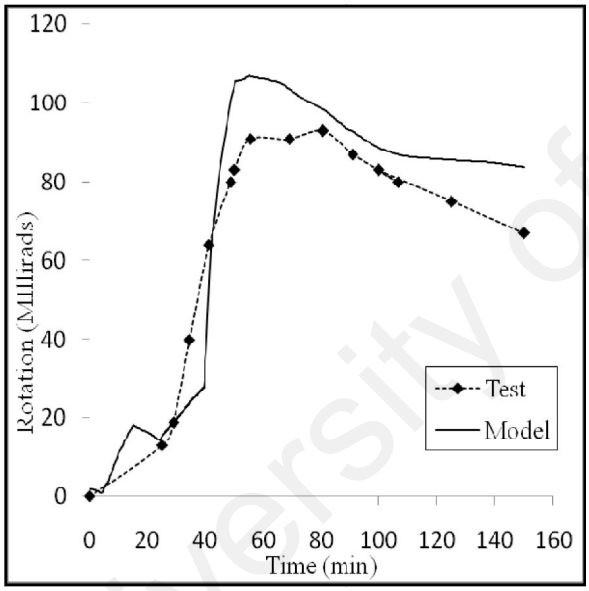

(c)

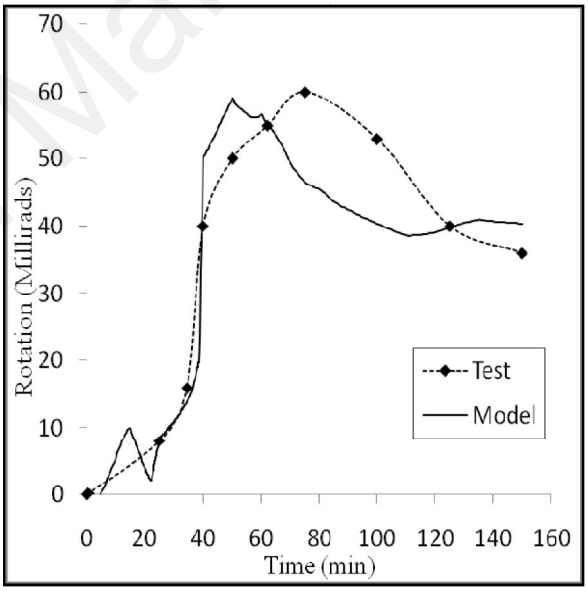

(d)

Figure 4.13 Rotation of connection for (a) FJ01 (b) FJ02 (c) FJ03 and (d) EJ01

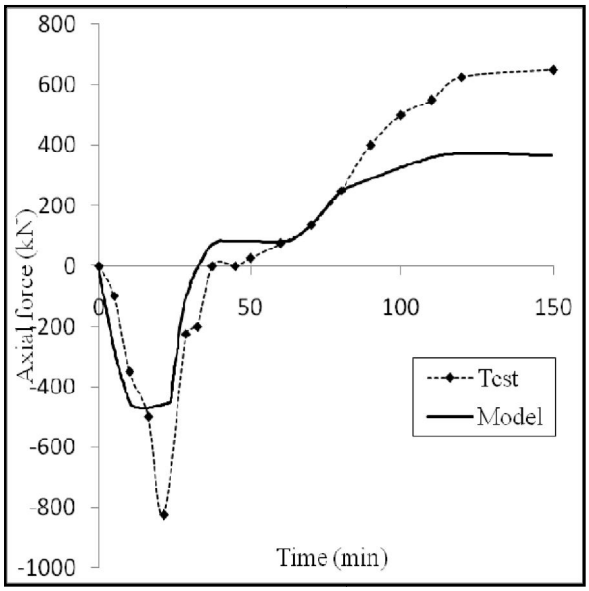

(a)

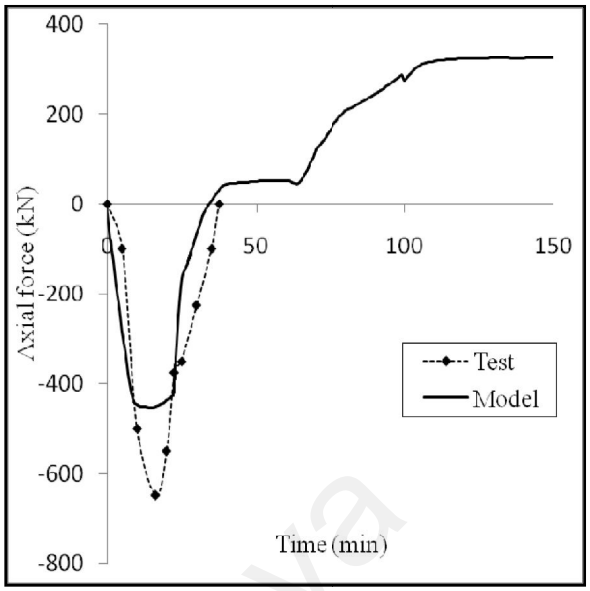

(b)

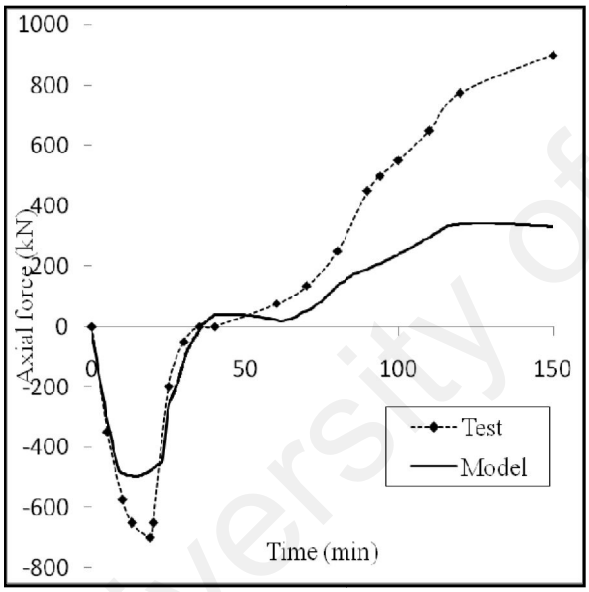

(c)

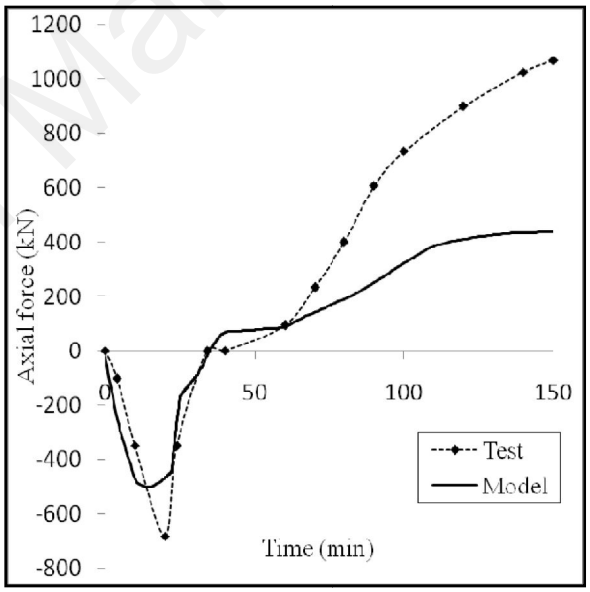

(d)

Figure 4.14 Axial force in the connection (a) FJ01 (b) FJ02 (c) FJ03 and (d) EJ01

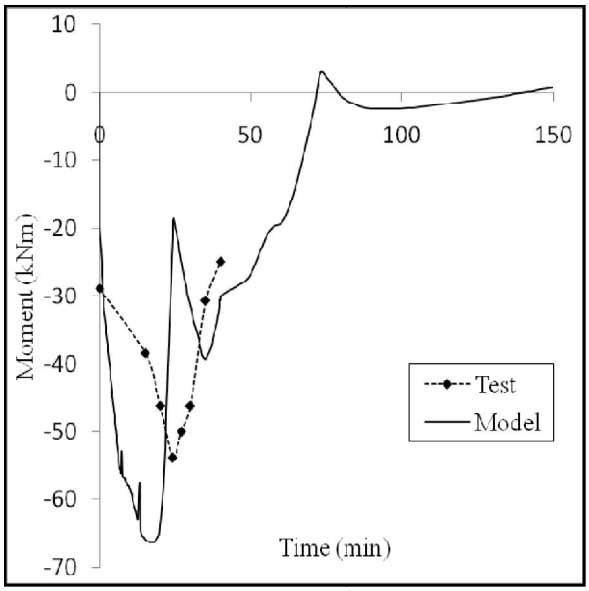

(a)

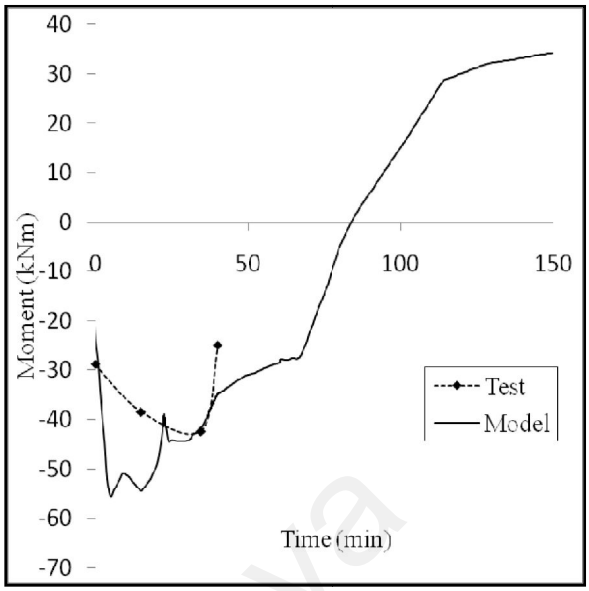

(b)

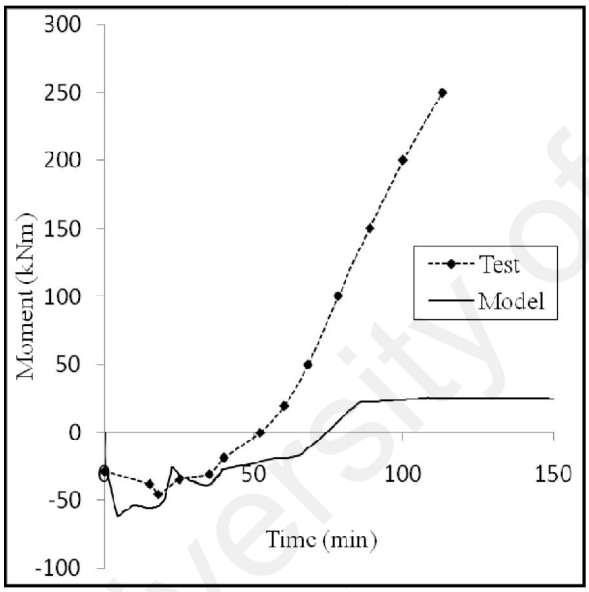

(c)

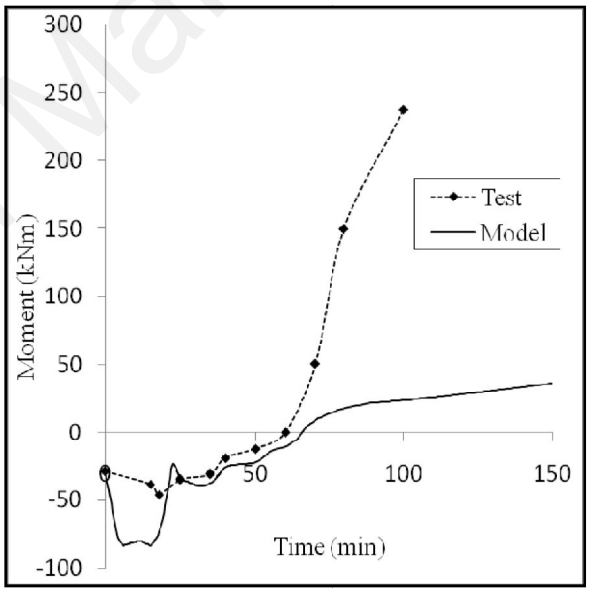

(d)

Figure 4.15 Moment of connection (a) FJ01 (b) FJ02 (c) FJ03 and (d) EJ01

As explained by Santiago (2008c) and also shows in Figure 4.12 to Figure 4.15 the analysis of model can divided into different stages. In Phase 1 ($t < 9$ min) the thermal expansion was converted into thermal stresses that increase the level of axial compression and hogging moment without large displacements and rotation. Phase 2, starts approximately after 9 min of the fire exposure, corresponds to the increase of the internal forces. In Phase 3 ($26 \text{ min} \leq t < 45$ min) a decrease of the internal forces is noted because of the material strength degradation and large deflections. In Phase 4 (45

min ≤ t ≤55 min), the beam behaviour changes from bending to catenary action and tensile forces are developed. Bending moments reduce and become similar to those observed at room temperature. Phase 5 (t > 55 min) corresponds to the cooling phase – increasing of the tensile forces and sagging moment because of the recovering of strength and stiffness.

Based on the measured axial and vertical displacements of the beam and the axial stiffness of the beam and end-restraints from the test, estimation of the axial force in the beam and the bending moment at the joints were developed Santiago (2008c). The measured moment in tensile force keep increasing base on the capacity of beam near to joint area. As for the model, the moment is limited by the connection moment, due to failure of critical component in tension zone.

4.4 CONCLUDING REMARKS

Validations of the connection model develop in ADAPTIC Finite Element programs were carried out by comparing with available experimental results at ambient and elevated temperature. At ambient temperature, closed prediction of the key parameters within the force-deformation or moment-rotation response was obtained for all connection types. The validation work at ambient temperature is important as it serves as a base in developing the model at elevated temperature. From the validation study the discrepancy of the modeling is depending on the accuracy of mechanical and geometrical properties applied on the model. In addition, for angle connections the discrepancies particularly are due to bolt slippage/bolt pretension, residual stresses and imperfections which are not included in the model. At elevated temperature, the analytical simulations also provided a faithful representation of the experimental results, particularly for endplate connections. They were considered as either isolated joints or incorporated within structural sub-frames. For angle connections, although there was good agreement between the analysis and tests, there is room for further investigation of the behaviour and refinement of the model in order to capture the influence of active components at elevated temperature more accurately. This simulation work is important in further understanding the behaviour of semi-rigid connection and collects unrecorded data from experimental test. Beside this component based method can be an alternative way in understanding the behaviour of the connection under elevated temperature in economical way. Gurun Fire Test was validated by considering a model as isolated connection, isolated steel beam and overall compartment. The overall compartment model which taken into consideration the influences of connected members, temperature on each members and accurate representation of boundary condition have yielded to closed prediction of the actual response. For the verification of connection response in steel sub-frame, in general, some discrepancies between the experimental

results and numerical simulations were observed. These are largely attributed to inevitable inaccuracies in defining the temperature-dependant material properties, this can overcome by determine the actual material properties from experimental test. In addition to other factors which were not covered in the model such as bolt slippage, residual stresses and imperfections. Overall, this investigation highlighted the need for further experimental studies on the response of connections at elevated temperature, particularly angle configurations, in order to provide data for additional validation. From overall validation, the models were capable of capturing the main response characteristics of a number of typical connection configurations under elevated temperature conditions, including the possible influence of boundary condition, loading applied and mechanical properties applied on the model. Based on validation work carried in this chapter, parametric studies were performed in order to identify several factors which gave influence to steel connection under fire.

CHAPTER 5.0 PARAMETRIC STUDIES

5.1 INTRODUCTION

Due to the complexity and diversity of steel joints, as well as to the expense of such large-scale testing, it is impractical to conduct sufficient high-temperature tests over a wide range of joint types and assemblies. It is practical to develop a model using numerical method to study the parametric influence of the structural behaviour.

Studies have proved that numerical model can validate the actual behaviour of joint under fire. Some of researches carried out numerical studies using component based method to validate and investigate the performance of joint in steel sub-frame under fire condition such as Santiago (2008) and other development based on isolated connection (Al-Jabri, 2006; Block, 2007 and Wang, 2007).

This chapter focuses on investigating wide range of parameter affecting the behaviour of joint/structures under fire based on a series of parametric studies. Experimental data of Gurun Fire Test and Coimbra Fire Test as mentioned in chapter 4 were utilized in this parametric studies.

Studies on ductility behaviour of connection at elevated temperature were presented at the end of this chapter. Existing researches focus on the behaviour of structure at ambient temperature but there is a need to identify the requirement and ductility behaviour of connection at elevated temperature. This chapter will also discuss on the requirement of ductility in the existing Eurocode. Deformation capacity and ductility demand on isolated beam by using five different types of connections are analysed at elevated temperature. This is followed by the overall joint ductility in a sub-frame at elevated temperature.

5.2 ISOLATED BEAM

This section focuses on the parametric studies on isolated steel and composite beam under elevated temperature. Several factors are considered such as influence of supported conditions, temperature effects, connection geometric properties and loaded ratio.

5.2.1 Influence of Support Conditions

Three support conditions are considered namely rigid, pin and actual connection used in Gurun Fire Test. As mentioned in section 3.4.1, the type of connection used to connect the secondary to main beam is DWA connection. The isolated beam model explained in section 3.4.2 is adopted to investigate the influence of axial and rotational restraint of the joint on the beam response.

In order to understand the structural response under fire conditions, the knowledge of connection and beam capacities at elevated temperature should be considered. Based on the beam geometric and material properties given in section 3.4.2.1, the beam plastic moment capacity and axial tension/compression capacity at ambient temperature are calculated. For the connection, based on connection model in ADAPTIC, the moment capacity, axial capacity in tension and compression are computed. By using strength and stiffness reduction factor adopted from Al-Jabri et.al (2004), the reduction of moment and axial capacities for both beam and connection at elevated temperature are calculated and presented in Table 5.1 and Figure 5.1.

Table 5.1 Results for connection and beam moment and axial force capacity, Strength and stiffness reduction factors for S275 steel at 1% strain level and proportional limit, respectively (Al-Jabri et al., 2004)

T (^oC)	Moment capacity, Mc (For connection)	Moment capacity, Mc (For beam)	Strength reduction Factor	Axial compression and tension capacity, Fx (For beam)	Axial tension capacity, Fx_t (For connection)	Axial compression capacity, Fx_c (For connection)
100	6.37	391.2425	1.000	2281.675	164	9950
200	6.18	379.891	0.971	2215.506	164	9950
300	5.98	368.159	0.941	2147.056	159	9650
400	5.79	356.813	0.912	2080.888	154	9350
500	4.31	282.086	0.721	1645.088	150	9050
600	2.82	172.538	0.441	1006.219	111	6730
700	1.34	80.596	0.206	470.025	72.8	4410
800	1.07	43.037	0.110	250.984	34.5	2090
900	0.708	23.475	0.060	136.901	27.6	1670
1000	0.213	15.650	0.040	91.267	20.7	1250

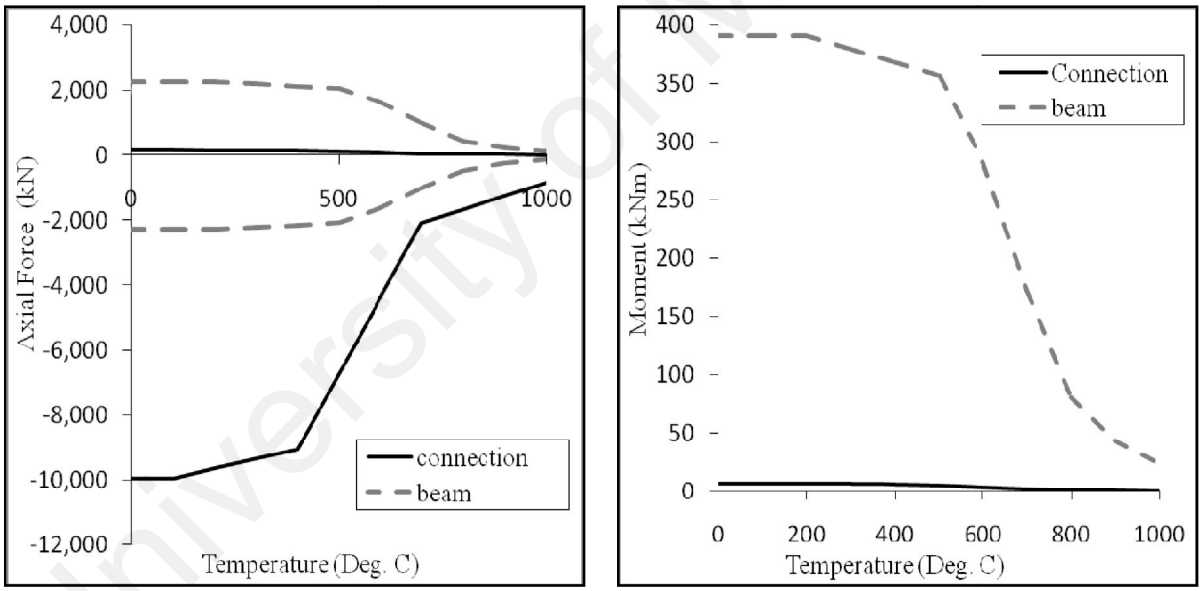

(a) Axial force (b) Moment

Figure 5.1 Member capacities

For a restrained secondary steel beam connected with three different supported conditions under applied initial load and temperature loading as described in 3.4.2.1, the vertical displacement obtained at the mid-span of the beam is shown in Figure 5.2. The actual connection type which is DWA is shown as ‘dwa’ curve. For pinned and rigid

connection, a 2D joint element (jel2) with uncoupled axial, shear and moment action is adopted in ADAPTIC model.

The result shows the importance of accounting for actual connection type, as the beam response is substantially influenced by the supported condition. Due to very low capacity of the actual connection, the beam respond incorporating DWA connection is similar to the behaviour of pinned connection under compressive force. Further, under tensile force the capacity of the beam with DWA is very low due to failure of connection's component i.e. angle in bending (as shown in Figure 5.3). As the temperature applied to structural member's moves to cooling stage, the connection is subjected to tensile forces which resulted in lower axial resistance, shown in Figure 5.3, where Time > 18 min. Due to lower tensile capacity of the connection in relation to earlier yielding of the most critical component in the connection at elevated temperature, very small recovery of the beam displacement is observed. Variations of mid-span moment of the beam and connection moment with different support conditions are shown in Figure 5.4 and Figure 5.5 respectively.

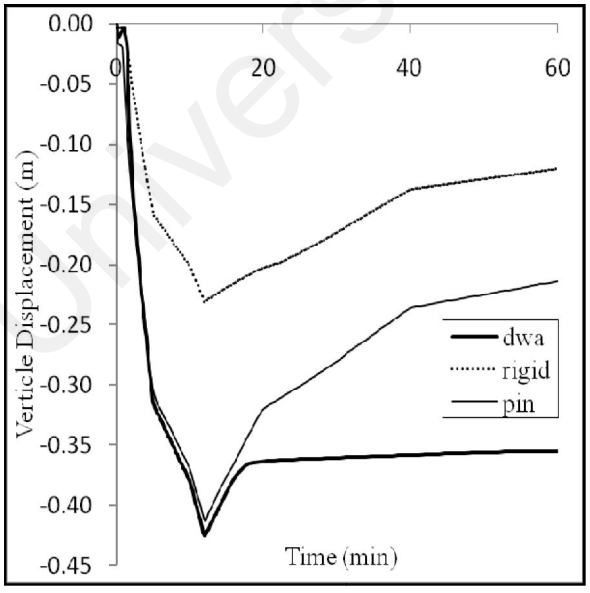

Figure 5.2 Test result for vertical displacement against time at mid span of steel beam and for different support condition

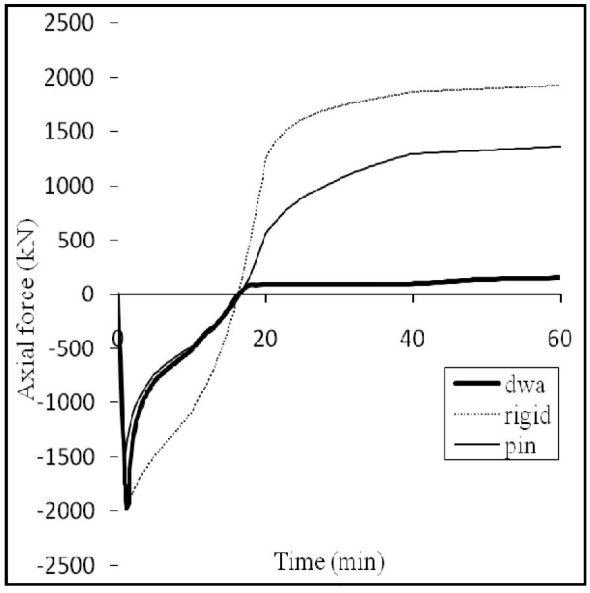

Figure 5.3 Axial force against time at connection for steel beam under different support condition

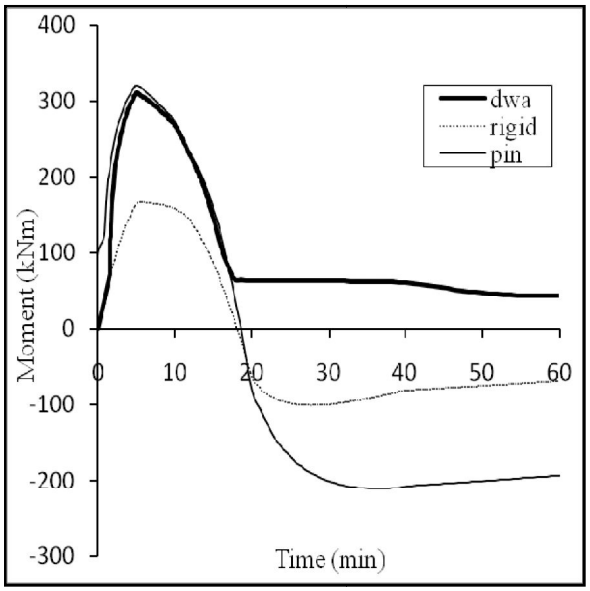

Figure 5.4 Moment against time at mid span for steel beam under different support condition

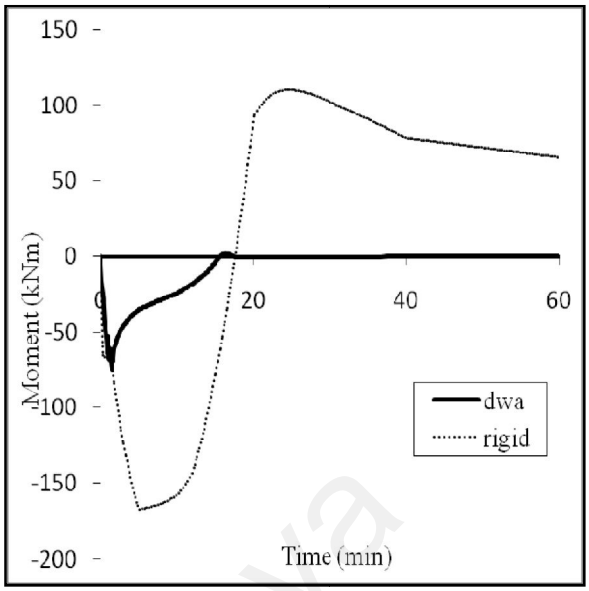

Figure 5.5 Moment against time at connection for steel beam under different support condition

The influence of support conditions in a restrained composite beam for secondary beam is shown in Figure 5.6 to 5.9. In general, the composite beam response incorporating pinned and rigid connection is very much similar due to the contribution of composite action and continuity of the steel reinforcement besides slab restraint gives a rigid connection between the slab and secondary beam surface. However, when actual connection is modeled, the beam capacity is lower due to yielding of the connection components in tensile region. Comparison of the beam support conditions shows that this restraint condition is significantly affecting the distribution of internal forces and deformation in the structural member beside proven that the compartment behaviour is significantly influenced by the continuity of the slab.

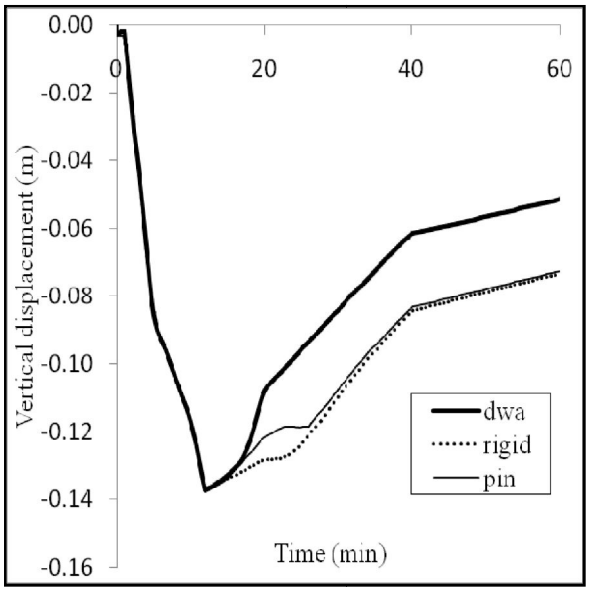

Figure 5.6 Test result for vertical displacement against time at mid span of composite beam for different support condition

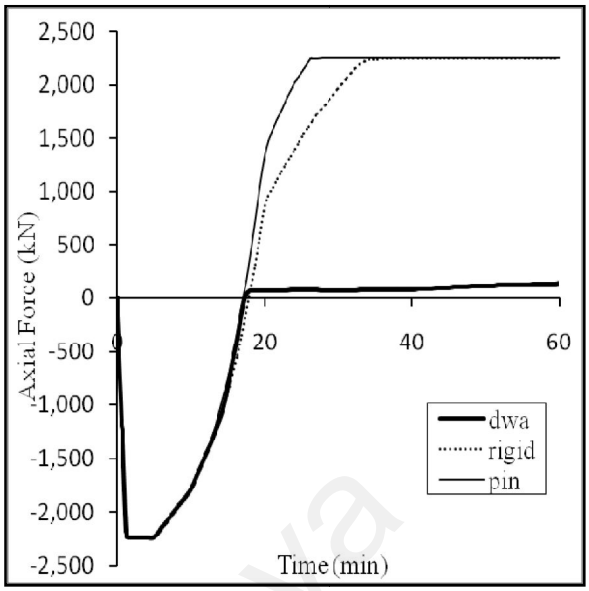

Figure 5.7 Axial force against time at connection for composite beam under different support condition

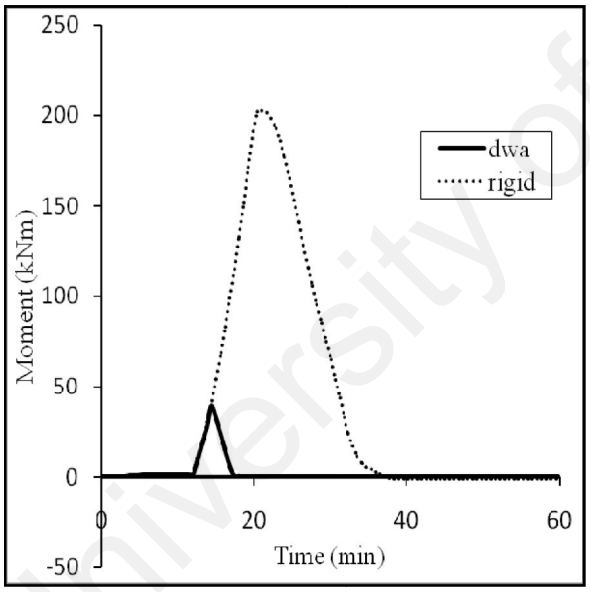

Figure 5.8 Moment against time at connection for composite beam under different support condition

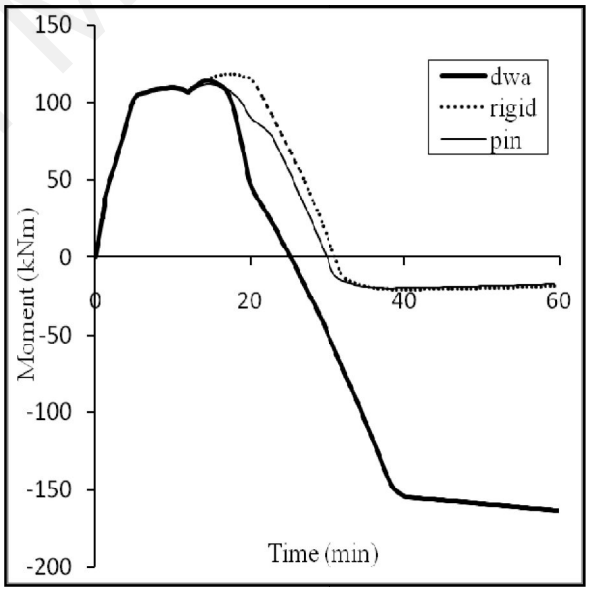

Figure 5.9 Moment against time at mid span for composite beam for different support condition

5.2.2 Temperature Effects

5.2.2.1 Temperature Loading

The influence of temperature loading is described in this section. The actual temperature profile applied to the beam and the connection recorded in Gurun Fire Test shows that the members are subjected to heating up to the maximum temperature, and going through temperature reduction during the cooling stage. The response of isolated steel and composite beam under actual temperature profile is compared against the beam response subjected to standard Time-Temperature curve BS 476 Part 20/ISO 834. The standard fire curve only considers continuous heating on the member, as shown in Figure 5.10.

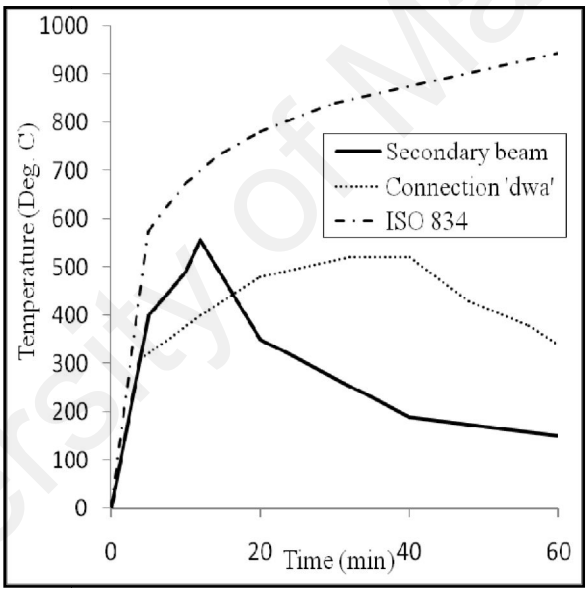

Figure 5.10 Time-temperature curve use in modelling the structure

For isolated steel beam, the beam response under the actual temperature curve (heating + cooling) and standard fire curve (heating) is shown in Figure 5.11 to 5.13. In this case, the steel beam is connected to the adjacent member through actual connection type i.e. DWA. The results show that temperature loading is significantly affecting the beam load carrying capacity, as the beam is continuously subjected to large displacement due to high temperature applied on the member. Kodur (2009) proves that the mid span deflection and the axial restraint force are dependent on fire scenario.

Result shows that for the case of severe fire scenario, large deflection occurs within the short growth phase of the fire.

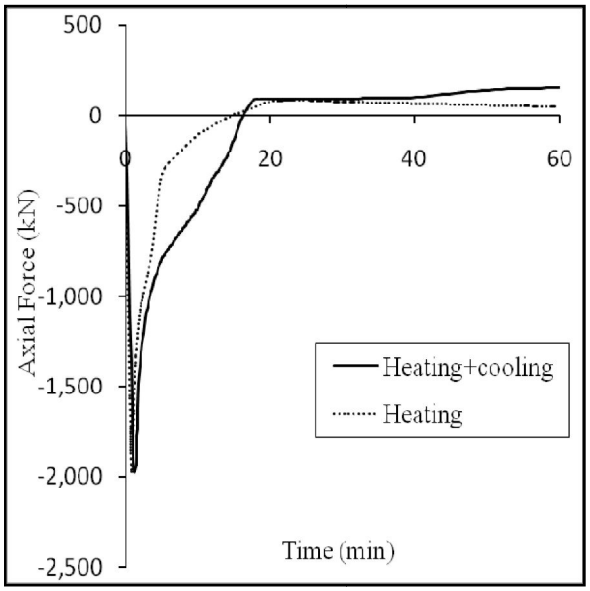

Figure 5.11 Axial force against time at connection for steel beam under different fire loading

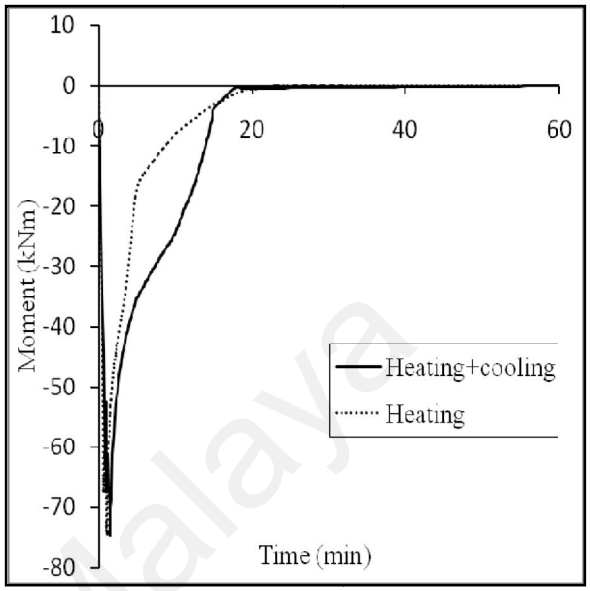

Figure 5.12 Moment against time at connection for steel beam under different fire loading

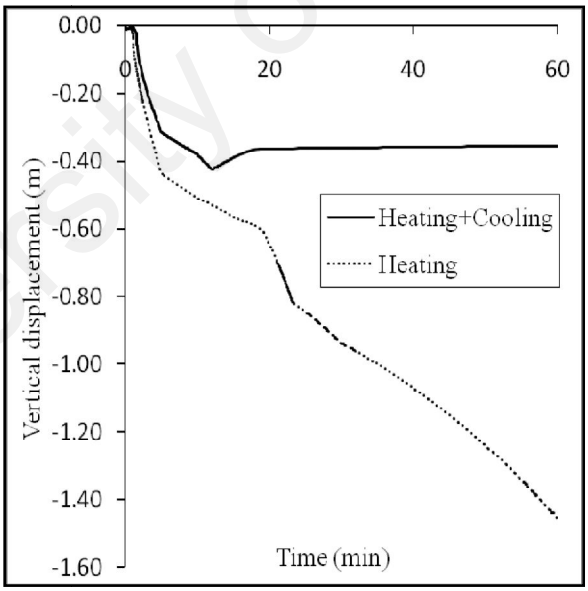

Figure 5.13 span of steel beam under different applied fire loading

Similar response is observed on the composite beam as shown in Figure 5.14 and 5.15. Smaller deformation is recorded compared to steel beam due to restraint of the concrete slab. As the beam is allowed to enter the cooling stage, vertical displacement begins to recover and ultimately the beam response is governed by the tensile capacity of the connection. Strain reversal happens during the cooling phase, which cooling can

be treated as an unloading behavior when considering thermal effects as the equivalent loading.

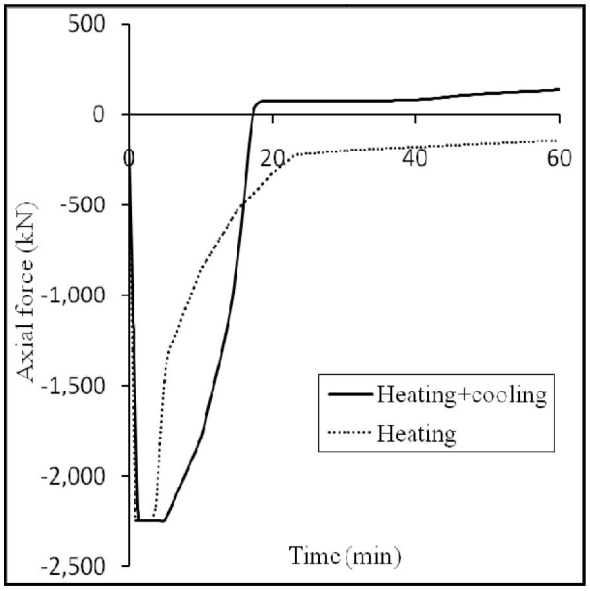

Figure 5.14 Axial force against time at connection for composite beam under different fire loading

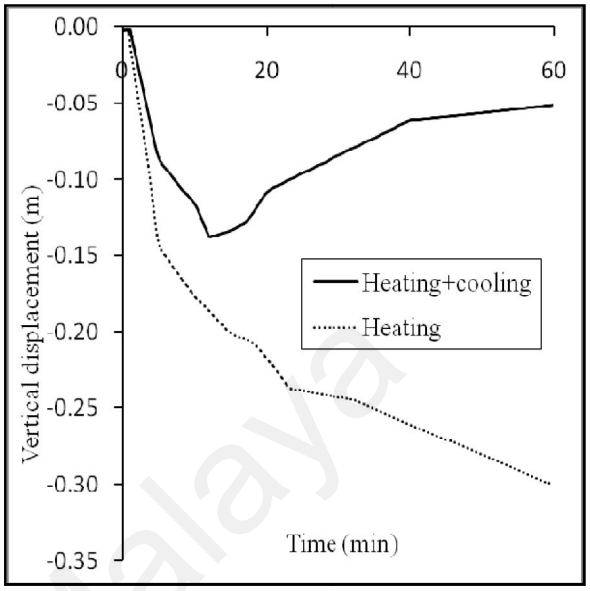

Figure 5.15 Vertical displacement against time at mid span of composite beam under different applied fire loading

Studies by Lien (2009) on the steel structures considering the heating and cooling phase in fire indicate that the steel beam with axial constraint will suppress the displacement effectively due to a catenary action. However, the structures with constraints in fires will induce thermal stresses, and the members of those structures will reach the plastic stage at lower temperatures when they are cooled to room temperature. This incident will cause the structures move into plastic phase in the early stage of a fire, and causes great damage even after the fire is put out. Bailey et al. (2011) in the studies also highlights the fact that the performance of structures must be checked in design under a range of possible fire scenarios, which must include both the heating and cooling stages of a fire. From the result of the studies indicates that the behaviour of composite slabs is dependent on the heating rate, the maximum temperature reached and the cooling rate.

5.2.2.2 Connection Temperature

The influence of connection temperature on the response of isolated steel beam is examined here. Due to concentration of mass at the joint, it is recognized that the connection temperature is normally lower than the beam temperature. A range of connection temperature including 0.1, 0.3, 0.5, 0.7, and 0.9 of temperature applied at centre of the beam is compared to the actual connection temperature measured in the fire test. The beam responses with various connection temperatures are shown in Figure 5.16. It can be concluded that for this selected DWA, its temperature is merely influenced by the beam response due to its lower capacity as illustrate in Figure 5.1. For other types of partial strength connection with larger capacity, it is anticipated that the connection temperature somehow should influence the beam response.

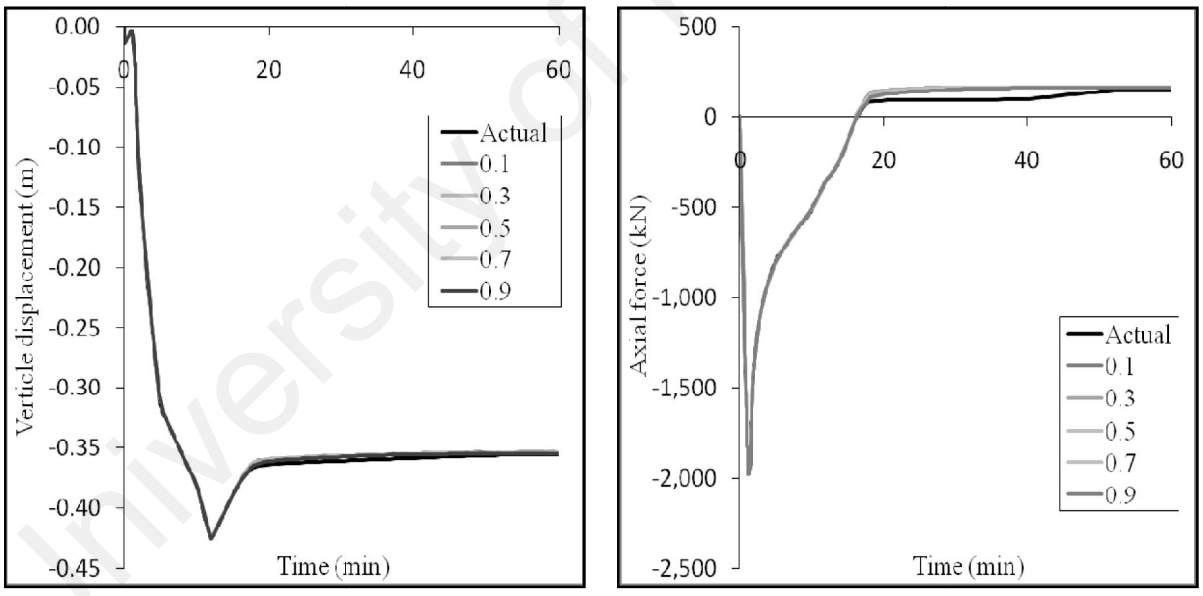

(a) Vertical displacement (b) Axial force

Figure 5.16 Effect of connection temperature

5.2.2.3 Thermal Gradient

This section examines the influence of temperature gradient on the response of a restrained steel beam by utilizing the data of secondary beam B2 in Gurun Fire Test. Structural members may be subjected to a temperature gradient across its section depending on the heat transfer. This is the case of beams supporting concrete or composite slabs, where high temperature gradients can develop due to the slow rate of heat transfer to the slab. Similar loading conditions as explained earlier are used in the analysis, with four temperature gradients (TG) across the beam section as illustrated in Figure 5.17, are investigated.

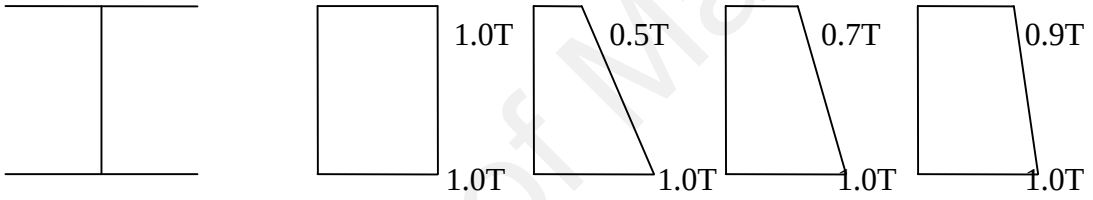

Figure 5.17 Temperature distributions across the beam section

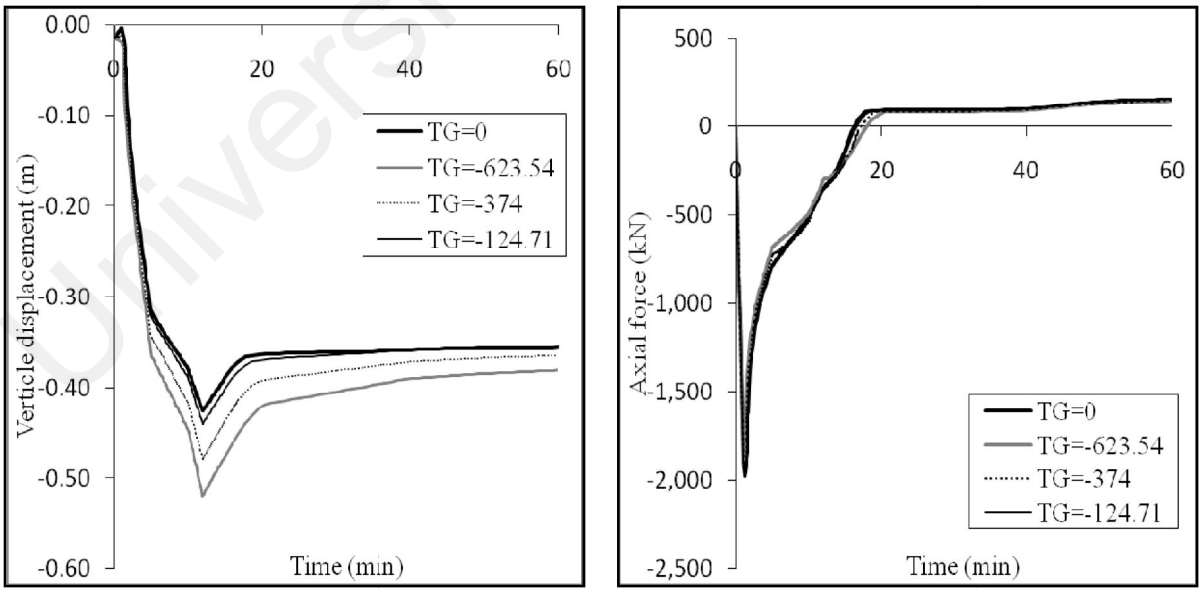

(a) Vertical displacement **(b) Axial force**

Figure 5.18 Effect of temperature gradient

As shown in Figure 5.18, temperature gradient significantly affects the beam displacement. As the gradient increases, the vertical displacement also increases

because the bottom beam section is subjected to higher temperature, which induces additional bending in the beam. However, this effect is not significant on the axial forces exerted at the beam end.

This phenomenon is proven by recent research by Dwaikat et al. (2011) whom carried out experiment to investigate the mechanics and capacity of steel beam-columns that develop a thermal gradient through their depths when exposed to fire. The specimens were tested with several combinations of load level, fire scenario, and direction of the thermal gradient. The authors indicate that the plastic resistance to combinations of axial load and moment was also affected by the thermal gradients where the critical section located in the hottest region along the column length. Result shows that all specimens failed by plastic yielding under combination of axial load and moment. Besides load level, fire scenario, and the direction of the thermal gradient had a significant influence on the fire response of beam-columns.

5.2.3 Connection Geometrical Properties

5.2.3.1 Web Angle Thickness

The influence of web angle thickness on the overall steel beam response is examined. The response of the beam with the actual web angle thickness of 10 mm is compared against two larger thicknesses i.e. 12 mm and 15 mm. This study shows the significant effect of the geometrical property of the connection selected on the beam response.

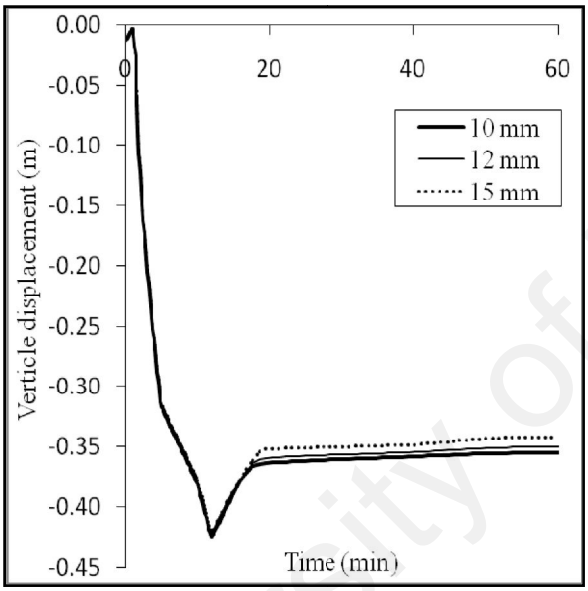

(a) Vertical displacement

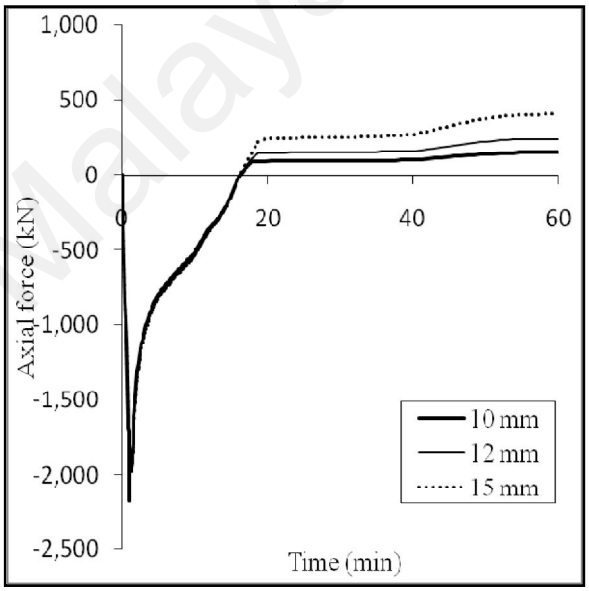

(b) Axial force

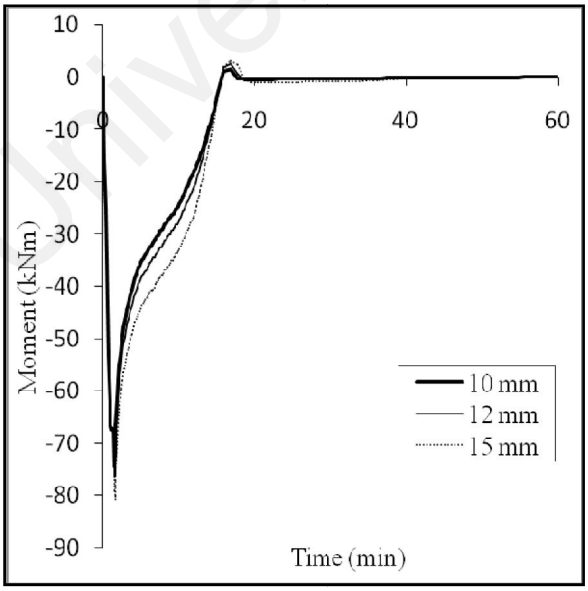

(c) Connection moment

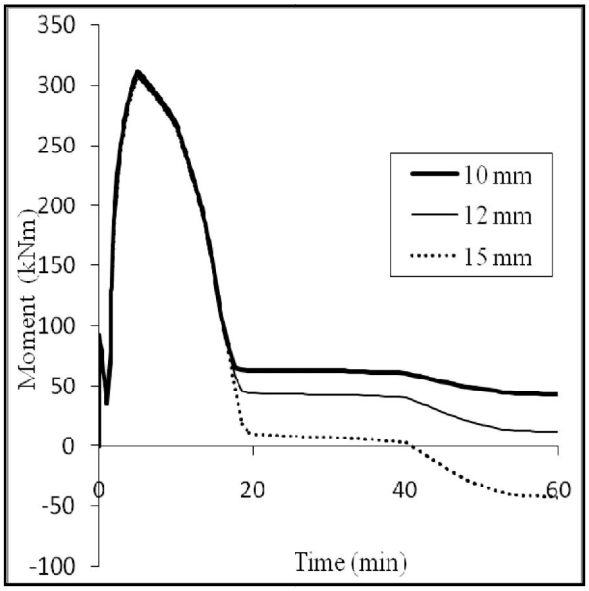

(d) Mid-span moment

Figure 5.19 Effect of web angle thickness

Generally, web angle thickness may contribute to the load carrying capacity of the beam especially in the tension region due to the characteristic of partial strength connection, which significantly governed the response as shown in Figure 5.19 (a-d). Increment in angle thickness leads to higher strength of the component angle in bending, consequently it increases the connection capacity.

5.2.3.2 Bolt Diameter

Three different bolt diameters were studied to see their effect on the beam response. From figure 5.20 it was shown that there is no difference in the behaviour of the beam because the failure is governed by the weaker component of the joint. Metric Structural Bolts are made to the requirements of ASTM A325M or A490M. An ASTM A325M Bolt has equivalent properties to an ASTM F568M Property Class 8.8 Bolt. An ASTM A490M Bolt has equivalent properties to an ASTM F568M Property Class 10.9 Bolt. These properties are essentially identical to Property Class 8.8 and 10.9 requirements in ISO 898/1. As expected, mechanical and geometrical properties of bolt do not give any influence on the response of the beam because of the failure of this particular connection is due to yielding of angle in bending.

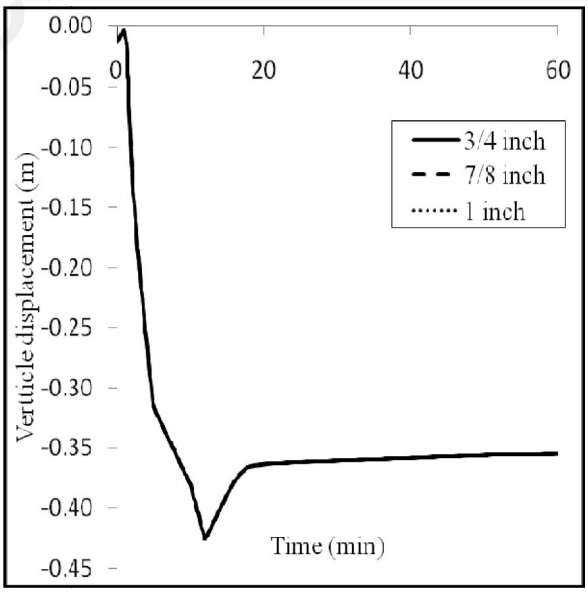

Figure 5.20 Effect of different bolt diameter

5.2.4 Load Ratio

Load ratio is defined in BS5950: Part 8 as the applied load or moment at the time of fire divided by the load or moment capacity at 20°C. According to current design approaches, the design load is based on a proportion of the ambient capacity of an isolated member, typically in the range of 40% to 60%. In order to investigate the effect of load ratio on the response of the beam, the beam as described above is subjected to an initial load in the range of 0.2, 0.3, 0.4, 0.6, 0.7 and 1.0. The actual load ratio applied in the test i.e. 0.25 is also included in the analysis.

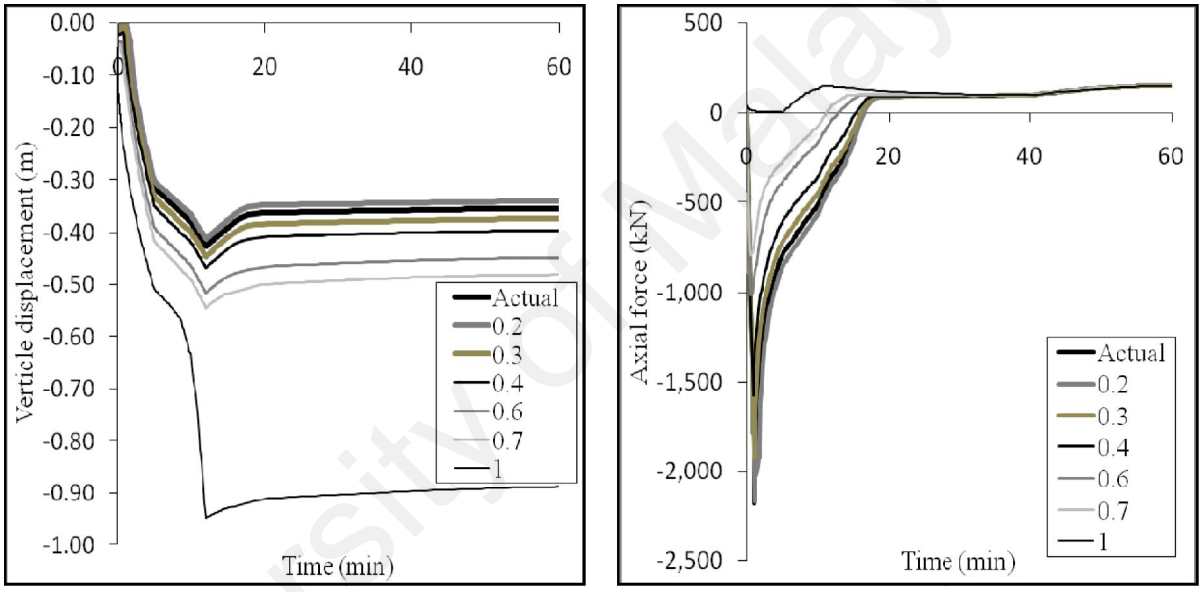

(a) Vertical displacement at mid span (b) Axial force

Figure 5.21 Effect of load ratio

The beam responses for various load ratios are depicted in Figure 5.21. At lower temperature, the response of the restrained beam is dominated by the effects of thermal expansion except for the case of load ratio equal to 1.0. As shown in Figure 5.21 (b), higher load ratio relieves the compressive forces in the beam. As the load ratio increases, the beam reaches tensile membrane behaviour at earlier stage. At any level of load ratio, the response is governed by the failure of DWA in the tension region.

Parametric studies carried by Kodur (2009), on the effect of load level show that higher load levels produce larger downward deflections in the restrained steel beam. On the other hand, the detrimental compressive axial force, which develops due to thermal

expansion of the steel beam, reduces with the increased load level. However, the increasing load level produces larger deflection, which makes the beam go into catenary action at earlier stages of fire exposure. The higher tensile forces develop in the restrained steel beam under catenary action as the load level is increased.

The same result was reported by Mao (2009), in the numerical results which show that the applied moments have significant effects on the stiffness of steel moment connections. The higher tensile forces would develop in the restrained steel beam under catenary action as the load level is increased. However, the axial load of column, shear and axial force of beam has been less affected. The stiffness of steel beam-column connection is not affected by the transverse load pattern of beam. For the cases of constant temperature (including ambient temperature case) with increasing transverse load on beam, the connection stiffness is constant when the connection is elastic, and it decreases with respect to the increase of transverse load of beam when the plastic strain occurs.

5.3 FLOOR SYSTEM

Parametric study on the floor system investigates several factors influencing the behaviour of compartment at elevated temperature such as restraint conditions, slab temperature, connection types, temperature gradient and temperature loading. Detail explanation of model development is given in chapter 3.

5.3.1 Influence Of Slab Restraint

Influence of slab restraint is referring to the rigid conditions applied on link (shear stud) between steel beam and concrete element. This is to represent full continuity of concrete slab on the floor. The result of floor responses with and without the slab restraint is given in Figure 5.22. In the model, the link between concrete slab and steel beam is modeled to give restrain on vertical direction which in this case referring to without slab restraint. As shown in the Figure 5.22, 21% reduction of vertical displacement is recorded in the internal secondary beam at nod 16 when the slab is restrained, correspond to resistance provided by the continuity of the floor slab. This proves that the compartment behaviour is significantly influenced by the continuity of the slab.

For the case of slab restraint, the responses on the connection in terms of strength and deformations are given in Figure 5.23 to 5.26. Compressive force is exerted on the connection as temperature increases. Then, the connections undergo tensile region with variation of tensile capacity depending on the type of connections as shown in Figure 5.23. Depending on the location and types of connection, variations in the moment developed in each connection are shown in Figure 5.24.

Deformations recorded in the connection in terms of axial displacement and rotation is given in Figure 5.25 and 5.26. By referring to graph time-axial displacement and time-rotation, the behaviour for all types of connection except EXTEP connection, no response under elastic phase was indicated until it reach to T = 17 min. This is due to

the tensile force which starts to develop in the connections in plastic region. Under tensile region, axial displacement and rotation response keep increasing until the end of analysis. Analysis shows that the connection referring to EXTEP, which connected main beam to column at major axis resist the highest compressive force, which resulting lowest axial displacement and rotation. Compared to other connections, the axial displacement and rotation keep increasing due to exposure to higher temperature and lower resistance of compressive forces.

It can be seen that from Figure 5.23 until 5.26, the different respond between Figure 4.7 until Figure 4.10 in chapter four is the response of DWA connection. By applying slab restraint, the connection resists higher value of compressive force, this can be seen from comparison without slab restraint in Figure 4.7. The restraint provided by the composite floor has developed a stiffer beam response compared to the case of without slab restraint (Figure 4.10), where DWA start to rotate from the beginning of analysis.

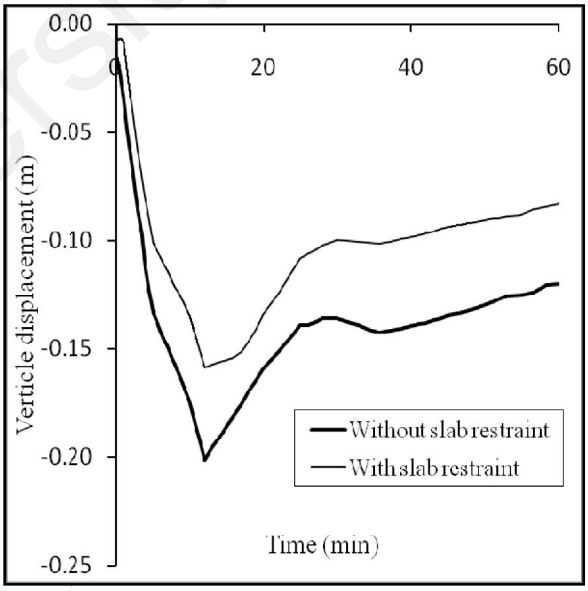

Figure 5.22 Time-vertical displacement for with and without slab restraint

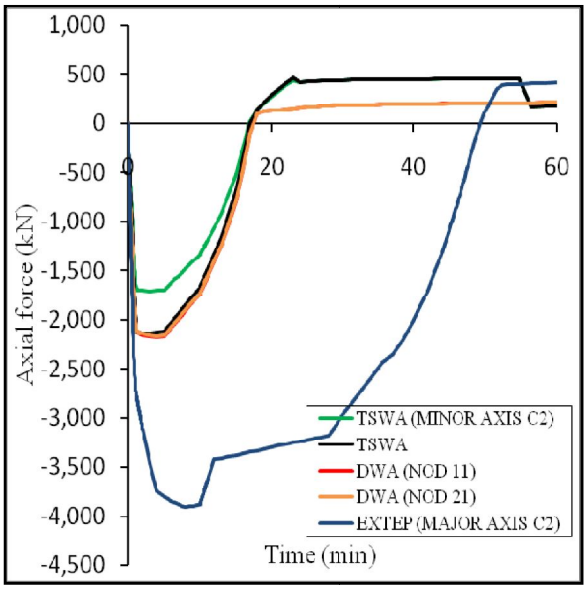

Figure 5.23 Time-axial force for slab restraint

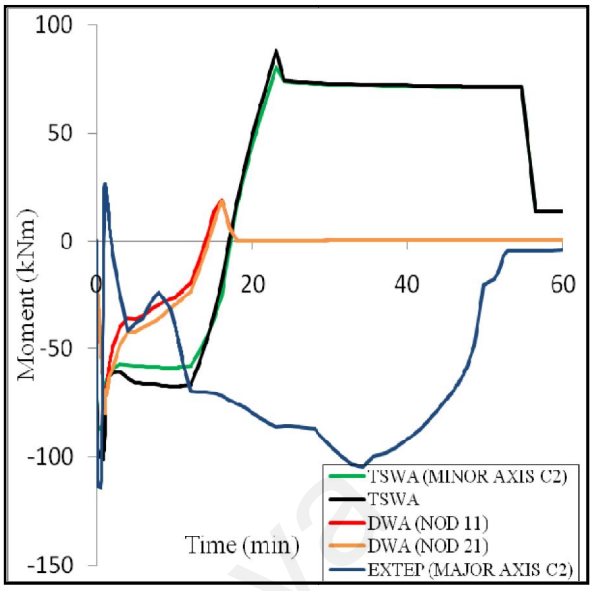

Figure 5.24 Time-moment for slab restraint

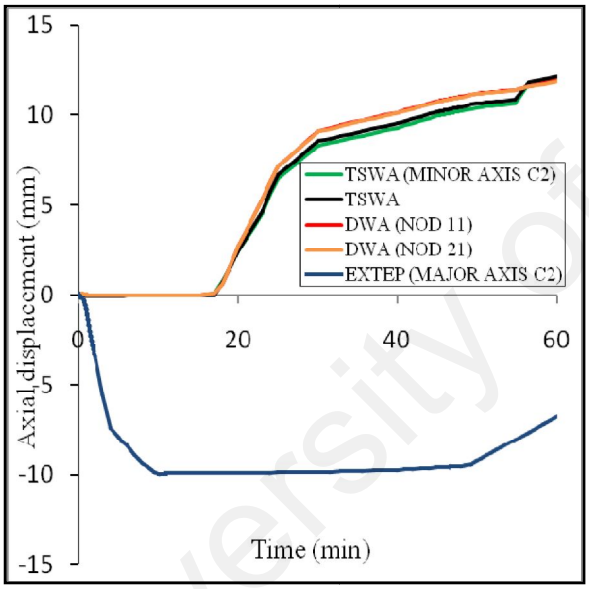

Figure 5.25 Time-axial displacement for slab restraint

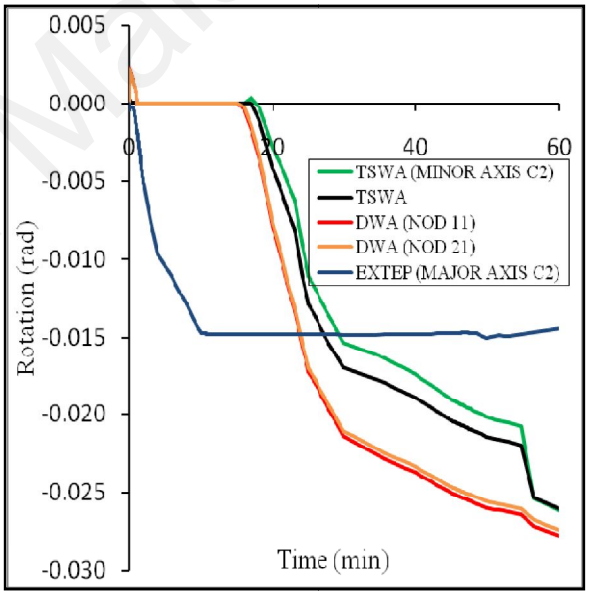

Figure 5.26 Time against rotation for slab restrain at node of connection

5.3.2 Influence Of Slab Temperature

Due to insufficient data of temperature applied on the slab, parametric studies were carried out to see the influence of slab temperature on the behaviour of floor system. A range of temperature was applied on the slab between 0.2 T to 0.8 T, where T is referring to temperature applied on the main beam, with maximum temperature of T= 600^0C at 12 min. The influence of slab temperature is given in Figure 5.27 to Figure 5.29.

The result shows that with an increasing temperature applied on the slab, the deformation at mid-span increases. This is due to decreasing of material properties of wire mesh in the slab and also degradation of material properties of concrete. The results were compared with actual model without applying temperature on the slab, which this condition will not happen in real situation. It can be concluded that the temperature recorded on the floor is very important to identify the time of maximum temperature experienced on the floor. Variations of vertical displacement with different slab temperature begin when compressive forces at the connection start to reduce until the end of analysis. Large deflection variations were observed because the mean temperature changes result in changes in length which have a much stronger effect on deflections relative to the changes in through depth gradients.

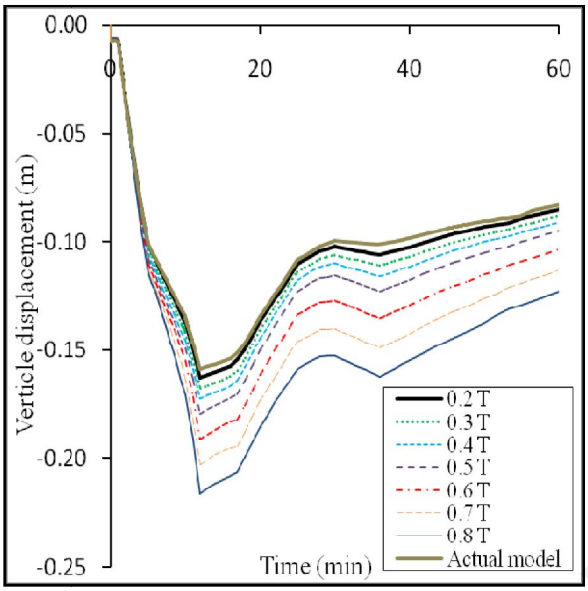

Figure 5.27 Time against vertical displacement at mid span of secondary beam for different ratio of slab temperature, (Node no 126)

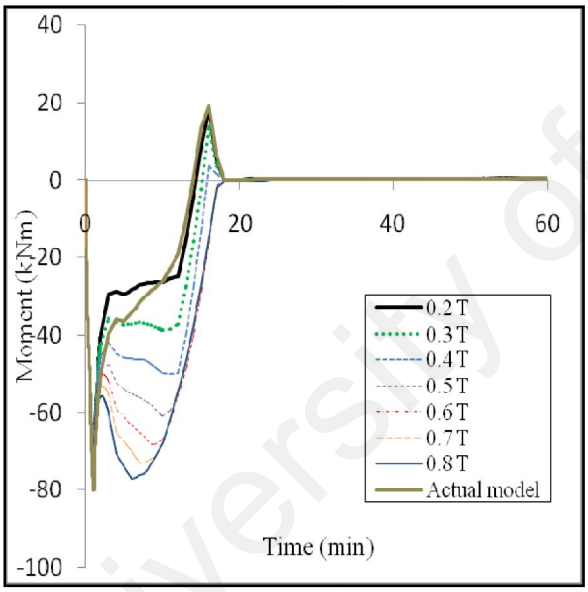

Figure 5.28 Time-moment for DWA connection for secondary beam (Element no. 11 to15 of secondary beam)

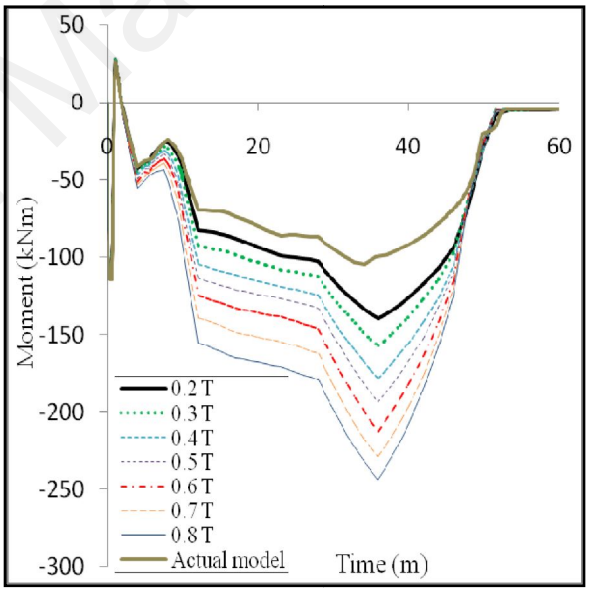

Figure 5.29 Time-moment for EXTEP connection at main beam, (Element 50 to 55 of beam)

5.3.3 Influence Of Boundary Conditions

In this section, the influence of boundary conditions on the floor system is examined by modelling three types of connections i.e. (i) all connections are pinned, (ii) all connections are rigid and (iii) actual connections types. In all cases, the edges of the concrete slab were left unrestrained. Results of the three models recorded at the secondary beam are shown in Figure 5.30. In the early stage, the beam's response incorporating actual connection types is similar to rigid connection until T = 17 min, when connection tensile capacity starts to govern the response.

Axial forces recorded in the connections at fire different locations are given in Figure 5.31 to 5.35. Overall, it can be concluded that the actual connections behaviour are similar to rigid connection in compression region. However, very large reduction in tensile region is observed for actual connection due to failure of the connection component i.e. angle in bending for the DWA and combined TSWA connection.

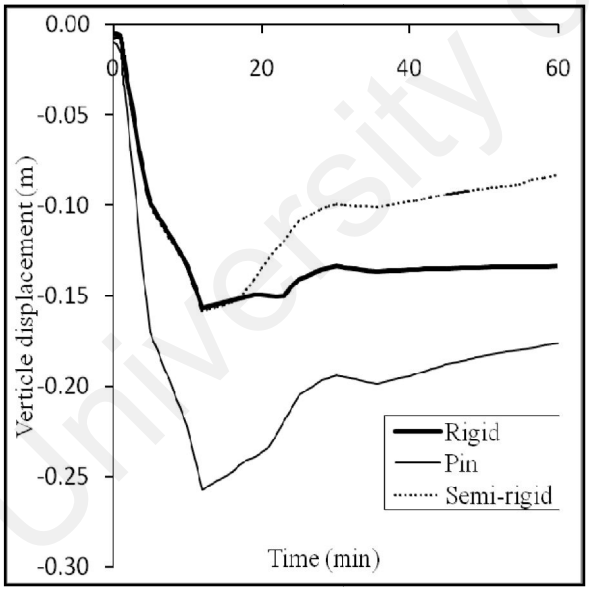

Figure 5.30 Time against vertical displacement for different boundary condition

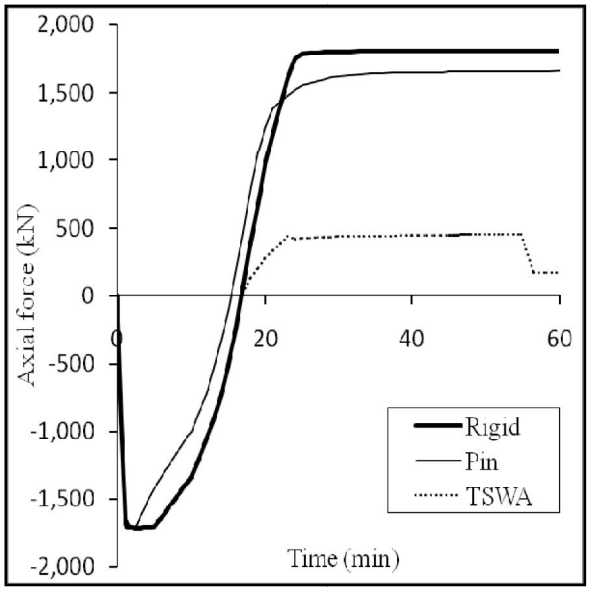

Figure 5.31 Time-axial force at the joint (minor axis C2), connected secondary beam B3 to column

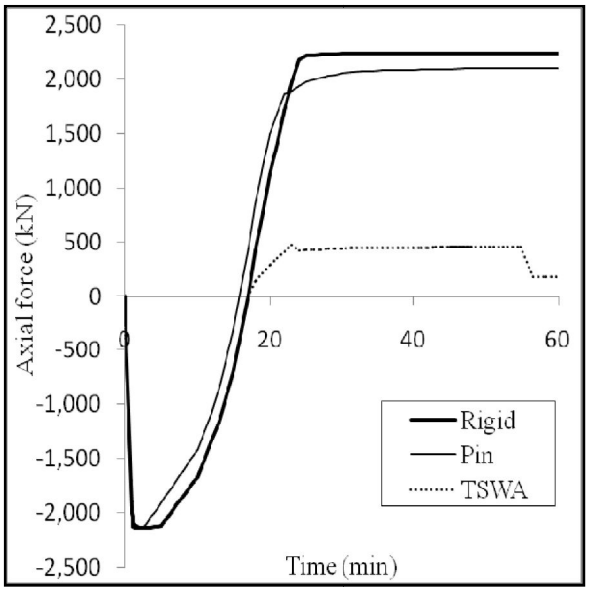

Figure 5.32 Time-axial force at tswa (connected secondary beam B2a to main beam B1)

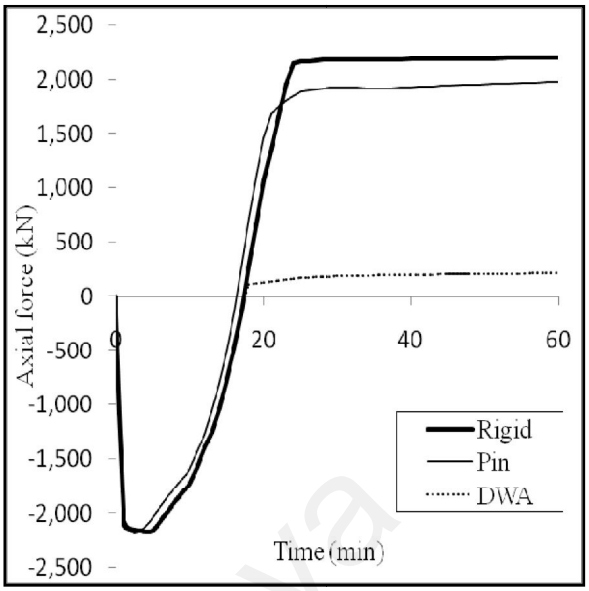

Figure 5.33 Time-axial force at the joint (nod 11 in Figure 3.17), connected secondary beam to main beam, B2c

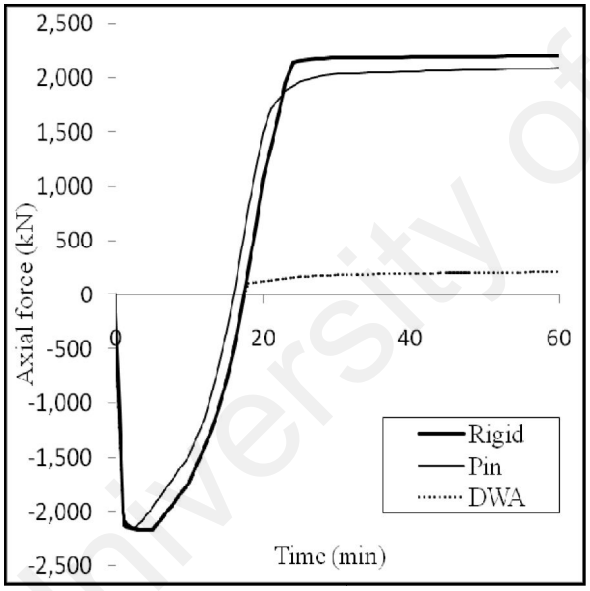

Figure 5.34 Time-axial force at the joint (nod 21 in Figure 3.17), connected secondary beam to main beam, B2b

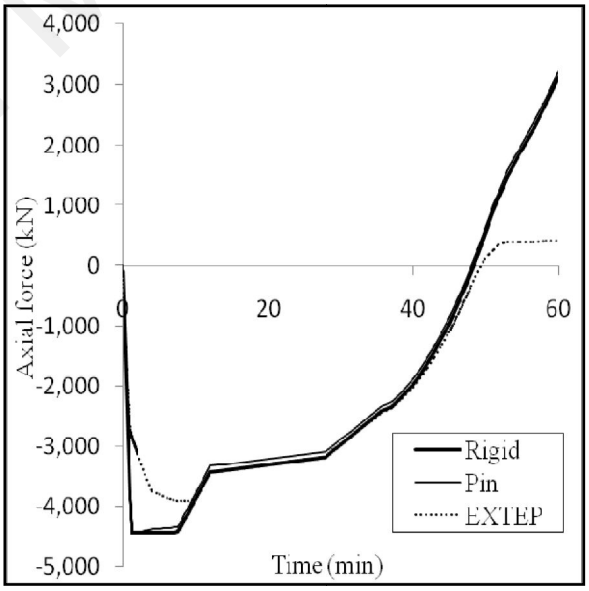

Figure 5.35 Time-axial force at the joint (major axis C2), connected main beam B1 to column.

5.3.4 Influence Of Temperature Gradient

5.3.4.1 Temperature Gradient on the Steel Beam Cross-Section

The influence of the steel beam cross-section temperature gradient on the floor system is examined here. Three different temperature gradient are applied i.e. 0.5 T, 0.7 T and 0.9 T, where T refers to centroidal temperature applied on the beam. It is noted that temperature in the floor slab is ignored in this study.

The response of the floor system under different temperature gradient is compared with uniform temperature case, as shown by the recorded vertical displacement at the mid-span of secondary beam in Figure 5.36. It can be seen that beam temperature gradient has large influence on the response, as decreasing temperature gradient results in larger displacement due to restraints of thermal actions.

The effect of temperature gradient contributes to the change of moment applied on the connection, but not on the axial forces, this is due to the response of the outermost layer of the bolt which is not affected much by the temperature gradient in this case, as shown in Figure 5.37 and 5.38. As explained in Sanad et al. (2000) the development of internal forces and moment in the beam is governed by the interaction of the mean temperature and through depth thermal gradients and end restrains available to translation and rotation.

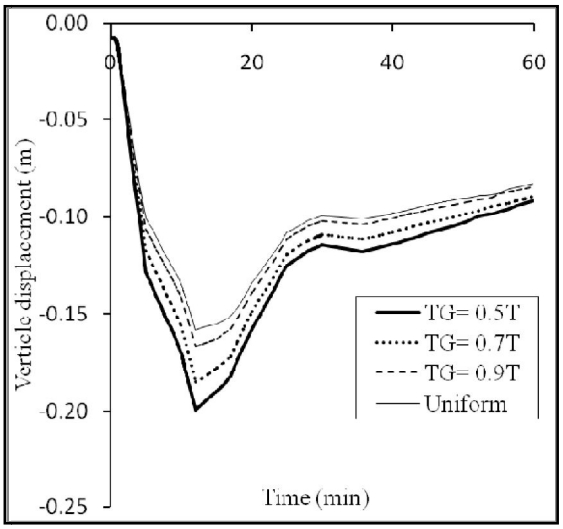

Figure 5.36 Time-vertical displacement for different temperature gradient at mid-span of secondary beam

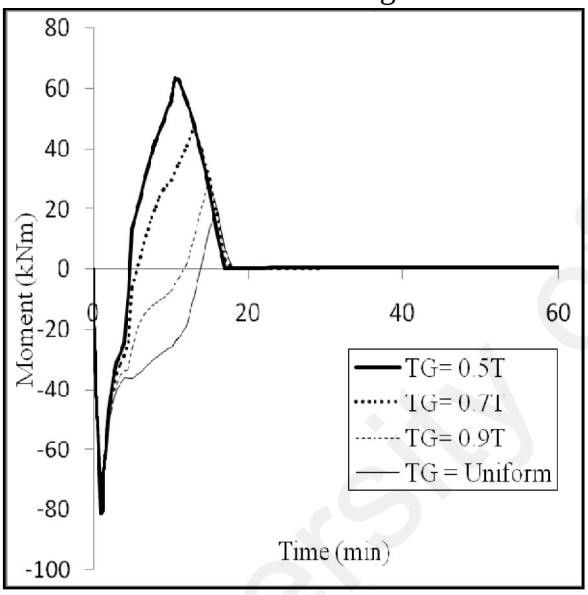

Figure 5.37 Time-moment for different temperature gradient applied on the secondary beam

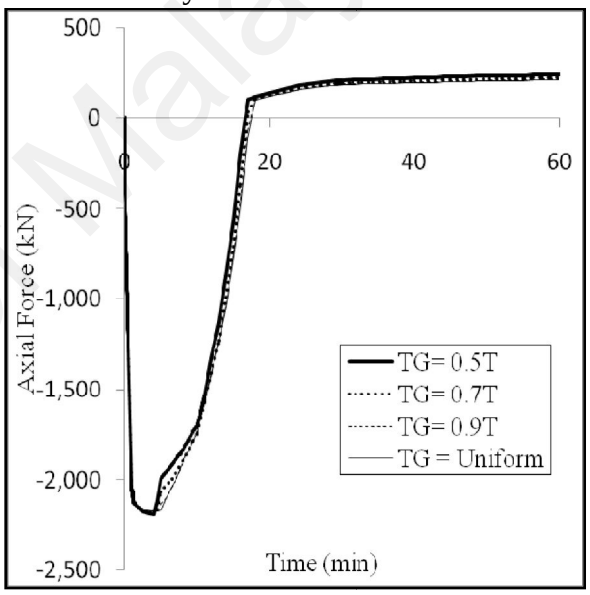

Figure 5.38 Time-Axial force for different temperature gradient applied on the secondary end beam

5.3.4.2 Temperature Gradient on the Floor Slab

In this section, the influence of slab temperature gradient on the floor response is examined. The slab is assumed to be restrained as mention in section 5.3.1 and subjected to temperature curve same as applied on main beam B1 (Figure 3.6). No temperature gradient applied on all steel beams. Three differences temperature gradient are assumed on the slab i.e. 0.5 T, 0.7 T, and 0.9 T. where T is temperature applied at main beam B1.

The influence of slab temperature gradient on the floor response as recorded in the section in the section beam mid-span displacement and end moment are presented in Figure 5.39 and 5.40. It can be concluded that the slab temperature gradient has mere influence on the floor response, as shown in the displacement curve. The developments of axial forces at the end of secondary beam are not sensitive to the gradient variation applied on the floor. However, small amount of reductions of moment is observed at the end of secondary beam with increasing temperature gradient, as shown in Figure 5.40.

Study carried by Sanad et al. (2000) justifies that with an increasing thermal gradient on the floor initially produces an increase in the hogging moment. The hogging moment starts to reduce because of the imposed deflection caused by the composite beam which begins to act as a point load at mid-span. A small different in hogging moment under compressive force also can be seen in Figure 5.40 below.

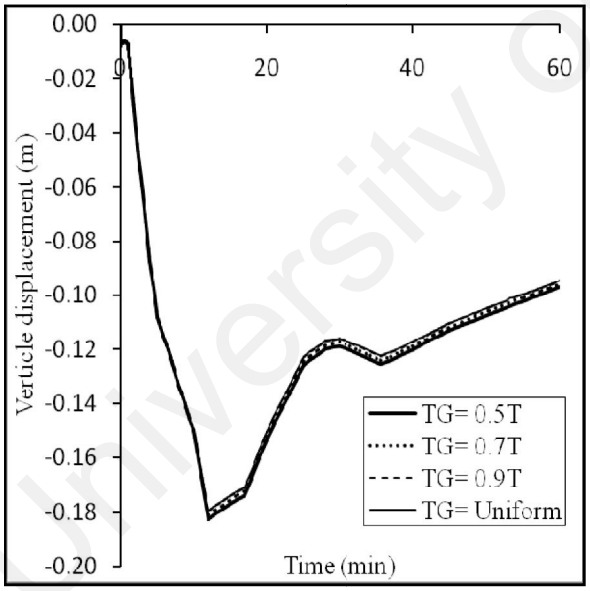

Figure 5.39 Time-vertical displacement for different temperature gradient applied on the floor

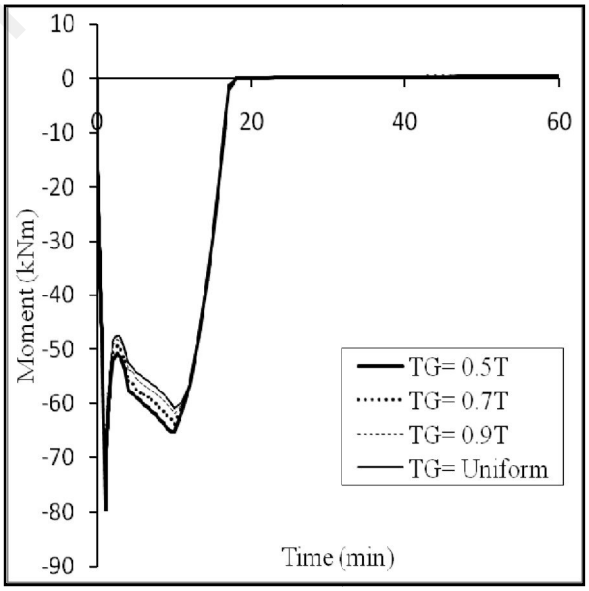

Figure 5.40 Time-moment for different temperature gradient on the secondary end beam

5.3.5 Influence Of Temperature Loading

Similar to fire scenario applied on isolated steel beam as mentioned in section 5.2.2.1, this section investigates the influence of temperature loading on the floor system for the case of restrained slab. Two fire curves are considered i.e. actual fire condition (heating + cooling phase) and standard fire test BS 476 part 20/ISO 834 (heating only). The effect of temperature loading is shown in Figure 5.41 to 5.43. Very large displacement is observed beyond T = 17 min for the heating case only, due to temperature applied on the compartment area keep increasing and there is no tensile force can be resisted by connections and at this point, all the forces applied are resisted by the beam itself. At 25th min, the temperature applied on the compartment area is about 800 ^{0}C where the strength of the beam right now can only resist about 11% from the beam capacity.

Developments of axial forces at different connection location are compared between the two fire curves. It can be seen that due to high temperature exposed on the members, compressive forces are relieved sooner for the heating only regime. This is highly associated with the faster material properties reduction of the elements until failure of the connection components under tensile region.

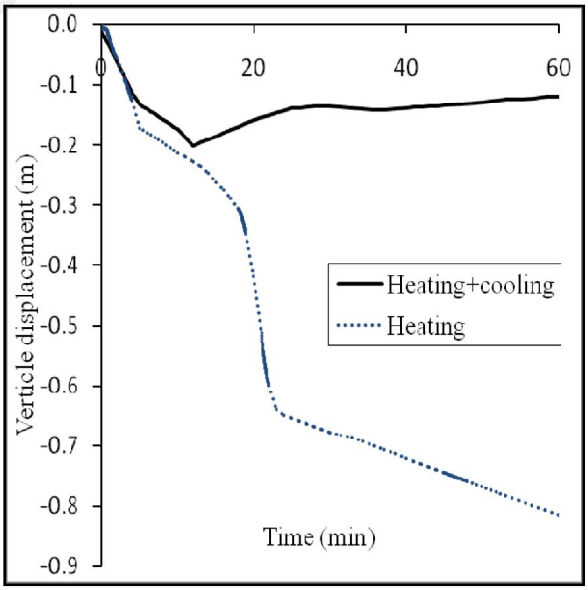

Figure 5.41 Time-vertical displacement under different applied fire loading

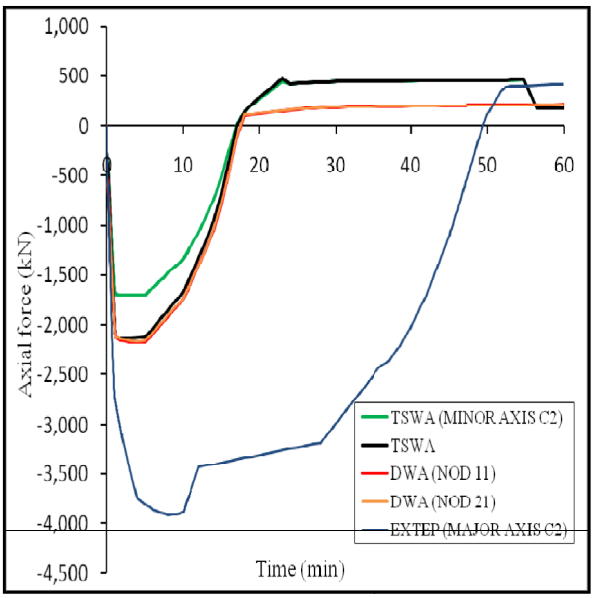

Figure 5.42 Time-axial force under actual fire scenario (heating + cooling)

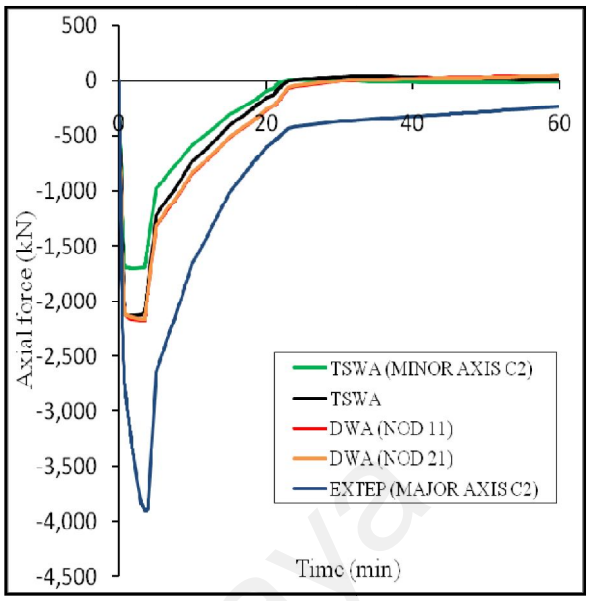

Figure 5.43 Time-axial force under standard time-temperature curve BS 476 Part 20/ISO 834 (heating)

Usmani and Cameron (2004) introduces a new three-step method that analyses the limited capacity of laterally restrained RC slabs in fire. This study proves that structural response to fire, depends upon the rate of heating as well as the temperature of the structure, and that different fires can produce very different stress/strain patterns in composite floor systems. This is because most of the pre-failure responses of structural members depend upon the two geometric effects produced by heating, a mean temperature increase and a mean thermal gradient. The material effects of reduction in strength and stiffness with temperature increase also require accurate estimates of the temperature distribution. In this case of study by considering different condition of heating case and combination of heating and cooling case influence the response of the structure as a whole.

5.4 SUB-FRAME

Two tests were selected for parametric studies i.e. FJ03 and EJ01 from the Coimbra Fire Test (Santiago, 2008). The difference between the tests is joint typology. Table 5.2 shows specimen description of the two tests. Parametric studies were carried out in order to determine the influences of some parameters such as temperature and temperature gradient applied on connection, different connection type and reduction of strength and stiffness using EC3 (EN 1993-1-8-2005). Result shows that factors which effect the connection characteristic will give influence to overall behaviour of the sub-frame structure.

Table 5.2 Specimen description

Test ID	Joint typology	End-plate dimentions(mm) and steel grade	Bolt and grade
FJ03	FEP	320x200x16; S275	2 bolt row M20, 8.8
EJ01	EXTEP	385x200x16; S275	3 bolt row M20, 8.8

5.4.1 Connection Temperature

This section discusses the influence of temperature applied on the connection element. In the case of fire protection applied on connection zone, the overall behaviour of sub-frame will be influenced by the installment of fire protection. Figure 5.44 and 5.45 illustrate reduction of deformation for model without temperature applied on connection. By comparing the final displacement, about 40% and 10% reduction was obtained for FJ03 and EJ01, respectively.

The result shows that the beam displacement reduces if the temperature at connection is lower than connected members, where the cooler member takes action in giving restrain to connected members. In the model, actual temperature recorded on connection is adopted in simulation work to ensure that the validation of model can be as precise as possible to reduce inaccuracy in the results.

Huge reduction of rotation is observed for both connection types for the case of no temperature applied at connection element. Actual connection temperature

distribution applied at connections is important in identifying the true behaviour of the structure. For flush end plate, because of lower stiffness, variation of the rotation can be seen from the beginning of analysis. For EXTEP, similar behaviour is observed at lower temperature as it possess high stiffness, then reduction of material properties governed the response together with the yielding of end plate in bending.

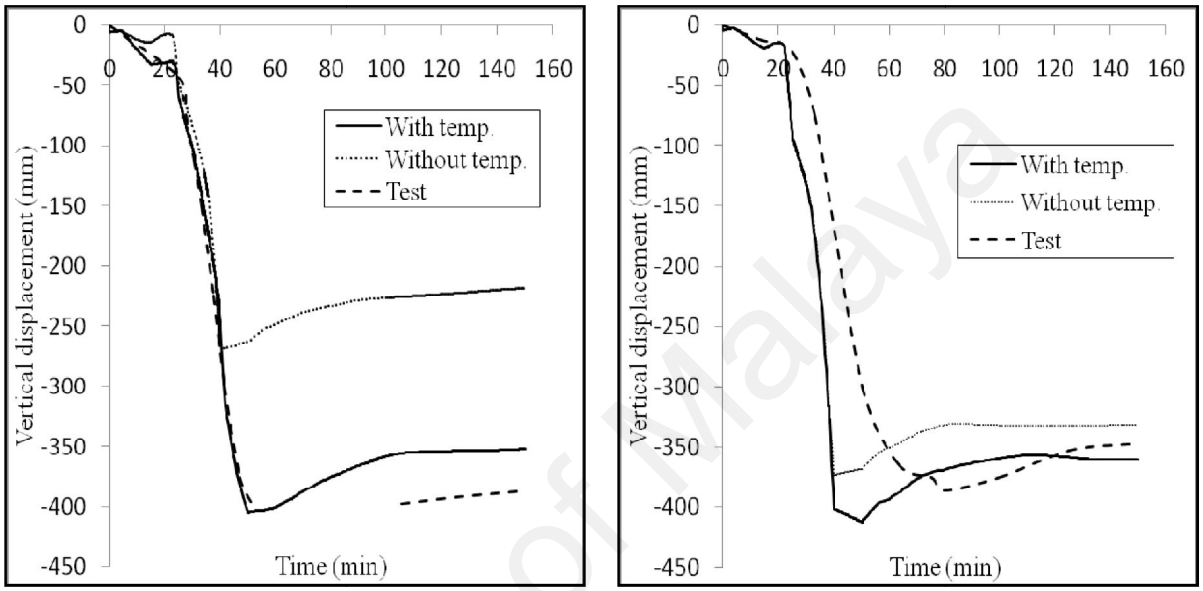

(a) (b)

Figure 5.44 Time-mid-span displacement curve for model (a) FJ03 and (b) EJ01 with and without fire applied on connection element.

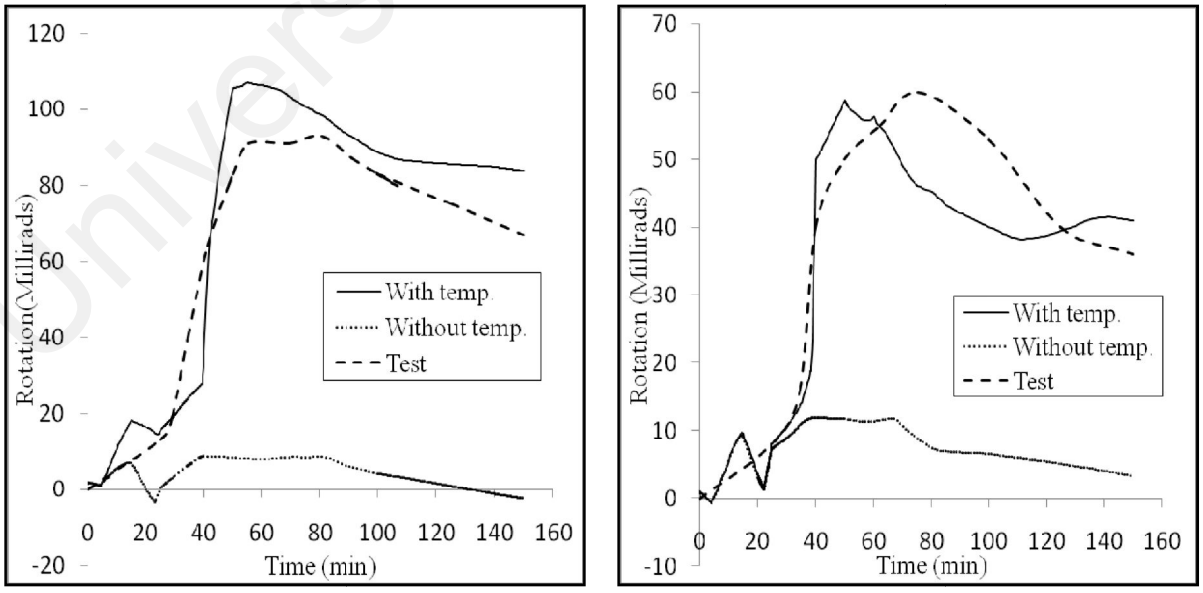

(a) FJ03 (b) EJ01

Figure 5.45 Time-rotation curve for model (a) FJ03 and (b) EJ01 with and without fire applied on connection element.

5.4.2 Temperature Gradient

Temperature gradients here refer to temperature gradient applied across the connection elements, as given in the test. Comparisons between the case of applied temperature gradient on connection element (With Tg) and without applied temperature gradient (Without Tg) are discussed in this section.

Small reduction of displacement at mid-span beam for without Tg was measured for both connections below 10% (Figure 5.46(a and b)). The recovery of the displacement takes action under cooling phase.

It can be seen from the time-rotation curve in Figure 5.46(c) and (d), a huge reduction of rotation is observed For EJ01 model compared to FJ03. This is due to high resistance from cooler bending component in particular from EXTEP.

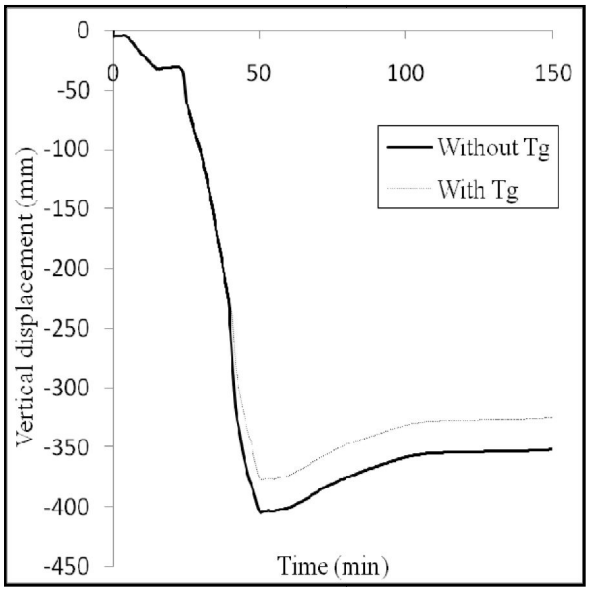

(a)

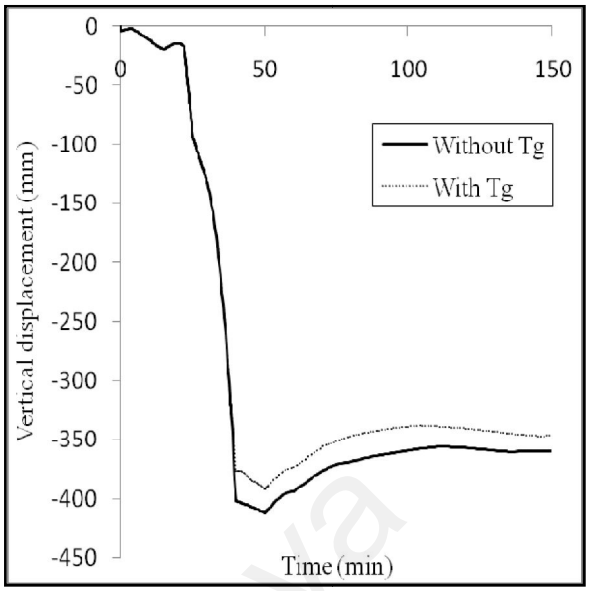

(b)

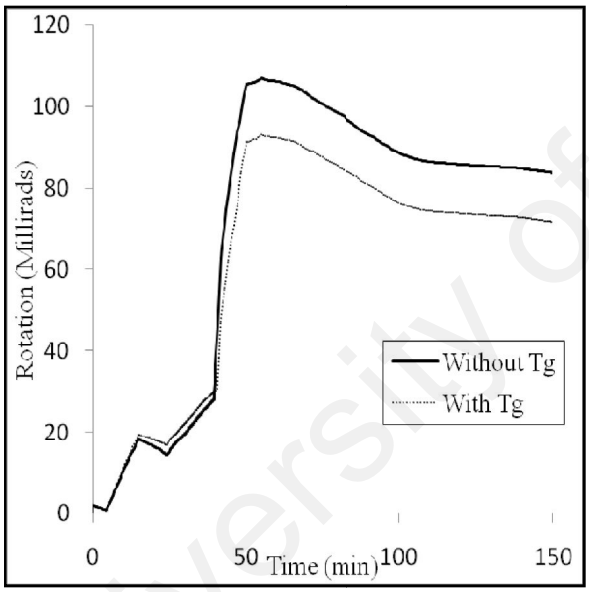

(c)

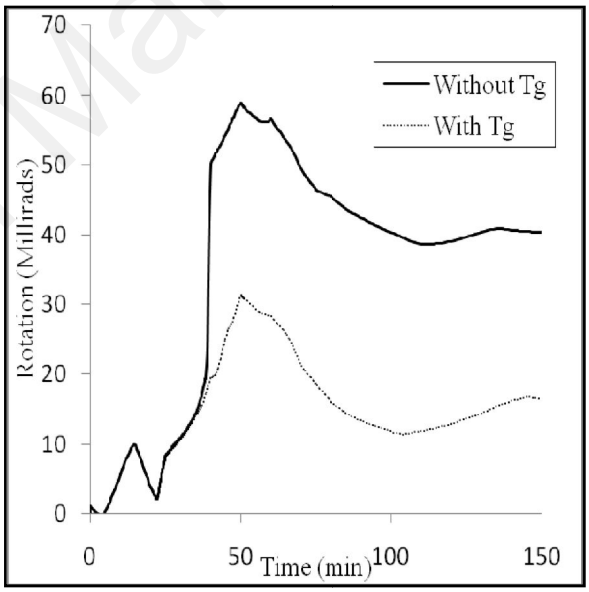

(d)

Figure 5.46 Time-mid-span displacement curve for model (a) FJ03, (b) EJ01 with and without temperature gradient applied on connection element.Time-rotation curve for model (c) FJ03, (d) EJ01 with and without temperature gradient applied on connection

5.4.3 Different Connection Typology

Four connection types are studied i.e. pin, rigid, FEP and EXTEP connection. The last two can be grouped as semi rigid connection. For all model same time-temperature were applied at beam and semi-rigid connection element except for rigid and pin connection element.

The behaviour can be divided into three phases, where at early stage under compressive forces T < 18, Figure 5.47 (a), the displacement of semi-rigid model is between pin and rigid connection model. After that, the displacement shows almost similar behaviour with rigid connection under reduction of compressive force. Under tensile forces, for flush end plate, the deformation is between rigid and pin connection, but for EJ01 the connection behaves like rigid connection.

Huge difference can be seen from time-rotation curve. Figure 5.47 (b) shows that FEP and EXTEP can be classified as semi-rigid connection due to capability to rotate and yet able to resist moment.

From time-axial force graph, Figure 5.47 (c), the capacity of semi-rigid is almost similar for pin and rigid connection up to maximum compressive force where semi-rigid is located between pin and rigid connections. Capacity of semi-rigid connection is similar to rigid connection when compressive force reduced. At the end of analysis, the maximum capacity of tensile force of semi-rigid connection is closer to pin connection.

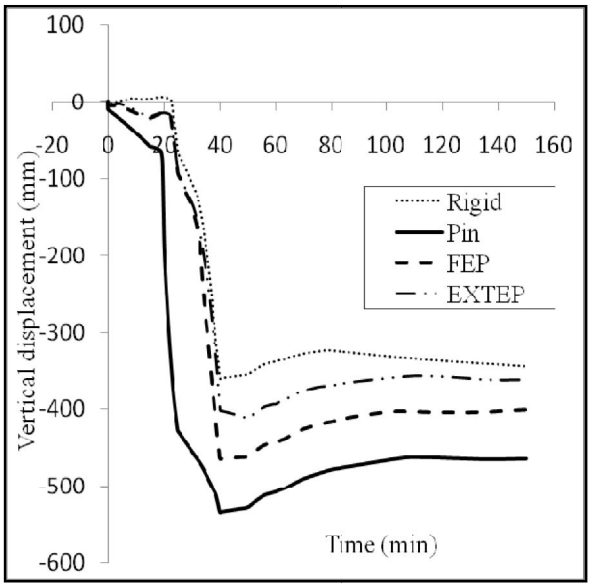

(a)

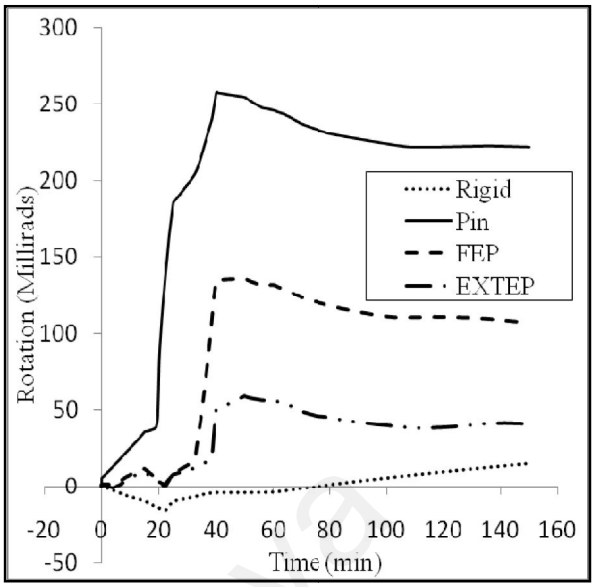

(b)

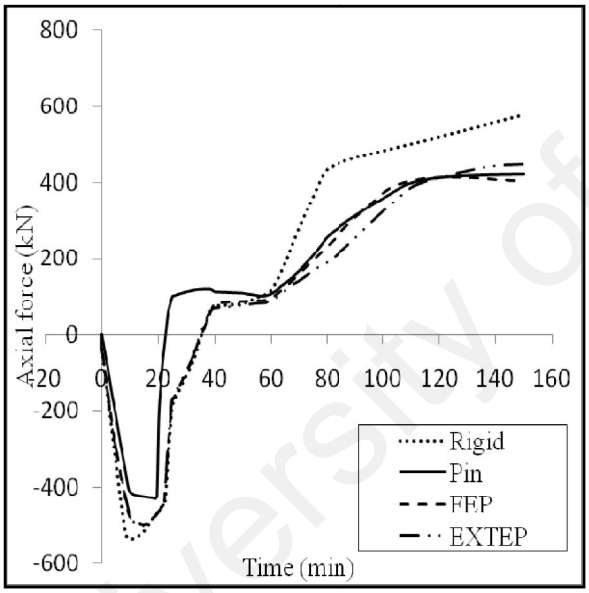

(c)

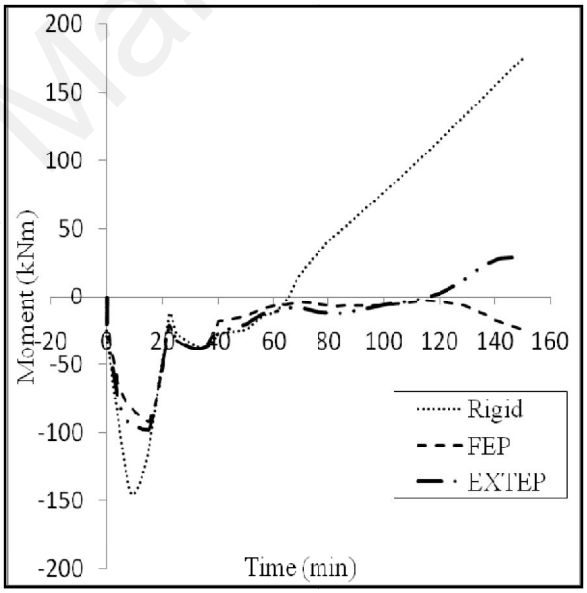

(d)

Figure 5.47 (a)Time-mid-span displacement curve, (b) Time-rotation curve, (c) Time-axial force curve and (d) Time-moment curve for different connection typology.

5.4.4 Effect of Reduction Factor

In Figure 5.48 model EC3 refers to the degeneration of the strength and stiffness of the connection material with increasing temperatures for connection element using the temperature-dependent strength reduction factors for mild steel given in EC3: Part 1.2 for endplate and connected member. For the bolts, however, the temperature reduction factors for strength derived by Kirby (1995). For actual model, the reduction of strength and stiffness of the connected member is according to experimental data given, others follow as mentioned earlier. Small difference of behaviour can be seen between the models under tensile forces, this is due to the reduction of strength and stiffness of end plate connection.

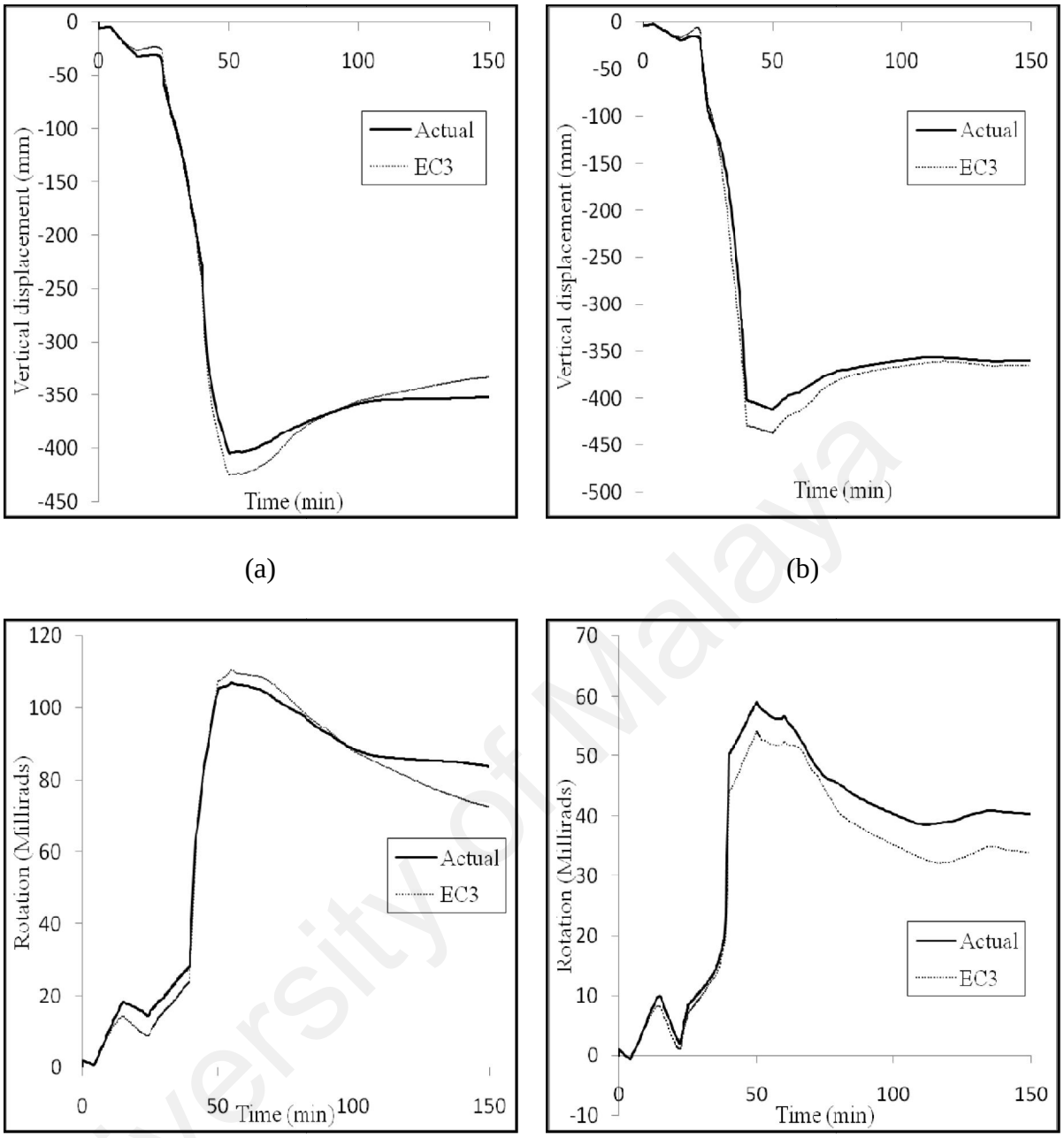

Figure 5.48 Time-mid-span displacement curve for model using actual reduction factor from test compared by using reduction factor from EC3: Part 1.2 (a) FJ03, (b) EJ01 and Time-rotation curve for model using actual reduction factor from test compared using reduction from EC3: Part 1.2 (c) FJ03, (d) EJ01.

5.5 DUCTILITY STUDY ON STEEL SUB-FRAME AT ELEVATED TEMPERATURE

In this section, the deformation and rotation demands from different semi-rigid connection types when subjected to fire for steel sub-frame are examined. This study adopts internal steel sub-frame used in Cardigton test. Two conditions are considered in this study; (i) where the sub-frame is applied with a linear increasing uniform temperature applied across and along the steel section and (ii) the sub-frame is subjected to heating and cooling phases and uniform temperature is considered across and along the steel section.

5.5.1 Structural Modelling and Layout

Five connection configurations are examined in investigating ductility demand including FEP, EXTEP, DWA, TSA, and combination of TSWA. Figure 5.49 shows the geometrical properties used for semi-rigid connections in this study. Different connection types are adopted, to identify their ductility demand on steel sub-frame under fire (Figure 5.50).

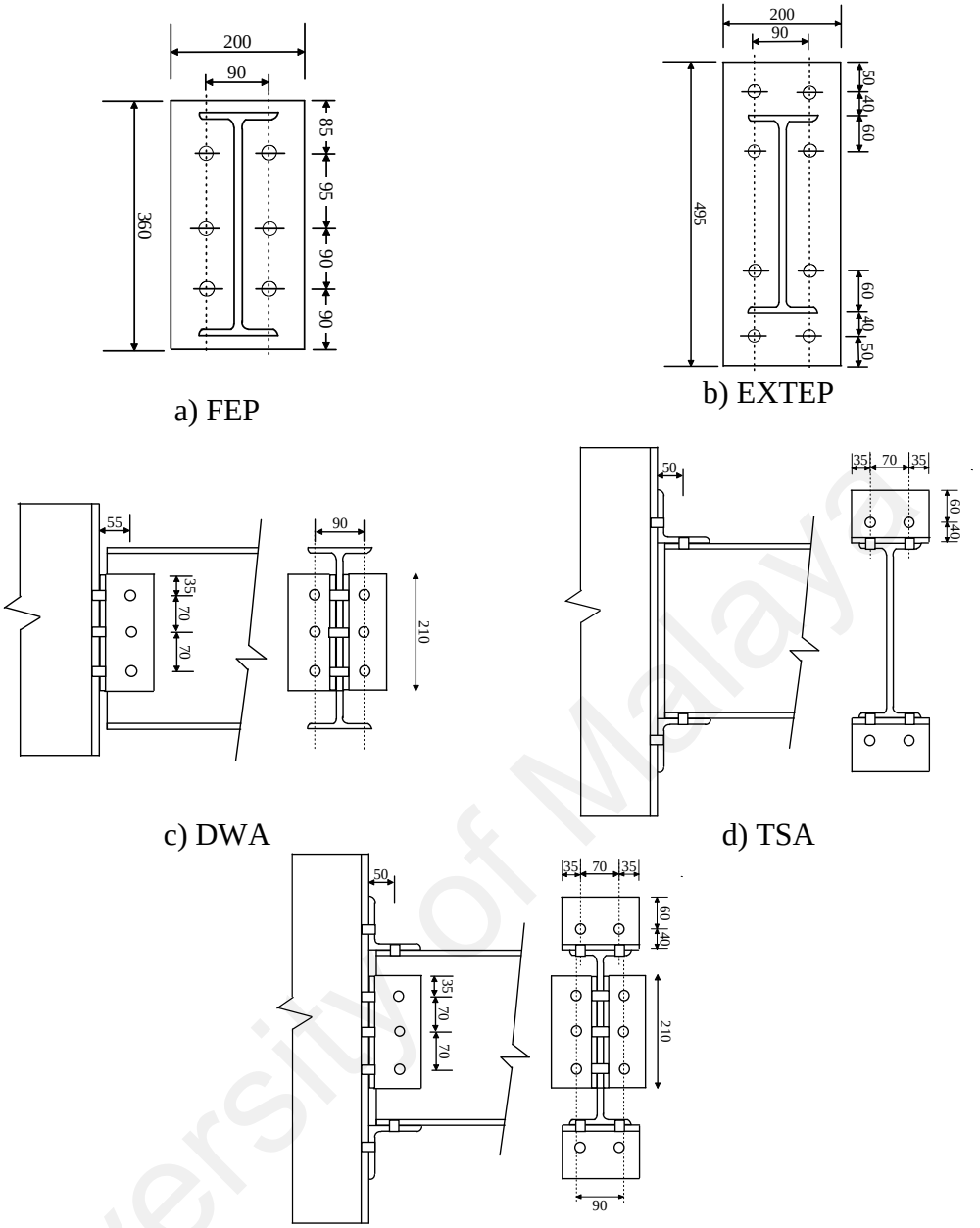

Figure 5.49 Geometrical properties of selected connections

The beam and column elements are modelled by using cubic elasto-plastic 2D beam-column elements (cbp2). Joints are modelled using 2D joint elements (jbc2). The beam size is taken as 305 x 127 x 37 UB and the column size is 254 x 254 x 73 UC with nominal yield stress of 275 N/mm^2 and an elastic modulus of 210 kN/mm^2 is used for all steel material.

The beams are subjected at mid-span with an initial load representing a load ratio of 0.6. The temperature distribution used for the sub-frame configuration is as

shown in Figure 5.51. The beam above the fire is assumed to have uniform temperature distribution along its length and a uniform temperature distribution within its cross-section. For the connection at the end of the heated beam, its temperature is assumed to be 70% of the beam temperature. For the beam as well as its connection adjacent to the heated beam, the temperature is assumed to remain at 20^{o}C. The column temperature in the fire compartment is taken as 50% of the heated beam temperature. While the column above the fire compartment is assumed to be at ambient temperature.

The model is carried out in two conditions, firstly the steel sub-frame is applied with heating temperature up to 1000^{o}C (Figure 5.52). For the other case, the sub-frame was applied with time-temperature curve as shown in Figure 5.53 where the heating and cooling phases are taken into consideration.

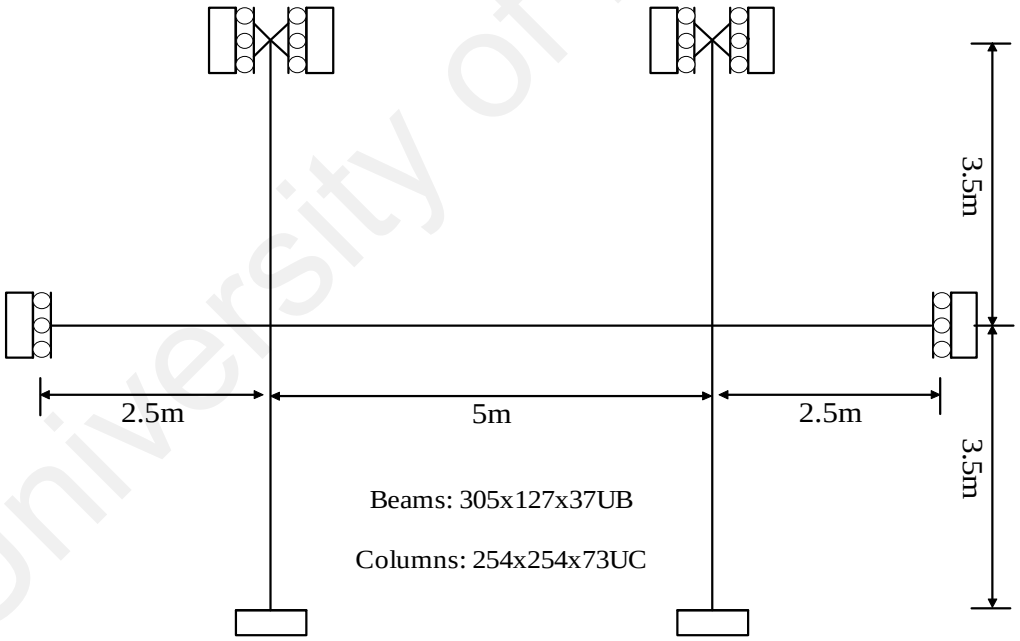

Figure 5.50 Internal sub-frame layout

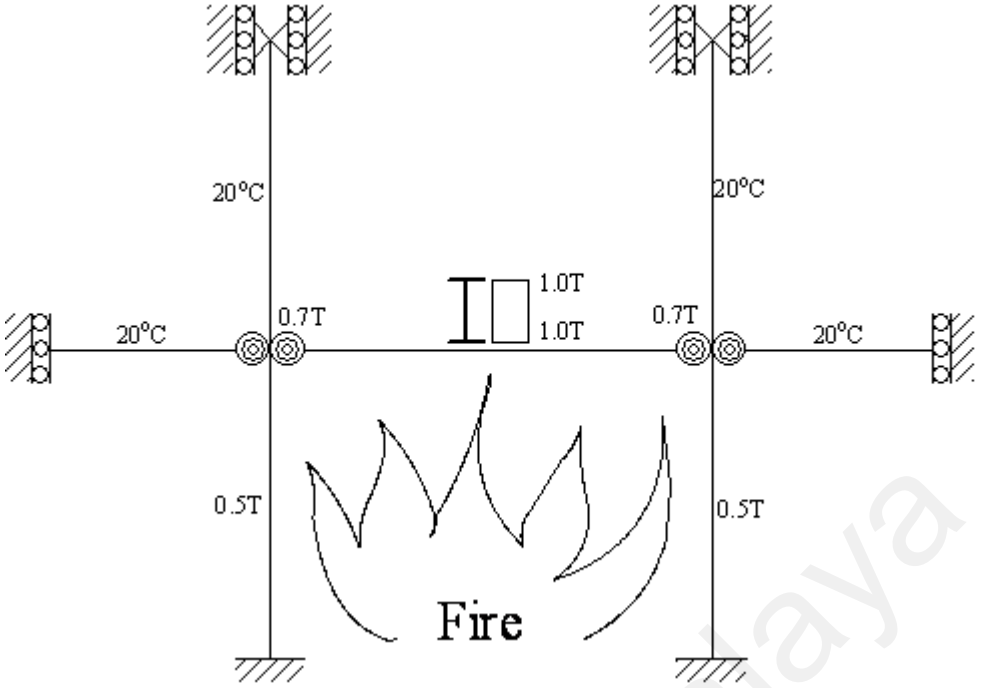

Figure 5.51 Sub-frame arrangement and temperature profile used

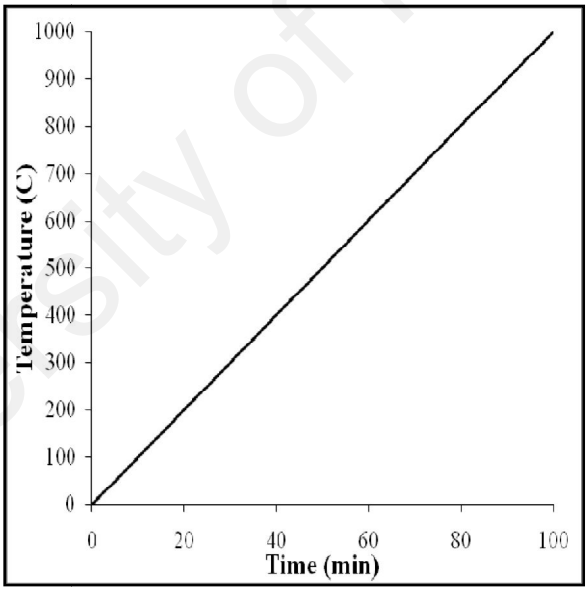

Figure 5.52 Time-temperature curve of a beam for heating case

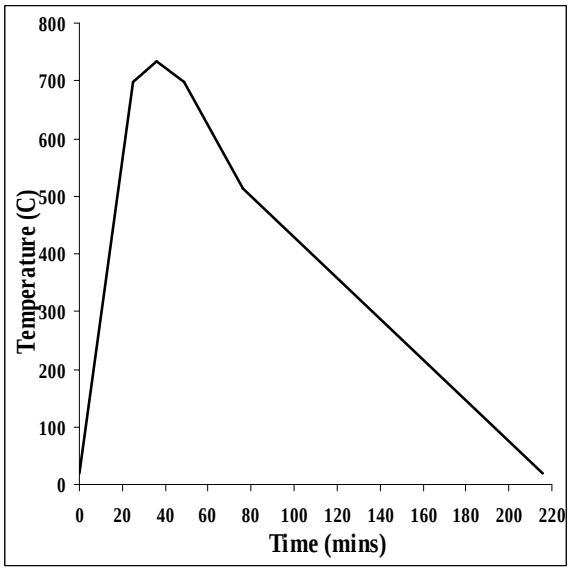

Figure 5.53 Time-temperature curve of a beam including the cooling phases (Bailey et al., 1996)

5.5.2 Analysis of Isolated Beam

The analysis on isolated beam is carried out by considering a fully restrained steel beam (UB 305 x 127 x 37) of 5 m span subjected to an initial load representing a load ratio of 0.6. Result of this isolated beam is then compared with frame structure analysis. Subsequently, a linear temperature history is applied uniformly along the beam up to a centroidal beam temperature T of 1000^{o}C. The connection temperature is considered as 0.7T, uniformly distributed along its depth.

The deformation demand in terms of rotation and axial deformation for the overall connection response is shown in Figure 5.54 and 5.55, respectively. As shown in the figures, high demands are imposed on the connection at elevated temperature. In the tension zone, the demand on the critical components (in the outermost layer) is shown in Figure 5.56. The overall connection response is influenced by the restraint to thermal expansion until the compressive effect is released after T=100^{0}C. In the compression region, the rotational stiffness of the connection governs the behaviour until the tensile membrane action in the beam dominates the response beyond T = 750^{0}C as shown in Figure 5.57.

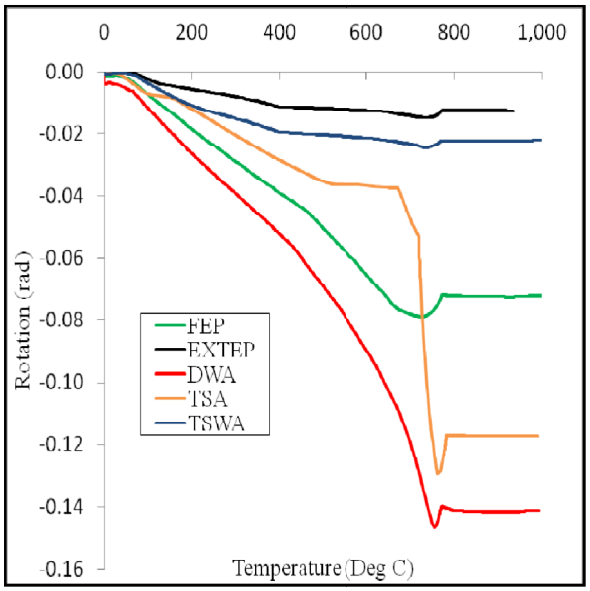

Figure 5.54 Connection rotation-temperature curves

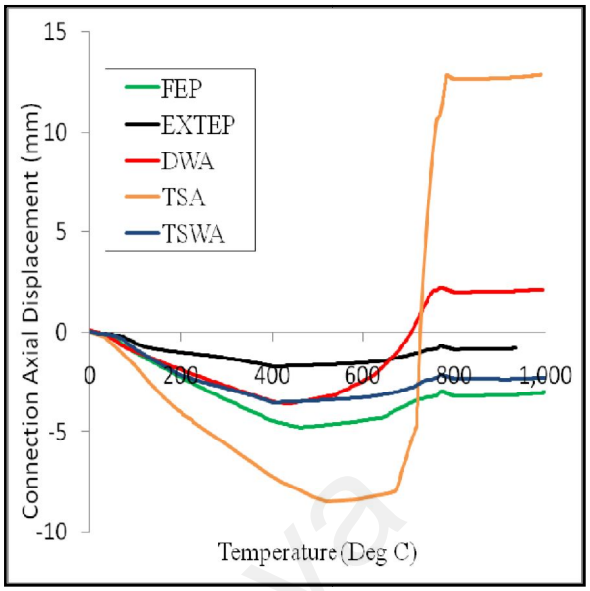

Figure 5.55 Connection axial displacement-temperature curves

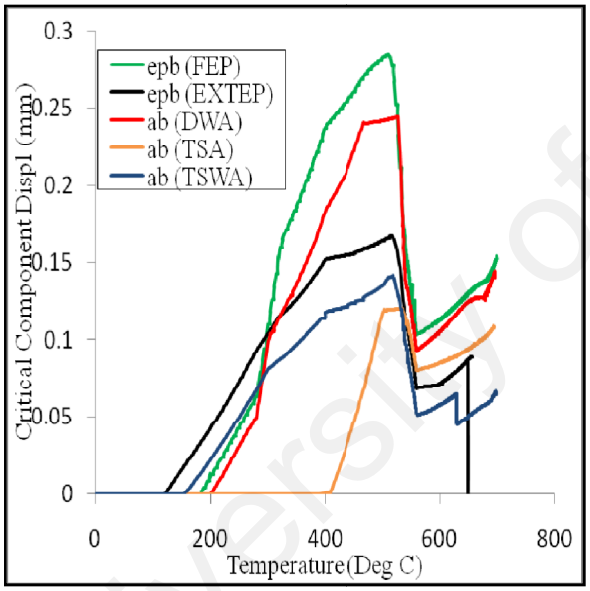

Figure 5.56 Critical component axial displacement-temperature curves (in tension zone)

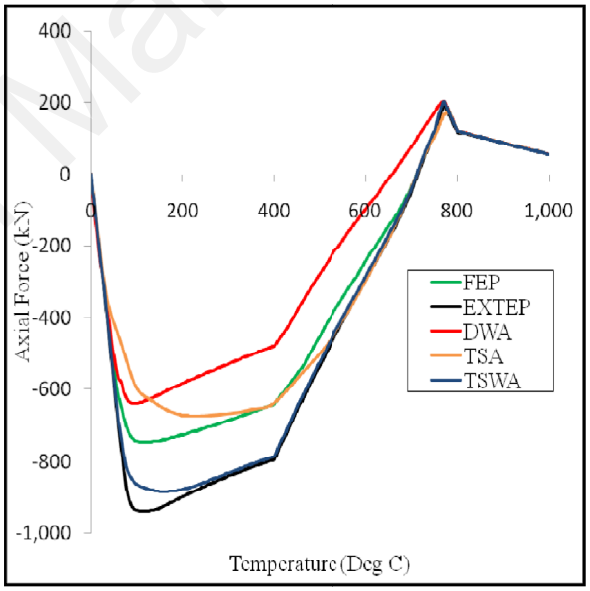

Figure 5.57 Connection axial force-temperature curves

5.5.3 Deformation Response of Frame Structure

5.5.3.1 Heating case

Linear temperature up to maximum temperature of 1000 ^{o}C is applied on the sub-frame. The fire is confined to the middle bay. As for isolated beam model, the deformation demand can be represented in term of deformation and rotation of overall connection with temperature. Comparisons were made between all connections, in terms of mid-span displacement, axial displacement at connection and rotation at connections. By comparing the sub-frame response with five different supported conditions as presented in Figure 5.58 (a) to (c), the effect of rotational restraint can be observed. The overall response can be depicted through the mid-span displacement of the middle beam. Figure 5.58 (a) shows that the displacement at mid-span of the beam starts increasing gradually until it reaches up to temperature of 700^{o}C under tensile force, after that the displacement increases rapidly due to failure of beam structure.

Due to longitudinal restraint, the beam has exerted compressive force to the joint from the beginning to temperature near 200 ^{o}C to 400 ^{o}C and after that the displacement reduces due to decreasing compressive force resisted by the connection. From the analysis, it shows that EXTEP is very stiff to axial response by the lowest value of axial displacement given. It then followed by DWA, TSWA, FEP and finally TSA connection.

Due to different degree of rotational stiffness of these types of connection, the rotational demand varies as shown in Figure 5.58 (c). The EXTEP and combined TSWA connections have the highest capacities, followed by TSA, FEP and DWA.

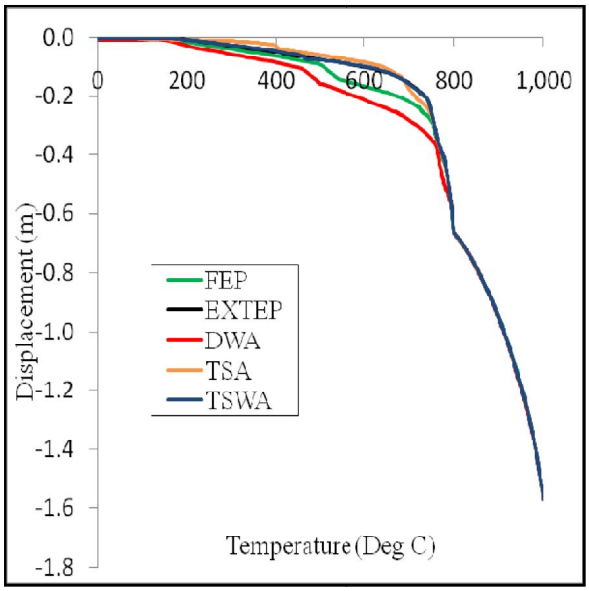

(a) Mid-span displacement

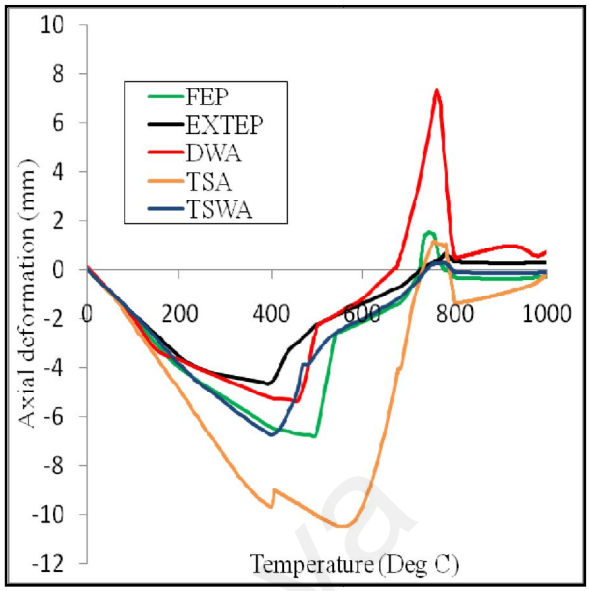

(b)Axial deformation of connection

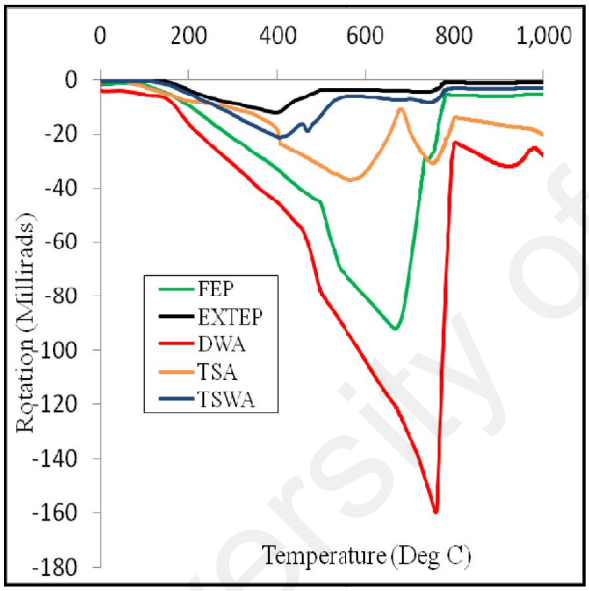

(c)Rotation at connection

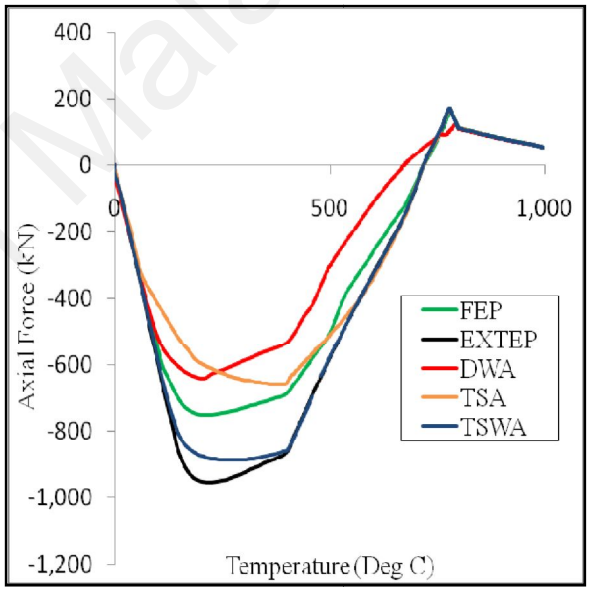

(d)Axial force at connections

Figure 5.58 Deformation and rotation for internal frame subjected to heating

It seems that result for axial force against temperature for isolated beam (Figure 5.57) and for connection under internal sub-frame (Figure 5.58 (d)) is similar. For axial displacement against temperature, the bahaviour under compressive force is almost similar between isolated beams and for sub-frame. In the tension region, result shows that for sub-frame model, axial deformation goes nearest to 0 values due to beam response.

Sub-frame analysis illustrates that the recovery of rotation under tensile force is huge compared to isolated analysis, this is due to restraint from boundary condition

governed by the column and also by cooler members. As a conclusion, a huge difference between analysis of structure for isolated beam analysis and frame analysis is the behaviour under tensile forces which the structure will highly recover under tensile force for frame depends on restrain and temperature exposed to the structure.

5.5.3.2 Heating and cooling case

For heating and cooling case, the time-vertical displacement at mid span (Figure 5.59 (a)) clearly shows that the maximum displacement occurs at maximum temperature and the beam starts to recover slightly during the cooling stage. From the analysis, EXTEP gives maximum displacement of 200mm, followed by TSWA connection 199 mm, TSA connection 229 mm, FEP connection 260 mm and finally DWA connection (DWA) is 320 mm. This is due to the resistance and stiffness of different connections' components of each semi-rigid connection..

At the early phase of analysis, axial force developed by connection is transfered to the column with an increasing temperature. Under cooling phase, the connection expands outward of the column due to extraction from the beam until the end of analysis. Axial displacements through cooling phase (Figure 5.59 (b)) keeps rising due to increasing tensile force until the end of analysis which resulting higher tensile force towards the connection in this case.

Time-rotation curve (Figure 5.59 (c)) for connection keeps increasing rapidly at early of analysis until it reaches maximum temperature. A massive recovery of rotation is observed with the reduction of temperature until the end of analysis. A rapid heating at the beginning of analysis will also result a rapid increasing rotation. A huge drop for DWA is due to the weaker component resistant compared to other connection types.

For heating only case, the overall displacement at mid-span of beam shows that the displacement keeps increasing due to increasing temperature and the reduction of

strength and stiffness of the structure. On the other hand, for heating and cooling cases, the maximum displacement reaches at maximum temperature and after that a recovery of displacement is observed due to reduction of temperature. Except for TSA and combination of TSWA connections, the recovery of displacement is slower due to resistance from the TSA. As for the rotation, it increases rapidly in the early stage of analysis due to rapid increasing temperature increase at the early stage of analysis and the rotation dropped back in cooling stage. In terms of capacity of axial force at connection, Figure 5.59 (d) illustrates that the connections resist maximum compressive force at early stage of analysis for heating and cooling case.

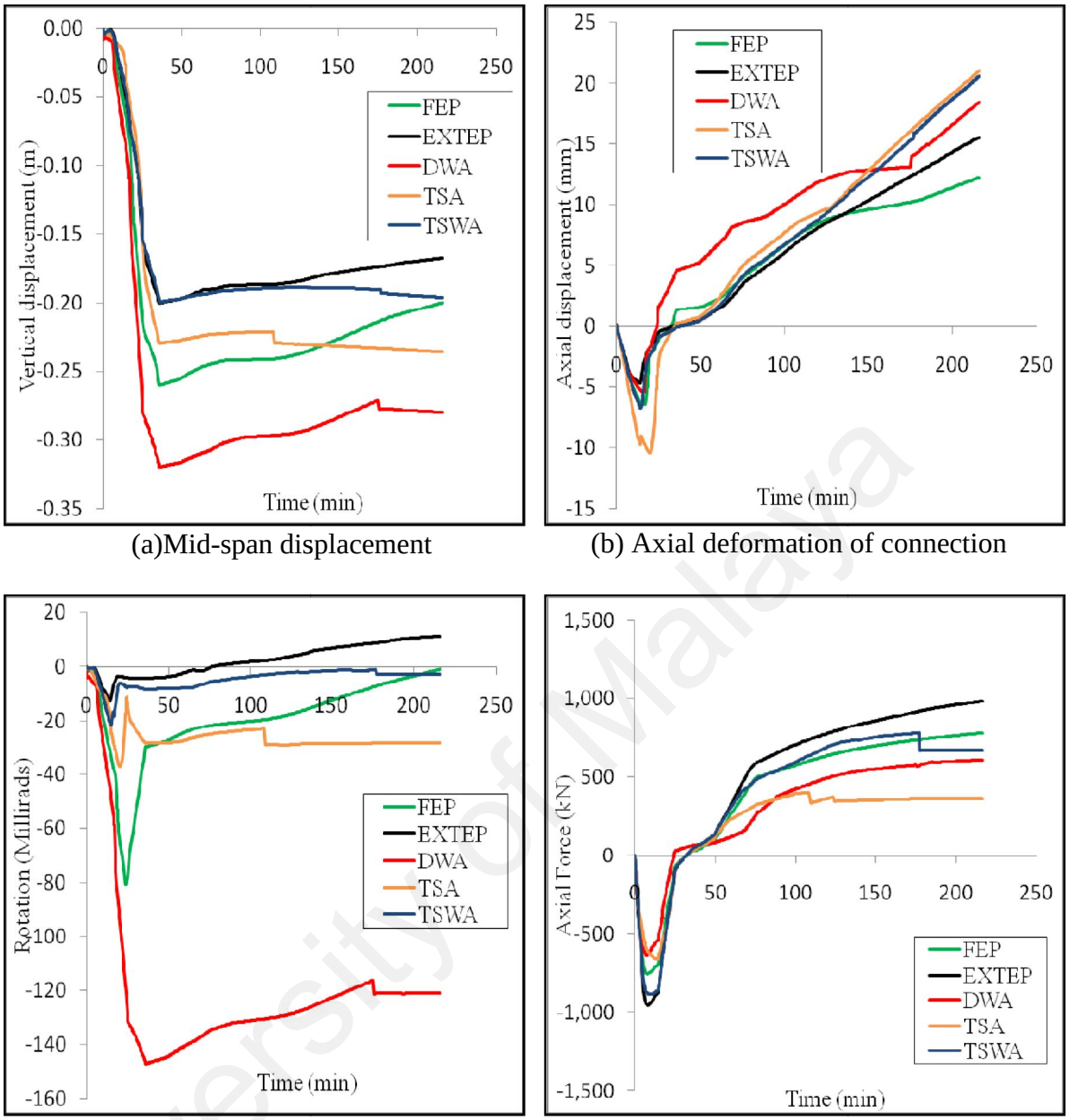

(a)Mid-span displacement (b) Axial deformation of connection

(c)Rotation at connection (d)Axial force at connections

Figure 5.59 Deformation and rotation for internal frame subjected heating and cooling temperature

5.5.4 Response of Critical Component on Frame Structure

5.5.4.1 For heating and cooling case

According to analysis on isolated beam by focusing to critical component failure for each connection type, a comparison of axial displacement was made with modelling as sub-frame structure. Results discussed are referring to behaviour of the first layer of

bolt which referring to end plate in bending (epb) for FEP as well as EXTEP and angle in bending (ab) for DWA, TSA as well as combination of TSWA.

Figure 5.60 and Figure 5.61 illustrate that the axial displacement of endplate in bending for FEP and angle in bending for TSA and DWA start to increase at temperature near 300^{o}C, endplate in bending in EXTEP already starts to increase after temperature 200^{o}C and angle in bending in TSWA starts to raise at temperature near to 400^{o}C. Note that the axial displacement of these components is developed when axial forces are in the tension region.

From five connection type models, three of them which are EXTEP, TSA and TSWA displaced to maximum value at maximum temperature which is assumed 0.7 from temperature applied on beam and after that axial displacement reduces slowly under cooling phase until it reaches to a stage where the response is given from connected members. As for flush end plate connection, the response of displacement reaches maximum value before maximum temperature achieved, this is because the tensile force is higher at maximum displacement, after that although tensile force keeps increasing, axial displacement reduces until the end of analysis. Different for DWA connection, the response from Figure 5.61 shows that, after reaching maximum temperature, the deformation keeps increasing in cooling phase until 112 ^{o}C. After that, a sudden drop can be seen due to overall deformation.

Axial force shows that TSA connection can resist higher capacity under compressive force which resulting lower axial displacement. Other connections resist compressive force below 150 kN for first layer. From all connections, Figure 5.62 illustrates that DWA resists higher tensile force which resulting higher axial displacement under cooling phase.

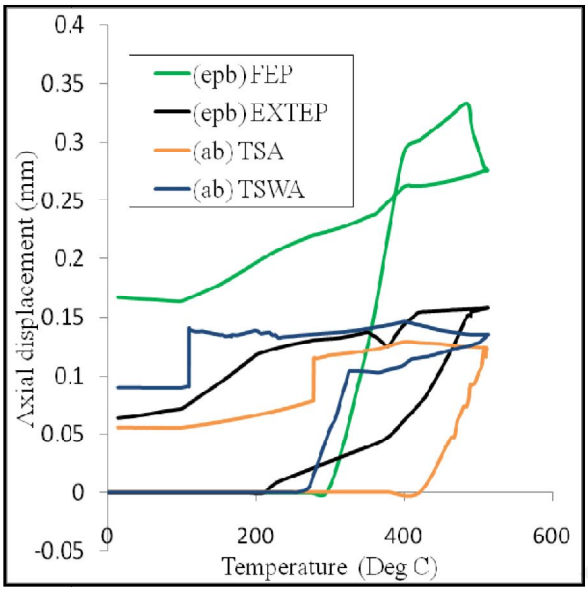

Figure 5.60 Axial displacement againts temperature for critical component

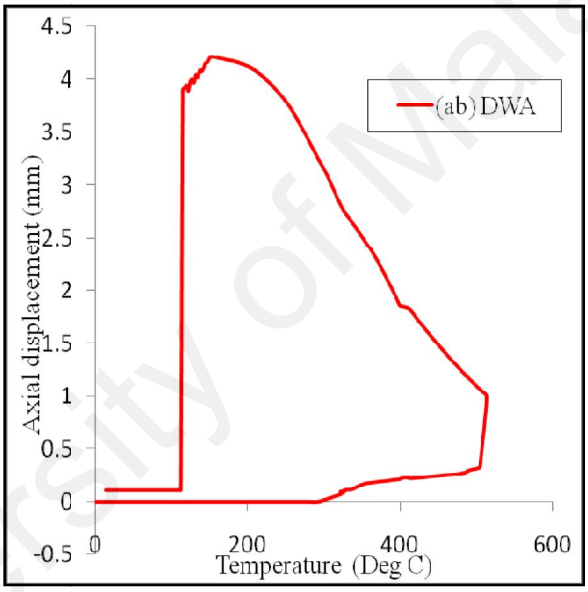

Figure 5.61 Axial displacement vs temperature for critical component for DWA connection.

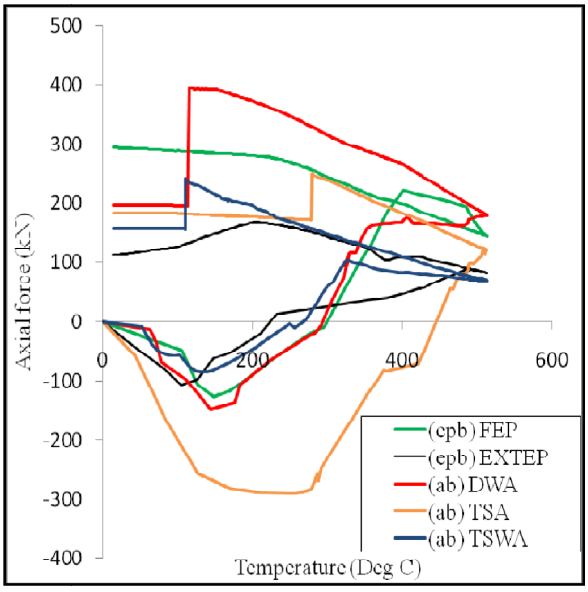

Figure 5.62 Axial force vs temperature for critical component

5.5.4.2 Heating case

In heating case, the critical component shows that for EXTEP axial displacement (Figure 5.63) starts to displace at temperature 220^{o}C, last connection starts to displace is TSA at temperature 430^{o}C. Other connections displace when temperature near to 300^{o}C. As compared to model as isolated beam, all models for sub-frame start to displace after a certain period at the beginning of analysis. The higher maximum displacement recorded governed by DWA connection followed by FEP, EXTEP, TSWA connection and finally TSA connection. Although the temperature keeps increasing, the displacement of connection drops back when reaching its limit.

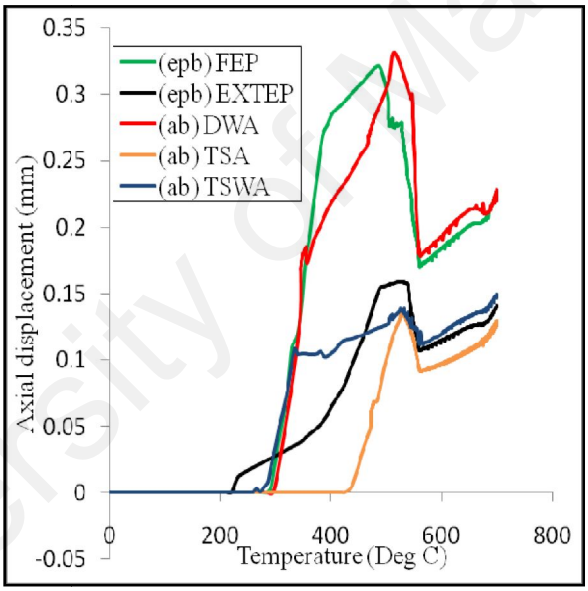

Figure 5.63 Axial displacement against temperature for critical component

Figure 5.64 shows axial force for the critical components againts temperature. The behaviour under compressive force at heating phase almost similar with heating and cooling case. Different with heating and cooling case, the heating case as the temperature increases, tensile force reduces after reaching maximum tensile capacity until the end of analysis, this is due to reduction of strength and stiffness with incresing temperature

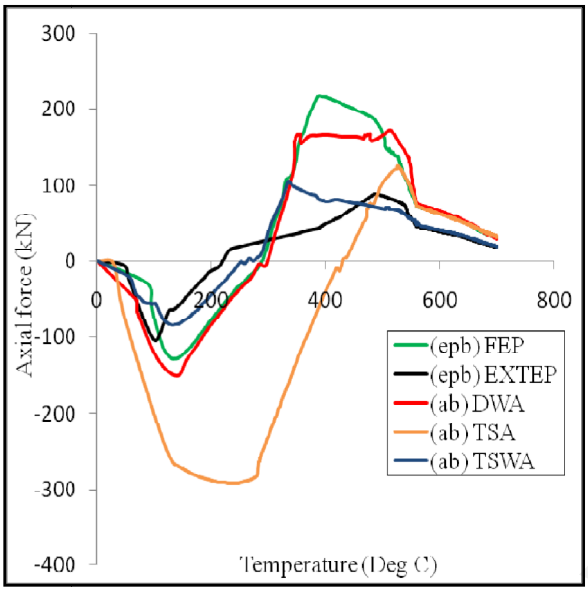

Figure 5.64 Axial force against temperature for critical component

5.6 CONCLUDING REMARKS

This chapter presents parametric studies to assess the behaviour of isolated beam and floor system for Gurun Fire Test and sub-frame model for test carried by Santiago et. al 2008. In understanding the influence of connection at elevated temperature, parametric studies were carried out in order to determine factors affecting the performance of connection at elevated temperature. Under fire condition, the connection is worse compared to actual performance at ambient. This is because of reduction of strength and stiffness of the structure under various factors.

Results highlight the need to review actual connection temperature and temperature gradients in order to reduce inaccuracy in simulation work of structure under elevated temperature. Temperature gradient across the beam illustrates very high contribution to displacement and it is more realistic at actual condition and should be considered in analysis.

Different connection types behave differently according to its geometrical properties and capacity of each component. There is slightly small different of behaviour by considering the influence of reduction of strength and stiffness with temperature for connected members. The influence of connection behaviour on the response of a steel and composite beam is also discussed. Investigation on the supported conditions shows that the rotational restraint and capacity of the connection can significantly influence the response of the beam. The load carrying capacity of the connection can be improved by changing its configurations as well as geometric and material properties.

The effect of temperature loading is significantly influence the structural response, where the beam is capable of reducing the displacement during the cooling stage. Under actual time-temperature curve, the response of the member is fully governed by the failure of the component in tension zone. Again, the effect of

temperature loading for this particular connection configuration is not significant in the tension region due to very low connection capacity.

Simulation results on the floor system behaviour in Gurun Fire Test considering the actual connection configuration show that the support conditions have significant influenced on the floor response as the response of the member is fully governed by the failure of the connection components in tensile region, especially for seat and web angle connection, as well as DWA connection. This is due to geometric properties of the angle connection, particularly the angle thickness, which cause failure due to angle in bending when the connection is subjected to tension. Findings in the parametric studies also indicate the importance of accounting for the slab temperature and temperature gradient of the steel beam. However, temperature gradient in the slab has mere influence on the floor response. In addition, investigating the structural behaviour under actual fire scenario is very important as the members show recovery of displacement under cooling stage and exhibit failure of the connection component in tension. However, the cooling stage induces tensile forces on the structural elements which eventually cause failure to partial strength connections, particularly to DWA due to lower resistance.

Under fire conditions, higher levels of ductility demand would be imposed on the connections. It was observed that different connection typology shows different ductility demand for structure under isolated beam and under sub-frame. Beside resistance of connected member, the response of the structure also influenced by the condition of temperature applied on the structure. From the analysis, the failure of the structure is governed by the critical component located at the outer layer of the connection. In this study, EXTEP and TSWA connection have the highest capacity, followed by TSA, FEP and DWA according to the geometrical arrangement and lever arm of the connections. In the following chapter, conclusions and recommendations will be made for this entire study.

CHAPTER 6.0 CONCLUSIONS AND RECOMMENDATIONS

6.1 CONCLUSIONS

The first objective of this thesis is to investigate the steel connection behaviour at elevated temperatures through numerical modeling based on the recent developed joint model by Ramli Sulong (2005). Several conditions were considered in studying the behaviour of steel connection under elevated temperature, such as analyzing connections in isolated beam, floor systems and in frame structures. This thesis highlights the importance of using Component Based method as one of the alternative and economical way in carrying out studies on steel connection behaviour at elevated temperature. From the validation work with Gurun Fire Test results, the floor system modeled by using 2D-grillage model gives close prediction of mid-span displacement with percentage error less than 10%.

Second objective of this thesis is to conduct parametric and sensitivity studies on steel connection and floor systems under fire loading based on Gurun Fire Test. Based on the connection model , parametric studies were carried out to identify parameters of several connections that affected the overall structural performance. From these studies, several factors have been identified such as influence of slab restraint, slab temperature, boundary condition, temperature gradient and temperature loading. Floor system is significantly influenced by the continuity of the slab. By considering a restraint between slab and steel beam, it has resulted in a reduction of mid-span deformation. Large deformation was observed when the ratio of slab temperature to secondary steel beam temperature is above 0.5T. These parametric studies also highlighted the importance of considering the actual semi-rigid connection compared to by simply assuming connection as rigid or pin connection. The mid-span displacement incorporating semi-rigid connection is similar to the case of pin connection under compressive forces. However, in the tensile region, the mid-span deformation is between the pin and rigid connection applied on overall floor. This is due to the failure

of connection components. The temperature gradient across the steel beam cross section gives more influence to overall structural response compared to minimum effect when temperature gradient was applied across the slab. Furthermore, temperature loadings give huge effect on the mid-span response especially under catenary action, where the mid-span displacement has capability to recover in the cooling stage.

Parametric studies on isolated steel beam were carried out by using DWA connection. From the analysis of the results, it shows that selected semi-rigid connection behave similarly to pin connection under tensile force, however, under cooling phase, the beam capacity is lower due to yielding of the connection components in tensile region. The load ratio applied on the steel beam also influence the performance, where an enormous increase of mid-span displacement was observed when the load ratio above 0.6 was applied. Considering the effect of web angle thickness, significant reduction of deformation of the beam was observed especially in the cooling phase for a thicker web angle. The third objective is to investigate the steel connection behaviour at elevated temperature in the frame structures by using frame tests conducted in Coimbra University, Portugal. Validation and numerical studies on the steel connection behaviour in the frame structures at elevated temperature were carried out. Two types of connections were studied i.e. three specimens of flush end plate connections and one specimen of EXTEP connection. It was found that the model is capable of accurately predicted the experiment results especially for flush end plate connections under elastic phase. Once the cooling phase started, the heated beams began to recover the strength and stiffness from an inelastic stage. For parametric studies, two specimens were selected from the frame test carried out by Santiago (2008), i.e FJ03 and EJ01. Several factors were investigated including connection temperature, temperature gradient across steel connection, different connection typology and effect of reduction factor of strength and stiffness. From the results of parametric studies, connection temperatures, temperature gradient applied on the

connection element and connection typology give a significant effect on the beam's mid-span displacement and rotation at the connection under cooling phase. On the other hand, reduction factor of strength and stiffness give minor affect of the performance of the frame structure.

The last objective is to investigate the ductility demand of connection components and rotation capacity of steel joints at elevated temperature. An internal steel sub-frame used in Cardigton test were selected. Two conditions are considered; (i) where the sub-frame is subjected to heating only with a uniform temperature applied across and along the steel section and (ii) the sub-frame is subjected to heating and cooling phases and uniform temperature is considered across and along the steel section. Five connection configurations are examined in investigating ductility demand including FEP, EXTEP, DWA, TSA, and combination of TSWA. From five connection types selected, the rotation demand varies according to the different degree of rotation stiffness of each connection. From the analysis, based on the first layer of bolt and critical component for each connection types, EXTEP and TSWA connections have the highest capacities to resist forces, followed by TSA, FEP and DWA. The critical component for each connection is referring to end plate in bending for FEP as well as EXTEP and angle in bending for DWA, TSA as well as combination of TSWA. By comparing the response of axial displacement, EXTEP is very stiff connection, which gives the lowest value of axial displacement followed by DWA connection, TSWA connection, FEP connection and finally TSA connection. From rotation–temperature curve, it shows that DWA gives the higher rotation value compared to others. For heating and cooling case, a different phenomenon of response can be seen under cooling phase, where under this phase, a recovery of displacement is observed due to reduction of temperature. This study highlights the importance of considering the actual performance of semi-rigid connection, where different connection types behave

differently according to its geometrical properties and capacity of each component to resist applied loading.

6.2 RECOMMENDATIONS

1. A few studies of steel connection have been carried out, especially focusing on angle connection at elevated temperature. The true behaviour of connections at elevated temperature needs to be studied to fill the gaps in current guidelines. Experimental work is quite expensive method to be used compared to component based method which gives a valuable result to create a simulation model that can be used for references in parametric studies. Further studies on detail active component of angle connection need to be considered in component based method.

2. To make sure the Component Based Method developed by Ramli Sulong (2005) is user friendly, a modification needs to be done. For example, output data, a tool needs to be created to differentiate the different components for different types of connection in output result when analyzing the floor system.

3. More experimental test on steel connection under elevated temperature need to be carried out, to study the actual moment-rotation demand. The finding will be useful for designer in designing stage of joint, by considering the actual performance of the connection at ambient as well as at elevated temperature.

4. More studies on semi-rigid connection need to be done in identifying the ductility demand of different connection types. Currently very limited guideline on ductility demand under elevated temperature where current design guidelines only refer to ambient temperature. A continuous research work should be made in this area and a valuable finding should be proposed.

5. Need further studies on variable that affects the reduction factor of strength and stiffness of steel structure under fire.

6. Current model of floor system using 2D grillage model, furthermore a 3D model needs to be considered to develop more accurate model.

REFERENCES

Abecassis-Empis, C., Reszka, P., Steinhaus, T., Cowlard, A., Biteau, H., Welch, S., Rein, G. & Torero, J. L. (2007). Characterisation of Dalmarnock fire Test One. Experimental Thermal and Fluid Science, Article in Press.

Al-Jabri, K. S. (1999). The Behaviour of steel and composite Beam-Column Connections in fire. PhD thesis, Department of Civil and Structural Engineering, University of Sheffield.

Al-Jabri, K. S., Burgess, I. W. & Plank, R. J. (2004). Prediction of the degradation of connection Characteristics at elevated temperature. *Journal of Constructional Steel Research,* 60**,** 771-781.

Al-Jabri, K. S. (2004). Component-based model of the behaviour of flexible end-plate connections at elevated temperatures. *Composite Structures,* 66(1-4), 215-221.

Al-Jabri, K. S., Burgess, I. W., Lennon, T. & Plank R. J. (2005). Spring-stiffness model for flexible end-plate bare-steel joints in fire. *Journal of Constructional Steel Research,* 61, 1672–1691.

Al-Jabri, K. S., Burgess, I. W., Lennon, T. & Plank R. J. (2005). Moment–rotation–temperature curves for semi-rigid joints. *Journal of Constructional Steel Research,* 61, 281–303.

Al-Jabri, K. S., Seibi, A. & Karrech, A. (2006). Modelling of unstiffened flush end-plate bolted connections in fire. *Journal of Constructional Steel Research*, Vol 62(1-2), 151-159.

Al-Jabri, K. S., Seibi, A. & Karrech, A. (2006). Modelling of unstiffened flush end-plate bolted connections in fire. *Journal of Constructional Steel Research,* 62, 151-159.

Andrew H. B. (2002). Structural design for fire safety, John Wiley & Son, England.

Anthony, K. A., Burgess, I. W. & Roger J. P. (2006). Effects of thermal gradients on membrane stresses in thin slabs. *4th International Workshop*, Aveiro, Portugal.

Anthony, K. A., Burgess, I. W. & Roger J. P. (2008). Effects of edge support and reinforcement ratios on slab panel failure in fire. *Proceedings of the 5th Structure in Fire Conference*, Singapore.

Azizinamini, A., Bradburn, J. H. & Radziminski, J. B. (1987). Initial stiffness of semi-rigid steel beam-to-column connections. *Journal of Constructional Steel Research*, 8, 71-90.

Bailey, C. G., Burgess, I. W. & Plank, R. J. (1996). Analyses of the effects of cooling and fire spread on steel-framed buildings. *Fire Safety Journal*, 26, 273-279.

Bailey, C. G. (2007). One Stop Shop in Structural Fire Engineering, http://www.mace.manchester.ac.uk/project/research/structures/strucfire/Design/performance/thermalAnalyses/testData/default.htm.

Bailey, C. G. & Moore D. B. (1999). The influence of local and global forces on column design. Final report for DETR. Partners in Technology contract no. CC1494, September.

Bailey, C. G. & Guo, S. (2011). Experimental behaviour of composite slabs during the heating and cooling fire stages. *Engineering Structures*, 33, 563–571.

Beg, D., Zupancic, E. & Vayas, I. (2004). On the rotation capacity of moment connections. *Journal of Constructional Steel Research,* 60, 601–620.

BS 5950: Part 8 (2003). Structural use of steelwork in building- Code of Practice for Fire Resistance Design, British Standards Institution.

Chen, K. Y, Chen, S. J. & Ho, M. C. (2009). Behavior of beam-to-column moment connections under fire load. *Journal of Constructional Steel Research*, 65, 1520-1527.

Chlouba, A. U. J., Sokol, Z. & Wald, F. (2008). Unrestrained beam under naturalfire test. *EUROSTEEL*, Graz, Austria.

Chung, H. Y., Su, W. J. & Lin, R. Z. (2010). Application of fire-resistant steel to beam-to-column moment connections at elevated temperatures. *Journal of Constructional Steel Research,* 66, 289-303.

Dai, X. H., Wang, Y. C. & Bailey, C. G. (2010). Numerical modelling of structural fire behaviour of restrained steel beam-column assemblies using typical joint types. *Engineering Structures*, 32, 2337-2351.

Danesh, F., Pirmoz, A. & Saedi Daryan, A. (2007). Effect of shear force on the initial stiffness of top and seat angle connections with double web angles. *Journal of Constructional Steel Research,* Vol 63(9), 1208-1218.

Dharma, R. B. (2007). Buckling Behaviour of Steel and Composite Beams at Elevated Temperatures. PhD Thesis, School of Civil and Environmental Engineering.

Ding, J. & Wang, Y. C. (2007). Experimental study of structural fire behaviour of steel beam to concrete filled tubular column assemblies with different types of joints. *Engineering Structures*, 29, 3485–3502.

Dubina, D., Grecea, D., Ciutina, A. & Stratan, A. (2000). Influence of connection typology and loading asymmetry, RECOS: moment resistant connections of steel frames in seismic area, design and reliability. RECOS. London: E&FN Spoon.

Dwaikat, M. M. S., Kodur, V. K. R., Quiel, S. E. & Garlock, M. E. M. (2011). Experimental behavior of steel beam-columns subjected to fire-induced thermal gradients. *Journal of Constructional Steel Research*, 67, 30-38.

Elghazouli, A. Y. & Izzudin, B. A. (2001). Analytical assessment of the structural performance of composite floors subject to compartment fires. *Fire Safety Journal*, 36, 769-793

Eurocode 3: Part 1.2 (1995). Design of steel structures: Part 1.2 General Rules, Structural Fire Design. ENV 1993-1-2, Commission of European Communities, Brussels, Belgium.

Eurocode 3: Part 1.2 (2002). Design of steel structures: Part1.2 General Rules, Structural fire design. EN 1993-1-2, Commission of European Communities, Brussels, Belgium.

Eurocode 3: Part 1.8 (2002). Design of steel structures: Part1.8 Design of Joints. EN 1993-1-8, Commission of European Communities, Brussels, Belgium.

Florian, M. B., Burgess, I. W., Davison, J. B. & Plank, R. J. (2007).The development of a component-based connection element for endplate connections in fire. *Fire Safety Journal*, 42, 498–506.

Girao Coelho, A. M., Bijlaard, F. S. K. & Silva, L. S. (2004). Experimental assessment of the ductility of extended end plate connections. ***Engineering Structures,*** 26, 1185–1206.

Heidarpour, A. & Bradford, M. A. (2010). Non-discretisation formulation for the non-linear analysis of semi-rigid steel frames at elevated temperatures. *Computers and Structures*, 88, 207–222.

Izzuddin, B. A. (1991). Nonlinear Dynamic Analysis of Framed Structures. London, Imperial College of Science, Technology and Medicine, ADAPTIC.

Kirby, B. R. (1995). The Behaviour of High-strength Grade 8.8 Bolts in Fire. *Journal of Constructional Steel Research*, 33, 3-38.

Kodur, V. K. R. & Dwaikat, M. M. S. (2009). Response of steel beamcolumns exposed to fire. *Engineering Structures*, 31, 369-379.

Kuhlmann, U., Davison, J. B. & Kattner, M. (1998). Structural systems and rotation capacity. In: Proceedings of COST conference on control of the semi-rigid behaviour of civil engineering structural connections, Liege, Belgium. 167–76.

Lamont, S. & Usmani, A. S. (2003). Possible 'panel instability' in composite deck floor systems under fire. *Journal of Constructional Steel Research,* 59, 1397-1433.

Lamont, S., Gillie, M. & Usmani, A. S. (2007). Composite steel-framed structures in fire with protected and unprotected edge beams. *Journal of Constructional Steel Research,* 63, 1138-1150.

Lawson, R. M. (1990). Behaviour of steel beam-to-column connections in fire. *The Structural Engineer,* Vol. 68(14/17), 263-271.

Leston-Jones, L. C., Burgess, I. W., Lennon, T. & Plank R. J. (1997). Elevated-temperature moment-rotation tests on steelwork connections. Proceedings of the Institution of Civil Engineers: *Structures and Buildings*, Vol. 122(4), 410-419.

Leston-Jones, L. C. & Burgess, I. W. (1997). The influence of Semi-Rigid Connections on the Performance of Steel Framed Structures in Fire. PhD thesis, Department of Civil and Structural Engineering, University of Sheffield.

Lien, K. H., Chiou, Y. J., Wang, R. Z. & Hsiao, P. A. (2009). Nonlinear behavior of steel structures considering the cooling phase of a fire. *Journal of Constructional Steel Research,* 65, 1776-1786.

Liu, T. C. H., Fahad, M. K. & Davies, J. M. (2002). Experimental investigation of behaviour of axially restrained steel beams in fire. *Journal of Constructional Steel Research,* Vol 58, 1211–1230.

Maggi, Y. I., Goncalves, R. M., Leon, R. T. & Ribeiro, L. F. L. (2005). Parametric analysis of steel bolted end plate connections using finite element modeling. *Journal of Constructional Steel Research,* Vol. 61(5), 689-708.

Mao, C. J., Chiou, Y. J., Hsiao, P. A. & Ho, M. C. (2009). Fire response of steel semi-rigid beam column moment connections. *Journal of Constructional Steel Research.* 65, 1290-1303.

O' Connor, M. A. & Martin, D. M. (1998). Behavior of multistory steel framed buildings subjected to fire attack. *Journal of Construction Steel Research,* Vol. 46(1–3), 295.

Petterson, O., Magnusson, S. E. & Thor, J. (1976). Fire engineering design of steel structures. Publication No. 50, Swedish Institute of Steel Construction, Sweden.

Pirmoz, A., Khoei, A. S., Mohammadrezapour, E. & Saedi Daryan, A. (2009). Moment-rotation behavior of bolted top-seat angle connections. *Journal of Constructional Steel Research,* Vol. 65(4), 973-984.

Poh, K. W. (2001). Stress strain-temperature relationship for structural steel. *Journal of Material Civil Engineering*, 13(5), 371-379.

Qian, Z. H., Tan, K. H. & Burgess, I. W. (2008). Behavior of steel beam-to-column joints at elevated temperature: Experimental investigation. *Journal of Constructional Steel Research,* Vol. 34(5), 713-26.

Qian, Z. H., Tan, K. H. & Burgess, I. W. (2009). Numerical and analytical investigations of steel beam-to-column joints at elevated temperatures. *Journal of Constructional Steel Research*, Vol. 65, 1043-1054.

Ramli Sulong, N. H. (2005). Behaviour of steel connections under fire conditions. PhD thesis, Imperial College London, University of London.

Ramli Sulong, N. H., Elghazouli, A. Y. & Izzuddin, B. A. (2007). Behaviour and design of beam-to-column connections under fire conditions. *Fire Safety Journal*, Vol 42, 437-451.

Real, P. V. & Franssen, J. M. (1999). Lateral buckling of steel I beams under fire conditions. Comparison between the EUROCODE 3 and the SAFIR code. Internal report no. 99/02, Institute of Civil Engineering, Service Ponts et Charpents of the University of Liege.

Real, P. V., Piloto, P. A. G. & Franssen, J. M., (2003). A new proposal of a simple model for the lateral-torsional buckling of unrestrained steel I-beams in case of fire: experimental and numerical validation. *Journal Construct Steel Research*, 59, 179–199.

Real, P. V., Cazeli, R., Silva, L. S., Santiago, A. & Piloto, P. (2004). The effect of residual stresses in the lateraltorsional buckling of steel I-beams at elevated temperature. *Journal of Constructional Steel Research,* 60, 783–793.

Saedi Daryan, A. & Bahrampoor, H. (2009). Behavior of Khorjini connections in fire. *Fire Safety Journal,* Vol. 44(4), 659-664.

Saedi Daryan, A. & Yahyai, M. (2009). Behavior of bolted top-seat angle connections in fire. *Journal of Constructional Steel Research,* Vol. 65(3), 531-541.

Sanad, A. M., Usmani, A. S. & Rotter, J. M. (2000). Structural behaviour in fire compartment under different heating regimes - Part 1(slab thermal gradients). *Fire Safety Journal,* 35, 99-116.

Sanad, A. M., Usmani, A. S. & Rotter J. M. (2000). Structural behaviour in fire compartment under different heating regimes - part 2: (slab mean temperatures). *Fire Safety Journal*, 35, 117-130.

Santiago, A. (2008a). Behaviour of Beam-to-Column Steel Joints Under Natural Fire. phd thesis, Coimbra, Portugal.

Santiago, A., Real, P. V. & Veljkovic, M. (2008b). Numerical study of a steel sub-frame in fire. *Computers and Structures,* 86, 1619–1632.

Santiago, A., Silva, L. S., Real, P. V., Vaz, G. & Lopes, A. G. (2008c). Experimental Evaluation Of The Influence Of Connection Typology On The Behaviour Of Steel Structures Under Fire. *Engineering Journal*, Vol 46 (2), 81-98.

Silva, L. S. & Girao Coelho, A. M. (2000). A analytical evaluation of the response of steel joints under bending and axial force. *Computers & Structures*, 79, 873-881.

Silva, L. S., Santiago, A. & Real, P. V. (2002). Post-limit stiffness and ductility of end plate beam-to-column steel joints. *Computers & Structures*, 80, 515-531.

Silva, L. S. & Gervasio, H. (2004). A probabilistic evaluation of the rotation capacity of end-plate beam-to-column steel joints. *Connections in Steel Structures V*. Amsterdam.

Silva, L. S. (2008). Towards a consistent design approach for steel joints under generalized loading. *Journal of Constructional Steel Research,* 64, 1059–1075.

Silva, L. S. & Santiago, A. (2005). Behaviour of steel joints under fire loading. *Steel and Composite Structures*, 5, 485-513.

Spyrou, S. (2002). Development of a component-based model of steel beam-to-column joints at elevated temperatures. PhD thesis, Department of Civil and Structural Engineering, University of Sheffield.

Spyrou, S., Davison, J. B., Burgess, I. W. & Plank, R. J. (2004). Experimental and analytical investigation of the 'compression zone' component within a steel joint at elevated temperatures. *Journal of Constructional Steel Research,* 60, 841–865.

Spyrou, S., Davison, J. B., Burgess, I. W. & Plank, R. J. (2004). Experimental and analytical investigation of the 'tension zone' components within a steel joint at elevated temperatures. *Journal of Constructional Steel Research*, Vol. 60 (6), 867-896.

Sarraj, M., Burgess, I. W. & Davison, J. B. (2007). Finite element modelling of steel fin plate connections in fire. *Fire Safety Journal*, Vol. 42(6-7), 408-415.

Swanson, J. A. (1999). Characterization of the strength, stiffness and ductility behavior of T-stub connections. PhD thesis, Georgia Institute of Technology, Atlanta, USA.

Tapsir, S. H. (2004). Structural Fire Engineering: Investigation of Gurun Fire Test. Universiti Teknologi Malaysia Skudai, Johor, Malaysia, ISBN no. 983-52-0352-0.

Usmani, A. S. & Cameron, N. J. K. (2004). Limit capacity of laterally restrained reinforced concrete floor slabs in fire. *Cement & Concrete Composites,* 26, 127–140.

Wald, F., Silva, L. S., Moore, D. & Santiago, A. (2004). Experimental behaviour of steel joints Under natural fire. Connections in Steel Structures V. Amsterdam, June 3-4.

Wald, F., Silva, L. S., Moore, D. B., Lennon, T., Chladna, M., Santiago, A., Benes, A. & Borges, L. (2006). Experimental behaviour of a steel structure under natural fire. *Fire Safety Journal,* 41, 509–522.

Wald, F., Sokol, Z. & Moore, D. B. (2009). Horizontal forces in steel structures tested in fire. *Journal of Constructional Steel Research,* 65, 1896-1903.

Wang, W. Y., Li, G. Q. & Dong, Y. L. (2007). Experimental study and spring-component modelling of extended end-plate joints in fire. *Journal of Constructional Steel Research,* 63, 1127–1137.

Witteveen, J., Twilt, L. & Bijlaard, F. S. (1977). The stability of braced and unbraced frames at elevated temperatures. International symposium of stability of steel structures, Liege.

Wang, Y. C. (2002). Steel and composite structures 'Behaviour and design for fire safety. SPON PRESS, Tylor and Francis Group.

Yin, Y. Z. & Wang, Y. C. (2004). A numerical study of large deflection behaviour of restrained steel beams at elevated temperatures. *Journal of Constructional Steel Research,* 60, 1029–1047.

Yang, J. G. & Lee, G. Y. (2007). Analytical models for the initial stiffness and ultimate moment of a double angle connection. *Engineering Structures,* Vol. 29(4), 542-551.

Yang, J. G., Chen, K. C., Ho, S. J. & Chin, M. (2009). Behavior of beam-to-column moment connections under fire load. *Journal of Constructional Steel Research*, Vol. 65(7), 1520-1527.

Hu, Y., Davison, B., Burgess, I. W. & Plank, R. J. (2008). Experimental study on flexible end plate connections in fire. *EUROSTEEL*, Graz, Austria.

Yu, H., Burgess, I. W., Davison, J. B. & Plank, R. J. (2007). Experimental Investigation of the Robustness of Fin Plate Connections in Fire. *5th International Conference on Advances in Steel Structures*, Singapore.

Yu, H., Burgess, I. W., Davison, J. B. & Plank, R. J. (2008). Experimental investigation of the tying capacity of web cleat connections in fire. *EUROSTEEL*, Graz, Austria.

Yu, H., Burgess, I. W., Davison, J. B. & Plank, R. J. (2009). Tying capacity of web cleat connections in fire, Part 1: Test and finite element simulation. *Engineering Structures*, Vol. 31(3), 651-663.

Yu, H., Burgess, I. W., Davison, J. B. & Plank, R. J. (2009). Tying capacity of web cleat connections in fire, Part 2: Development of component-based model. *Engineering Structures*, Vol.31(3), 697-708.

Yu, H., Burgess, I. W., Davison, J. B. & Plank, R. J. (2009). Development of a yield-line model for endplate connections in fire. *Journal of Constructional Steel Research*, 65, 279-1289.

Zhao, M. R. B. & Vassart, O. (2008). Full Scale Test Of A Steel And Concrete Composite Floor Exposed to ISO Fire and Corresponding Numerical Investigation. *EUROSTEEL*, Graz, Austria

APPENDICES

APPENDIX A1 – Data file of Isolated steel beam model for Gurun Fire test.

```
#unit kN,m
#
analysis 2d static
#
#
materials
mat.name     model      properties
steel        stl4       205e6 41.0e6 100 700 1200 &
                        275e3 27.5e3 400 800 1200 &
                        0.0 0.0 200 600 1200 &
                        0.010125 0.01485 750 850 1200
#
 mat.name    model      properties
    mat1       gen1 460e3 100.0 1.0 400.0 0.91 700.0 0.21 1200.0 0.0 &
                    205e6 100.0 1.0 400.0 0.43 700.0 0.077 1200.0 0.0&
                    0.0000001 500.0 1.0 600.0 1.0 700.0 1.0 1200.0
1.0&
                    275e3 100.0 1.0 400.0 0.91 700.0 0.21 1200.0 0.0 &
                    0.02 500.0 1.0 600.0 1.0 700.0 1.0 1200.0 1.0

    mat2       gen1 827.0e3 300 1.0 680.0 0.17 1000 5.84e-3 1200 0.0 &
                     210e6 100 1.0 400.0 0.43 700.0 0.077 1200.0 0.0 &
                     0.0000001 500.0 1.0 600.0 1.0 700 1.0 1200 1.0 &
                     634.32e3 300 1.0 680 0.17 1000 5.84e-3 1200 0.0 &
                     0.001 500.0 1.0 600.0 1.0 700.0 1.0 1200.0 1.0

    mat3       gen1 446.16e3 100 1.0 400 0.91 700 0.21 1200 0.0 &
                     205e6 100 1.0 400 0.43 700 0.077 1200 0.0 &
                     0.0000001 500 1.0 600 1.0 700 1.0 1200 1.0 &
                     275e3 100 1.0 400 0.91 700 0.21 1200 0.0 &
                     0.02 500 1.0 600 1.0 700 1.0 1200 1.0
#
#
sections
sec.name    type  mat.name    dimensions
ub          isec  steel       0.199 0.012 0.199 0.012 0.422 0.008
#
#
groups
type.of.element = cbp2
grp.name    sec.name  monitoring.points
beam        ub           200
#
type.of.element = jbc2
 grp.name   type                  mat.name(s)   parameters
joint  steel web.angle rigid  mat1 mat2 mat3    19.05e-3 285.02e-6 &
                                                155.0e-3 10e-3 0.1e-3
&
                                                2.0e-3 75e-3 43.4e-3 &
                                                40.0e-3 0.5 12.0e-3 &
                                                16e-3 130e-3 100.0e-3
&
                                                50e-3 50e-3 13e-3 &
                                                75e-3 200e-3 5e-3 &
                                                446e-3 12e-3 8e-3 &
                                                2 0.3 1
#
#
```

```
structural.nodal.coordinates
nod.name          x       y
        1a      0.0     0.0
f       1       0.0     0.0
r       1       0.16    0.0 27
        29      4.5     0.0
#
#
non.structural.nodal.coordinates
nod.name    x     y
500         10    0
#
#
element.connectivity
grp.name = beam
elm.name    nod.name(s)
f 1             1  2
r 1             1  1   27
#
grp.name = joint
elm.name    nod.name(s)
100         1a    1     500
#
#
restraints
nod.name    direction
1a                x+y+rz
1                  y
29                x+rz
#
#beam
linear.curves
 start.time = 0.0
 crv.name = crv1
  time  load.factor
    5     0.72
    10    0.88
    12    1.0
    20    0.63
    40    0.34
    60    0.27
#
#conn.
#conn.
crv.name = crv2
  time  load.factor
   4     0.6
   12    0.77
   20    0.92
   32    1.0
   40    1.0
   48    0.83
   56    0.73
   60    0.65
#
#
applied.loading
initial.loads
    elm.name  type  value
 f   1    udl1   0  -9.6
 r   1      -    0   0     27
#
#
  time.history
  elm.name   type  crv.name   value
```

```
f   1        tmp1   crv1    556.2 0 556.2 0
r   1         -       -     0   0  0  0    27
#
  100   tmp5      crv2  520 0 0
#
equilibrium.stages
 end.of.stage     steps
     15         100
     60         50
#
#
iterative.strategy
number.of.iterations = 20
initial.reformations = 20
step.reduction = 10
divergence.iteration = 20
maximum.convergence = 1e+30
#
#
convergence.criteria
tolerance = 0.1e-2
# disp = 0.5
# rota = 0.1
  work = 1800
#
#
output
frequency 0 stress
#
#
end
#
```

APPENDIX A2 – Data file of composite beam model for Gurun Fire test.

```
#unit kN,m
#
analysis 2d static
#
#
materials
mat.name    model        properties
steel        stl4        205e6 41.0e6 100 700 1200 &
                         275e3 27.5e3 400 800 1200 &
                         0.0 0.0 200 600 1200 &
                         0.010125 0.01485 750 850 1200
#
reinf       stl4        205e6 41.0e6 100 700 1200 &
                        460e3 46.0e3 400 800 1200 &
                        0.0 0.0 200 600 1200 &
                        0.010125 0.01485 750 850 1200
#
con         con6        25e3 300 1 1100 0.04 1200 0 &
                        2.5e-3 600 5 900 6 1200 6 &
                        20e-3 1200 2.5 1200 2.5 1200 2.5 &
                        1 1200 9.6e-3 1200 9.6e-3 1200 9.6e-3
#
 mat.name    model      properties
  mat1       gen1   460e3 100.0 1.0 400.0 0.91 700.0 0.21 1200.0 0.0 &
                    205e6 100.0 1.0 400.0 0.43 700.0 0.077 1200.0 0.0
&
                    0.0000001 500 1.0 600.0 1.0 700.0 1.0 1200.0 1.0 &
                    275e3 100.0 1.0 400.0 0.91 700.0 0.21 1200.0 0.0 &
                    0.02 500.0 1.0 600.0 1.0 700.0 1.0 1200.0 1.0

  mat2       gen1   827.0e3 300 1.0 680 0.17 1000 5.84e-3 1200 0.0 &
                    210e6 100 1.0 400 0.43 700 0.077 1200 0.0 &
                    0.0000001 500 1.0 600 1.0 700 1.0 1200 1.0 &
                    634.32e3 300 1.0 680 0.17 1000 5.84e-3 1200 0.0 &
                    0.001 500.0 1.0 600.0 1.0 700.0 1.0 1200.0 1.0

  mat3       gen1   446.16e3 100 1.0 400 0.91 700 0.21 1200 0.0 &
                    205e6 100 1.0 400 0.43 700 0.077 1200 0.0 &
                    0.0000001 500 1.0 600 1.0 700 1.0 1200 1.0 &
                    275e3 100 1.0 400 0.91 700 0.21 1200 0.0 &
                    0.02 500 1.0 600 1.0 700 1.0 1200 1.0
#
sections
sec.name    type  mat.name    dimensions
ub          isec  steel       0.199 0.012 0.199 0.012 0.422 0.008
#
cslab       rcgs  reinf con   1.0 0.15 0 0 0 0 193e-6 0.105 193e-6 &
                              0.045
#
Groups
type.of.element = cbp2
grp.name    sec.name  monitoring.points
beam          ub           200
gcs           cslab         40
#
type = lnk2
 grp.name       stiffness.parameters
   gp1           rigid rigid   rigid
#
type.of.element = jbc2
 grp.name   type                  mat.name(s)   parameters
joint  steel web.angle rigid  mat1 mat2 mat3    19.05e-3 285.02e-6 &
```

```
                                                    155.0e-3 10e-3 0.1e-3 &
                                                    2.0e-3 75e-3 41.4e-3 &
                                                    40.0e-3 0.5 12.0e-3 &
                                                    16e-3 130e-3 100e-3 &
                                                    50e-3 50e-3 13.0e-3 &
                                                    75e-3 200e-3 5.0e-3 &
                                                    446e-3 12e-3 8e-3 &
                                                    2 0.3 1
#
structural.nodal.coordinates
nod.name         x       y
# jnt + beam
        1a      0.0     0.0
f       1       0.0     0.0
r       1       0.16    0.0  27
        29      4.5     0.0
#slab
f       101      0.0     0.298
r        1       0.16    0.0   27
        129      4.5     0.298
#
non.structural.nodal.coordinates
nod.name    x     y
500         10    0
#
element.connectivity
grp.name = beam
elm.name    nod.name(s)
f 1             1  2
r 1             1  1   26
  28           28  29
#
grp.name = gcs
elm.name    nod.name(s)
f 101          101 102
r 1             1   1  26
  128          128 129
#
grp.name = gp1
elm.name    nod.name(s)
f 201        2 102
r 1          1  1  27
#
grp.name = joint
elm.name    nod.name(s)
1000        1a    1     500
#
#
restraints
nod.name    direction
1a               x+y+rz
29               x+rz
1                 y
101              x+y+rz
#
#secondary beam, b2 b&c
linear.curves
 start.time = 0.0
 crv.name = crv1
  time  load.factor
    5     0.72
    10    0.88
    12    1.0
    20    0.63
    40    0.34
```

```
    60    0.27
#
#conn. for b2c
crv.name = crv2
  time  load.factor
   4     0.6
   12    0.77
   20    0.92
   32    1.0
   40    1.0
   48    0.83
   56    0.73
   60    0.65
#
applied.loading
initial.loads
 elm.name  type  value
 f   1    udl1   0  -9.6
 r   1      -    0   0     27
#
  time.history
  elm.name   type  crv.name   value
f    1        tmp1  crv1      556.2 0 556.2  0
r   1           -    -         0  0  0  0   27
#
  1000        tmp5      crv2  520 0 0
#

#
equilibrium.stages
 end.of.stage     steps
     60          100
#
#
iterative.strategy
number.of.iterations = 10
initial.reformations = 10
step.reduction = 5
divergence.iteration = 5
maximum.convergence = 0.1e+8
#
convergence.criteria
tolerance = 0.1e-4
& disp = 1.0
& rota = 1.5
  work = 2000
#
output
frequency 0 stress
#
end
```

APPENDIX A3 – Data file of floor system model for Gurun Fire Test.

```
# symmetric floor systems
analysis 3d static
#
materials
mat.name      model   properties
 mat1         stl4   205e6 41.0e6 100 700 1200 &
                     275e3 27.5e3 400 800 1200 &
                     0.0 0.0 200 600 1200 &
                     0.010125 0.01485 750 850 1200

 mat2         con6   25e3 300 1 1100 0.04 1200 0 &
                     2.5e-3 600 5 900 6 1200 6 &
                     20e-3 1200 2.5 1200 2.5 1200 2.5 &
                     1 1200 9.6e-3 1200 9.6e-3 1200 9.6e-3

 mat3        stl4    460e6 41.0e6 100 700 1200 &
                     275e3 27.5e3 400 800 1200 &
                     0.0 0.0 200 600 1200 &
                     0.010125 0.01485 750 850 1200
#
 mat4       gen1     460e3 100 1.0 400 0.91 700 0.21 1200 0.0 &
                     205e6 100 1.0 400 0.43 700 0.077 1200 0.0 &
                     0.0000001 500 1.0 600 1.0 700 1.0 1200 1.0 &
                     275e3 100 1.0 400 0.91 700 0.21 1200 0.0 &
                     0.02 500 1.0 600 1.0 700 1.0 1200 1.0

 mat5       gen1     827.0e3 300 1.0 680 0.17 1000 5.84e-3 1200 0.0 &
                     210e6 100 1.0 400 0.43 700 0.077 1200 0.0 &
                     0.0000001 500 1.0 600 1.0 700 1.0 1200 1.0&
                     634.32e3 300 1.0 680 0.17 1000 5.84e-3 1200 0.0 &
                     0.001 500 1.0 600 1.0 700 1.0 1200 1.0

 mat6       gen1     446.16e3 100 1.0 400 0.91 700 0.21 1200 0.0 &
                     205e6 100 1.0 400 0.43 700 0.077 1200 0.0 &
                     0.0000001 500 1.0 600 1.0 700 1.0 1200 1.0 &
                     275e3 100 1.0 400 0.91 700 0.21 1200 0.0 &
                     0.02 500.0 1.0 600.0 1.0 700.0 1.0 1200.0 1.0
#
sections
sec.name         type  mat.name     dimensions
 cbeam1          isec   mat1   0.300 0.017 0.300 0.017 0.548 0.012
 cbeam2          isec   mat1   0.199 0.012 0.199 0.012 0.422 0.008
 cbeam3          isec   mat1   0.199 0.011 0.199 0.007 0.374 0.008
#
#
 cslab1   rcts   mat3 mat2 mat2     0.150 0.0001 0.060 0.045005 1.0 &
                                    0.01 0.9 0.001 193e-6 0.050 0.2 &
                                    193e-6 0.105 0.2
#
groups
type.of.element = cbp3
 grp.name       sec.name        monitoring.points
   gcb1           cbeam1                5
   gcb2           cbeam2                5
   gcb3           cbeam3                5
   gcs1           cslab1               20
#
type.of.element = lnk3
 grp.name       stiffness.parameters
   gp1           rigid rigid   rigid     rigid rigid rigid
#
type.of.element = jbc2
```

```
 grp.name   type                    mat.name(s)   parameters
#secondary beam b2b1, b2c, b2b
joint1  steel web.angle rigid  mat4 mat5 mat6  19.05e-3 285.02e-6 &
                                                155.0e-3 10e-3 0.1e-3 &
                                                2.0e-3 75e-3 41.4e-3 &
                                                40.0e-3 0.5 12.0e-3 &
                                                16e-3 130e-3 100.0e-3 &
                                                50e-3 50e-3 13e-3 &
                                                75.0e-3 200e-3 5.0e-3 &
                                                446e-3 12e-3 8e-3 &
                                                2 0.3 1
#secondary beam b2b1, b2a
joint2 steel combination.web/top/seat rigid  mat4 mat5 mat6 19.05e-3 &
                                                285.02e-6 155.0e-3 &
                                                10e-3 1e-3 2.0e-3 &
                                                75.0e-3 41.4e-3 40e-3 &
                                                0.5 12.0e-3 16e-3 &
                                                19.05e-3 285.02e-3 &
                                                0.3 25e-3 10e-3 2e-3 &
                                                90e-3 0.1e-3 0.1e-3 &
                                                40e-3 10e-3 19.05e-3 &
                                                285.02e-3 155e-3 &
                                                12e-3 35.4e-3 2e-3 &
                                                75e-3 1e-3 1e-3 47e-3 &
                                                12e-3 294.0e-3 &
                                                302e-3 50e-3 50.0e-3 &
                                                13e-3 75e-3 200e-3 &
                                                5e-3 446e-3 12.0e-3 &
                                                8.0e-3 4 0.3 1

#main beam, b1c
joint3 steel extended.endplate rigid mat4 mat5 mat6 25.4e-3 506.71e-6&
                                            17.46e-3 25e-3 3.98e-3&
                                            20.95e-3 38.1e-3 &
                                            78.162e-3 800e-3 25e-3&
                                            300e-3 130e-3 4.75 &
                                            25.4e-3 506.71e-6 &
                                            17.46e-3 25.0e-3 &
                                            3.975e-3 20.95e-3 &
                                            38.1e-3 30.66e-3 800e-3&
                                            25e-3 300e-3 130.0e-3 0&
                                            294.0e-3 302.0e-3 12.0e-3 &
                                            12.0e-3 13.0e-3 130.0e-3 &
                                            40.0e-3 97.21e-3 582.0e-3 &
                                            17.0e-3 12.0e-3 5 0.3
#
#
type.of.element = jel3
 grp.name   curve.types                      parameters
  beamj1    lin rigid rigid rigid rigid lin      0 0
#
structural
  nod.name  x     y      z
#
#steel beam
f       1       0      0        0
r       1       0      0        0.9   5
r       10      3.2    0        0     2

f       31      9.5    0        0
r       1       0      0        0.9   5

f       49      0      0        0
r       1       1.6    0        0     5
        55      9.5    0        0
```

```
#slab
f       101       0      0.337    0
r         1       0      0        0.9   5
r        10       3.2    0        0     2

f       131       9.5    0.337    0
r         1       0      0        0.9   5

f       150       1.6    0.337    0
r         1       3.2    0        0     1
         152      7.95   0.337    0
#
#connection nodes
   1a       0      0      0
#
non.structural.nodal.coordinates
  nod.name      x       y      z
#secondary beam in z axis
f     3001  0     0.5   20
r     1     3.2   0     0     2
      3004  9.5   0.5   20
      4001  20    0.5   0

f     5001  20     0.5  0
r     1      0     0    0.9    5

      6002    3.2      0.5    20
      6003    6.4      0.5    20
      6001    0        0.5    20
      6004    9.5      0.5    20
#
element.connectivity
 elm.name   grp.name    nod.name
# Steel Beams, secondary beam 2
f       1      gcb3          1       2      3001
r       1       -            1       1       0       4
#
f       31      gcb2          31      32      3004
r       1       -             1       1       0       4
#
f       12      gcb2          12     13      3002
r       1       -             1      1       0       3
r       10      -             10     10      1       1
        11      gcb2          11     12      6002
        21      gcb2          21     22      6003
#main beam
        50      gcb1          49     50     4001
        51      gcb1          50     51     4001
        52      gcb1          51     52     4001
        53      gcb1          52     53     4001
        54      gcb1          53     54     4001
        55      gcb1          54     55     4001
# slab
f       101     gcs1          101     102      6001
r       1       -             1       1        0       4
r       10      -             10      10       1       3

        150     gcs1          101     150       5001
        151     gcs1          150     111       5001
        152     gcs1          111     151       5001
        153     gcs1          151     121       5001
        154     gcs1          121     152       5001
        155     gcs1          152     131       5001
#
        160     gcs1          102     112       5002
```

```
        161     gcs1            112     122       5002
        162     gcs1            122     132       5002
        170     gcs1            103     113       5003
        171     gcs1            113     123       5003
        172     gcs1            123     133       5003
        180     gcs1            104     114       5004
        181     gcs1            114     124       5004
        182     gcs1            124     134       5004
        190     gcs1            105     115       5005
        191     gcs1            115     125       5005
        192     gcs1            125     135       5005
        200     gcs1            106     116       5006
        201     gcs1            116     126       5006
        202     gcs1            126     136       5006
#
#link
        1001    gp1             1a      101     6001
F       1002    gp1             2       102     6001
r       1       -               1       1       0     4
r       10      -               10      10      1     3

        1011    gp1             51      111     6002
        1021    gp1             53      121     6003
        1050    gp1             50      150     4001
        1051    gp1             52      151     4001
        1052    gp1             54      152     4001
        1031    gp1             55      131     4001
#
# connection tswa
      10001    joint2          1a     1    2   102
      10002    joint2          55     31   32  132
#
# connection   dwa
      10003     joint1         51     11   12  112
      10004     joint1         53     21   22  122
# connection extep
      10005     joint3         1a     49   50  150
#pin
       10011     beamj1         1a     1    2   102
       10012     beamj1         55     31   32  132
       10013     beamj1         51     11   12  112
       10014     beamj1         53     21   22  122
       10015     beamj1         1a     49   50  150
#
restraints
nod.name direction
1a      x+y+z+rx+ry+rz
55      x+y+z+rx+ry+rz
6       x+z+rx+ry+rz
16      x+z+rx+ry+rz
26      x+z+rx+ry+rz
36      x+z+rx+ry+rz
#
#beam 2(2bnc also side and beam 3)
linear.curves
 start.time = 0.0
 crv.name = crv1
  time  load.factor
    5     0.72
    10    0.88
    12    1.0
    15    0.863
    18    0.719
    20    0.63
    25    0.45
```

```
    30    0.378
    40    0.34
    45    0.315
    50    0.297
    55    0.288
    60    0.27
#conn.dwa
 crv.name = crv2
  time  load.factor
   4     0.6
   12    0.77
   20    0.92
   32    1.0
   40    1.0
   48    0.83
   56    0.73
   60    0.65
# beam 1(main beam)
#linear.curves
# start.time = 0.0
 crv.name = crv3
  time  load.factor
   4     0.53
  12     0.83
   28    0.87
   36    1.0
   52    0.67
   60    0.58
#temperature at extend end plate
#linear.curves
# start.time = 0.0
 crv.name = crv4
  time  load.factor
   4    0.234
   8      0.195
   12     0.234
   15     0.351
   20     0.351
   28     0.584
   30     0.805
   35     1.0
   41     0.805
   48     0.805
   54     0.779
   60     0.727
#
applied.loading
 initial.loads
      elm.name  type    value
#slab
f     101   udl1  0  -11.520  0
r     1     -     0     0  0  4
r     30    -     0     0  0  1

f     150     udl1      0   -3.420  0
r     1     -           0     0     0     5
f     160   udl1  0   -6.840  0
r     1     -     0     0  0  2
r     10    -     0     0  0  3

f     200   udl1  0   -3.420  0
r     1     -     0     0  0  2
time.history
 elm.name       type    crv.name        value
#B1
```

```
f     50    tmp1  crv3  600   0     0     600   0     0
r     1     -     -     0     0     0     0     0     0     5
#B3
f     1     tmp1  crv1  556.2 0     0     556.2 0     0
r     1     -     -     0     0     0     0     0     0     4
#B2b n c
f     11    tmp1  crv1  556.2   0   0     556.2   0   0
r     1     -     -     0     0     0     0     0     0     4
r     10    -     -     0     0     0     0     0     0     1
#B2
f     31    tmp1  crv1  556.2   0   0     556.2   0   0
r     1     -     -     0     0     0     0     0     0     4
#connection
  10003       tmp5      crv2  520 0 0
  10004       tmp5      crv2  520 0 0
  10005       tmp5      crv4  385 0 0
#
equilibrium.stages
 end.of.stage  steps
     5          10
     10         10
     20         10
     30         10
     40         7
     45         5
     55         5
     60         3
#
iterative
 number = 20
 initial = 10
 step = 20
 dive = 20
 maxi = 0.1e20
#
convergence
 toler = 0.1e0
 disp = 1
 rota = 0.05
# work = 2000
#
output
 frequency 0
#
end
#
```

Academic Journal

Ramli Sulong, N. H., Elghazouli, A. Y., Izzuddin, B. A., Ajit, N. (2010). Modelling of Beam-to Column Connection at Elevated Temperature using the Component Methods. Steel and Composite Structures, Vol. 10(1), 23-43.

Conference Papers

Ramli Sulong, N. H., Ajit, N. (2008). Parametric Investigations Of Steel Connection Behaviour In Gurun Fire Test, Chulalongkorn University. University of Malaya Civil and Envirobmental Engineering Research Symposium, 7-8 May, Department of Civil Engineering, Chulalongkorn University Bangkok, Thailand.

Ramli Sulong, N. H., Ajit, N. (2008). Connection Performance In Gurun Fire Test The. International Conference on Construction And Building Technology (ICCBT), 16-20 June, Hotel Grand Seasons, Kuala Lumpur, Malaysia.

Ramli Sulong, N. H., Elghazouli, A. Y., Izzuddin, B. A., AJIT, N. (2008). Deformation Capacity and Ductility Demand of Steel Connections at Ambient and Elevated Temperature. EUROSTEEL, 3-5 September, Graz, Austria,

Ramli Sulong, N. H., Ajit, N. (2009). Analytical Investigation Of Connection Influence On The Floor System In Gurun Fire Test. 7th Asia Pacific Structural Engineering And Construction Conference (APSEC), 4-6 August, Awana Porto Malai, Langkawi, Malaysia.

Ramli Sulong, N. H., Ajit, N. (2009). Investigation on Beam-to-Column Connection Of Steel Sub-Frame Under Fire. International Conference for Technical Postgraduates, 14-15 December, Legend Hotel, Kuala Lumpur, Malaysia.